Development of novel synthetic methodologies in photocatalysis

Cristofer Pezzetta

A thesis submitted in partial fulfilment of the requirements for the degree of

Doctor of Philosophy

under the supervision of

Prof. Davide Bonifazi (Cardiff University)

Dr Robert Davidson (Dr. Reddy's Laboratories, Cambridge)

Cardiff University – School of Chemistry

April 2020

This PhD was funded by the Marie Skłodowska-Curie Actions within the Innovative Training Network (ITN) PHOTOTRAIN (722591).

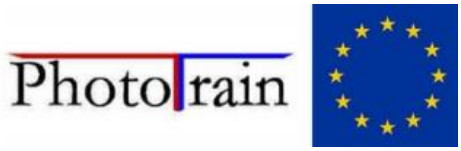

Abstract

The last decade has seen an impressive number of studies in the field of photocatalysis: the mild conditions used for the generation of radical intermediates and the possibility to couple it with other catalytic manifolds are among the reasons of such popularity. In this thesis, the use of some photocatalytic strategies in organic synthesis is presented.

The development of a dual Ni-photoredox strategy for the asymmetric synthesis of *N*-benzylic heterocycles, interesting drug-like compounds, is described in **Chapter 2**: a privileged ligand system was found for inducing chirality, and the effect of different heterocycles (in particular bearing directing groups) was addressed.

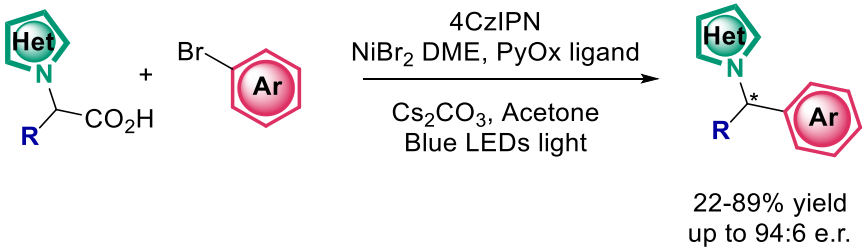

A different perspective is taken in **Chapter 3**: in this case the focus is not on the transformation, but on PXX (*peri*-xanthenoxanthene) as a new photocatalyst. Possessing a relatively high reduction potential in the excited state, PXX is capable of promoting a variety of reactions, from the addition of aryl radicals to radical traps, to the organocatalytic β-arylation of cyclic ketones, to Ni-catalysed carbon-heteroatom cross-couplings.

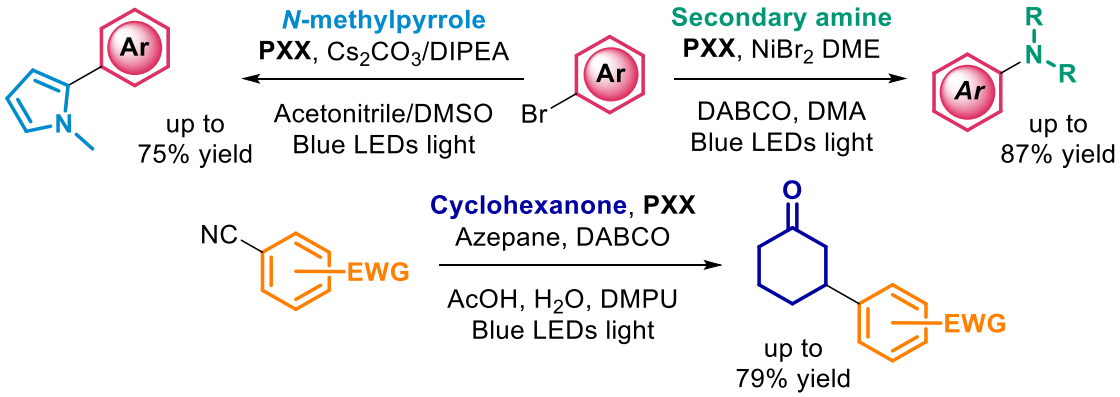

The focus moves to organocatalysis in **Chapter 4**, in particular to the use of chiral iminium ions as photoredox-active species: paired with 4-alkyldihydropyridines as radical precursors, an asymmetric β-alkylation of enals is thus demonstrated.

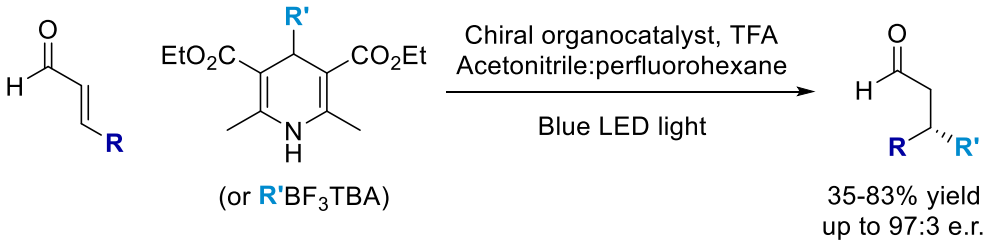

Chapter 5 takes back themes encountered in the previous chapters to briefly introduce some attempted but not successful transformations: an organocatalytic β-fluorination of aldehydes, and a cross-coupling strategy towards an API intermediate.

Acknowledgements

I would like to start by thanking both my supervisors for the invaluable help, support and advice given to me during these years of work. Thanks to Dr Robert Davidson for the constant presence and help, for the number of discussions and ideas, and for being a model chemist to look up to. Thanks to Prof. Davide Bonifazi for accepting to have me in his group despite the "long distance relationship", and also for the trust, kindness and scientific advice.

Many thanks to all the people who actively contributed to this work. First I must thank Prof. Armando Carlone, my original industrial supervisor, who made my PhD possible in the first place and who was a constant source of ideas. Thanks to Victor Kronig, Thomas Mahoney, Colin Dewar and Hugo Morren, analytical chemists in Dr. Reddy's, for precious analytical support. Thanks to Dr Andrea Folli for the EPR analyses, and Dr Emma Richards for teaching me the use of the glove-box. Thanks to Nurtalya Alandini, with whom I have shared four great (but tough) months of secondment in ICIQ, Tarragona. Thanks to Prof. Paolo Melchiorre for having me in his ICIQ group in the first place and for advice and discussions during that period and beyond. Thanks to Oliwia Matuszewska for all the support while working in Cardiff University and for the work done together. Thanks to Tommaso Battisti for his help with analytical instruments in Cardiff University. Thanks to the analytical teams in Cardiff University and ICIQ for all the work performed on my samples.

Special thanks go to all the people in Dr. Reddy's that made these years much easier, both personally and scientifically: thanks to Dr Tamara Fanjul for having been a wonderful mentor, and to Dr Shahed Hussain, Dr Justine Peterson, Dr Graham Meek, Dr Chris Cobley and Dr Martin Fox.

I would like to add all the people in the Phototrain consortium who made our meetings scientifically interesting and personally entertaining. Thanks again to Nurtalya, Oliwia and Tommaso, and also to Daniele, Amedeo, Argyri, Ewelina, Thien, Alex, Gustavo and

Kaituo. Thanks to Prof. Giacomo Bergamini for the scientific discussions, and to Lucy for getting everything organised.

Thank you to all who helped me settle in and work during my secondment in ICIQ, Tarragona, and helped me not feeling lonely: thanks Eva for your all your help, and thanks Giacomo, Pablo, Sara, Giulio, Bertrand, Alexis and Tamal.

Thanks to all in Cardiff University who helped and have been nice to this "outsider" during my work there: Grazia, Cataldo, Melina, André.

Un ringraziamento particolare va a tutti gli amici che, lontani o meno, mi hanno supportato in questi anni con il loro sostegno e affetto: Luca, Luciana, Riccardo, Emanuele, Pizza, Cate, Jac, Serena (x2), Marta (x2), Francesca, Alice, Angelica, Chiara, Giulia, Lorenzo, Marco, Daniele, Luce, Phil.

Tutto questo non sarebbe stato possibile senza l'appoggio della mia famiglia, che continua a credere in me e a sostenermi nonostante la distanza e gli sparuti incontri dal vivo: dai miei genitori, a Micky, ai nonni, grazie di cuore. Ora sarete contenti, ho finito di studiare! (sto mentendo…)

Fede: semplicemente, Grazie.

Contents

Publications, presentations and secondment

Some of the results presented in this thesis have been published:

- C. Pezzetta, D. Bonifazi, R. W. M. Davidson, Enantioselective Synthesis of *N*-Benzylic Heterocycles: A Nickel and Photoredox Dual Catalysis Approach, *Org. Lett.* **2019**, *21*, 8957-8961. (**Chapter 2**).
- C. Verrier, N. Alandini, C. Pezzetta, M. Moliterno, L. Buzzetti, H. B. Hepburn, A. Vega-Peñaloza, M. Silvi, P. Melchiorre, Direct Stereoselective Installation of Alkyl Fragments at the β-Carbon of Enals via Excited Iminium Ion Catalysis, *ACS Catal.* **2018**, *8*, 1062-1066. (**Chapter 4**).

The contents of **Chapter 3** will also be part of a forthcoming publication: Application of PXX as photocatalyst in organic synthesis (in preparation).

Some of the results in Chapter 2 have been presented at various events:

- Young Chemists in Industry 2019, 4th November 2019, UCB (Slough, UK) – oral presentation.
- International Symposium on Synthesis and Catalysis (ISySyCat) 2019, 3rd-6th September 2019, Évora – poster presentation.
- European Symposium on Organic Chemistry (ESOC) 2019, 14th-18th July 2019, Vienna – poster presentation.

Most of the experimental work presented in this thesis has been performed in Dr. Reddy's Laboratories, Cambridge under the supervision of Prof. Armando Carlone (January 2017 – August 2017) and Dr Robert Davidson (September 2017 onwards). I have spent four months (June-September 2017) in secondment in ICIQ (Institute of Chemical Research of Catalonia), Tarragona, under the supervision of Prof. Paolo Melchiorre, where I worked at the project described in **Chapter 4** together with Nurtalya Alandini (PhD candidate in the Melchiorre group).

List of abbreviations

4CzIPN	2,4,5,6-Tetra(carbazol-9-yl)isophthalonitrile (photocatalyst)
acac	Acetylacetonate
API	Active Pharmaceutical Ingredient
BD	2,3-Butanedione
BET	Back Electron Tranfer
Box	Bis-oxazoline (ligand)
bpy	2,2′-Bipyridine (ligand)
BTMG	2-*tert*-Butyl-1,1,3,3-tetramethylguanidine (Barton's base)
CFL	Compact Fluorescent Lamp
CN-Box	Cyano-bis-oxazoline (ligand)
CV	Cyclic Voltammetry
DABCO	1,4-Diazabicyclo[2.2.2]octane
DBU	1,8-Diazabicyclo[5.4.0]undec-7-ene
DCA	9,10-Dicyanoanthracene (photocatalyst)
DFT	Density Functional Theory
DHP	1,4-Dihydropyridine radical precursors
DIBAL	Diisobutyl Aluminium Hydride
DMA	*N*,*N*-Dimethylacetamide
DMBP	Bis(4-methoxyphenyl)methanone
DME	1,2-Dimethoxyethane
DMF	*N*,*N*-Dimethylformamide
DMPU	*N*,*N*′-Dimethylpropyleneurea
DMSO	Dimethylsulfoxide
DRL	Dr. Reddy's Laboratories, Cambridge (PhD host institution)
d.r.	Diastereoisomeric ratio
dtbbpy	4,4′-Di-*tert*-butyl-2,2′-bipyridine (ligand)
EDA	Electron Donor-Acceptor
e.e.	Enantiomeric eccess
e.r.	Enantiomeric ratio
EI	Electron Ionisation
EPR	Electron Paramagnetic Resonance
ESI	ElectroSpray Ionisation
FT-IR	Fourier Transform – Infrared spectroscopy
FWHM	Full Width at Half Maximum
GC	Gas Chromatography
HAT	Hydrogen Atom Transfer
HFIP	1,1,1,3,3,3-Hexafluoroisopropanol
HOMO	Highest Occupied Molecular Orbital
HPLC	High Performance Liquid Chromatography
HRMS	High-Resolution Mass Spectrometry
ICIQ	Institute of Chemical Research of Catalonia (secondment host institution)
ISC	Intersystem Crossing
LED	Light Emitting Diode
LUMO	Lowest Unoccupied Molecular Orbital
MS	Mass Spectrometry

NFPy	*N*-Fluoropyridinium tetrafluoroborate
NFSI	*N*-Fluorobenzenesulfonimide
NMR	Nuclear Magnetic Resonance
PBN	*N*-*tert*-Butyl-α-phenylnitrone (EPR radical trap)
PC	Photocatalyst (in schemes)
PDI	Perylenediimide (photocatalyst)
PET	Photoinduced Electron Transfer
phen	Phenanthroline (ligand)
pin	Pinacolate (substituent)
PPO	2,5-Diphenyloxazole
PTH	10-Phenylphenothiazine (photocatalyst)
PXX	*Peri*-xanthenoxanthene (photocatalyst)
PyBox	Pyridine 2,5-bis(oxazoline) (ligand)
PyOx	Pyridine 2-oxazoline (ligand)
PyrrOx	Pyrrole 2-oxazoline (ligand)
R&D	Research & Development
r.t.	Room temperature
RRC	Radical-Radical Coupling
RVC	Reticulated Vitreous Carbon electrode
SCE	Standard Calomel Electrode
SET	Single Electron Transfer
SFC	Supercritical Fluid Chromatography
SOMO	Singly Occupied Molecular Orbital
SulfOx	*N*-Phenylmethanesulfonamide 2′-oxazoline (ligand)
TBA^+	Tetrabutylammonium cation
TBADT	Tetrabytylammonium decatungstate (photocatalyst)
TBAF	Tetrabutylammonium fluoride
TDS	Texyldimethylsilyl
TEA	Triethylamine
TFA	Trifluoroacetic acid
TFE	2,2,2-Trifluoroethanol
THF	Tetrahydrofuran
TMEDA	Tetramethylethylenediamine
TMG	1,1,3,3-Tetramethylguanidine
TMS	Trimethylsilyl
TMU	1,1,3,3-Tetramethylurea
TTA	Triplet-Triplet Annihilation
TTET	Triplet-Triplet Energy Transfer
UV	Ultraviolet light

Chapter 1
Introduction

1.1 A new light in radical chemistry

During most undergraduate courses on organic chemistry (mine included), radical chemistry is little considered: after learning how to photochemically make organic halides from hydrocarbons, most of the scene is occupied by nucleophilic substitutions, carbonyl, enolate or arene chemistry, heterocycle formation, Pd catalysis. This is usually justified by the notion that radicals are very reactive and uncontrollable species, thus difficult to use for selective transformations. The historical methods of radical generation, typically involving initiators, heating or UV irradiation, certainly did not help with radicals' reputation. It took at least four years of studies before reality was slowly unveiled, and a number of efficient radical transformations were revealed to me. Recent years have indeed witnessed a dramatic increase in the number of works on radical chemistry as more and more groups studied their reactivity, efficient methods of formation and even their use in enantioselective transformations.[1]

Very recently, radical chemistry was gifted with a revisited strategy for radical generation that prides itself for efficiency and the mild conditions employed: photocatalysis.[2,3] While the first applications of photocatalysts were reported over 40 years ago, they were rediscovered only in the last 12 years, starting in 2008 with pioneering works from the MacMillan,[4] Yoon[5] and Stephenson[6] groups. From there interest grew exponentially, making photocatalysis one of the hottest topics of the decade, accompanying the general renewed interest into radical chemistry.

As the name implies, photocatalysis involves the use of a catalyst activated by light, and visible light is usually considered in this case. Upon light absorption, the photocatalyst accesses an excited state, which can be considered a new chemical species, behaving markedly differently from its ground state.[7] For example, the excited state is both a better reductant and oxidant than the ground state, and a single electron transfer (SET) to/from a suitable substrate can take place (**Scheme 1a**): this step (PET or photoinduced electron transfer) generates two new radical species (one from the photocatalyst, one from the substrate) that can engage into useful chemistry. This is the basis of the sub-

field of photoredox catalysis, so named because it involves a redox step (reduction/oxidation) with the substrate of interest. If a substrate (electron donor) reduces the excited state photocatalyst (PC*), then a reductive quenching cycle takes place (**Scheme 1b**), and the now reduced photocatalyst ($PC^{\cdot-}$) needs to be turnovered by another species (a sacrificial electron acceptor, another substrate or reaction intermediate). Conversely, in an oxidative quenching cycle the excited state photocatalyst is oxidised by a substrate (electron acceptor), and its oxidised form ($PC^{\cdot+}$) turnovered by another electron donor species (**Scheme 1c**). Every SET is governed by the redox potentials of the species involved, which can be experimentally determined and provide an approximate guide for the thermodynamic feasibility of the redox steps.[8] While these full catalytic cycles are typically considered, radical chain pathways where the photocatalyst works as a redox initiator are also possible.[9]

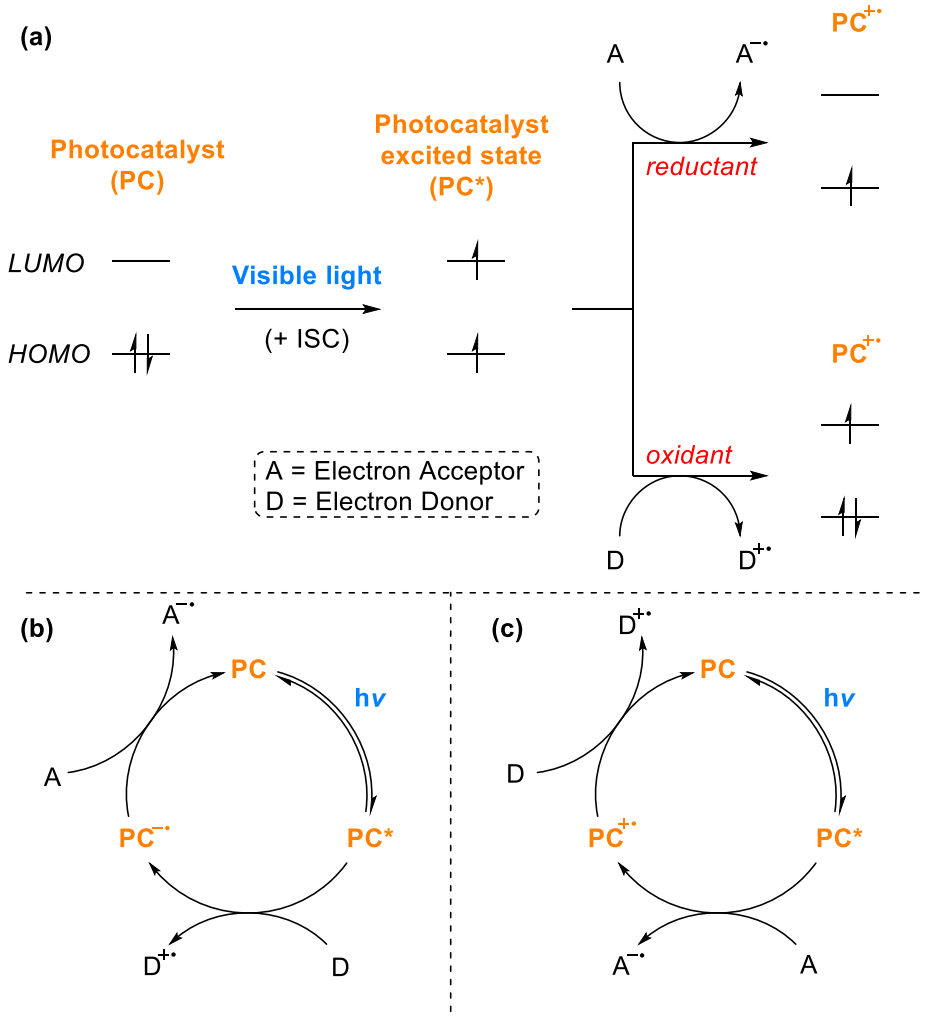

Scheme 1

General orbital scheme for the redox activity of a photoredox catalyst **(a)**. General depiction of reductive **(b)** and oxidative **(c)** quenching cycles in photoredox catalysis.[7]

As both an oxidant and a reductant are formed in the same reaction vessel, photoredox catalysis offers the unique opportunity to obtain redox-neutral reactions, where donation and capture of electrons happen in two different points of the mechanism. This puts it in direct contrast with the use of stoichiometric oxidants/reductants or with electrochemistry, for which redox-neutral transformations are more challenging.[2]

A less exploited activation method involves energy transfer (EnT) from the excited state photocatalyst to another species, raising it to a higher state (**Scheme 2**), a phenomenon typically called sensitisation.[10] Excited states can thus be accessed for species with low absorption coefficients, or for those which would require higher energy irradiation, allowing for milder conditions to be employed. The energy transfer can proceed through dipole-dipole interactions (Förster mechanism) or *via* intermolecular exchange of ground and excited state electrons (Dexter mechanism). Many photocatalysts can engage into EnT as well as SET, which can make understanding their real mechanism of action difficult.

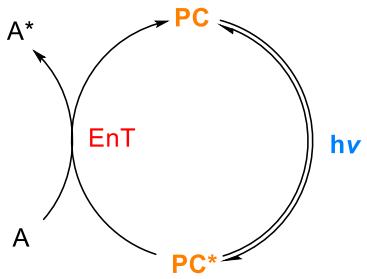

Scheme 2

General photocatalytic cycle involving energy transfer to an acceptor (A).[10]

Photocatalysis proved very effective also when combined with other catalytic platforms.[2,11] Dual catalytic systems allow unprecedented transformations, often complementary to existing single catalytic ones. It is for example the case of Ni and photoredox dual catalysis: radical species are photocatalytically generated and engage in C–C or C–heteroatom bond formation *via* the Ni centre, offering reactivity for a variety of C(sp^3) radical precursors which are not accessible with the more common Pd and Ni catalytic manifolds.[12,13] From the early days, merging with organocatalysis has allowed the development of interesting enantioselective transformations, using organocatalysts with both covalent and non-covalent modes of action.[2,14] In a similar fashion, Lewis and Brønsted acid catalysis were also combined with photocatalysis towards useful

enantioselective reactions.[11] Numerous cases of dual catalysis involving photocatalysis will be discussed later in this thesis.

The most commonly employed photocatalysts are polypyridyl complexes of ruthenium(II) and iridium(III): they absorb light in the visible region of the electromagnetic spectrum and possess long-lived (in the range of the μs) excited states, sufficiently long to participate in bimolecular SET and EnT reactions.[7] They have been largely employed in inorganic and material sciences, and their properties have become of interest to the synthetic community only in response to the growing interest into photocatalytic reactions. While very effective, these complexes are often expensive and their production (and price) depends on the supply of the precious metal. Many groups have thus focused on the use of organic photocatalysts (dyes) as alternatives to the common metal-based ones.[15,16] Very inexpensive dyes such as EosinY have been applied to a variety of transformations.[17] The development of specific dyes also allowed tackling difficult reactions: it's the case of Fukuzumi's highly oxidising acridinium salts such as Mes-Acr-Me,[18,19] or of 4CzIPN that is becoming a valid alternative to the most oxidising Ir(III) photocatalysts.[20] In **Section 3.1** an overview of highly reducing photocatalytic systems will be given as a representative example of the type of development in the field of photocatalyst structures and properties. In the end, the photocatalyst of choice will come from a compromise between efficiency, cost, availability and ease of use. It is thus important to have access to the widest range possible of dyes and metal complexes, so to apply the right photocatalyst for every occasion. **Figure 1** summarises the photocatalysts mentioned in this document, along with a selection of their photophysical and electrochemical properties.

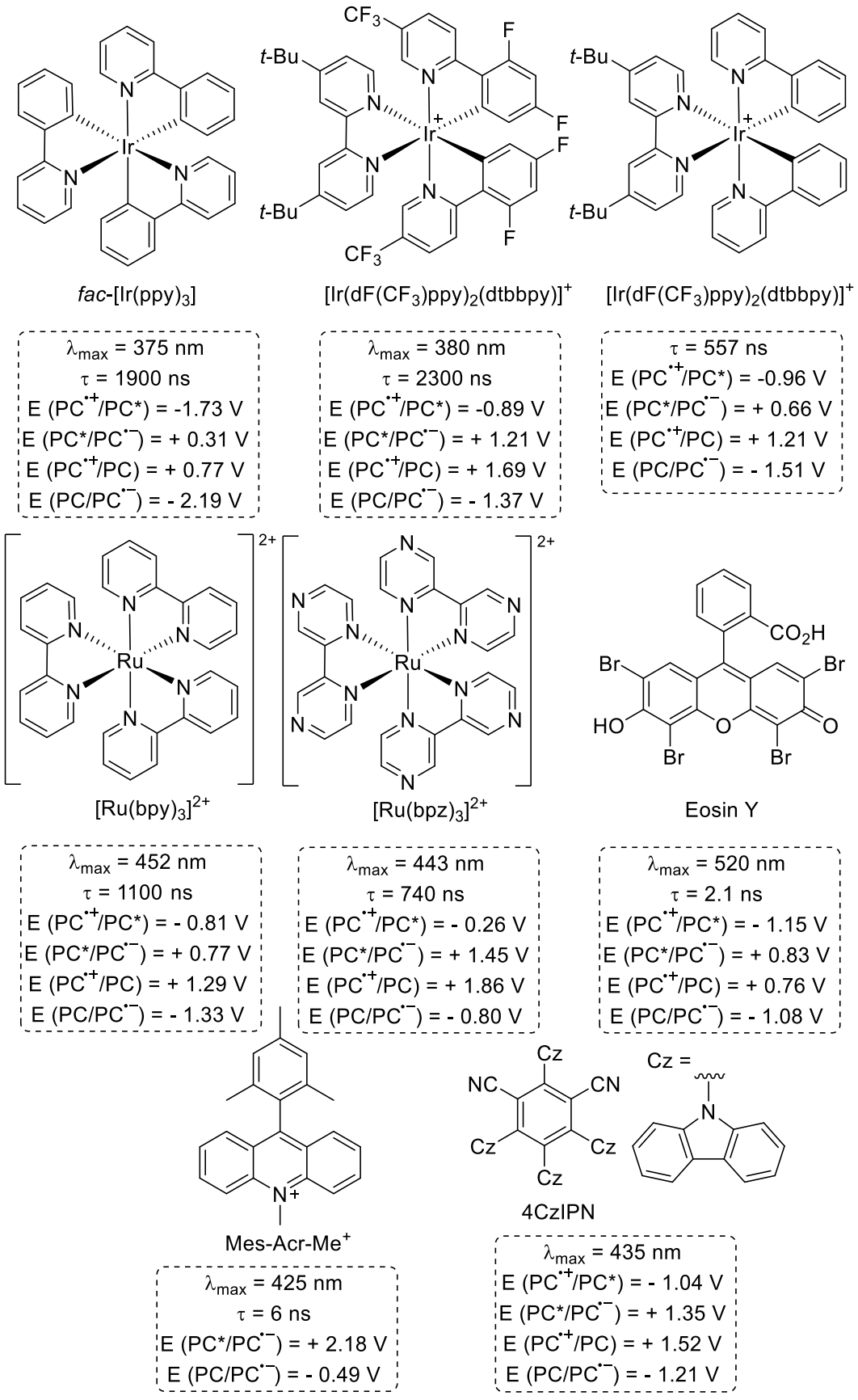

Figure 1

Overview of photocatalysts mentioned in this thesis, along with some of their photophysical and electrochemical properties.[7,15,20]

1.2 Thesis overview

The aim of this thesis is to demonstrate novel and interesting reactivity in photocatalysis, tackling some open challenges in the field with particular attention to accessing compounds of pharmaceutical interest.

For example, the development of enantioselective radical transformations is of uttermost importance in pharmaceutical research. In photocatalytic reactions, dual catalytic platforms are particularly useful as asymmetry can be introduced *via* a second catalyst, being it a metal centre, an organocatalyst or a Lewis acid: for this reason dual catalytic systems will be the focus of most of the thesis, and in particular of **Chapters 2** and **4** (**Scheme 3**). **Chapter 2** will describe an enantioselective method for the preparation of *N*-benzylic heterocycles, an important class of molecules in pharmaceutical chemistry. A Ni catalyst along with a chiral bidentate ligand is used to promote this transformation, with 4CzIPN as organic photocatalyst.[21] **Chapter 4** will describe the work performed

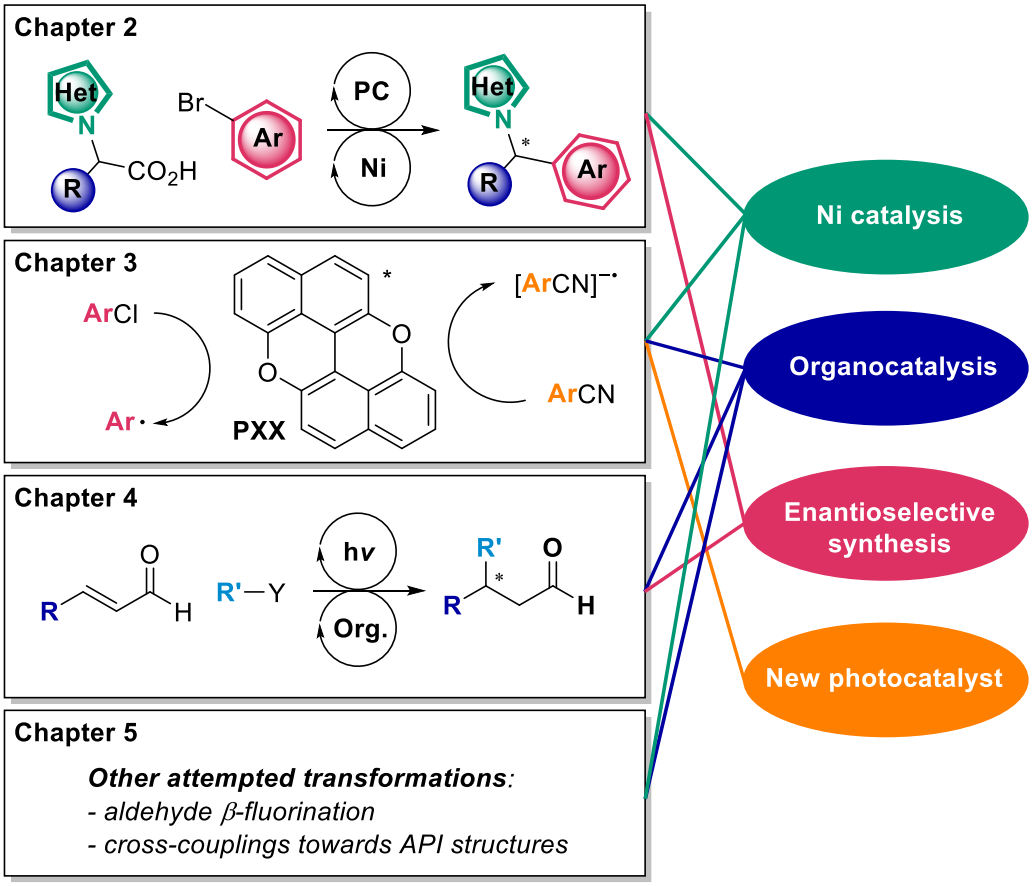

Scheme 3

Overview of the thesis chapters associated with some common themes.

during my secondment in the Melchiorre laboratory. A photomediated enantioselective β-alkylation of enals is reported, where no photocatalyst is added but the intrinsic photoactivity of a transient iminium ion is exploited.[22]

The replacement of precious metal photocatalysts with efficient organic alternatives is also a topic of current research.[15] The recent developments of highly reductive photocatalytic systems and our contributions in this regard are described in **Chapter 3** (**Scheme 3**), which will focus on the application of PXX, a dye under study in the Bonifazi group,[23] as an highly reducing photocatalyst. Applications to aryl halide activation, organocatalytic β-functionalisation and Ni-catalysed C–heteroatom bond formation will be described, encompassing three of the main themes in one project.

Chapter 5 will briefly report on two attempted transformations (a β-fluorination of aldehydes and attempted cross-coupling strategies towards an API structure) that did not show any of the desired reactivity, but from which something interesting was learned.

Chapter 2
Asymmetric synthesis of *N*-benzylic heterocycles

In this chapter a modular approach for the preparation of enantioenriched *N*-benzylic heterocycles is presented. α-Heterocyclic carboxylic acids, easily obtainable from common commercial materials, are reported as suitable substrates for a decarboxylative cross-coupling strategy in conjunction with a chiral pyridine–oxazoline (PyOx) ligand, providing quick access to enantioenriched drug-like products. The presence of a directing group on the heterocyclic moiety is shown to be beneficial, affording improved stereoselectivity in a number of cases.

2.1 Nickel- and photoredox-catalysed cross-coupling reactions

Transition metal-catalysed cross-couplings are amongst the most useful and widespread strategies for the formation of C–C bonds.[24] In the typical scenario, an organic halide or pseudohalide is coupled to an organometallic nucleophile in the presence of a transition metal catalyst, often palladium-based. The mechanism consists of oxidative addition of the organic halide, transmetalation with the organometallic reagent and final reductive elimination (**Scheme 4**). Although it's a very efficient process for the formation of C(sp^2)-C(sp^2) bonds, when the reaction involves C(sp^3) centres the generality is lost.[13] This is typically due to lower rates of transmetalation, leaving space for competing mechanisms, including β-hydride elimination. The development of novel ligand systems

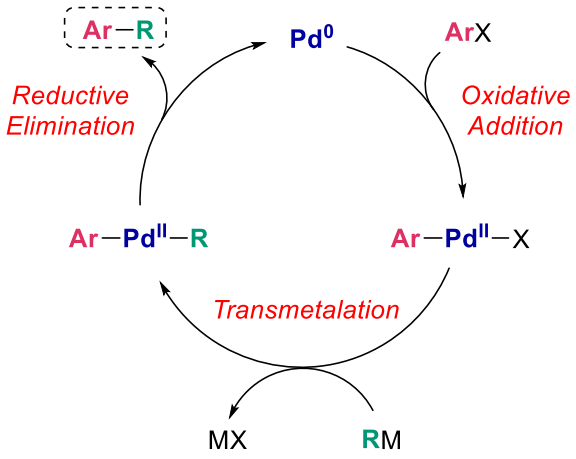

Scheme 4
Typical mechanism for a Pd-catalysed cross-coupling reaction.[13]

or the use of other transition metals (Ni, Fe) has allowed the use of alkyl halides as electrophilic partners.[25] The introduction of alkylic nucleophiles, however, has been limited to the use of reactive organometallic species (organo-Zn and organo-Mg) or harsh conditions.[13]

In the last ten years, a new mechanistic perspective has opened up opportunities for C–C cross-couplings with C(sp^3) "nucleophilic" partners.[12,13] The well-known ability of Ni complexes to access various oxidation states through one electron-reductions and oxidations was combined with photoredox SET activation: radical species in the reaction mixture could thus be trapped by the Ni centres and engaged in cross-coupling reactions. In this scenario, the coupling partner to the aryl halide is no more an organometallic nucleophile, but an alkyl radical precursor amenable of SET for the generation of alkyl radicals. The typical mechanism for these Ni-photoredox dual catalytic transformations is depicted in **Scheme 5**.[26] Upon visible light irradiation, the excited state photocatalyst is capable of oxidising the radical precursor, leading to fragmentation of an auxiliary group (Y in the scheme) and formation of alkyl radical **1**. Oxidative addition of the organic halide onto a Ni(0) complex can lead to Ni(II) intermediate **2a**, which can intercept radical **1** forming Ni(III) complex **2b**. The order of events can also be reversed: the initial Ni(0) complex can capture alkyl radical **1** leading to **2c** before oxidative addition. Computational studies have revealed that in some cases these two pathways compete. In either case, reductive elimination from complex **2b** leads to the final product. The resulting Ni(I) complex **2d** can be reduced by the reduced state of the photocatalyst, allowing turnover of both the photoredox and Ni catalytic cycles.

2.1.1 Cross-couplings initiated by the oxidation of a radical precursor

Pioneering works in this field have come independently from the Molander and the MacMillan and Doyle groups. In the first case, in 2014 organic trifluoroborate salts were introduced as radical precursors for efficient cross-couplings with aryl halides (**Scheme 6**).[27] A typical Ir(III) photocatalyst was used, along with $Ni(cod)_2$ and dtbbpy as Ni catalytic system. Addition of the alkyl radical to the Ni centre has a very low energetic barrier,[26] circumventing the slow transmetalation encountered with these substrates in classical two-electron chemistry. While the initial scope was limited to benzyl and α-alkoxy trifluoroborate salts, extensive work from the Molander group demonstrated

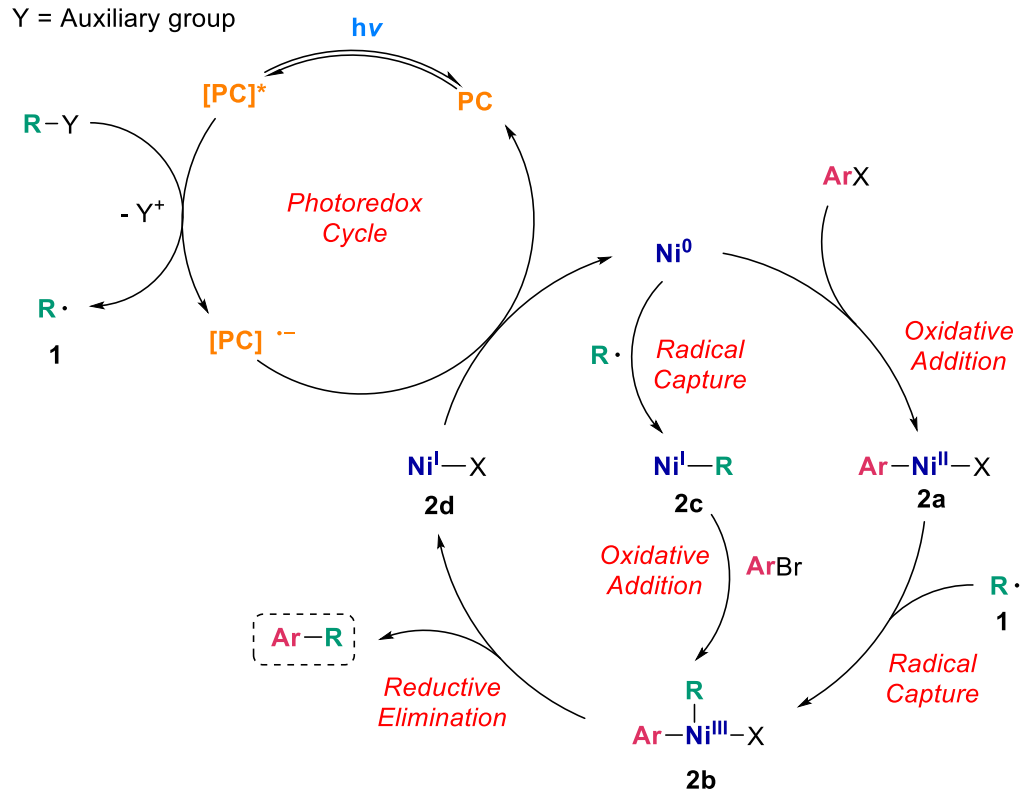

Scheme 5

Typical mechanism for a Ni-photoredox dual catalytic cross-coupling. Other ligands on Ni are omitted for clarity, as they depend on specific conditions. PC = Photocatalyst.[13]

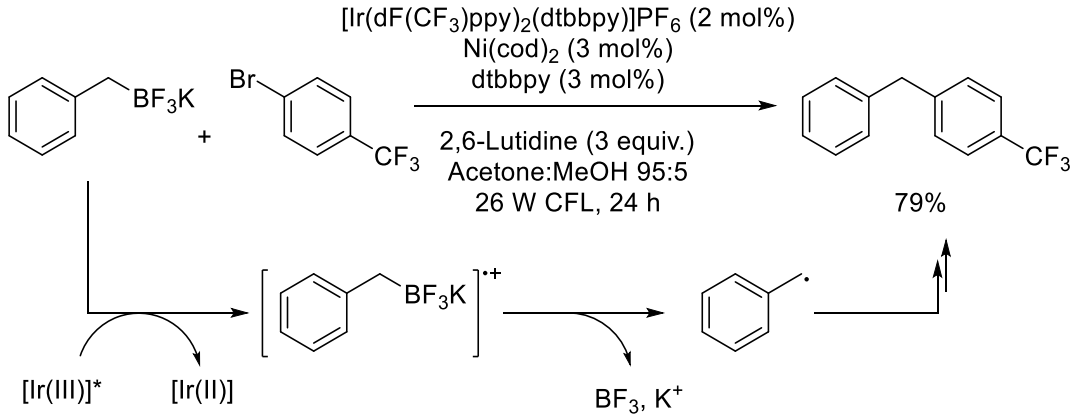

Scheme 6

General conditions and radical generation mechanism for Molander's Ni-photoredox cross-coupling of benzyltrifluoroborate salts and aryl halides.[27]

wide applicability of these reagents to the generation of α-alkoxy, α-hydroxy, secondary and tertiary alkyl radicals.[28–33]

The second seminal study revolves around a decarboxylative approach: in 2014 the MacMillan and Doyle groups reported the use of α-heteroatom carboxylic acids as radical precursors for cross-coupling reactions with aryl halides (**Scheme 7**).[34] In this

case, the *in situ*-formed carboxylate anion can be oxidised by the excited state Ir(III) photocatalyst, leading to a carboxy radical that, expelling CO_2, delivers the α-heteroatom alkyl radical. The method efficiently delivered coupled products from a variety of aminoacids, and α-oxo derivatives as well. It is of note the remarkable use of widely available, stable and inexpensive starting materials as radical precursors. Subsequent work from the MacMillan group further expanded this decarboxylative chemistry.[35–37]

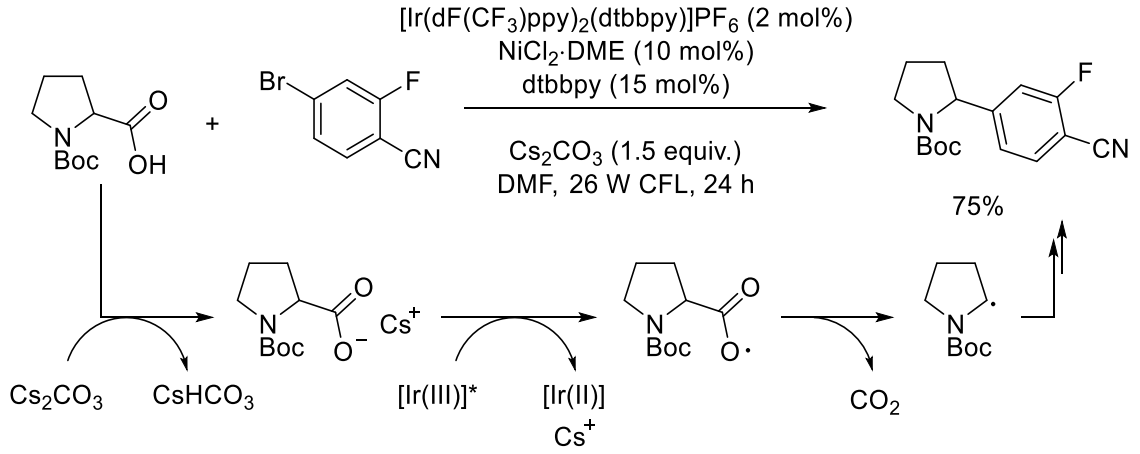

Scheme 7

General conditions and radical generation mechanism for MacMillan and Doyle's Ni-photoredox decarboxylative cross-coupling with aryl halides.[34]

These findings opened the way to the use of a variety of radical precursors in Ni-photoredox cross-couplings. Initial work from Fensterbank and co-workers followed by the Molander group introduced alkylbis(catecholate)silicate salts (**Scheme 8**).[38,39] When compared to trifluoroborates or carboxylates, these salts show reduced oxidation potentials allowing the use of a wider range of photocatalysts, display improved solubility in organic solvents and release non-acidic byproducts, so no base is required. Interestingly, these compounds allowed access to a variety of secondary and primary alkyl radicals, much more difficult to obtain with the previously mentioned derivatives. The Nishibayashi and Molander group independently reported the use of 4-alkyldihydropyridine (DHP) as radical precursors for cross-coupling reactions (**Scheme 9**).[40,41] The advantage here lies in the possibility to access the aldehyde feedstock, as DHPs can be easily obtained from the corresponding alkylic aldehyde *via* construction of the heterocycle. With these derivatives α-activated and non-activated radicals could be obtained, and it is of note the possibility to use sugar-derived DHPs as radical precursors.[42,43] They also display an instrinsic photoredox activity, which has

been later exploited by the Melchiorre group for coupling with cyanoarenes or Ni-catalysed cross-couplings with aryl bromides and acyl chlorides.[44]

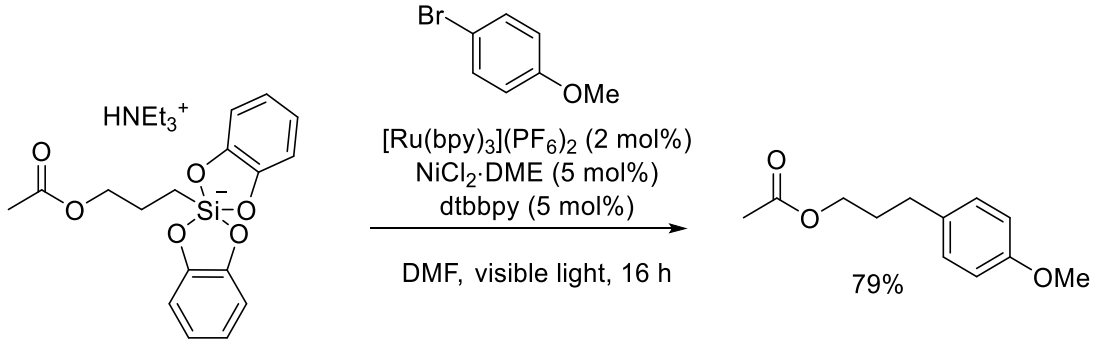

Scheme 8

General conditions for Molander's Ni-photoredox cross-coupling with silicate salts.[39]

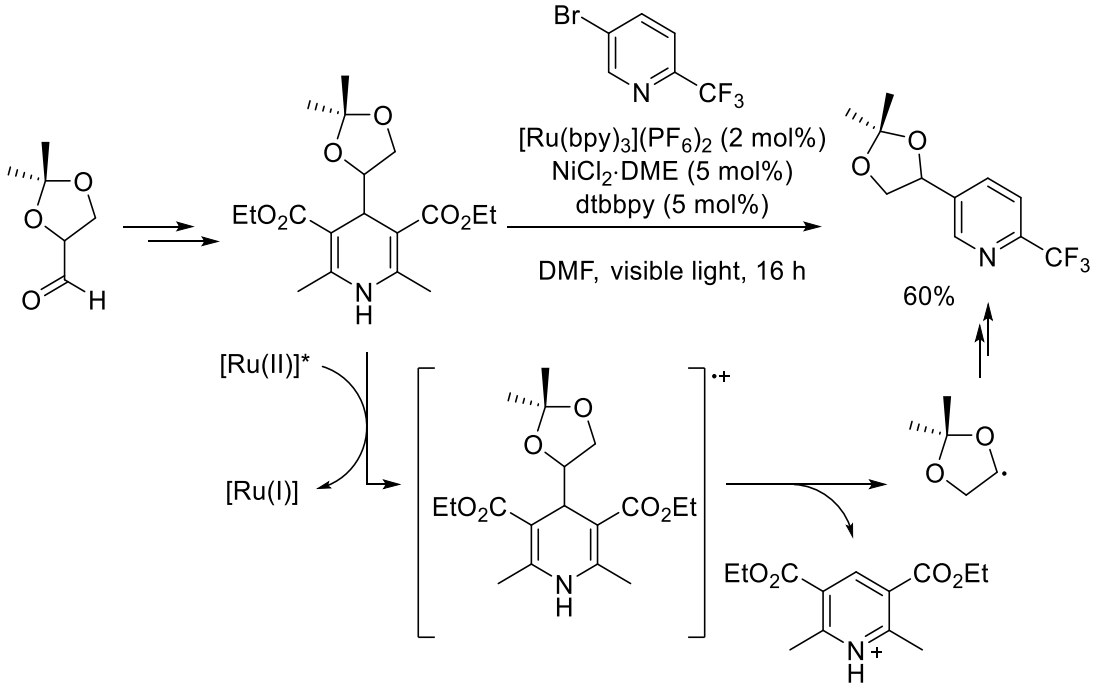

Scheme 9

General conditions and radical generation mechanism for Molander's Ni-photoredox cross-coupling with dihydropyridine precursors.[41]

Tetraalkylsilanes[45] and alkylsulfinate salts[46] are other radical precursors with more limited applications. The cross-coupling mechanism with these derivatives still involves their photo-oxidation with subsequent fragmentation and release of the desired alkyl radical.

A slightly different strategy was exploited in 2019 by Leonori and co-workers: oxidation of cyclobutanone oximes bearing a carboxylate auxiliary group leads to a nitrogen-centred radical, and subsequent ring opening leads to the formation of an alkyl radical.[47]

In this way, cross-couplings with aryl (**Scheme 10**) and alkyl bromides were obtained in good yields.

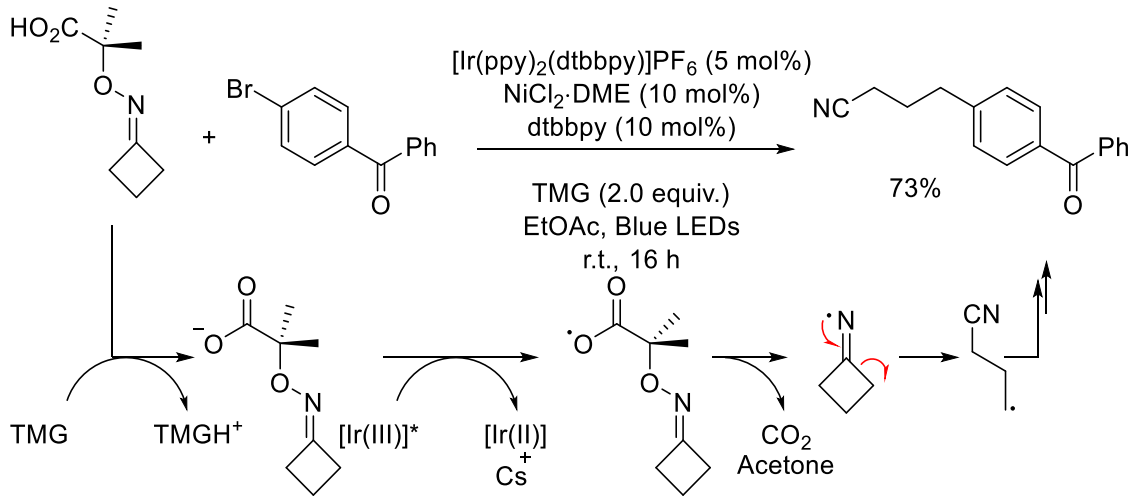

Scheme 10

Leonori's ring-opening procedure for the formation of alkyl radical from oximes and subsequent cross-coupling with aryl bromides.[47]

2.1.2 Cross-couplings based on the activation of C–H bonds

While all these derivatives bear a suitable auxiliary group to aid in the oxidation event, an even more advantageous approach is the use of simple hydrocarbons as radical precursors through a formal C-H activation for the generation of the alkyl radical. This has been the case of the α-arylation of *N*,*N*-dimethylaniline as described by the MacMillan and Doyle groups in the same work of the decarboxylative coupling.[34] In this case, oxidation of dimethylaniline leads to the corresponding radical cation which, upon deprotonation on the acidic α-position, releases the alkyl radical (**Scheme 11**). This strategy has been later expanded by the Doyle group for the α-functionalisation of cyclic *N*-aryl amines.[48]

In 2016, an elegant cross-coupling strategy for non-functionalised protected amines was devised by the MacMillan group by introduction of an hydrogen atom transfer (HAT) step in the catalytic cycle.[49] In this scenario, the excited state Ir(III) photocatalyst oxidises aceclidine (a quinuclidine-type base) to its radical cation, which can abstract an hydrogen from the α position of, for example, *N*-Boc pyrrolidine. The regioselectivity of the abstraction is controlled by the higher hydridic nature of the α-hydrogens, which matches the electrophilicity of the aceclidine radical cation. The α positions of amides, ureas, ethers and benzylic hydrocarbons are also amenable to this type of activation. The same approach was later applied to the cross-coupling with alkyl electrophiles.[50]

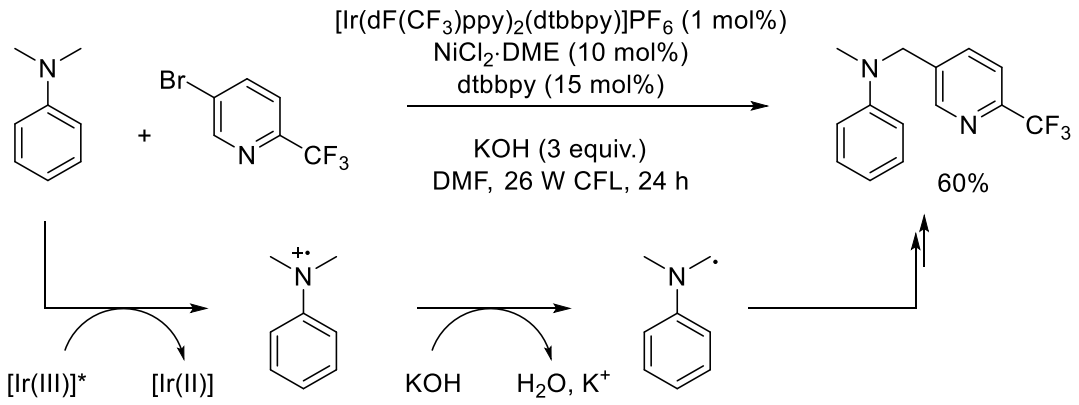

Scheme 11

General conditions and radical generation mechanism for MacMillan and Doyle's Ni-photoredox cross-coupling of dimethylaniline.[34]

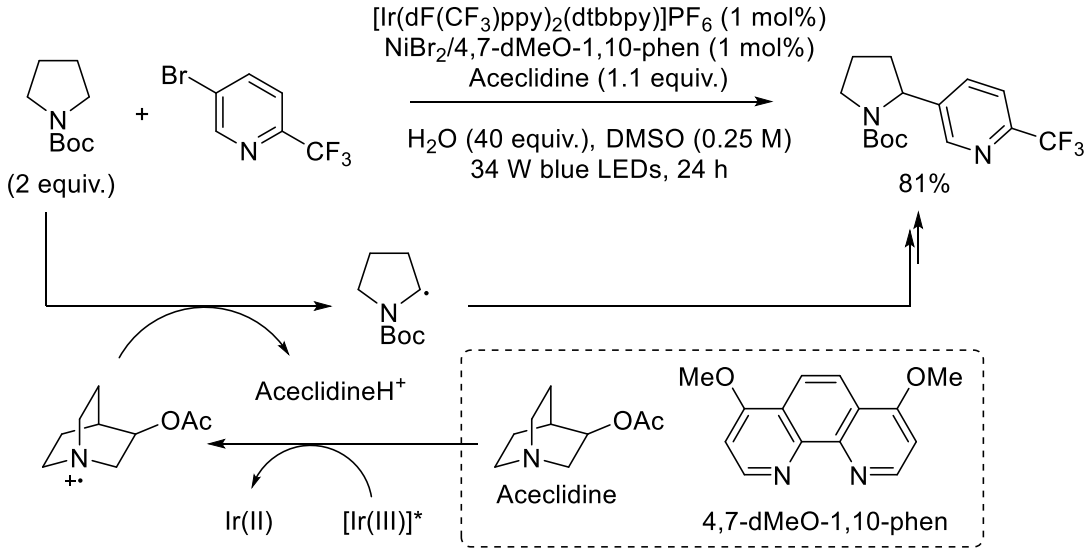

Scheme 12

General conditions and radical generation mechanism for MacMillan's Ni-photoredox HAT cross-coupling of protected amines.[49]

A similar strategy was used again by the MacMillan group with TBADT (tetrabutylammonium decatungstate) as photocatalyst for the activation of C-H bonds in simple hydrocarbons (**Scheme 13**).[51] In this case, the excited triplet state of the photocatalyst itself acts as the HAT reagent.

The triplet excited state of diarylketone **3** was exploited by Martin and co-workers, with the hydrocarbon reagent used as solvent (**Scheme 14**).[52] A wide scope was presented, including both aryl and alkyl bromides.

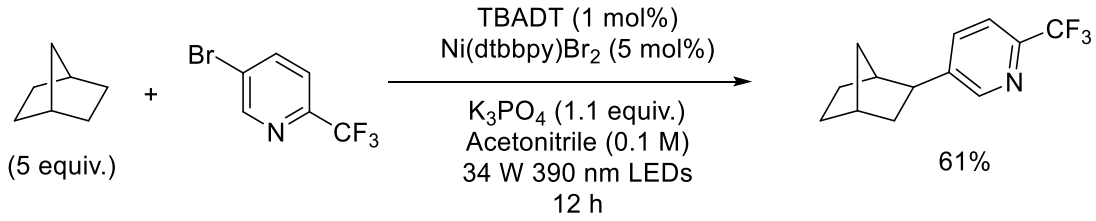

Scheme 13

General conditions for MacMillan's TBADT-photocatalysed Ni cross-coupling.[51]

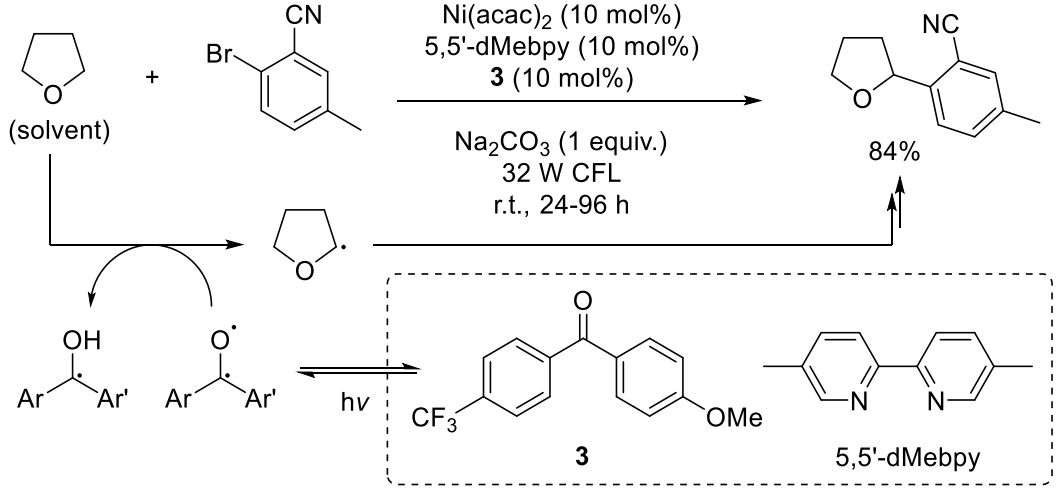

Scheme 14

General conditions for Martin's Ni-photoredox HAT cross-coupling with a diarylketone as photocatalyst.[52]

Doyle and co-workers demonstrated a cross-coupling in the absence of a formal HAT reagent. In their conditions, irradiation of a photo-oxidised Ni(III)-Cl complex releases a chlorine radical, which then behaves as HAT abstractor, extracting hydrogen from the solvent (**Scheme 15**).[53] The procedure worked well with different aryl chlorides and a range of ethers as solvents/reaction partners.

Lastly, a similar mechanism was also inferred by Molander and co-workers for their HAT cross-coupling reaction of aryl bromides and cyclic ethers.[54] While a diarylketone is present in the reaction mixture and seems to improve yields, the main pathway is believed to involve triplet-triplet energy transfer from the Ir(III) photocatalyst to a Ni(II) complex, with subsequent formation of a bromine radical that works as HAT reagent, in the same way as depicted in **Scheme 15**.

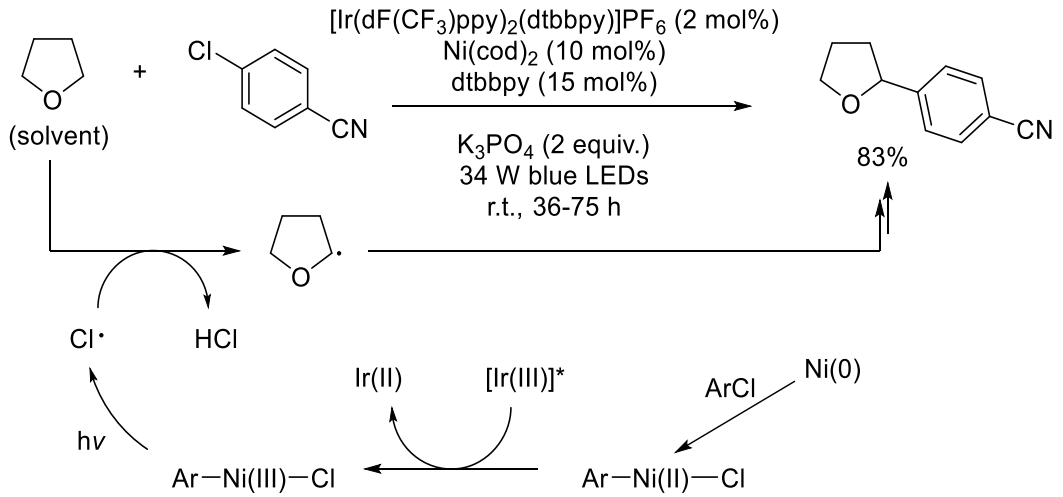

Scheme 15

General conditions and radical generation mechanism for Doyle's Ni-photoredox HAT cross-coupling.[53]

2.2 Ni-photoredox asymmetric cross-couplings

While we have witnessed growing interest in Ni-photoredox dual catalysed cross-coupling reactions, few studies have focused on asymmetric variants of these transformations.[55] A lot of the cases examined above generate racemates starting from prochiral/racemic radical precursors. While still very interesting, it is also true that chirality can have profound effects on the activity of, for example, pharmaceutical agents,[56] so the development of enantioselective cross-couplings is of utmost significance. The most immediate strategy for introducing chirality in these systems is through a chiral ligand for the Ni centre; indeed, every example in the following review introduces a different ligand for each transformation, and the best results stem from a careful choice of ligand.

The first attempt to obtain an asymmetric cross-coupling has been made by Molander and co-workers in 2014 in their seminal paper on the application of alkyltrifluoroborates as radical precursors.[27] A single example was reported where dtbbpy was replaced with the chiral bioxazoline ligand **BOX1** (**Scheme 16**). The 1,1-diarylethane product **4** was obtained in 52% yield and 75:25 e.r.

The mechanism of this reaction and the origin of the (if modest) enantioselectivity were studied computationally shortly after.[26] The two competing pathways reported in **Scheme 5** were found to be both operating: radical addition can occur both on the initial Ni(0) complex and on the Ni(II) complex after oxidative addition. The two pathways

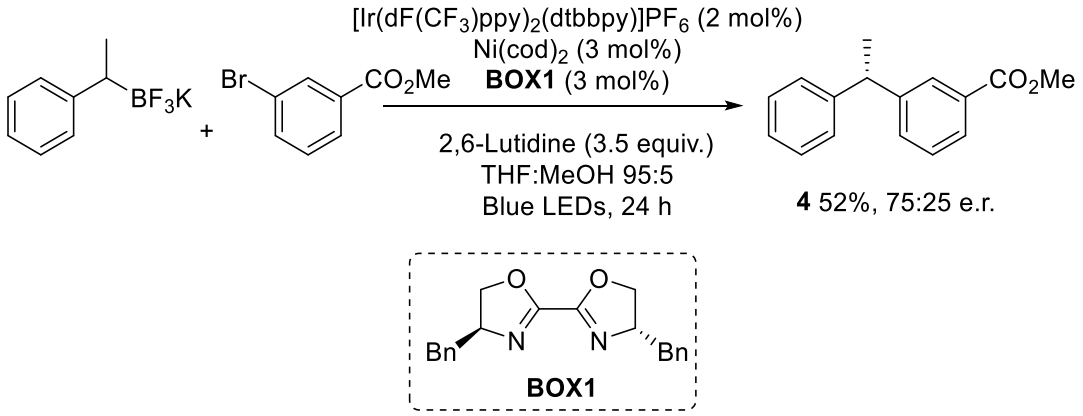

Scheme 16

Molander's first example of enantioselective Ni-photoredox cross-coupling with a racemic benzyltrifluoroborate.[27]

converge towards Ni(III) complex **5b** (**Scheme 17a**), but this can release the alkyl radical back forming again Ni(II) complex **5a** through C–Ni bond homolysis, in a situation of equilibrium. The subsequent reductive elimination has a higher barrier, and is the irreversible and enantiodetermining step. The system is thus under a Curtin-Hammett dynamic kinetic resolution model: there are two equilibrating diastereoisomeric Ni(III) complexes, of which one of the two provides reductive elimination faster than the other, leading to the major enantiomer of the product (**Scheme 17b**).

In 2016, the Fu and MacMillan groups published an enantioselective variant of the decarboxylative cross-coupling of protected amines.[57] In these conditions, a cyano-bis-oxazoline ligand (**L2**) was employed, affording good yields (46-84%) and very good enantioselectivities (up to 96:4 e.r.) for the resulting benzylic amine protected as carbamate (**Scheme 18**). While the starting material, derived from a natural amino acid, is enantiopure the chirality of the product does not depend on it: if the enantiomer of the ligand is used, the opposite enantiomer of the product is obtained. This is in line with the known phenomenon of racemisation of C(sp^3)-centred radicals.[58] The method allows the efficient preparation of different chiral benzylic amines, but suffers from limited scope: β-substitution or cyclic amines (for example from valine and proline) are not tolerated (< 10% yield) and only electron-poor aryl bromides are included. Iodobenzene as substrate provides coupling product in 64% yield but at a reduced 83:17 e.r.

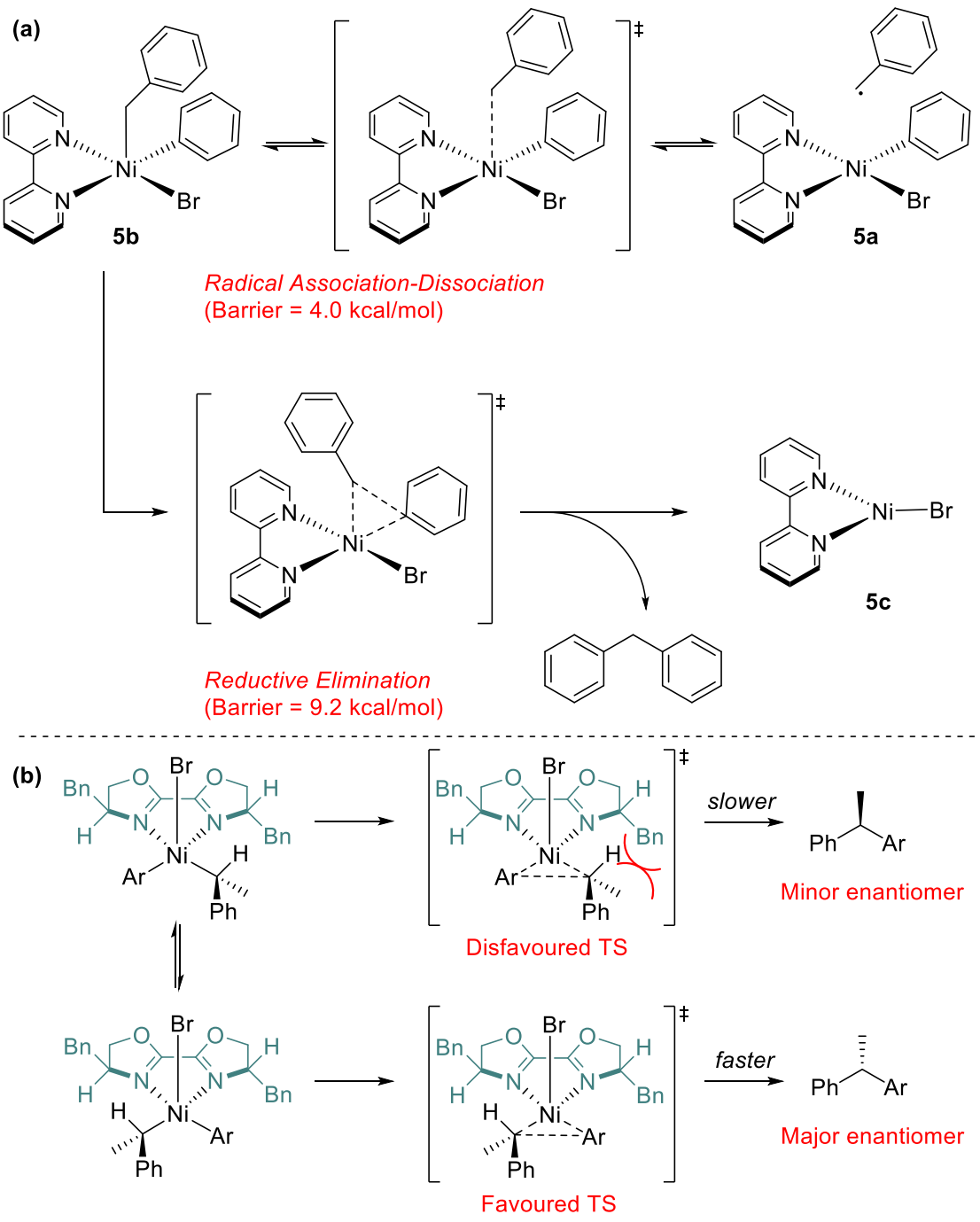

Scheme 17

Computed mechanism for the final C–C bond formation in the achiral Ni-photoredox cross-coupling of benzyltrifluoroborate and phenyl bromide **(a)**. Dynamic kinetic resolution in the case of chiral **BOX1** used as ligand **(b)**.[26]

The two subsequent reports both focus on desymmetrisation strategies. In 2017 Doyle and co-workers demonstrated the use of a bis-oxazoline ligand (**BOX4**) for the desymmetrisation of cyclic *meso*-anhydrides through a Ni-photoredox cross-coupling with benzyltrifluoroborate salts (**Scheme 19**).[59] In this cross-coupling, the anhydride takes the place of the aryl bromide and the oxidative addition of Ni(0) to the C–O bond is the enantiodetermining step. While yields are overall good, the enantioselectivity is

shown to highly depend on the structure of the starting anhydride, reaching as low as 68:32 e.r. if the substrates bears β-substitution.

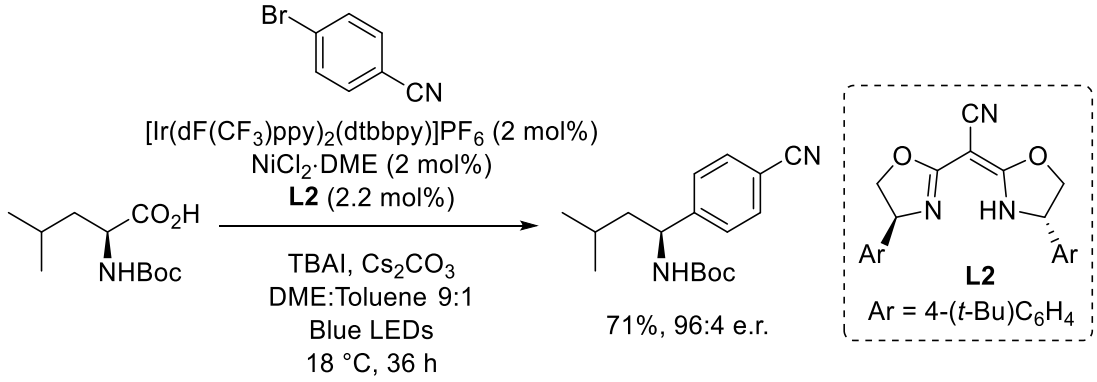

Scheme 18

Fu and MacMillan's enantioselective decarboxylative cross-coupling of protected amino acids with aryl bromides.[57]

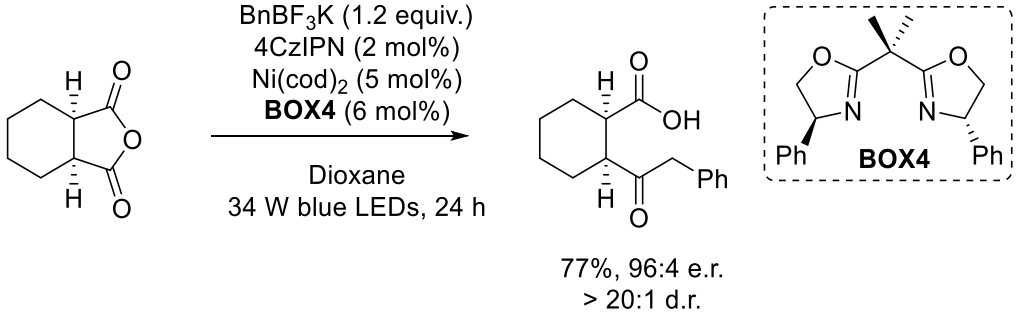

Scheme 19

Doyle's desymmetrisation of cyclic *meso*-anhydrides *via* acyl Ni-photoredox cross-coupling.[59]

In 2018 Xiao and co-workers described the desymmetrisation of specific aryl ethers through an intramolecular Ni-photoredox C–O bond-forming[I] cross-coupling reaction (**Scheme 20**).[60] Of note is the ligand used, different from the classical bis-oxazoline-type ligands: the authors reasoned that since bpy-type ligands are typically employed in the achiral reactions, a chiral bpy structure could afford products efficiently but in a stereoselective fashion. Indeed, using bipyridine **6** chiral 1,4-dioxanes, an interesting motif in the pharmaceutical setting, could efficiently be obtained with good enantiomeric ratios. Moreover, introduction of a methyl substitutent on the chiral centre allowed the formation of a quaternary stereocentre in 70:30 e.r.

[I] Despite this work not comprising C–C bond-forming cross-couplings, and the reaction thought to proceed through a different mechanism,[149] it is included as one more example of enantioselective Ni-photoredox cross-couplings.

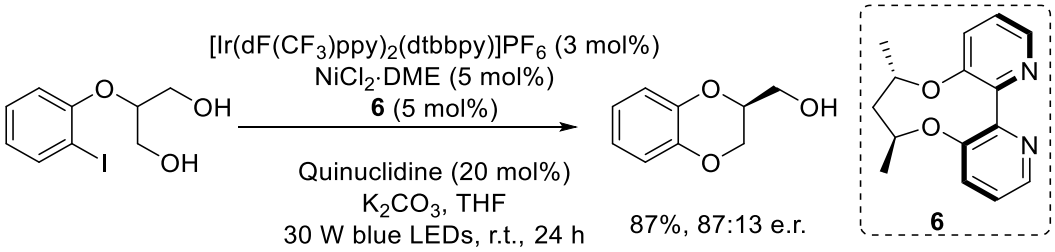

Scheme 20

Xiao's desymmetrisation of aryl ethers through a Ni-photoredox C–O bond-forming intramolecular cross-coupling.[60]

In 2019, during the publication process of the work described later in this chapter, two interesting reports appeared. First, the Lu group described the enantioselective C-H arylation of benzylic positions through a Ni-photoredox cross-coupling.[61] Besides the work from Fu and MacMillan,[57] the highest enantioselectivities in this type of cross-coupling were reported. This is due to the use of bi-imidazoline ligands, an alternative structural motif that proved more efficient than the classical bis-oxazolidine-based ligands. Steric hindrance and π-π interactions between the *N*-aryl groups on the ligand are thought to increase inflexibility, justifying the better performance. In the presence of **7** as ligand, chiral 1,1-diarylalkanes could be obtained in high yields and enantioselectivities almost always higher than 90:10 e.r. (**Scheme 21**); however, relatively high loadings of photocatalyst (2.2 mol%), Ni salt (20 mol%) and chiral ligand (20 mol%) are used, along with 5 equivalents of ethylbenzene. Similarly to the above mentioned Martin's procedure,[52] a diaryl ketone (DMBP) was introduced as co-catalyst, but the mechanism of HAT to generate the benzyl radical intermediate is not entirely clear.

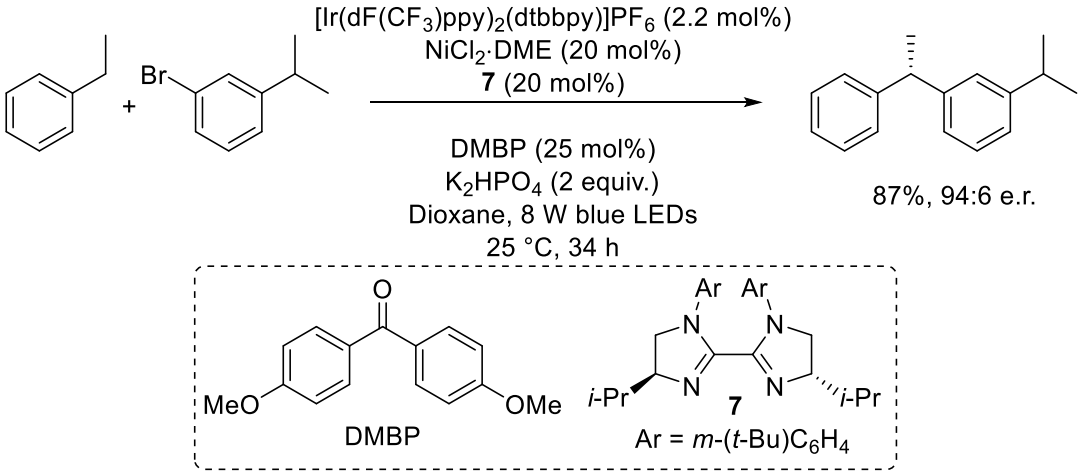

Scheme 21

Lu's enantioselective Ni-photoredox cross-coupling to 1,1-diarylalkanes.[61]

Shortly after, Melchiorre and co-workers reported an enantioselective Ni-catalysed acyl cross-coupling in the absence of an exogenous photocatalyst (**Scheme 22**).[62] The work is a direct extension of a cross-coupling obtained by exploiting the natural photoredox activity of dihydropyridine (DHP) radical precursors.[44] Upon visible light (405 nm) irradiation, DHPs can behave as strong reductants,[II] and are thus capable of promoting a typical Ni-photoredox catalytic cycle while also releasing the alkyl radical. 4-Alkyl DHP derivatives and symmetrical anhydrides were coupled using a catalytic system comprising a Ni salt in combination with **BOX4** as ligand: α-functionalised ketones were obtained in an efficient and enantioselective fashion. When α-indole DHPs were used, the system afforded modest to good yields (43-85%) and enantioselectivities (from 73:17 to 91:9 e.r.). When α-aryl DHPs were used, on average worse yields (39-83%) but better stereocontrol were obtained (94:6 to 98:2 e.r.).

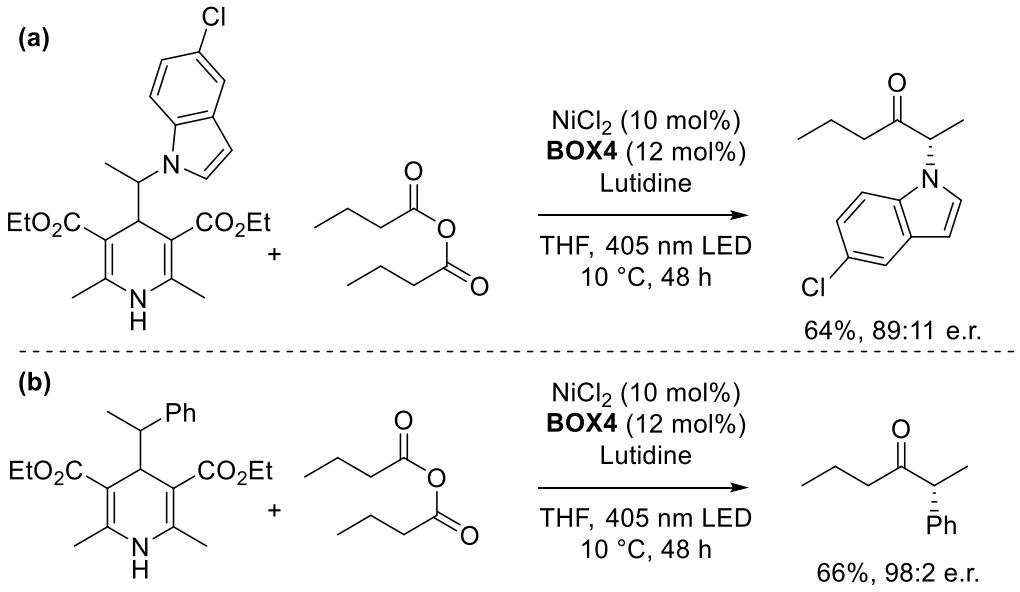

Scheme 22

Melchiorre's photochemical asymmetric Ni-catalysed cross-coupling of alkyl DHPs and symmetrical anhydrides: substartes with α-indole **(a)** and α-aryl **(b)** substituents.[62]

Over the past 5 years, other works on Ni-photoredox cross-couplings have reported single examples of the transformation applying commercial chiral ligands. In **Scheme 23** the examples from the works of Molander **(a)**,[31] Doyle **(b)**[48] and Martin **(c)**[52] groups are reported.

[II] For more examples of the photoredox activity of organic intermediates, see **Section 4.2**.

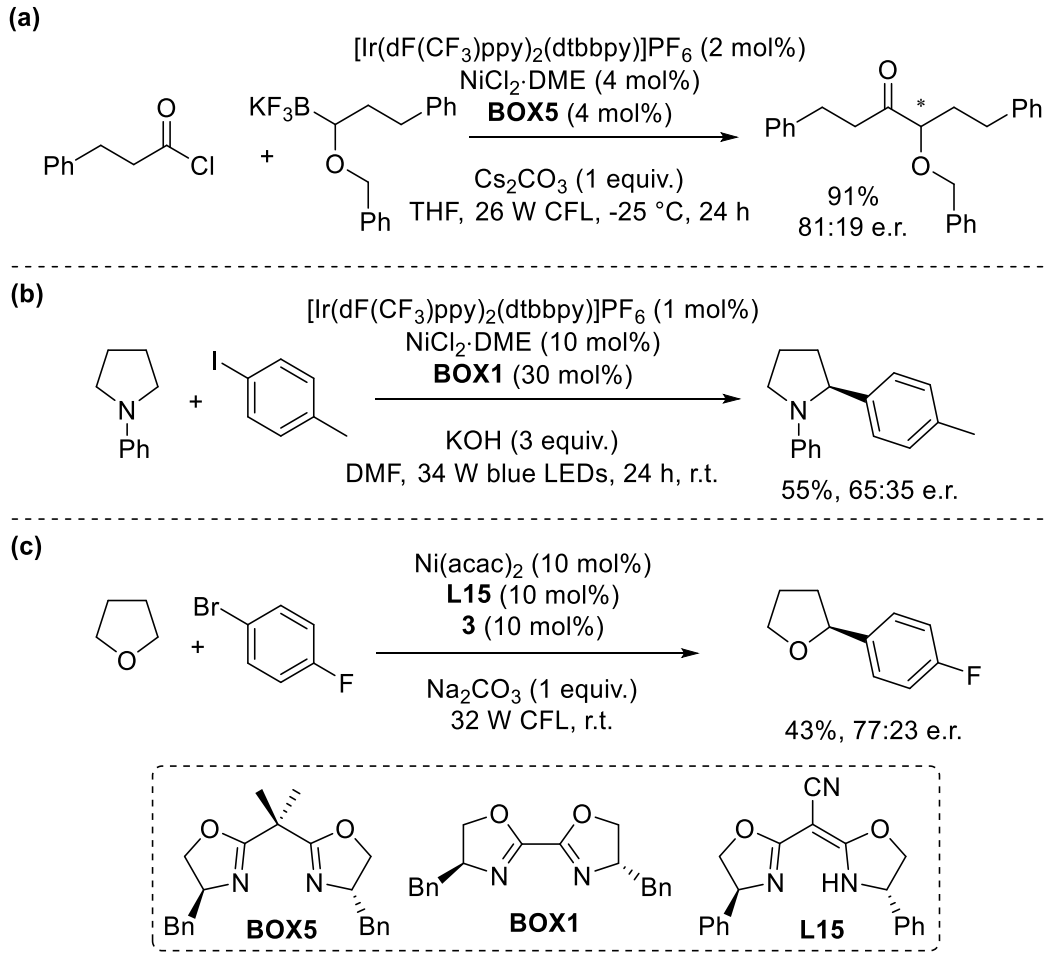

Scheme 23

Single examples of enantioselective Ni-photoredox cross-couplings from various groups: Molander **(a)**,[31] Doyle **(b)**[48] and Martin **(c)**.[52]

2.3 Aim of the project

The range of substrates and the performing ligand classes in enantioselective Ni-photoredox catalysis are still limited, and there is surely ample space for new discoveries. Mild conditions and sometimes low catalyst loadings are attractive features for a methodology to construct C–C bonds enantioselectively, making this field particularly interesting in a pharmaceutical setting. In this chapter, particular attention will be given to the preparation of enantioenriched *N*-benzylic heterocycles.

2.3.1 *N*-Benzylic heterocycles in the pharmaceutical industry

N-Benzylic heterocycles constitute an important class of heterocyclic compounds in the pharmaceutical industry with numerous examples of commercial drugs and bioactive molecules containing this motif. In a 2011 review on the 50 best selling drugs containing 5-membered heterocycles, eight of them were found to contain an *N*-benzylic

heterocyclic unit.[63] A subset of these molecules contain chirality at the α-position of the benzylic moiety (**Figure 2**), with important effects on their pharmacological properties. For example, the anesthetic drug etomidate contains an imidazole ring with a chiral *N*-benzylic substituent.[64] The anesthetic potency is one order of magnitude higher for the (*R*) enantiomer compared with the (*S*) enantiomer: for example the HD_{50} (hypnotic dose successful for 50% of the population) for induced hypnosis in mice upon intravenous injection is 6.0 μmol kg^{-1} for the (*R*) enantiomer and 61.3 μmol kg^{-1} for the (*S*) enantiomer.[65] Similar structural features are also found in the etomidate analogue carboetomidate,[66] in the exploratory drug MK-0893[67] and in the hormonal disorders drug osilodrostat.[68]

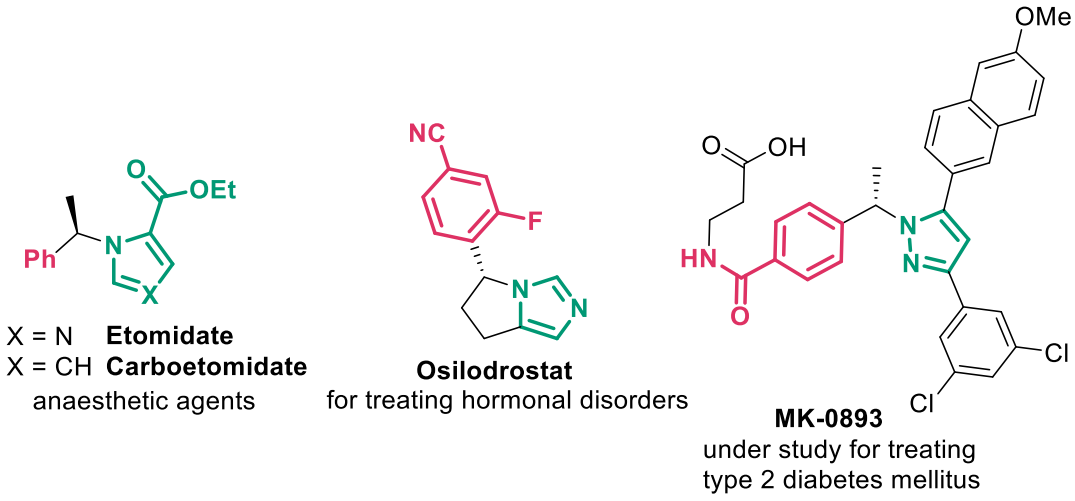

Figure 2
Examples of pharmaceutically-relevant compounds bearing a chiral *N*-benzylic heterocycle motif.

There are two typical routes towards their preparation: (i) synthesis of the heterocycle from a chiral benzylic amine (or analogue);[67,69–72] (ii) base-mediated nucleophilic substitution of a suitable chiral precursor with the nitrogen heterocycle.[73–75] While these methods can be effective, the lack of modularity hampers quick access to different structures, necessitating the preparation of an enantiopure precursor for every desired entry. Moreover, substitution using heterocycles with multiple nitrogen atoms can lead to the formation of isomers, resulting in low yields and difficulty of separation while consuming such precious chiral precursors. Indeed, orthogonal functionalisation of multiple heteroatoms has been highlighted as one of the challenges for organic synthesis in drug discovery.[76] A modular approach, allowing the use of prochiral and easily obtainable substrates, is thus desirable.

2.3.2 Aim and strategy

The recent advances in the field of Ni-photoredox dual catalysis inspired the modular approach developed for the preparation of chiral *N*-benzylic heterocycles. This method exploits a disconnection between the aryl group and the α-carbon, where the former can derive from an aryl (pseudo)halide, in the typical cross-coupling fashion, while the latter from a suitable radical precursor (**Scheme 24**). The introduction of a chiral ligand for the Ni catalyst enables control of the stereochemistry of the newly formed stereocentre. This route allows bypassing the preparation of enantiopure precursors, using instead simple, achiral or racemic starting materials. Before our work, only the Rueping group reported a single example of decarboxylative cross-coupling of an indole derivative with an aryl triflate,[77] while analogous non-photoredox disconnections had also been described.[78–80]

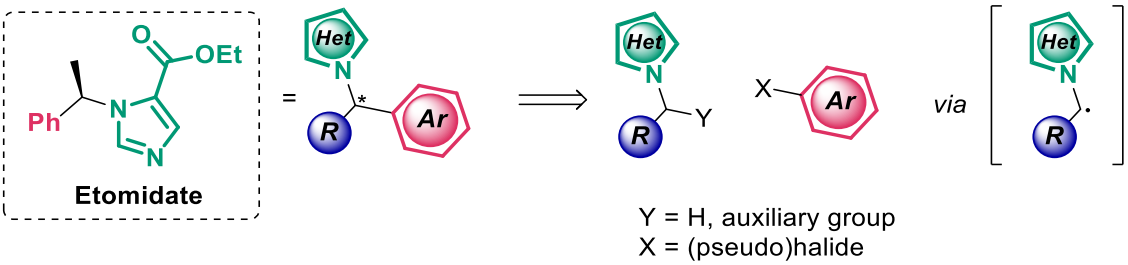

Scheme 24

Ni-photoredox approach towards the synthesis of *N*-benzylic heterocycles.

The success or failure of this methodology certainly depends on the choice of radical precursor for the generation of the desired α-heterocyclic alkyl radical. Based on the literature review presented in the previous sections, two alternatives were found:

i. Hydrogen atom transfer (HAT) based cross-coupling, starting from a simple *N*-alkyl heterocycle (**Scheme 25a**). The HAT step can take place with the help of an H atom abstractor such as a quinuclidinium ion or a ketyl radical.

ii. Oxidation-initiated cross-coupling, where the radical precursor contains an auxiliary group prone to photocatalytic oxidation; the resulting oxidised species fragments in a second moment to deliver the alkyl radical (**Scheme 25b**).

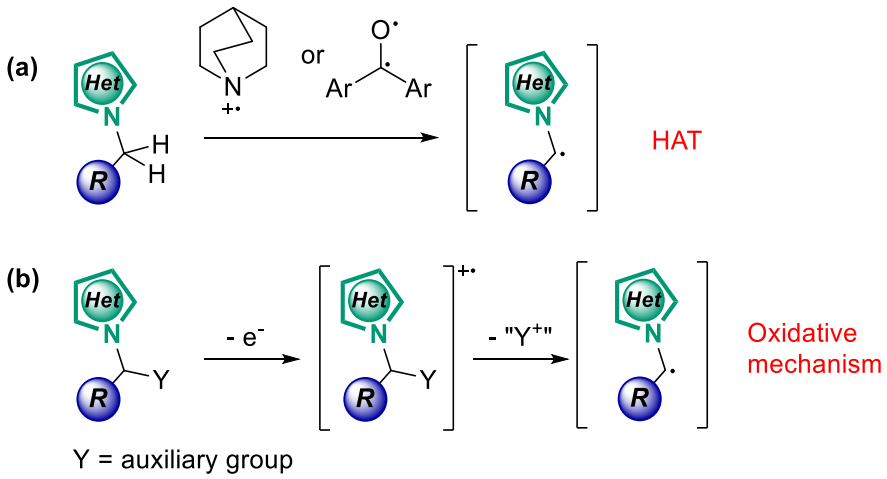

Scheme 25

Alternative methods for generation of the α-heterocyclic radical: **(a)** HAT mechanism; **(b)** oxidative mechanism.

Of the two alternatives, the HAT process seems immediately more convenient, since simpler starting materials can be used with very good atom economy; for this reason, initial efforts were directed towards this type of cross-coupling. However, better and more reliable reactivity was found with the second choice, employing a convenient auxiliary group on the alkyl moiety. The next sections will present attempts towards obtaining both types of reactivity, and the final development of a decarboxylative asymmetric cross coupling reaction towards *N*-benzylic heterocycles.

2.4 Preliminary results

2.4.1 Exploration of an HAT-based strategy

Investigations began by selecting *N*-ethylimidazole as model substrate, *in lieu* of the more complex imidazoles found in the pharmaceutical setting. Coupling conditions were inspired by the work of MacMillan and co-workers on the HAT coupling of carbamate-protected amines and amides with aryl bromides.[49] In these conditions, a catalytic system composed of $NiBr_2$ and a phenanthroline ligand was used alongside $[Ir(dF(CF_3)ppy)_2(dtbbpy)]PF_6$ as photocatalyst, in the presence of aceclidine as base and HAT reagent, to attempt the cross-coupling with 4-bromobenzonitrile. However, no product was detected, and only conversion of the aryl bromide to the corresponding phenol **8** was observed (**Scheme 26**). Variations in solvent, base, Ni precursor and Ni loading did not provide any product but only variable conversions to **8**. The exclusion of water from the reaction mixture simply provided no conversion of the aryl bromide.

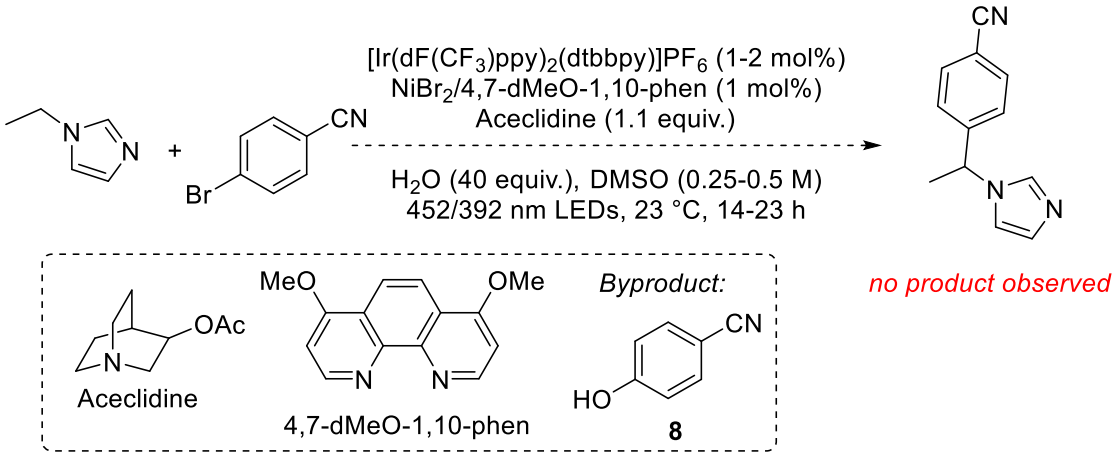

Scheme 26

Attempted HAT-based Ni-photoredox cross-coupling on *N*-ethylimidazole.

Control experiments were then performed. Tetramethylurea (TMU) is a known substrate for this reaction, and provided 58% NMR yield of coupled product with the conditions outlined above. However, when *N*-ethylimidazole was added to the reaction mixture at different times, the reaction stopped, affording limited yields of product (**Scheme 27**).

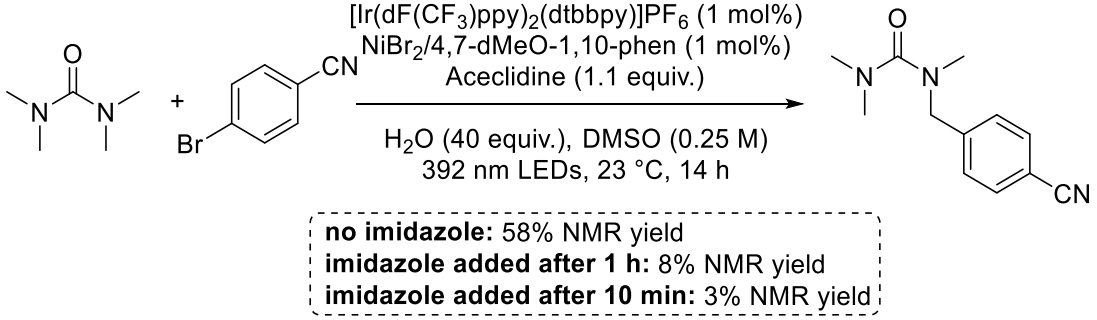

Scheme 27

Control and inhibition experiments with TMU as known substrate.

Based on these results, a poisoning effect of the imidazole ring on the Ni catalyst, in particular through the coordinating nitrogen on the ring, was hypothesised. *N*-Methylpyrrole was next used as model substrate: lacking the coordinating nitrogen atom, it should be more tolerated by the Ni system. The first attempt with the conditions outlined above revealed some reactivity, and traces amounts of the required product **9a** were found (**Scheme 28**); however, the majority of the aryl bromide was converted to **8**, and trace amounts of C2-arylation (product **9b**) were also observed. A screening of conditions including solvent, photocatalyst, HAT reagent, ligands, Ni precursor and temperature did not afford any improvement. Since the efforts on the HAT approach were not repaid with a good reactivity, the attention was then turned to the simpler auxiliary-directed oxidative approach.

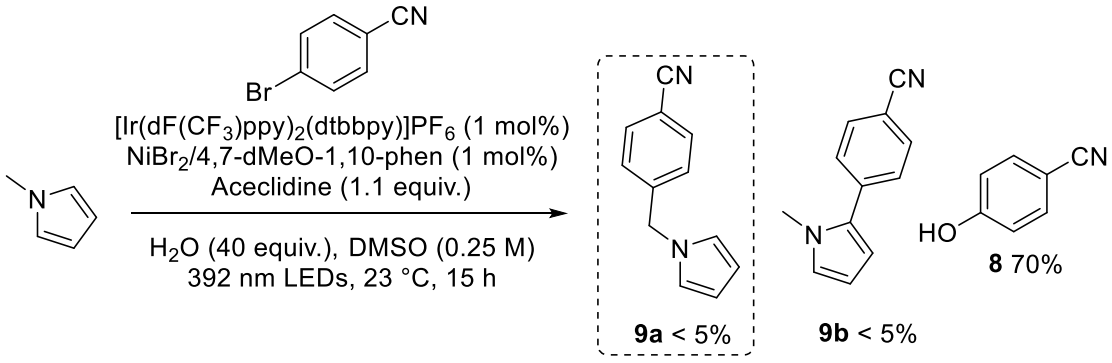

Scheme 28

Results for the HAT cross-coupling with *N*-methylpyrrole as substrate.

2.4.2 Exploration of an oxidative mechanism-based strategy

As no reaction was observed with the imidazole substrate, further investigations were conducted with pyrrole as heterocyclic core. The key feature of the oxidative approach is the presence of an auxiliary group prone to oxidation in the photoredox cycle which, upon fragmentation, delivers the desired alkyl radical: benefits of this strategy are an easier radical formation and control over its position. Among the auxiliary groups mentioned in **Section 2.1.1**, three were selected for efficacy and ease of synthesis. The corresponding silane **10a**, trifluoroborate **10b** and carboxylic acid **10c** were thus subjected to standard coupling conditions (**Scheme 29**).[34] Silane **10a** did not provide a good reactivity, even when conditions were slightly modified; however, both **10b** and **10c** afforded NMR yields higher than 85%, confirming the versatility of these classes of compounds within different substrate structures.

Of the two derivatives, the higher yield and easier substrate preparation directed the choice to the carboxylic acid auxiliary. A wide variety of α-amino acids and α-bromo acids are commercially available, allowing the potential preparation of a good range of α-heterocyclic derivatives *via* the already mentioned strategies: construction of the heterocycle from the amine or nucleophilic substitution on the halide.

For proof of concept, the same conditions used in **Scheme 29** were applied to carboxylic acids bearing other heterocycles (**Scheme 30**). While imidazole **9c** was obtained in traces amounts (verified by LCMS analysis of the crude mixture),[III] benzimidazole **9d** and

[III] Efforts to obtain higher yields of **9c** by changing conditions (solvent, Ni precursors, photocatalyst) or by addition of Lewis acids to coordinate the ring nitrogen in place of Ni were met with failure, and no more than traces (< 5% by NMR) of product were obtained.

pyrazole **9e** were obtained with promising 40% and 23% NMR yields, suggesting the applicability of such decarboxylative strategy to different heterocyclic moieties.

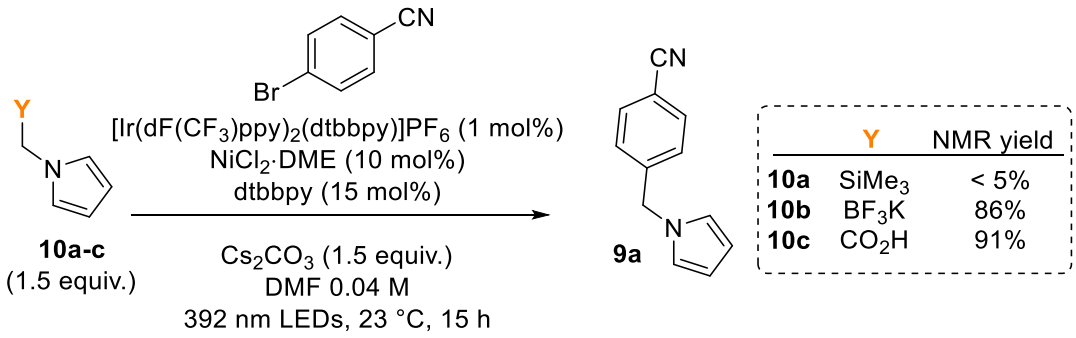

Scheme 29
Initial coupling results with different auxiliary groups.

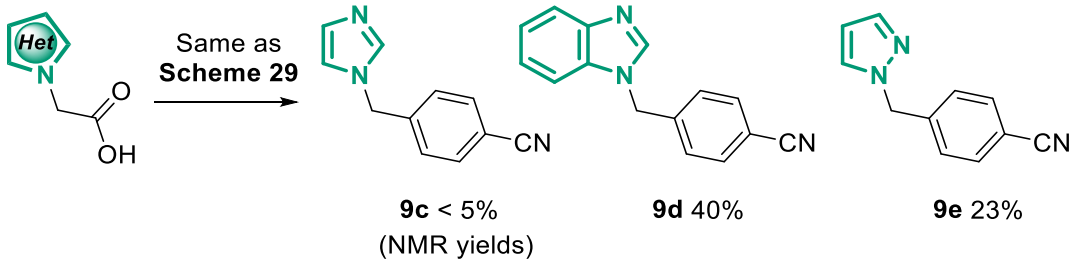

Scheme 30
Initial results for the decarboxylative coupling using substrates with different heterocycles.

2.5 Asymmetric cross-coupling: screening and optimisation

2.5.1 First ligand screening

The conditions for the achiral decarboxylative cross-coupling found during the preliminary tests (**Scheme 29**) were then extended to a catalytic system with a chiral ligand, in the attempt to obtain an enantioselective transformation. The reaction with pyrrole substrate **11a** derived from L-alanine and 4-bromobenzonitrile was examined as benchmark transformation (**Table 1**). The initial conditions involved the use of $NiCl_2$·DME complex as Ni source, 4CzIPN as photocatalyst,[IV] Cs_2CO_3 as base in DMF with blue light (452 nm) irradiation. Ligands are depicted in **Figure 3**. While the reaction using bpy as achiral ligand (entry 1) works well (86% yield), the majority of the ligands examined behaved poorly in this reaction. A range of chiral *N*,*N*-, *N*,*P*- and *P*,*P*-bidentate

[IV] Very low yields are obtained when the more typical $[Ir(dF(CF_3)ppy)_2(dtbbpy)]PF_6$ is used as photocatalyst in the presence of these chiral ligands.

ligands, obtained from DRL's ligand collection, failed to deliver measurable amounts of product **12a** (entries 4-7, 10-20). Interestingly, only a subset comprising a pyridine-oxazoline (PyOx) ligand (entry 2, **L1**), a cyano-bisoxazoline (CN-Box) ligand (entry 3, **L2**) and similar pyrrole-oxazoline and sulfonamide-oxazoline ligands (entries 8-9) provided **12a** in modest yields and enantioselectivity. Note that **L1** and **L2** provide product with opposite stereoselectivity.[V]

Table 1

Screening of ligands (first phase).[a]

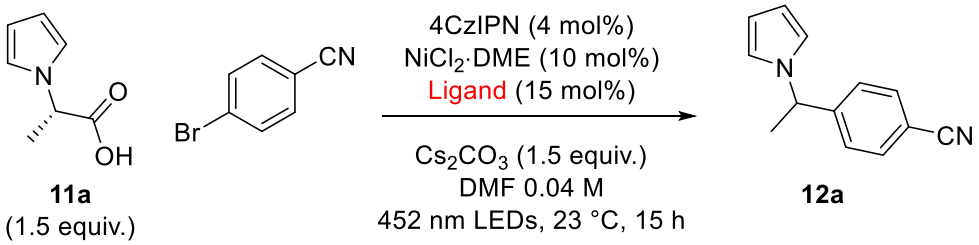

Entry	Ligand	Yield %[b]	e.r.[c]	Conversion %[d]
1	bpy	86	-	-
2	**L1**	42	69:31	95
3	**L2**	27	27:73	67
4	BOX1	traces	-	28
5	BOX2	traces	-	17
6	BOX3	traces	-	35
7	PyBOX	traces	-	13
8	PyrrOX	56	36:64	77
9	SulfOX	22	69:31	100
10	TROST1	5	51:49	30
11	TROST2	traces	-	26
12	TROST3	traces	-	30
13	PN1	traces	-	24
14	PN2	traces	-	26
15	PN3	0	-	14
16	PP1	0	-	16
17	PP2	traces	-	42
18	PP3	0	-	28
19	PP4	traces	-	33
20	PP5	traces	-	33

[a] In all examples, Cs_2CO_3 is added with Ni salt and ligand to make the Ni solution. [b] Yields determined by chiral SFC analysis of reaction mixtures, using calibration with a pure standard. [c] Enantiomeric ratio (e.r.) determined by chiral SFC analysis of reaction mixtures. Reported as the ratio first enantiomer : second enantiomer in order of elution (same SFC method used in all cases). [d] Calculated as 100 - % remaining 4-bromobenzonitrile in the reaction mixture, as analysed by chiral SFC analysis, using calibration with a pure standard.

[V] Later analyses (**Section 6.6** compound **12z**) revealed that PyOx ligands provide the major enantiomer with *S* configuration.

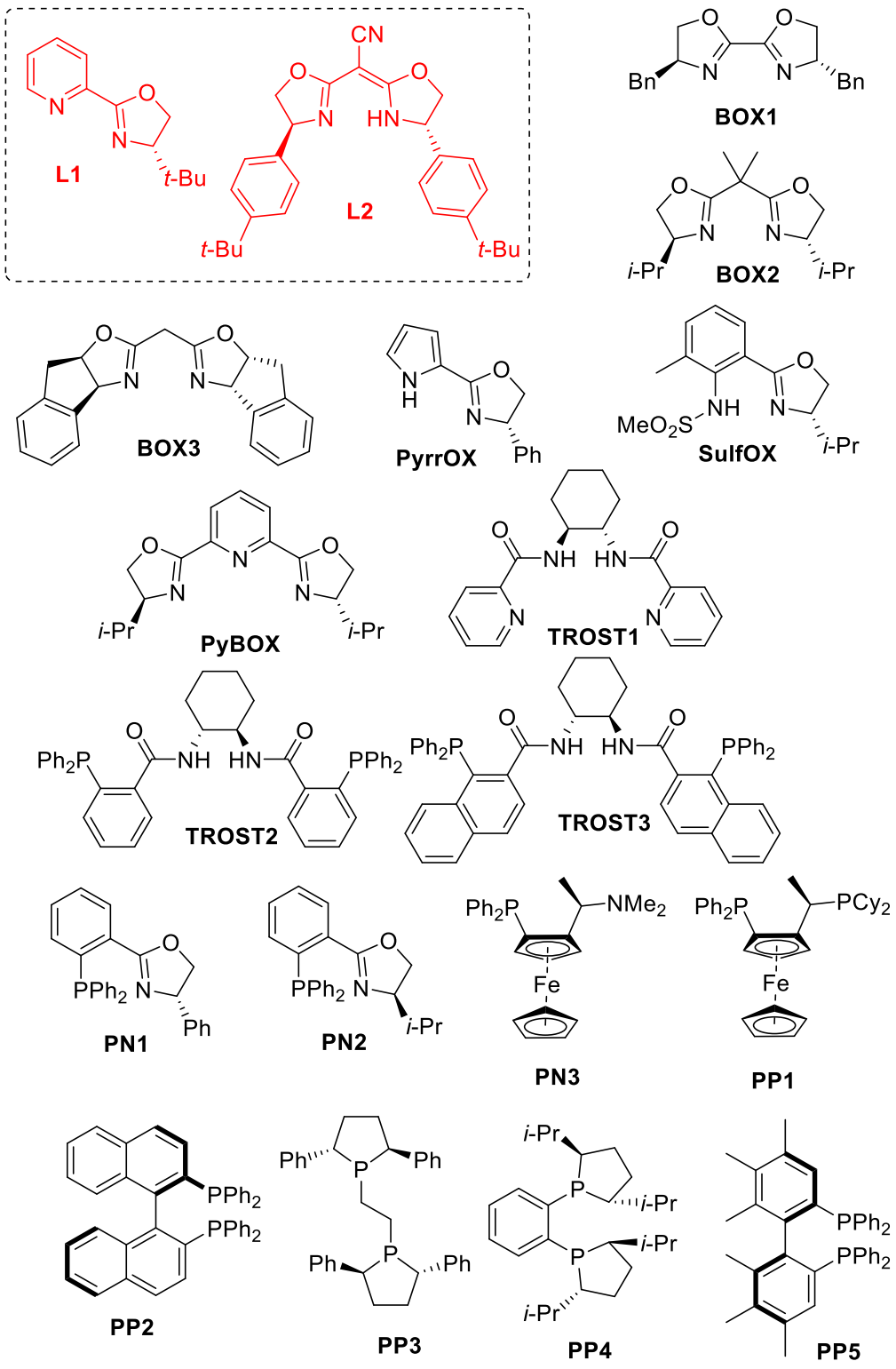

Figure 3
Ligands examined during the first screening.

2.5.2 Optimisation: part 1

Based on the results reported above PyOx ligand **L1** and CN-Box ligand **L2** were chosen for further evaluation. An initial round of optimisation was carried out in order to find the best set of conditions when using each ligand. The Ni source was the first parameter examined. Practically, reaction mixtures were set up by preparing a solution of the Ni salt and ligand in the presence of Cs_2CO_3, to which all other substrates were subsequently added. In this phase of optimisation, the influence of the presence or absence of Cs_2CO_3 in this initial mixture was also assessed. The results, reported in **Table 2**, suggest $NiBr_2$·DME (entry 5) and $Ni(ClO_4)_2$·$6H_2O$ (entry 8) to be the best Ni sources when **L1** is used, while $NiCl_2$·DME (entry 13) is the best when **L2** is employed. In the case of the former, $NiBr_2$·DME was chosen for subsequent studies because it is less hygroscopic and easier to weigh and use. For both ligands, excluding Cs_2CO_3 from the initial Ni-ligand mixture afforded better results (compare for example entries 4 and 5, and entries 12 and 13).

Table 2

Screening of Ni sources, **L1** and **L2** as ligands.[a]

Entry	Ligand	Change from conditions	Yield %	e.r.	Conversion %
1	**L1**	none ($NiCl_2$ DME)	42	69:31	95
2		none ($NiCl_2$ DME)[b]	50	69:31	91
3		$NiCl_2$[b]	52	69:31	87
4		$NiBr_2$ DME	48	69:31	85
5		$NiBr_2$ DME[b]	58	69:31	96
6		$NiBr_2$	38	69:31	72
7		$Ni(acac)_2$	50	52:48	19
8		$Ni(ClO_4)_2$ $6H_2O$[b]	59	69:31	95
9		$Ni(BF_4)_2$ $6H_2O$[b]	52	69:31	93
10		$Ni(NO_3)_2$ $6H_2O$[b]	52	69:31	92
11		Ni(*o*-tol)(TMEDA)Cl in Acetone[c]	28	71:29	52
12	**L2**	none ($NiCl_2$ DME)	27	27:73	67
13		none ($NiCl_2$ DME)[b]	40	28:72	68
14		$NiBr_2$ DME[b]	29	27:73	68
15		$Ni(acac)_2$[b]	8	31:68	20
16		$Ni(ClO_4)_2$ $6H_2O$[b]	36	27:73	56
17		$Ni(BF_4)_2$ $6H_2O$[b]	14	26:74	69
18		Ni(*o*-tol)(TMEDA)Cl in DME[c]	traces	-	8

[a] Substrates, conditions and notes as in **Table 1**. [b] Reaction run by excluding Cs_2CO_3 from the Ni solution, and adding it at the very end of the reaction setup. [c] See **Table 3**.

Solvents were subsequently examined (**Table 3**). A range of polar and, to a lesser extent, apolar solvents were tested with both ligands using the best Ni sources, as just found. In

the case of **L1**, a lot of solvents provide some product but acetone stands out (entry 8), affording 75% yield with a slight improvement in e.r. (from 69:31 in DMF to 73:27). In the case of **L2**, more solvents fail to deliver even modest yields of **12a**, and DME (entry 20) afforded the best 56% yield and 22:78 e.r. (improved from 28:72 in DMF).

Table 3

Screening of solvents, **L1** and **L2** as ligands.[a]

Entry	Ligand	Change from conditions	Yield %	e.r.	Conversion %
1	**L1**	none (DMF)	58	69:31	96
2		Acetonitrile	62	73:27	93
3		DMA	56	69:31	n.d.
4		EtOAc	43	70:30	92
5		DMSO	24	58:42	68
6		CH_2Cl_2	21	67:33	38
7		DME	52	66:34	94
8		Acetone	75	73:27	100
9		$CHCl_3$	0	-	0
10		THF	48	67:33	90
11		Propylene carbonate	58	65:35	90
12		Benzonitrile	14	67:33	37
13		Toluene	12	67:33	44
14	**L2**	none (DMF)	40	28:72	68
15		Acetonitrile	37	52:48	64
16		DMA	43	27:73	61
17		EtOAc	6	26:74	31
18		DMSO	9	26:74	18
19		CH_2Cl_2	0	-	0
20		DME	56	22:78	75
21		Acetone	41	25:75	75
22		$CHCl_3$	0	-	0
23		THF	25	25:75	52
24		Propylene carbonate	6	24:76	18
25		Benzonitrile	23	54:46	45
26		Toluene	0	-	1
27		DME:Toluene 1:9[b]	5	33:67	28
28		DME:Toluene 1:9[bc]	traces	-	< 5

[a] Substrates, conditions and notes as from **Table 2**. For **L1** and **L2**, $NiBr_2$ DME and $NiCl_2$ DME are chosen as Ni sources, respectively. Reactions are run by excluding Cs_2CO_3 from the Ni solution, and adding it at the very end of the reaction setup. [b] Concentration 0.01 M. As to mimic conditions found in ref.[57] for the enantioselective cross-coupling of carbamate-protected aminoacids with aryl bromides. [c] Run with $[Ir(dF(CF_3)_2ppy)_2(dtbbpy)]PF_6$ (1 mol%) as photocatalyst and violet light irradiation (400 nm).

Using the conditions found previously (**Table 2**, entries 8 and 20), the next parameter to be evaluated was the type of base (**Table 4**). With **L1** as ligand, some organic bases showed reactivity similar to Cs_2CO_3: DBU (entry 3) and MeTBN (entry 6) in particular. TMG afforded an improved 92% yield, but at the price of some erosion in stereocontrol

(from 73:27 to 69:31). The reaction with **L2** showed small improvements in e.r. with TBAOH·30H_2O (entry 21, but this might be due to water, see **Table 5**) and K_2CO_3 (entry 25, slightly better both in yield and e.r.). Overall, no great improvements from Cs_2CO_3 were observed.

Table 4

Screening of bases, **L1** and **L2** as ligands.[a]

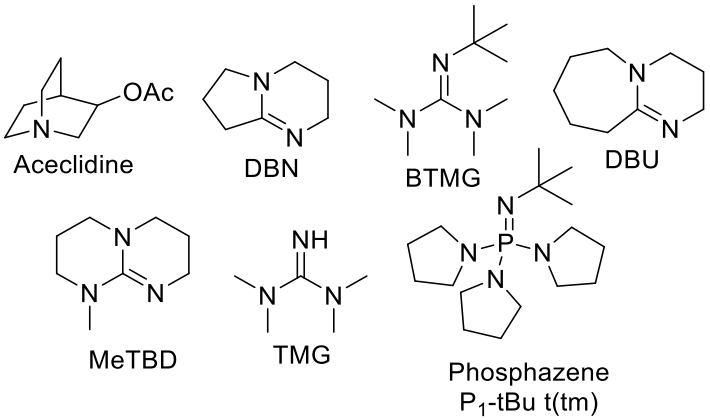

Entry	Ligand	Change from conditions	Yield %	e.r.	Conversion %
1	**L1**	none (Cs_2CO_3)	75	73:27	100
2		Aceclidine	23	70:30	83
3		DBU	78	73:27	100
4		DBU (3 equiv.)	traces	-	< 5
5		DBN	13	64:36	29
6		MeTBD	75	71:29	100
7		BTMG	79	67:33	97
8		TMG	92	69:31	100
9		Phosphaz P1-tBu t(tm)	70	66:34	100
10		TBAOH 30 H_2O	9	62:38	19
11		2,4,6-Collidine	traces	-	34
12		2,6-Lutidine	0	-	18
13	**L2**	none (Cs_2CO_3)	56	22:78	75
14		Aceclidine	26	25:75	97
15		DBU	19	18:82	70
16		DBN	traces	-	23
17		MeTBD	14	20:80	20
18		BTMG	11	20:80	23
19		TMG	12	15:85	23
20		Phosphaz P1-tBu t(tm)	16	20:80	38
21		TBAOH 30 H_2O	38	17:83	99
22		2,4,6-Collidine	1	-	17
23		2,6-Lutidine	0	-	21
24		$KOBu^t$	0	-	n.d.
25		K_2CO_3	64	21:79	n.d.

[a] Substrates, conditions and notes as from **Table 3**. For **L1** and **L2**, $NiBr_2$ DME / Acetone and $NiCl_2$ DME / DME are chosen as combination of Ni source / solvent, respectively.

As last parameter, the influence of some protic co-solvents (added in 20 equiv.) was examined (**Table 5**). While they seem to have an overall detrimental effect when **L1** is used as ligand (entries 1-5), some improvements in enantioselectivity are observed when **L2** is used instead. Going from MeOH (entry 8, 18:82 e.r.) towards more acidic alcohols such as TFE (entry 11, 15:85 e.r.) and HFIP (entry 12, 10:90 e.r.) a gradual increase in enantioselectivity is observed, accompanied by a similar decrease in reactivity (from 58% yield to 38% to 15%). Phenol, instead, completely shuts down the reaction (entry 13). Different attempts have been made using HFIP as co-solvent to obtain an improved yield; the reaction was revealed to be poorly reproducible, and no yield higher than the one here reported was ever obtained. For these reasons, after some effort this possible route for improvement was abandoned.

Table 5

Screening of protic co-solvents, **L1** and **L2** as ligands.[a]

Entry	Ligand	Added co-solvent	Yield %	e.r.	Conversion %
1	**L1**	none	75	73:27	100
2		H_2O (20 equiv.)	60	69:31	>95
3		MeOH (20 equiv.)	76	71:29	100
4		TFE (20 equiv.)	60	67:33	92
5		HFIP (20 equiv.)	24	67:33	52
6	**L2**	none	56	22:78	75
7		H_2O (20 equiv.)	48	20:80	>95
8		MeOH (20 equiv.)	58	18:82	82
9		iPrOH (20 equiv.)	27	14:86	41
10		tBuOH (20 equiv.)	27	14:86	40
11		TFE (20 equiv.)	38	15:85	82
12		HFIP (20 equiv.)	15	10:90	29
13		PhOH (20 equiv.)	0	-	88

[a] Substrates, conditions and notes as from **Table 3**. For **L1** and **L2**, $NiBr_2$ DME / Acetone and $NiCl_2$ DME / DME are chosen as combination of Ni source / solvent, respectively. Reactions are run by excluding Cs_2CO_3 from the Ni solution, and adding it at the very end of the reaction setup. TFE = 2,2,2-trifluoroethanol; HFIP = 1,1,1,3,3,3-hexafluoroisopropanol.

2.5.3 Second ligand screening

Having found the best conditions for reactions with **L1** (**Table 2**, entry 8) and **L2** (**Table 2**, entry 20), a range of structural modifications of PyOx and CN-Box ligands was examined,[VI] applying the specific conditions for each class of ligands (**Table 6**, ligands depicted in **Figure 4**). Concerning PyOx ligands, remarkable improvements (90% yield,

[VI] Preparations of all these ligands, unless commercially available, are detailed in the **Experimental Section**.

77:23 e.r.) were obtained using **L3** (entry 2), bearing a 3-Me substituent on the pyridine ring. If the methyl group is moved to position 4 (**L4**), the same results as when using **L1** are obtained, while substitution in position 6 (**L5**, and similarly **L9**) is deleterious. The presence of electron-withdrawing groups on the pyridine ring (**L6**, **L8**) also does not afford active catalytic systems. Other substitutions in position 3 (an hydroxy group in **L7** or a fused ring in **L10**) do not provide the same improvements as the 3-Me substitution. Replacing the *tert*-butyl group at the chiral centre with phenyl groups (**L11**-**L14**, in different variations) seems to provide some improvements in yields compared to **L1**, but usually with inferior enantiomeric ratios. On the other hand, among CN-Box ligands **L2** is confirmed as the best choice, since only **L15**, without *tert*-butyl groups on the aromatic rings, affords similar but slightly inferior results. Introducing rigidity (**L16**) or other groups in the chiral sections (**L17**, **L18**) seems to shut down reactivity.

Table 6

Screening of ligands (second phase).[a]

Entry	Ligand	Yield %[b]	e.r.[c]	Conversion %[d]
1	**L1**	75	73:27	100
2	**L3**	90	77:23	100
3	**L4**	74	72:28	100
4	**L5**	9	51:49	51
5	**L6**	15	50:50	44
6	**L7**	70	41:59	98
7	**L8**	16	55:45	45
8	**L9**	9	52:48	52
9	**L10**	39	47:53	96
10	**L11**	93	70:30	100
11	**L12**	82	68:32	100
12	**L13**	95	50:50	100
13	**L14**	89	53:47	100
14	**L2**	56	22:78	75
15	**L15**	49	25:75	79
16	**L16**	< 5	20:80	12
17	**L17**	traces	-	14
18	**L18**	20	32:69	62

[a] Substrates and notes as in **Table 1**. Conditions used with PyOx ligands (green): $NiBr_2$ DME (10 mol%), ligand (15 mol%), Cs_2CO_3 (1.5 equiv.), acetone 0.04 M. Conditions used with CN-Box ligands (blue): $NiCl_2$ DME (10 mol%), ligand (15 mol%), Cs_2CO_3 (1.5 equiv.), DME 0.04 M.

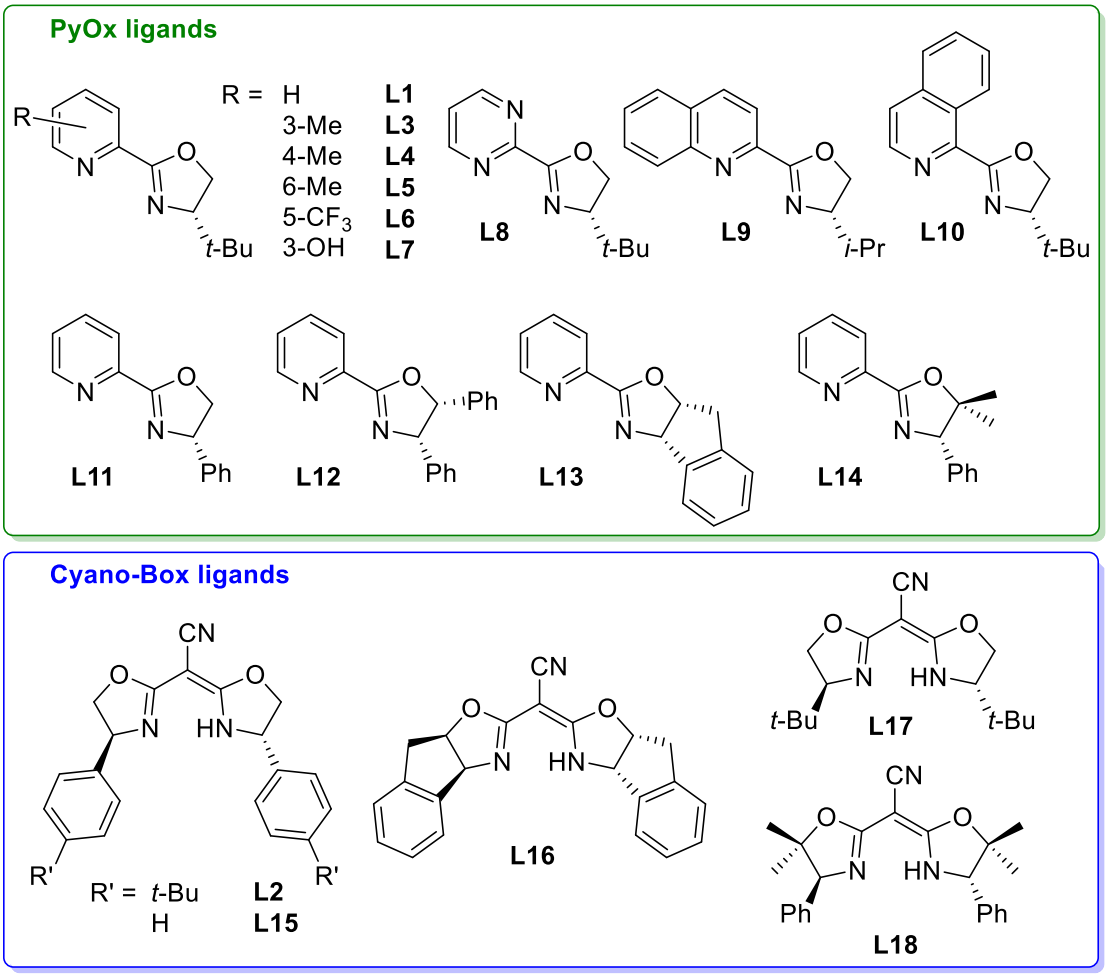

Figure 4

Ligands examined during the second screening.

After this second ligand screening, it became clear that PyOx ligands (**L3** in particular) provide higher reactivity (90% yield), while CN-Box ligands (**L2** in particular) afford less active catalytic systems (56% yield) but with slightly higher enantiocontrol (22:78 *vs* 73:27 e.r.). To better appreciate the differences in reactivity, reaction profiles were recorded for the reactions employing **L1**, **L2** and **L3** as ligands (**Figure 5**). This comparison shows how with **L3** full conversion of the aryl bromide to **12a** is obtained in the first 4 hours, while with both **L1** and **L2** overnight reactions are necessary to obtain good yields. Concerning e.r. there is little variation over the course of the reaction, and even at full conversion it is maintained constant for all ligands, suggesting that racemisation processes of the product are not taking place in this timeframe.

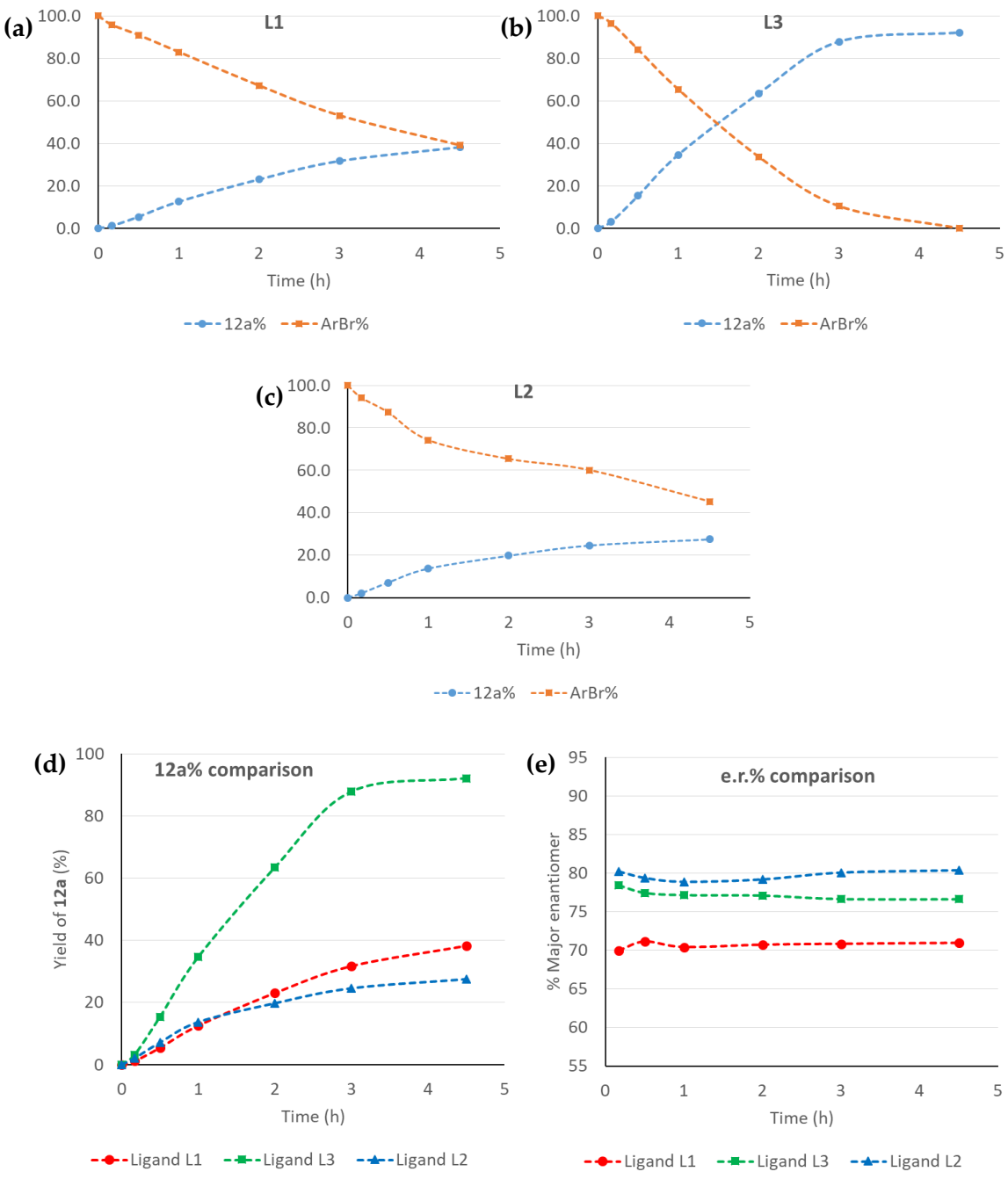

Figure 5

Reaction profiles: samples taken from reaction mixtures during the first hours and analysed by chiral SFC. Yield of product **12a** and remaining 4-bromobenzonitrile when using ligands **L1 (a)**, **L3 (b)** and **L2 (c)**. Direct comparison between the three ligands concerning yield of **12a (d)** and enantioselectivity **(e)**. In the latter, the percentage of major enantiomer over the total amount of **12a** is plotted.

When comparing **L3** and **L2**, the difference of reactivity seen so far with the model substrate suggests that turning to more complex/difficult substrates there would be more chances of good reactivity using the more active **L3** rather than **L2**. This was proved right with some preliminary substrate evaluation. While **L3** allowed a good range of substrates to be coupled under the same conditions (as will be described in **Section 2.6**),

using **L2** reactivity dropped drammatically when turning to more hindered substrates, either with hindrance on the heterocycle or on the alkyl group (**Table 7**). Concluding **L2** is unsuitable for lack of versatility, **L3** was employed for all further studies.

Table 7

Experiments with **L2** as ligand using other carboxylic acid substrates.[a]

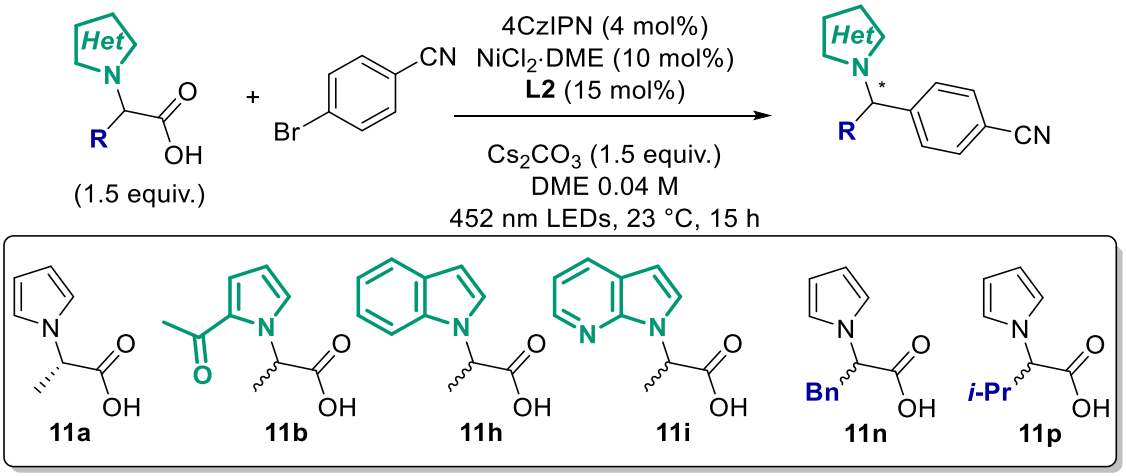

Entry	Substrate	Yield %	e.r.	Conversion %
1	**11a** (standard)	56	22:78	75
2	**11b**	< 5	25:75	31
3	**11h**	31	22:78	63
4	**11i**	< 5	28:72	n.d.
5	**11n**	16	75:25	37
6	**11p**	< 5	5:95	48

[a] Notes as from **Table 1**. Standard conditions: 4-bromobenzonitrile (1 equiv.), heterocyclic carboxylic acid (1.5 equiv.), 4CzIPN (4 mol%), $NiCl_2$ DME (10 mol%), **L2** (15 mol%), Cs_2CO_3 (1.5 equiv.), DME 0.04 M, blue light irradiation, 23 °C, 15 h.

2.5.4 Optimisation: part 2

The final round of optimisation using **L3** as ligand was then started (**Table 8**). Other bases provided very similar reactivity compared to the usual Cs_2CO_3: both inorganic ($CsOH·H_2O$, entry 9) or organic (DBU, TMG, or a phosphazene base, entries 2, 4 and 13). The latter are particularly interesting since organic, soluble bases are necessary if extention to a flow setup is desired, for example for scale-up.[81] Interestingly, an excess of base (2 equiv. of DBU, entry 3) shuts down the reaction completely (2% yield), likely interfering with the catalytic cycle. The reaction outcome depends on the concentration of the reaction mixture: while increasing concentration from 0.04 M to 0.1 M seems deleterious (9% yield, entry 14), only a slightly lower yield is obtained by diluting to 0.02 M (76% yield, entry 15). It is possible to lower the amount of photocatalyst to 2 mol% with only minor losses in yield (entry 16), but moving to 1 mol% the yield drops to 65%

(entry 17). [Ir(dF(CF$_3$)ppy)$_2$(dtbbpy)]PF$_6$ as photocatalyst also provides product, but in lower yields at the usual 1 mol% loading (entry 18). It is also possible to lower the loading of Ni catalyst from 10 mol% to 5 mol% (84% yield, entry 19), but at 2 mol% the system loses reactivity (34% yield, entry 20). Finally, the ligand **L3**:Ni ratio does not affect the reaction (entries 21-22), and a 1:1 ratio can also be used (91% yield, 76:24 e.r., entry 22).

Table 8

Second round of optimisation, using **L3** as ligand.[a]

Entry	Modification from conditions	Yield %	e.r.	Conversion %
1	none	90	77:23	100
2	DBU (1.5 equiv.) as base	88	77:23	100
3	DBU (3 equiv.) as base	2	54:46	10
4	TMG (1.5 equiv.) as base	88	74:26	100
5	K_2CO_3 (1.5 equiv.) as base	64	76:24	92
6	KH_2PO_4 (1.5 equiv.) as base	0	-	0
7	K_2HPO_4 (1.5 equiv.) as base	0	-	23
8	K_3PO_4 (1.5 equiv.) as base	65	77:23	100
9	CsOH H_2O (1.5 equiv.) as base	87	76:24	100
10	TBAOH 30 H_2O (1.5 equiv.) as base	30	70:30	50
11	*t*-BuOK (1.5 equiv.) as base	12	76:24	28
12	MeTBD (1.5 equiv.) as base	75	76:24	100
13	Phosphazene P1-tBu t(tm) (1.5 equiv.) as base	86	74:26	100
14	Concentration 0.1 M	9	75:25	42
15	Concentration 0.02 M	76	77:23	100
16	2 mol% of 4CzIPN	81	77:23	100
17	1 mol% of 4CzIPN	65	75:25	100
18	[Ir(dF(CF$_3$)$_2$ppy)$_2$(dtbbpy)]PF$_6$ (1 mol%) as photocatalyst	73	77:23	85
19	5 mol% Ni salt, 7.5 mol% **L2**	84	76 :24	100
20	2 mol% Ni salt, 3 mol% **L2**	34	75 :25	43
21	10 mol% **L2** (1:1 ligand:Ni)	91	76:24	100
22	20 mol% **L2** (2:1 ligand:Ni)	91	76:24	100

[a] Substrates and notes as from **Table 1**. Standard conditions: 4-bromobenzonitrile (1 equiv.), **11a** (1.5 equiv.), 4CzIPN (4 mol%), $NiBr_2$ DME (10 mol%), **L3** (15 mol%), Cs_2CO_3 (1.5 equiv.), Acetone 0.04 M, blue light irradiation, 23 °C, 15 h.

The use of other aryl (pseudo)halides in place of the bromide for the benzonitrile derivative is not advised (**Table 9**). Reactivity drops when using the chloride (entry 2), iodide (entry 3) or tosylate (entry 5), though enantioselectivity is mantained. The use of the triflate (entry 4) damages both yield and enantiomeric ratio.

Table 9

Aryl (pseudo)halide screening, using **L3** as ligand.[a]

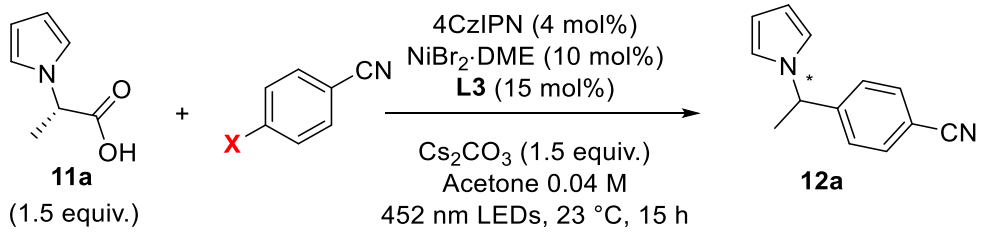

Entry	X	Yield %	e.r.	Conversion %
1	Br (standard)	90	77:23	100
2	Cl	42	77:23	n.d.
3	I	15	77:23	41
4	OTf	68	56:44	n.d.
5	OTs	36	78:22	45

[a] Substrates and notes as from **Table 1**. Standard conditions: 4-(pseudo)halobenzonitrile (1 equiv.), **11a** (1.5 equiv.), 4CzIPN (4 mol%), $NiBr_2$ DME (10 mol%), **L3** (15 mol%), Cs_2CO_3 (1.5 equiv.), Acetone 0.04 M, blue light irradiation, 23 °C, 15 h.

As a possible source of improvement for the still modest e.r., the effect of temperature on enantioselectivity was also examined. A jacketed vessel surrounded by LED strips was employed: a heated or cooled liquid flows through the jacket in order to obtain temperature control.[VII] A very limited effect of temperature on enantioselectivity was observed (**Table 10**). From 35 °C (maximum temperature tested) to 0 °C (minimum temperature tested) the e.r. changed from 75:25 to 78:22. The best yield (78%) was obtained at the usual 23 °C (entry 2), while at both higher (entry 1) and lower (entries 3-4) temperatures inferior yields (69-73%) were observed. Due to the limited improvements obtained with this strategy, this parameter was not investigated further. Control experiments confirmed the necessity of all the reaction components (photocatalyst, light, ligand, base) for the success of the transformation (**Table 11**, entries 1-6). Exclusion of chiral ligand (entry 5) showed the presence of a slow background reaction, affording 12% yield of racemic product overnight. If the enantiomer of the substrate ***ent*-11a** is employed the product is obtained with the same stereoselectivity (entry 14), confirming the enantioconvergent nature of the process and that stereoselectivity is entirely controlled by the catalytic system.

[VII] This simple setup was used for proof of concept. See **Section 6.2** for details.

Table 10

Effect of temperature, using **L3** as ligand.[a]

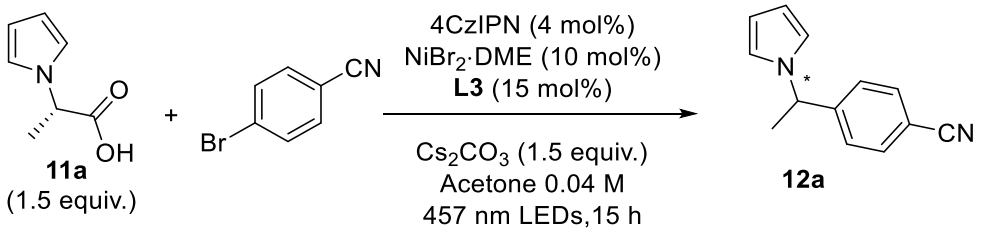

Entry	T [°C]	Yield %	e.r.	Conversion %
1	35	69	75:25	100
2	23 (standard)	78	76:24	100
3	10	73	77:23	100
4	0	72	78:22	100

[a] Substrates and notes as from **Table 1**. Reactions carried out in jacketed vessel surrounded by blue light LED strips, with cooling/heating liquid in the jacket, as described in the **Section 6.2**. Standard conditions: 4-bromobenzonitrile (1 equiv.), **11a** (1.5 equiv.), 4CzIPN (4 mol%), $NiBr_2$ DME (10 mol%), **L3** (15 mol%), Cs_2CO_3 (1.5 equiv.), Acetone 0.04 M, blue light irradiation, 23 °C, 15 h.

Table 11

Control experiments, using **L3** as ligand.[a]

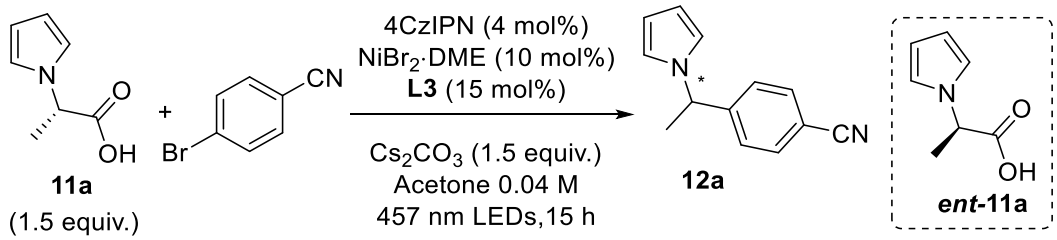

Entry	Modification from conditions	Yield %	e.r.	Conversion %
1	None	90	77:23	100
2	No photocatalyst	0	-	0
3	No light	0	-	0
4	No Ni salt	0	-	5
5	No ligand	12	51:49	20
6	No Cs_2CO_3	0	-	0
7	Run using ***ent*-11a** as substrate	86	76:24	100

[a] Substrates and notes as from **Table 1**. Standard conditions: 4-bromobenzonitrile (1 equiv.), **11a** (1.5 equiv.), 4CzIPN (4 mol%), $NiBr_2$ DME (10 mol%), **L3** (15 mol%), Cs_2CO_3 (1.5 equiv.), Acetone 0.04 M, blue light irradiation, 23 °C, 15 h.

2.6 Asymmetric cross-coupling: scope of the transformation

With optimised conditions in hand, a scope of the methodology was next defined (**Scheme 31**). Firstly, model product **12a** was obtained in 80% isolated yield when purified from 90% SFC yield. Pleasingly, the reaction can be successfully scaled up from

0.2 mmol to a more synthetically useful 1.0 mmol scale, affording 175 mg of **12a** in 89% yield and 77:23 e.r., with no loss in reactivity or enantioselectivity. The absolute

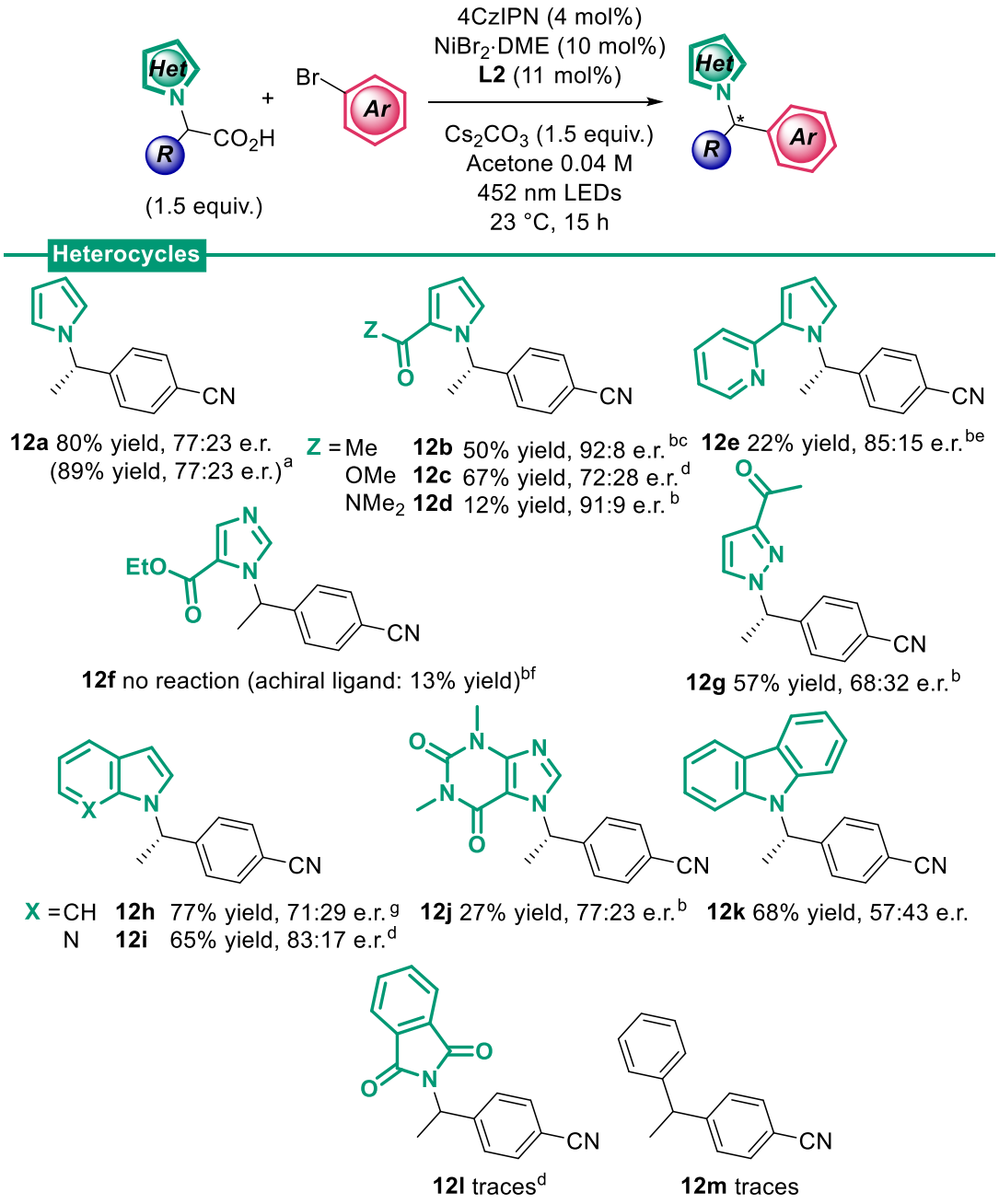

Scheme 31

Scope of heterocycles (isolated yields reported). Standard conditions as in **Table 6**, entry 2, with 11 mol% **L3**. Notes: [a] Reaction carried out on 1 mmol scale, see **Section 6.6** for details. [b] Reaction time: 64 h. [c] 8 mol% 4CzIPN used. [d] Reaction time: 40 h. [e] 1.1 equiv. of carboxylic acid and Cs_2CO_3 were used. [f] ^1H NMR yield of racemic product. Experiment run in DMF with $NiCl_2$·DME (10 mol%), dtbbpy (15 mol%), $[Ir(dF(CF_3)_2bpy)_2(dtbbpy)]PF_6$ (2 mol%), 1 equiv. of imidazolic acid and Cs_2CO_3. The standard conditions failed to deliver any product. [g] Experiment run with **L1** as ligand. Reaction with **L3** affords product in 97% chromatographic yield and 57:43 e.r..

configuration of the major enantiomer of **12a** and all other products was determined by analogy with an enantiopure sample of **12z** (see **Sections 2.6.3** and **6.6**).

2.6.1 Heterocycles and the effect of directing groups

Inspired by the good stereocontrol obtained by the Fu and MacMillan groups on carbamate-protected aminoacids (**Scheme 18**), it was hypothesised that the carbamate could play a role as a coordinating moiety in such systems.[57] The introduction of a directing group in C2 position on the heterocycle might have similar benefits.[82–84] Such a system could provide an additional binding site for the heterocyclic-alkyl fragment to the nickel centre, increasing rigidity in some key intermediate complexes of the catalytic cycle (**Scheme 32**, hypothetical intermediate **13**).

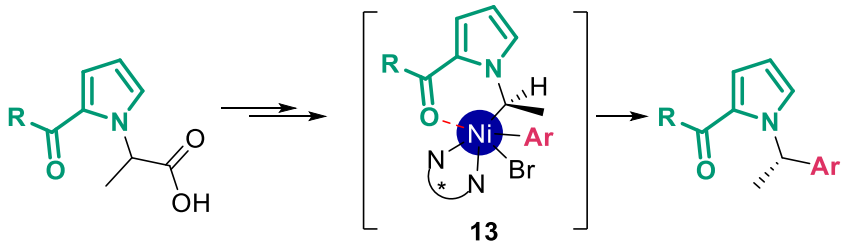

Scheme 32
Hypothetical chelation of the alkyl radical to Ni thanks to a directing group on the heterocyclic moiety.

Indeed, an increased stereocontrol is observed when a carbonyl functionality is introduced on the heterocycle (**Scheme 31**): ketone **12b** and amide **12d** are obtained in 92:8 and 91:9 e.r. respectively. Reduced reactivity is observed however, and extended reaction times are required to obtain useful yields. An ester group does not seem to provide directing group assistance, for **12c** is obtained with 72:28 e.r., similar to the model compound **12a**. A pyridine ring can also behave as a directing group: derivative **12e** is obtained in improved 85:15 e.r. and 22% yield. Unfortunately, imidazole-bearing etomidate analogue **12f** could not be obtained with this methodology. If the reaction is run with an achiral ligand a 13% NMR yield is obtained. This suggests that a bespoke designed catalytic system might be needed for efficient reactivity of imidazole-containing substrates.[VIII] Pleasingly, pyrazole-containing derivative **12g** was obtained in

[VIII] As was already observed with preliminary experiments (see **Section 2.4.1**), the imidazole ring might interfere with reactivity. Indeed, reaction of **11a** with 4-bromobenzonitrile in the presence of 1 equivalent of *N*-methylimidazole affords **12a** in a reduced 60% yield.

57% yield and 68:32 e.r.; as expected, an acetyl group positioned away from the reaction centre does not provide directing group assistance. Replacing the pyrrole with a bulkier indole ring, as for compound **12h**, has a detrimental effect on enantioselectivity when the ligand employed is **L3**. While the reaction goes to completion, the product obtained is almost racemic; however, if **L1** is used some stereocontrol is restored (71:29 e.r.) whilst maintaining good reactivity (77% yield). As further evidence of the concept of using a directing group, azaindole derivative **12i** was obtained in comparable 65% yield and 83:17 e.r. even when using **L3**. The coordinating ability of the additional nitrogen centre must thus overcome the steric hindrance provided by the two fused rings. A xanthine system, such as in **12j**, is also tolerated (77:23 e.r.), even if the product is obtained with 27% yield. A limitation is found when turning to carbazole derivative **12k**. Employing either **L2** or **L1** as ligands, an almost racemic compound is obtained with a good yield. Phthalimide-containing derivative **12l** and the simple diaryl compound **12m** were obtained in trace amount using the standard conditions.

2.6.2 Alkyl chains

Variations in the alkyl chain were then explored (**Scheme 33**): groups other than methyl such as *n*-butyl, benzyl and 3-methoxy-3-oxopropyl are tolerated on the substrate, affording products **12n**, **12o** and **12q** in 81-87% yield and enantioselectivities close to the model substrate's (76:24 e.r. on average). Valine-derived compound **12p** was obtained

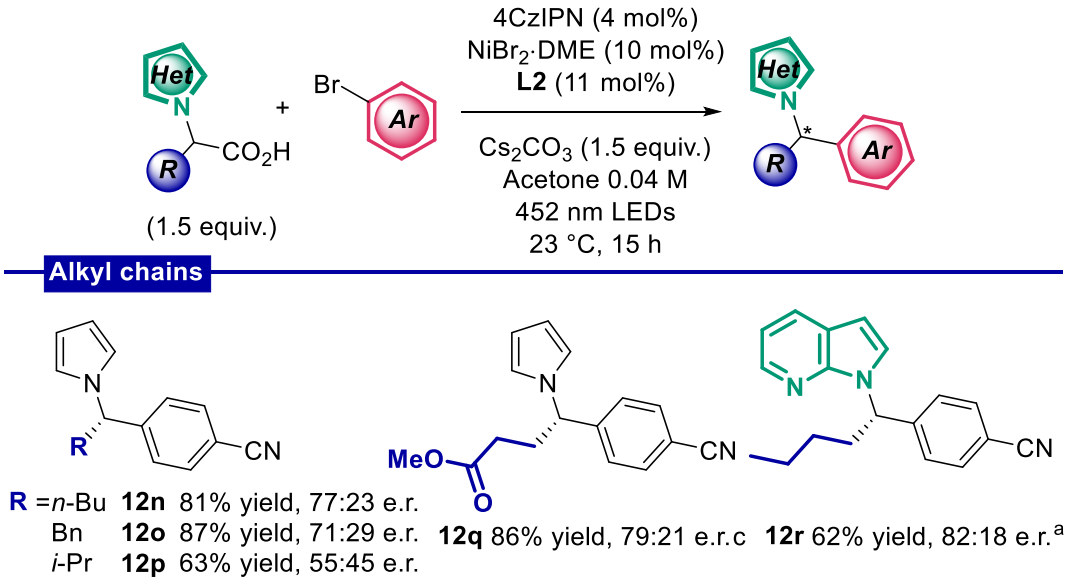

Scheme 33

Scope of alkyl chains (isolated yields reported). Standard conditions as in **Table 6**, entry 2, with 11 mol% **L3**. Notes: [a] Reaction time: 64 h.

with very low stereocontrol in 63% yield, suggesting β-substitution on the alkyl chain is not well tolerated. Azaindole derivative **12r**, bearing a *n*-butyl alkyl chain, could also be obtained with results comparable to those for **12i** (62% yield, 82:18 e.r.).

2.6.3 Aryl bromides

Lastly, an evaluation of aryl bromides was performed (**Scheme 34**). A range of *para*-substituted electron-poor derivatives can be successfully coupled with the model pyrrole carboxylic acid **11a**. Ketone **12s**, aldehyde **12t**, benzothiazole **12u** and oxadiazole **12v** can all be obtained in very good yields (75-88%) and enantioselectivity comparable to that of the model substrate (78:22 e.r. on average). Interestingly, the azole groups in **12u** and **12v** are well tolerated, allowing the preparation of these drug-like compounds

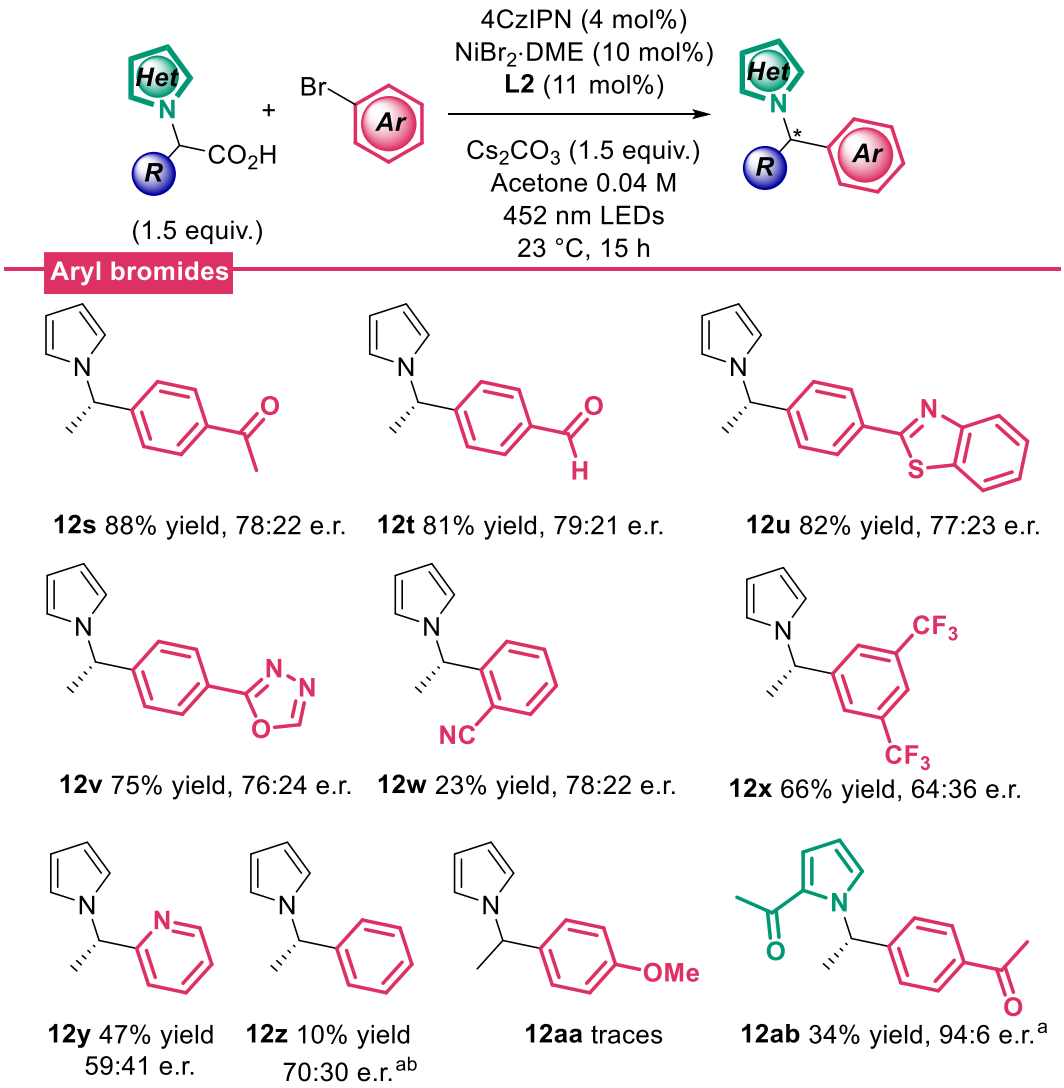

Scheme 34

Scope of heterocycles (isolated yields reported). Standard conditions as in **Table 6**, entry 2, with 11 mol% **L3**. Notes: [a] Reaction time: 64 h. [b] ^{1}H NMR yield: 20%.

in an efficient manner. Other substitution patterns including *ortho*- (**12w**), *meta*,*meta*- (**12x**) and 2-pyridine substitution (**12y**) seem more problematic, affording products in reduced yields and/or enantioselectivity. The use of electron-neutral or electron-rich aryl bromides is not advised, as poor yields are obtained in the former case (compound **12z**, 10% yield), while only traces of the desired reactivity are found in the latter (compound **12aa**). Compound **12ab**, bearing an acetyl directing group, was obtained with 94:6 e.r. but in 34% yield, similarly to **12b**.

2.7 Mechanistic considerations

The postulated mechanism of this transformation is analogous to the general Ni-photoredox mechanism described in **Section 2.1** (**Scheme 35**). While extensive mechanistic investigations were not tackled, a few experiments and observations support some steps of such mechanistic hypothesis.

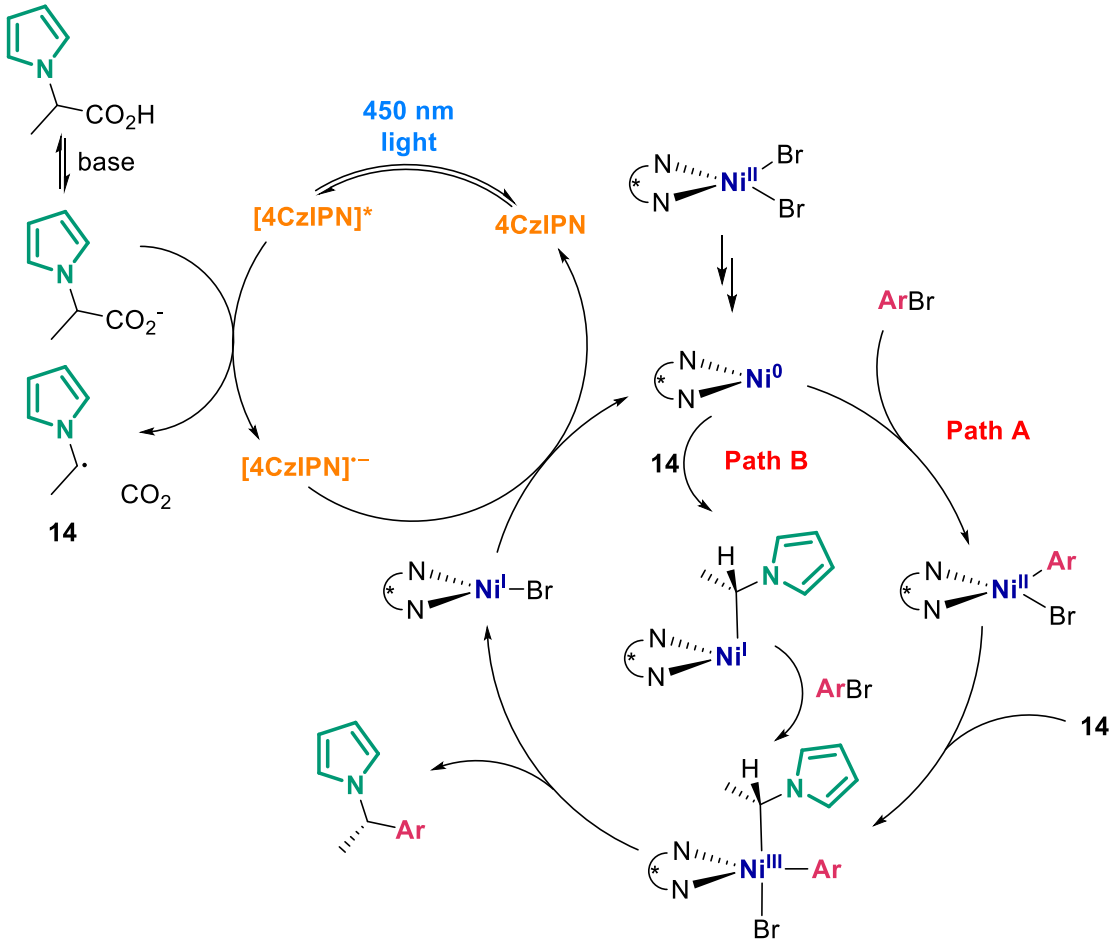

Scheme 35

Postulated mechanism for the asymmetric cross-coupling. Other possible ligands on Ni are omitted for clarity.

The first step of the transformation is thought to be the formation of the carboxylate and its subsequent oxidation by the excited state photocatalyst (4CzIPN) to the carboxyl radical, which readily decarboxylates yielding CO_2 and the desired alkyl radical **14**: this step is supported by both electrochemical and fluorescence quenching studies.

Cyclic voltammetry (CV) analysis[IX] of the caesium salt of **11a** in acetonitrile revealed two irreversible oxidation peaks, with half-peak potentials of +0.90 V and +1.45 V *vs* SCE in acetonitrile, which were assigned to the oxidation of the carboxylate anion and of the pyrrole ring, respectively.[X] The reduction potential of the excited state of 4CzIPN has been reported as +1.35 V (*vs* SCE in acetonitrile),[20] making the oxidation of the carboxylate a thermodynamically favourable process (ΔE = +0.45 V).

Fluorescence quenching studies were also performed using a 10^{-4} M solution of 4CzIPN in acetone and different potential quenchers (**Table 12**).[XI] Keeping constant emitter and solvent allows to use the Stern-Volmer constant (K_{SV}) to compare quenching efficiencies. As expected, the ionised form of carboxylic acid **11a** is quenched much more efficiently (K_{SV} = 654 M^{-1}, entry 2) compared to the non-ionised form (K_{SV} = 33 M^{-1}, entry 1), supporting the idea that it's the carboxylate salt to be oxidised by the excited state of the photocatalyst. In the case of neutral **11a**, we hypothesise that one-electron oxidation of the pyrrole ring might be the process occurring. Indeed, when *N*-methylpyrrole is taken as a comparison, a similar quenching efficiency is observed (K_{SV} = 108 M^{-1}, entry 3), where the decreased efficiency for **11a** might be due to the electron-withdrawing properties of the carboxylic group. 4-Bromobenzonitrile is not efficiently quenched by the photocatalyst (K_{SV} < 1 M^{-1}, entry 4).

Table 12

Results from quenching studies on 4CzIPN (10^{-4} M in acetone, intensity of fluorescence recorded at 530 nm).

Entry	Quencher	K_{SV} (M^{-1})
1	**11a**	33
2	**11a** + TBAOH	654
3	*N*-Methylpyrrole	108
4	4-Bromobenzonitrile	< 1

[IX] See **Section 6.10** for the CV trace.

[X] This is due to the oxidation potential of simple *N*-methylpyrrole being +1.04 V,[8] and having the additional electron-withdrawing effect of the carboxylic group which increases the oxidation potential of the ring.

[XI] See **Section 6.11** for Stern-Volmer plots.

As a last note, three main byproducts were usually formed in these reactions, in variable amounts depending on substrates and reaction conditions (**Scheme 36**). Omnipresent but typically in small amounts (5-10%) is the debromination product such as **15**, detected by SFC-MS, which is most likely derived from the activation of the C-Br bond from Ni(0) or Ni(I): it is usually postulated to derive from HAT of an aryl radical, formed during oxidative addition, from the solvent.[85,86] Reduction of the aryl bromide by the photocatalyst is also conceivable but seems to be thermodynamically unfavourable.[XII] Other typically observed byproducts are the decarboxylated *N*-alkyl heterocycle **16** and dimer **17**: both could derive from HAT and radical-radical coupling (RRC) of the corresponding alkyl radical.[87] Reduction of the radical to its carbanion and subsequent protonation is also a possible pathway for the formation of **16**.[88] The presence of **16** and **17** in various reaction mixtures has been detected by ^{1}H NMR and SFC-MS analyses.

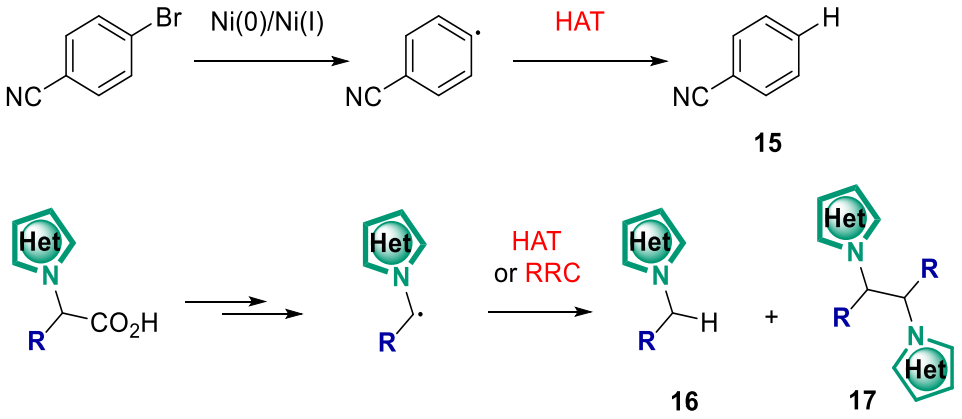

Scheme 36
Main reaction byproducts and hypothetical mechanisms of formation.

2.8 Conclusions

In conclusion, *α*-heterocyclic carboxylic acids can be successfully employed as substrates for the preparation of enantioenriched chiral *N*-benzylic heterocycles, an important class of compounds now accessible using Ni–photoredox dual catalysis. A variety of substrates was examined to find useful trends and limitations. Notably, the combination of yields and enantioselectivity obtained with cheap and easily obtainable chiral PyOx ligands proves advantageous over a comparable racemic synthesis (**Table 13**). Unsolved issues are the reduced reactivity of some heterocyclic substrates (e.g. imidazoles) and

[XII] E = -1.22 V *vs* SCE (in acetonitrile) for the couple 4CzIPN/4CzIPN(-),[20] while E = -1.83 V *vs* SCE for the reduction of 4-bromobenzonitrile in DMF.[130]

aryl halides, for which more work needs to be carrier out. Nonetheless, the modular and stereoconvergent nature of this strategy will allow rapid screening and diversification of structures, especially useful in a drug discovery setting, exploiting the commercial accessibility of aryl bromides and carboxylic acid precursors.

Table 13

Comparison between the asymmetric transformation using selected substrates with **L3** as chiral ligand and conditions employing an achiral ligand.[a]

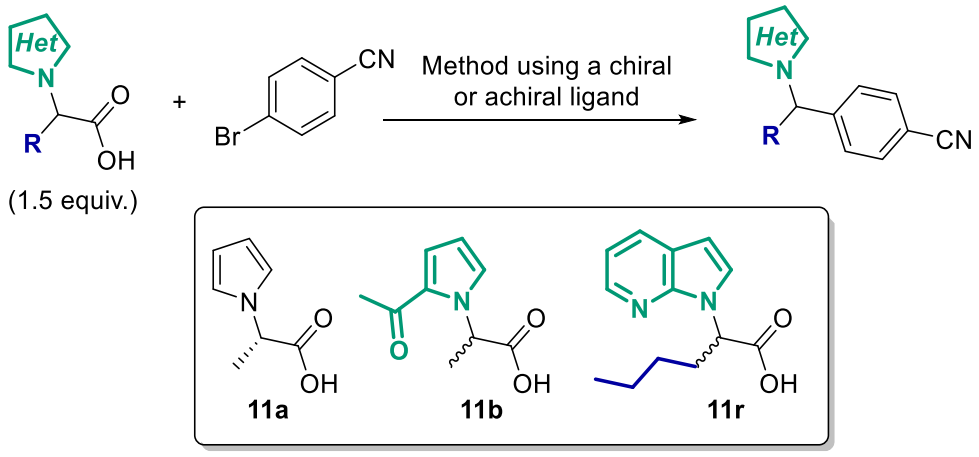

Entry	Substrate	Yield % (chiral)[b]	e.r. (chiral)[c]	Maj. ent. yield % (chiral)[d]	Yield % (achiral)[b]	Maj. ent. yield% (achiral)[d]
1	**11a**	90 (80)	77:23	69	86	43
2	**11b**	57 (50)	92:8	52	70	35
3	**11r**	67 (62)	81:19	54	86	43

[a] Standard conditions using the *chiral* ligand: 4-bromobenzonitrile (1 equiv.), heterocyclic carboxylic acid (1.5 equiv.), 4CzIPN (4 mol%), $NiBr_2$·DME (10 mol%), **L3** (11 mol%), Cs_2CO_3 (1.5 equiv.), Acetone 0.04 M, blue light irradiation, 23 °C. Standard conditions using the *achiral* ligand: 4-bromobenzonitrile (1 equiv.), heterocyclic carboxylic acid (1.5 equiv.), $[Ir(dF(CF_3)_2ppy)_2(dtbbpy)]PF_6$ (1 mol%), $NiCl_2$ DME (10 mol%), dtbbpy (15 mol%), Cs_2CO_3 (1.5 equiv.), DMF 0.04 M, blue light irradiation, 23 °C. Reaction times: 15 h for **11a**, 64 h for **11b** and **11r** using both methods. [b] NMR yield determined using nitromethane as internal standard. Isolated yields in parentheses. For **11a** using the chiral ligand, yield determined by SFC analysis of reaction mixture, compared to a pure standard. [c] Determined by chiral SFC analysis. [d] Intended as effective yield of single major enantiomer, calculated as NMR yield of product multiplied by the fraction of major enantiomer in the product. For reactions with the achiral ligand, the fraction of major enantiomer is equal to 0.5.

Chapter 3
PXX as photocatalyst in organic synthesis

This chapter focuses on a demonstration of the use of PXX (*peri*-xanthenoxanthene) as photocatalyst in organic synthesis. Its excited state has a relatively high reduction potential, allowing reduction of a number of substrates and thus triggering useful radical reactions. Benchmark transformations such as the addition of aryl radicals to radical traps are initially demonstrated. More complex dual catalytic manifolds, involving the coupling with organocatalysts or metallocatalysts, are also shown to be operative.

Part of the work described in ***Section 3.4.2*** *has been performed in collaboration with Oliwia Matuszewska, Phototrain PhD candidate from the Bonifazi group. Oliwia's contributions are acknowledged in the text and schemes.*

3.1 On the development of highly reducing photocatalytic systems

3.1.1 Metal complexes and dyes

In the field of photoredox catalysis, Ru(II)- and Ir(III)-based complexes are still the work-horses in terms of photocatalysts. Stability, long excited state lifetimes and tunability of the photoredox properties through ligand modifications are among the reasons for this preference in the community. Early works revealed that *fac*-[Ir(ppy)$_3$] (**Scheme 37**), a homoleptic complex of Ir(III), was particularly interesting for the highly reducing properties of its excited state. With a redox potential of -1.73 V *vs* SCE,[7] it could be used effectively for the activation of different compounds, in particular alkyl and aryl halides. In 2012 Stephenson and co-workers first demonstrated the utility of this complex in activating alkyl, alkenyl and aryl iodides for the formation of organic radicals (**Scheme 37**):[89] simple deiodination and cyclisation reactions were reported. In the former case, the alkyl radical is expected to abstract an hydrogen atom *via* HAT from either tributylamine or the Hantzsch ester, which are also suitable electron donors for the turnover of the photocatalytic cycle.

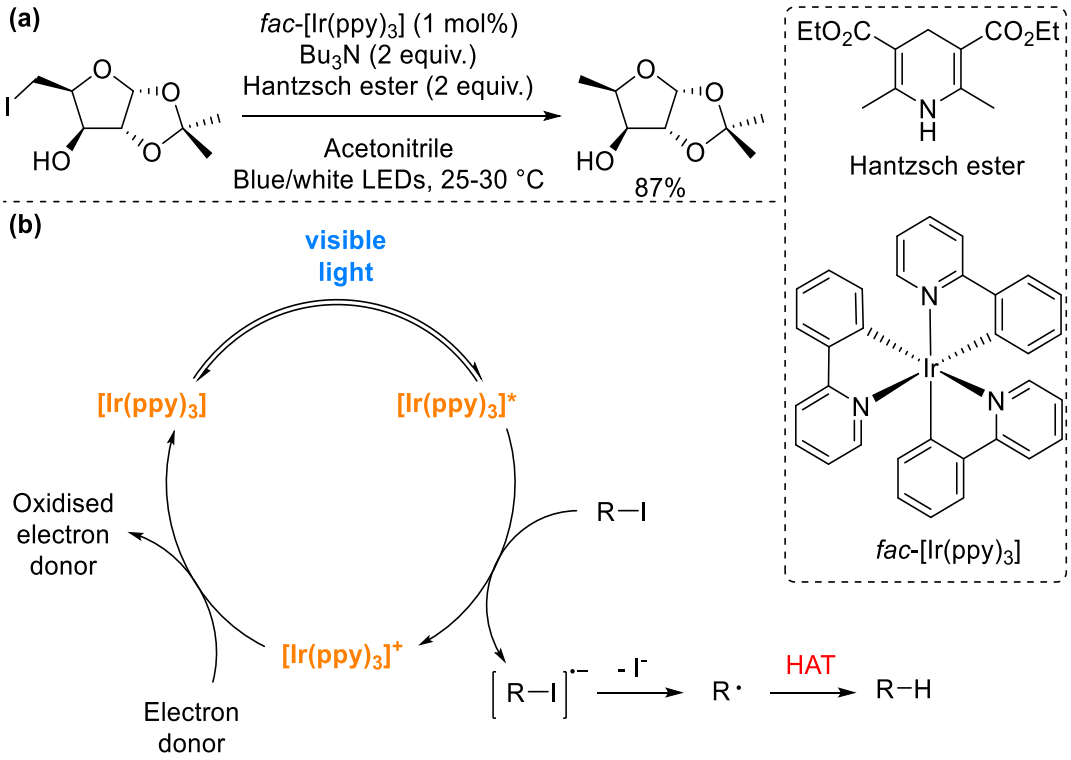

Scheme 37

General conditions **(a)** and proposed mechanism **(b)** for Stephenson's method for the photoredox dehalogenation of organic iodides with *fac*-[Ir(ppy)$_3$] as photocatalyst.[89]

Later on, the same photocatalyst was applied for the enantioselective α-benzylation of aldehydes from MacMillan and co-workers, since the high reduction potential of the excited state of *fac*-[Ir(ppy)$_3$] was sufficient to reduce electron-poor benzyl bromides.[90] The activation of electron-poor cyanoarenes also led to efficient C–C bond-forming reactions, some of which will be discussed more in detail in **Section 3.5**.[91–93]

Staying in the realm of organic halide reduction, in 2013 Li and co-workers demonstrated the use of *fac*-[Ir(ppy)$_3$] as photocatalyst for the activation of aryl iodides and bromides and the addition of the resulting radicals to benzene (**Scheme 38**).[94] The reaction proceeds efficiently at room temperature for aryl iodides, while higher photocatalyst loadings (2.5 mol% instead of 0.5 mol%) and heating (70 °C) are necessary for aryl bromides. It's interesting that the electronic nature of the substituents on the aryl halide did not affect the reactivity, and electron-rich systems actually afforded the best yields.

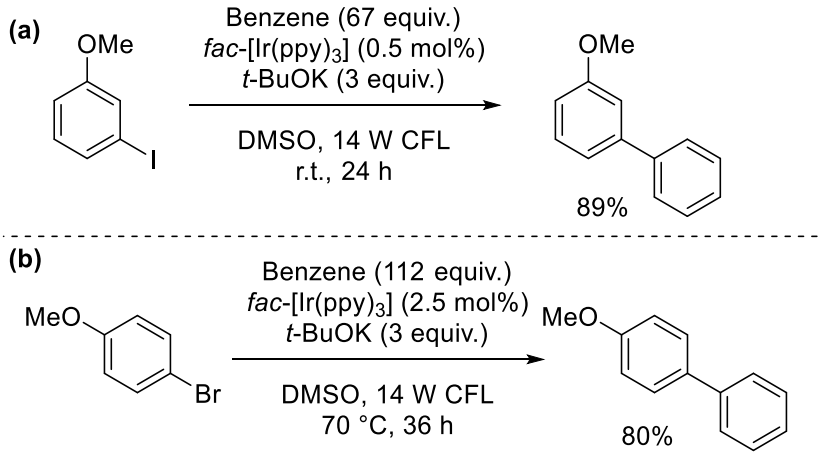

Scheme 38

Li's procedure for the activation of aryl halides and addition to benzene, for iodides **(a)** and bromides **(b)**.[94]

The useful reactivity found with *fac*-[Ir(ppy)$_3$] inspired further work towards alternative photocatalytic systems with comparable or higher reducing power (-1.73 V for *fac*-[Ir(ppy)$_3$]),[7] also in order to obtain photoredox activation of substrates non accessible because of lower reduction potentials. The interest focused mainly on the development of organic dyes, so that reaction mixtures could be devoid of metallic impurities due to the photocatalyst, and to avoid the use of expensive and supply-dependent precious metals. The reduction of organic halides is typically used as a benchmark reaction, either for dehalogenation and formation of the corresponding hydrocarbon, or for addition to electron-rich radical traps (benzene, pyrrole and similar).[95,96]

Many works concentrated on the development and application of phenothiazine- and phenoxazine-type photocatalysts to the activation of organic halides. 10-Phenylphenothiazine (PTH) was introduced by the de Alaniz group in 2015: with an excited state reduction potential of -2.1 V *vs* SCE, it represents a cheap and robust alternative to metal-based photocatalysts.[97] The dehalogenation of various aryl iodides and bromides was demonstrated, usually with excellent yields (**Scheme 39a**); however, a relatively high 5 mol% loading and near UV 380 nm light were used. The reactivity was subsequently extended to include the addition of the aryl radical to pyrrole as radical trap.[98] Of particular note is the intramolecular reaction depicted in **Scheme 39b** that allowed to obtain derivative **18**, with the core structure of lamellarins, a class of mollusk alkaloids.

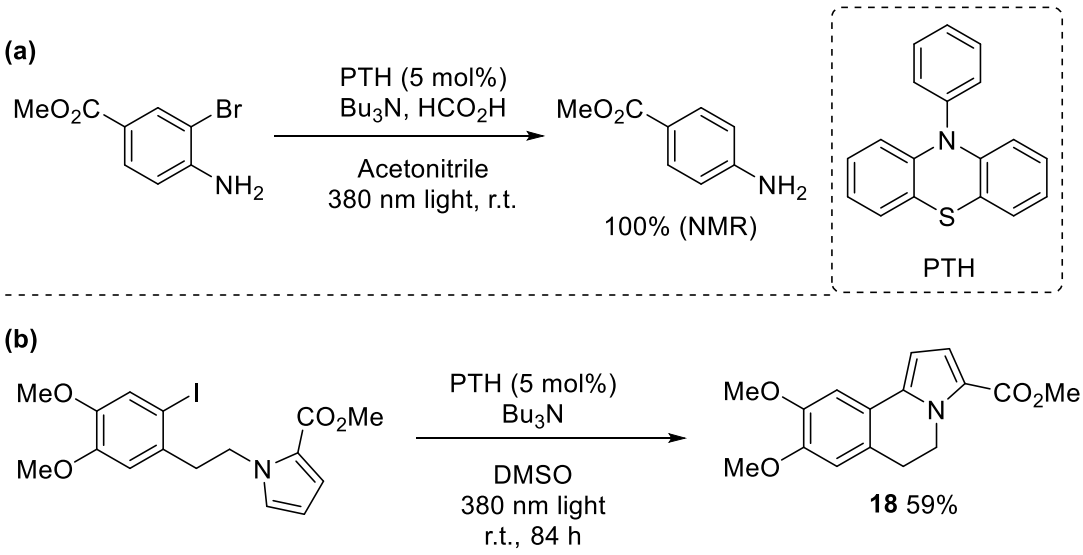

Scheme 39

Application of PTH as photocatalyst for the dehalogenation of aryl halides **(a)**[97] and addition to pyrroles as in the synthesis of derivative **18 (b)**.[98]

Very recently, the Procter group employed PTH as photocatalyst for the formal C-H/C-H coupling of arenes *via* an interrupted Pummerer rearrengement.[99] An arene substrate is reacted with a dibenzothiophene sulfoxide in the presence of triflic anhydride, leading to sulfenylation of the ring. Subsequent photoreduction with PTH releases the aryl radical, allowing formation of C–C bonds through addition to a radical trap. This strategy is very interesting as it allows the use of non-functionalised arenes through *in situ* activation. In this case, blue light was successfully employed for excitation of PTH.

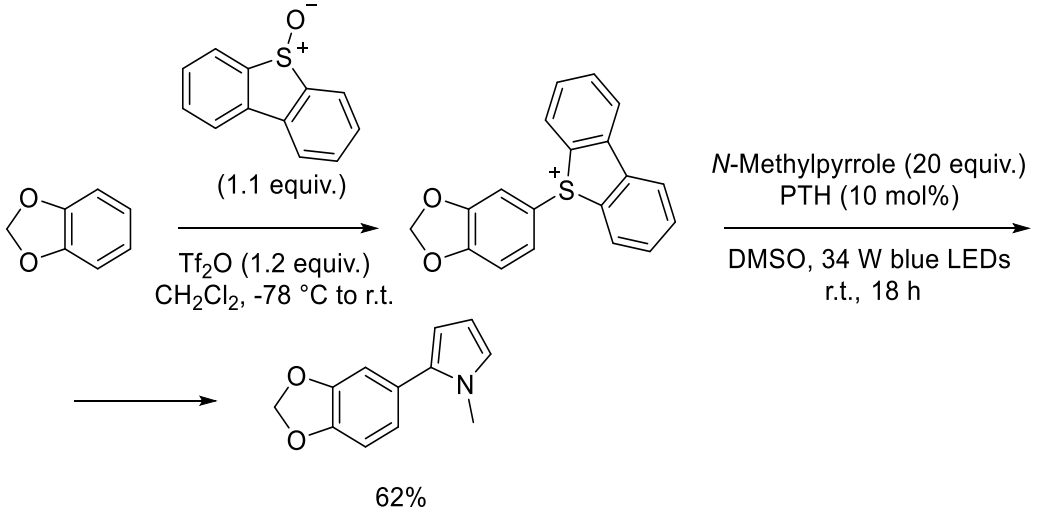

Scheme 40

Procter's formal C-H/C-H coupling of arenes *via* sulfenylation and subsequent photoreduction with PTH.[99]

Two similar dyes were introduced by Miyake and co-workers in 2017: dihydrophenazine **19** and phenoxazine **20** (**Scheme 41a**).[100] While the former has an excited state reduction potential comparable to that of *fac*-[Ir(ppy)$_3$] (-1.69 V *vs* SCE), the latter provides some improvement, with -1.80 V *vs* SCE. Dye **19** was applied to the photoreduction of trifluoromethyl iodide for the trifluoromethylation of arenes and alkenes (**Scheme 41b**) and to the Ni-catalysed amination of aryl bromides with secondary amines. With primary amines and sulfides, the Ni-catalysed cross-coupling was carried out with **20** (**Scheme 41c**). While the mechanism for the trifluoromethylation probably follows the usual pathway *via* photoreduction of ICF_3, subsequent mechanistic studies on the aminative cross-coupling revealed an energy transfer mechanism between the photocatalyst and the Ni centre to be more probable.[101] See **Section 3.6.1** for further details.

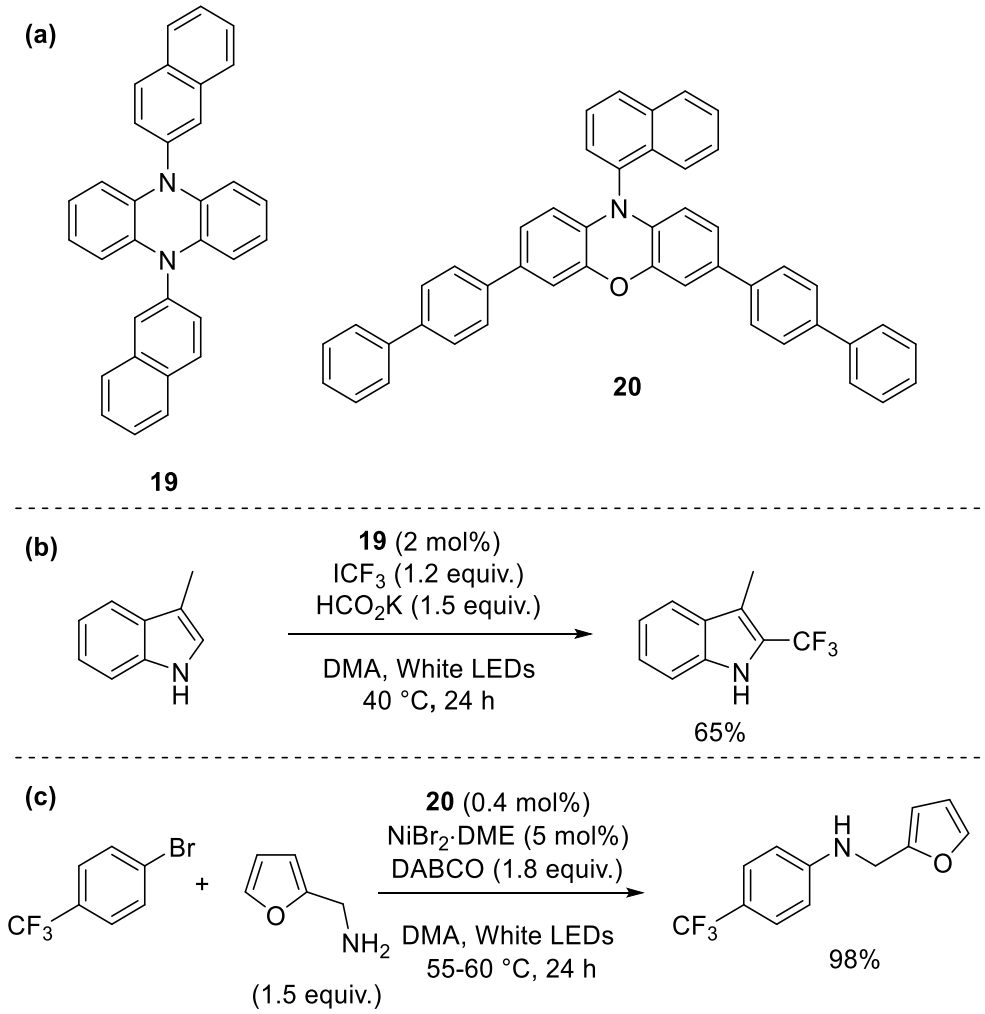

Scheme 41

Miyake's dyes **(a)** and their application to the trifluoromethylation of arenes **(b)** or to the Ni-catalysed amination of aryl bromides **(c)**.[100]

In 2019 Cho and co-workers developed the even more reducing phenoxazine **21** (E = -1.98 V *vs* SCE), which was used to activate a variety of aryl halides, among which electron-poor aryl chlorides.[102] Coupling partners were electron-rich aromatics as radical traps, along with some examples of reactions with B_2pin_2 for the formation of arylboronic esters (**Scheme 42**).

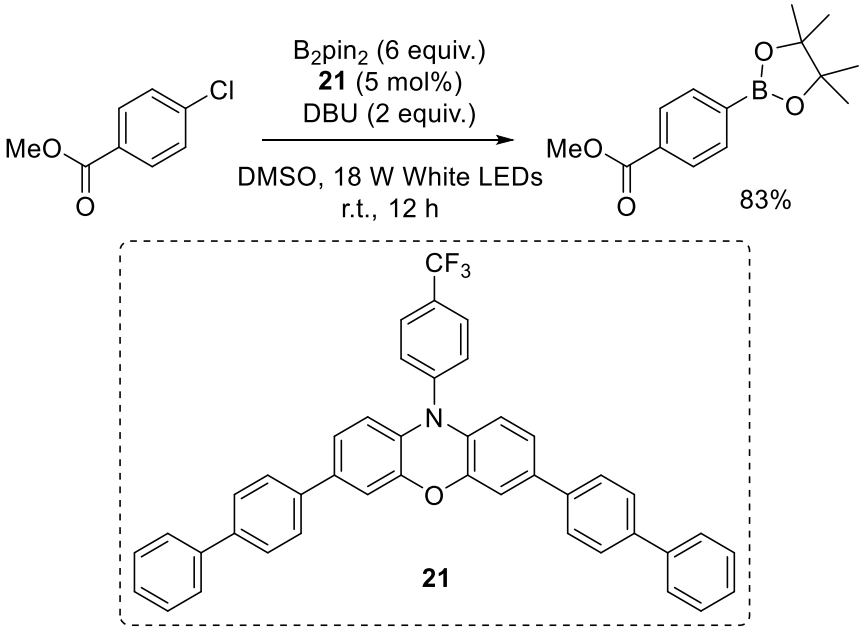

Scheme 42

Cho's phenoxazine **21** in the activation of electron-poor aryl chlorides for the formation of C-B bonds.[102]

Other groups moved from the phenothiazine/phenoxazine theme, and different dye structures were thus developed. In 2018 Zhang and co-workers described novel donor-acceptor-type dyes, of which Py-Btz-Py was the most efficient photocatalyst, with an excited state reduction potential of -2.04 V *vs* SCE.[103] It was used for the activation of aryl iodides and radical addition on furan and other electron-rich aromatics, also selectively in the presence of chlorine substitutents (**Scheme 43**).

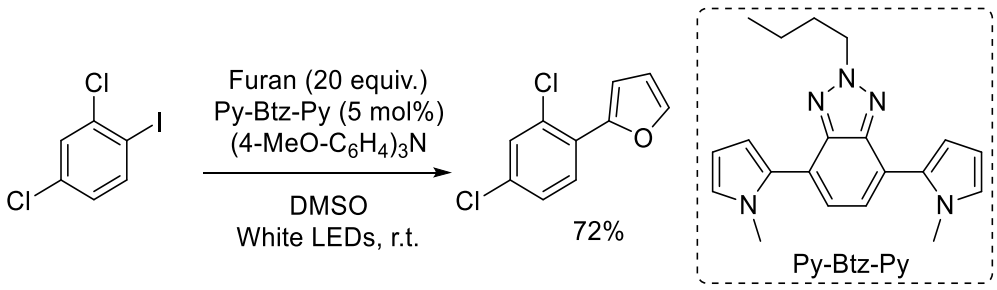

Scheme 43

Zhang's donor-acceptor dye and its application to the coupling of aryl iodides with electron-rich arenes.[103]

In the same year, the Sakata group revealed photocatalyst **22** with an impressive excited state reduction potential of -2.57 V *vs* SCE due to the presence of the electron-donating dimethylamino groups in the carbazole backbone.[104] Using this dye, under 365 nm light irradiation, the dehalogenation of both electron-poor and electron-rich aryl chlorides was obtained in high yields (**Scheme 44**). Alkyl chlorides were also competent substrates, with yields in the range 56-87%. An example of defluorination of a 4-alkylfluorobenzene was also reported in 62% yield. Moreover, the addition to arenes such as *N*-methylpyrrole and benzene was demonstrated, although in more moderate yields (22-66%).

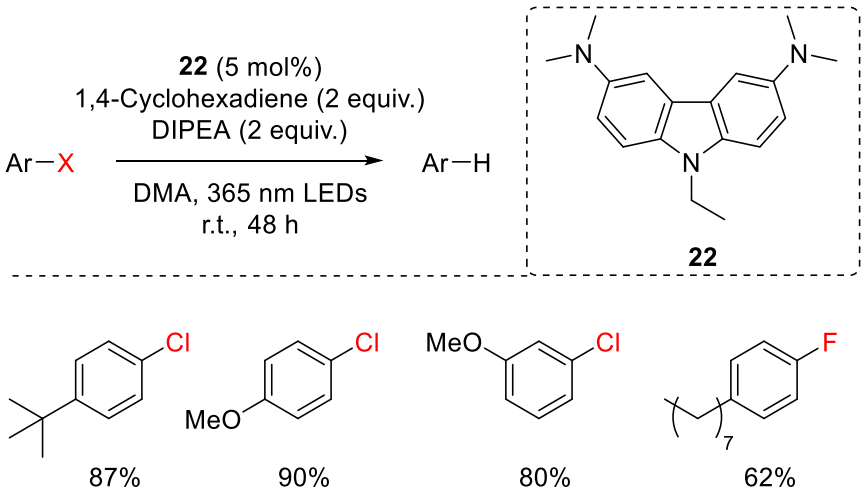

Scheme 44
Sakata's carbazole-based dye **22** and its application to the dehalogenation of aryl chlorides and fluorides.[104]

3.1.2 Excitation of anions and radical anions

While the systems described so far are all based on the development of a novel dye structure, the König group has instead applied a different approach to designing highly reducing photocatalytic systems. Focusing mainly on known dyes, they demonstrated that if the radical anion of the photocatalyst is formed *in situ*, this species can typically absorb visible light and become, in the excited state, an even more powerful reductant. It was the case, in 2014, of perylenediimide (PDI): after absorption of visible light, the photo-oxidation of a reducing agent (TEA in this case) results in the formation of the radical anion of PDI, a colored species which upon a second absorption has stored enough energy for the reduction of a variety of aryl halides (**Scheme 45**).[105] The resulting aryl radicals are then used for dehalogenation or addition to radical traps (pyrroles). Aryl halide activation worked well for aryl iodides, but was limited to electron-poor aryl

bromides and chlorides. Duan and co-workers later developed an heterogeneous version of the photocatalyst by organised aggregation of carboxylate-bearing PDI units with Zn^{2+} ions: the resulting system was more efficient and robust than its homogeneous counterpart.[106]

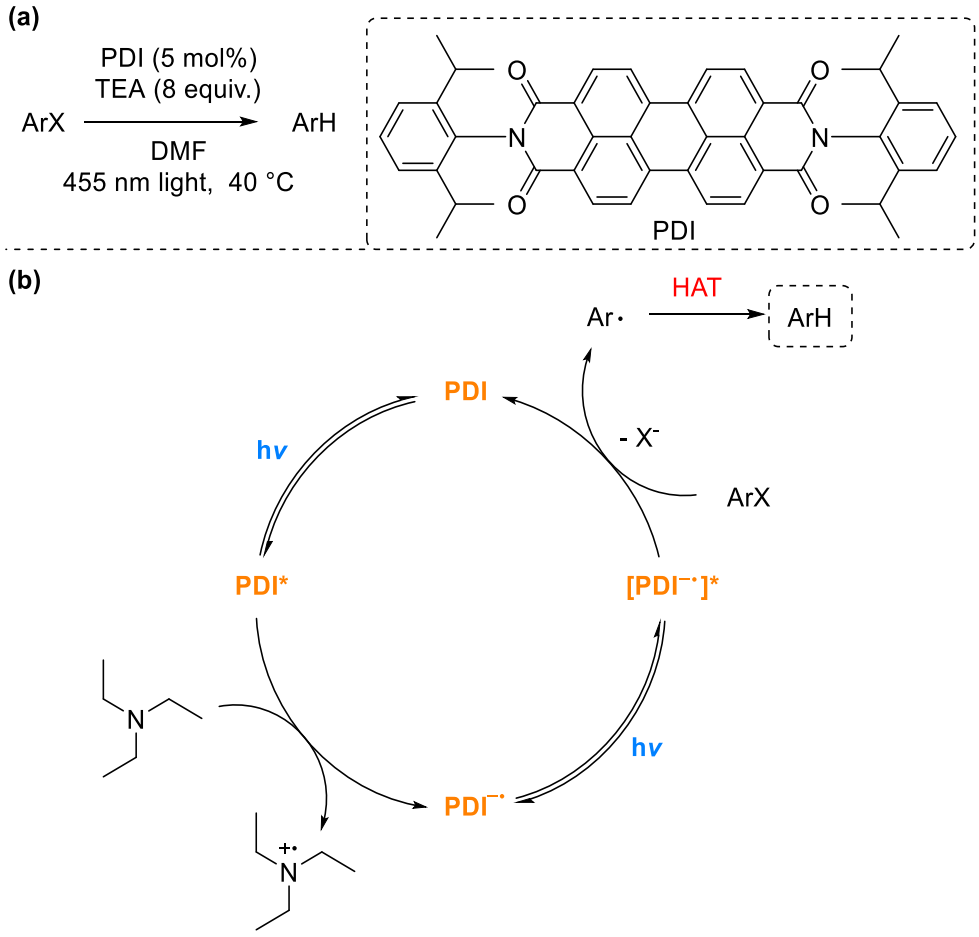

Scheme 45
General conditions **(a)** and proposed mechanism **(b)** for König's PDI-photocatalysed dehalogenation of aryl halides.[105]

The same concept was later applied to the more accessible dye rhodamine 6G (Rh6G): its radical anion has an estimated excited state reduction potential of -2.4 V *vs* SCE.[107] While the neutral dye absorbs both green and blue light, the radical anion is shown to absorb only blue light, allowing for tuning of the reductive power of the photocatalytic system with the wavelength (color) of the light. This was the case for consecutive functionalisations: when tribrominated substrate **23** was subjected to the reaction with 1,3,5-trimethoxybenzene under green light irradiation, only a single functionalisation occurred, since product **24a** is now out of the range of the photocatalyst radical anion. However, under blue light irradiation the radical anion can be excited, and its excited state is capable of catalysing a second functionalisation with, for example,

N-methylpyrrole to product **24b**. While this first work was focused on the coupling with electron-rich arenes, subsequent efforts expanded the scope to the addition to phosphites for C–P bond formation,[108] the functionalisation of nucleobases[109] and to reactions with isonitriles.[110]

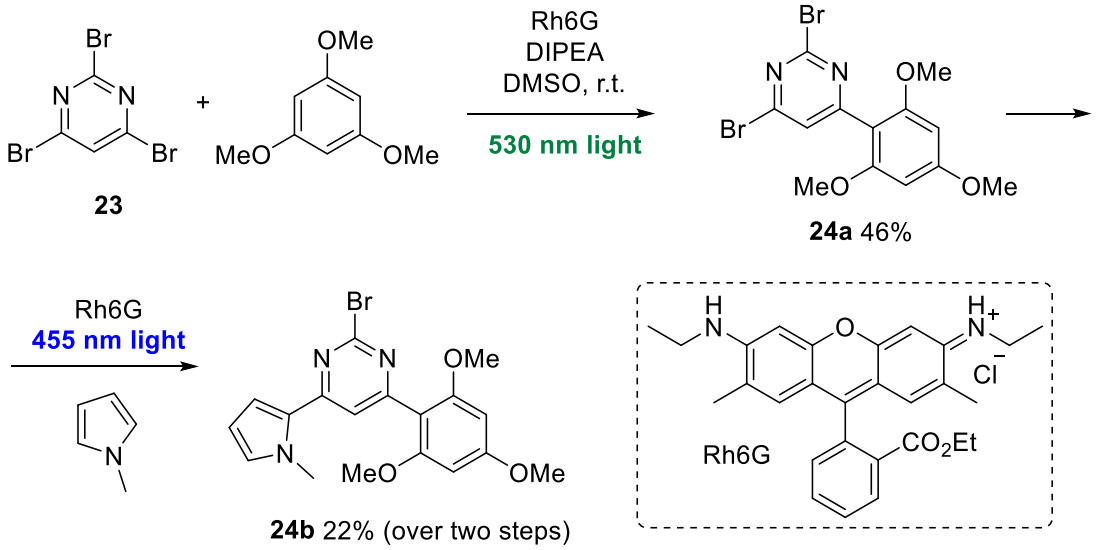

Scheme 46

Light wavelength-controlled selectivity in König's rhodamine 6G-photocatalysed debromination and attack on electron-rich arenes.[107]

The same group reported a similar phenomenon when using anthraquinone Aq-OH as photocatalyst (**Scheme 47a**): also in this case formation of the radical anion and its subsequent excitation by 455 nm light are employed for the reduction of electron-poor aryl bromides.[111] Dehalogenation and addition to electron-rich arenes were again used as benchmark reactions. Von Wangelin and co-workers also described double excitation when using 9,10-dicyanoanthracene (DCA) as photocatalyst: the excited state of its radical anion was found to have reduction potential of -2.47 V *vs* SCE (**Scheme 47b**).[112] Aryl bromides and chlorides are reacted with pyrroles as radical traps, but poor yields are obtained with electron-rich aryl halides. In another report from König and co-workers, anthrolate anion **25** was formed *in situ* from the corresponding ketone by treating with base (Cs_2CO_3 with 18-crown-6 as additive) and, upon absorption of 455 nm light, the excited state anion could behave as a strong reductant, with an estimated reduction potential of -3.0 V *vs* SCE (**Scheme 47c**): electron-poor aryl chlorides were thus reduced for reactions with a variety of radical traps, including pyrroles, benzothiazoles, triethyl phosphite and B_2pin_2.[113]

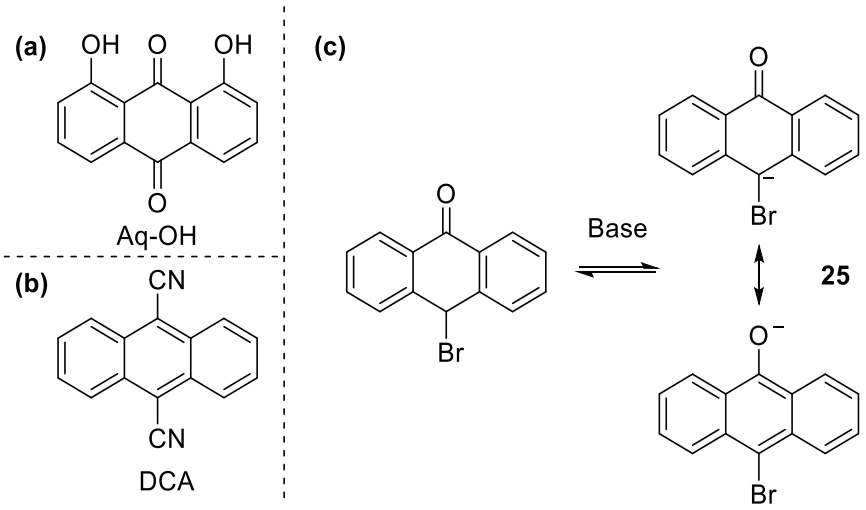

Scheme 47

Different photocatalytic systems: anthraquinone **Aq-OH (a)**,[111] 9,10-dicyanoanthracene **(b)**[112] and anthrolate anion **25 (b)**.[113]

The formation of a radical anion to be used as photocatalyst has been very recently tackled electrochemically: Wickens and co-workers demonstrated that electron priming NpMI as photocatalyst *via* an electrochemical cell allows access to impressive reduction potentials, in the order of the alkali metals (-3.0 V and beyond).[114] Indeed, the so-obtained radical anion of NpMI is able to reduce substrate **26** with a reduction potential of -3.4 V *vs* SCE, releasing the radical for subsequent C–P bond formation with triethyl phosphite in a good 51% yield (**Scheme 48**). Electron-rich aryl chloride substrates are also coupled with *N*-methylpyrrole, obtaining 41-56% yields of arylated pyrroles. The method is demonstrated as being more efficient than classical photoredox methods and direct electrolysis as it provides higher yields of product along with reduced amounts of protodehalogenation in selected cases.

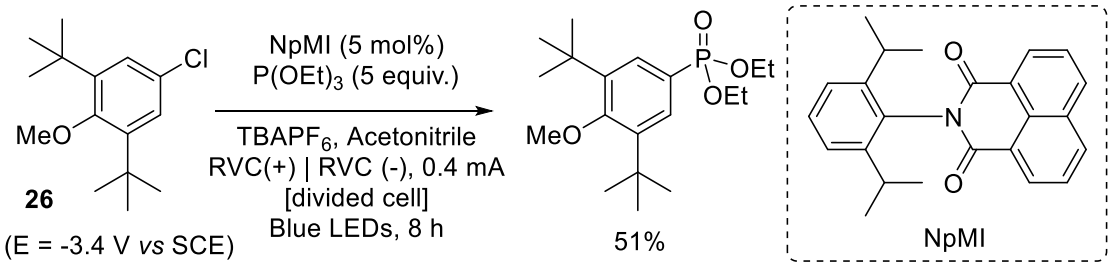

Scheme 48

Wickens' electrochemical and photocatalytic activation of highly electron-rich aryl chloride *via* photocatalyst electron priming.[114]

3.1.3 Sensitisation and triplet-triplet annihilation

Another strategy attempted by the König's group involved the sensitisation of a UV-absorbing polycyclic aromatic hydrocarbon (pyrene) with a visible light-absorbing photocatalyst ($[Ru(bpy)_3]Cl_2$): after reduction of the triplet excited state of pyrene by DIPEA, the highly reducing radical anion of pyrene (-2.1 V *vs* SCE) can thus be accessed by visible light irradiation (**Scheme 49**).[115] This mechanistic hypothesis has been questioned, and a group led by Balzani suggested a triplet-triplet annihilation (TTA)-based mechanism instead.[116] They argue that the above scenario is improbable due to the endoergonic SET step between DIPEA and the pyrene triplet state (ΔE = -1 V). They

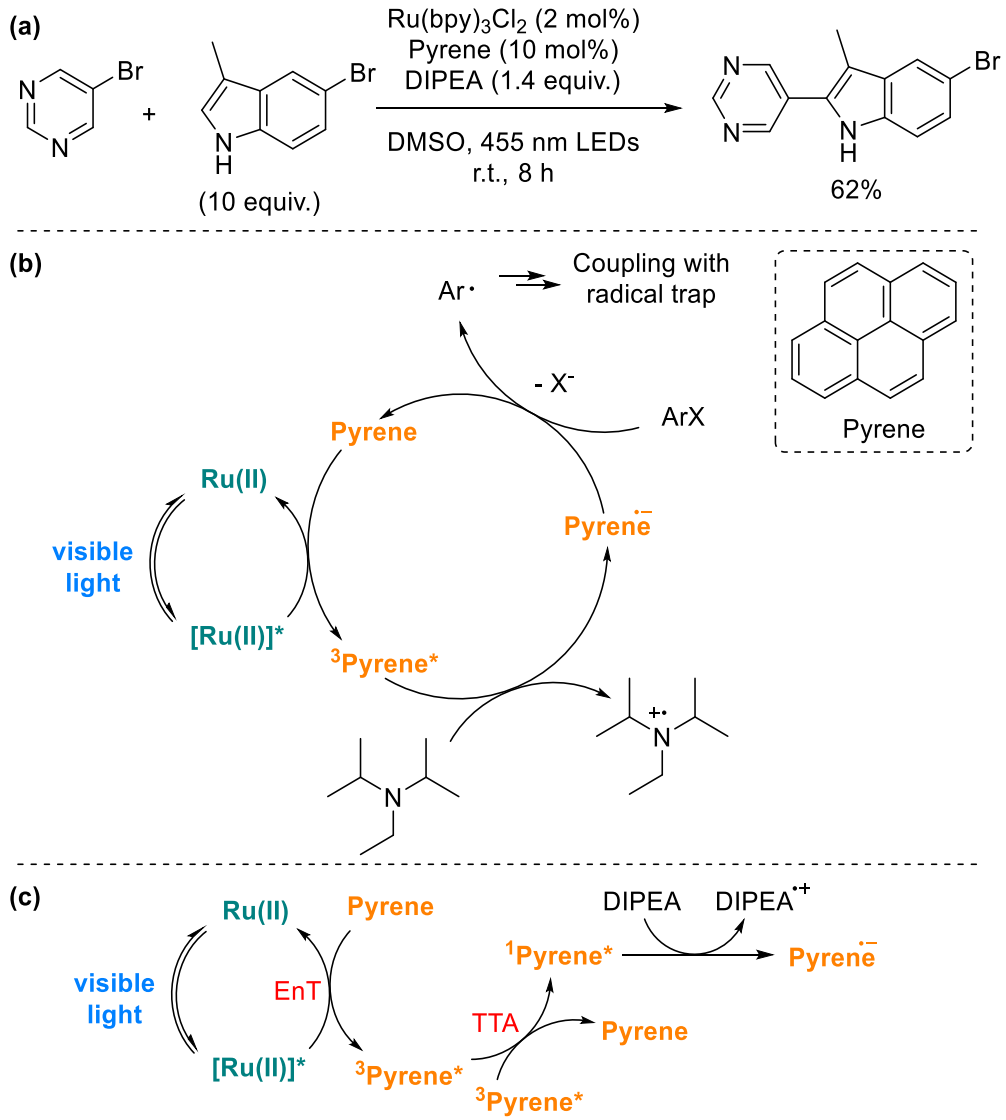

Scheme 49

König's procedure **(a)** and proposed mechanism **(b)** for aryl halide reduction involving sensitisation of pyrene with a Ru(II) photocatalyst;[115] **(c)** revised mechanism of formation of pyrene radical anion, as proposed by Balzani.[116]

alternatively propose that the collision between two triplet state pyrenes allows one of them to access the higher energy singlet state with their combined energy, while the other decays to the ground state (annihilation step). The so-obtained singlet excited state pyrene would be the oxidant for DIPEA, allowing formation of pyrene radical anion. This second proposal has been questioned and discussed further by the original authors.[117] Nonetheless, this procedure allowed functionalisation of electron-poor aryl chlorides and triflates with a variety of radical traps (arenes and phosphites) in typically good to excellent yields.

While a triplet-triplet annihilation (TTA) mechanism was simply suggested in the case above, von Wangelin and co-workers worked on applying this photophysical process to accessing high reduction potentials (**Scheme 50**).[118] In their mechanistic perspective, a sensitiser (2,3-butanedione, BD) absorbs visible light, and through ISC (intersystem crossing) accesses a triplet state. Energy transfer to an annihilator (2,5-diphenyloxazole, PPO) converts the latter to its triplet state, and TTA generates PPO in the singlet state. This is a reducing species and can effect SET on aryl halides. While in principle

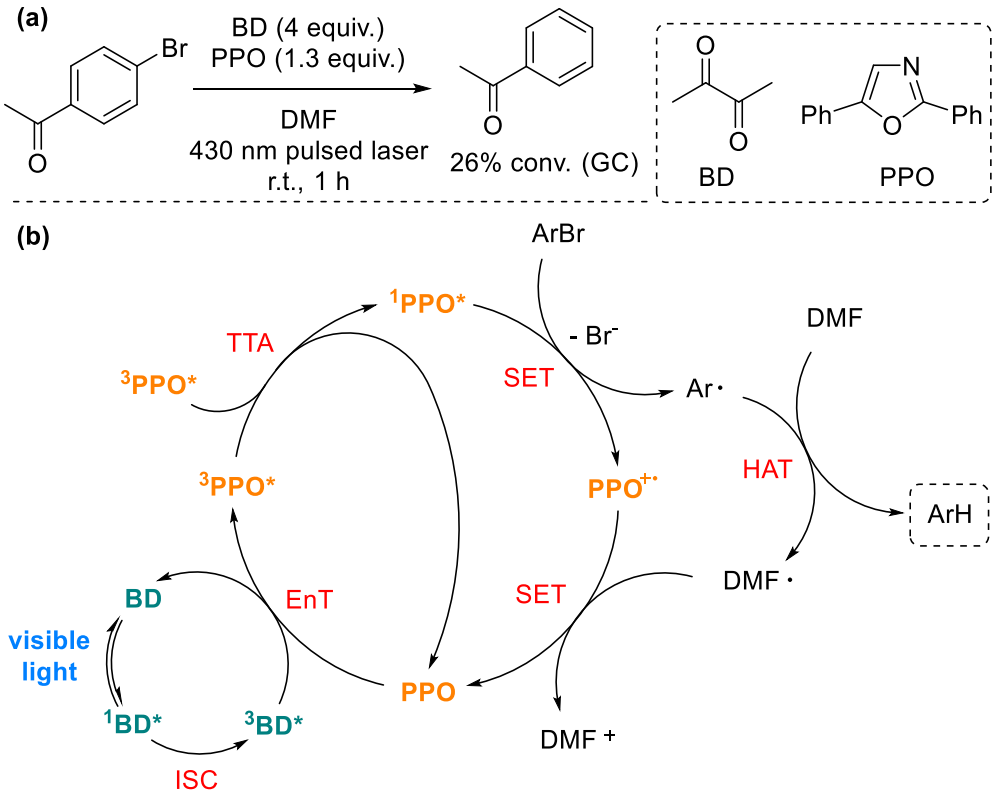

Scheme 50

Von Wangelin's triplet-triplet annihilation-based method for aryl halide reduction.[118]

interesting, the method was limited by the need of laser irradiation to obtain a sufficient light intensity, and by overall low conversions of the aryl halide.

3.2 PXX: properties and established reactivity

When looking at the research and use of metal-based photocatalysts, we realise that they have been known long before sustained organic synthesis applications. For example, the photophysical properties of the most popular $[Ru(bpy)_3]Cl_2$ complex have been exploited in a variety of inorganic and material applications, from water splitting to dye sensitized solar cells, to polymerisation initiation.[7] Organic synthesis came later, building on the photophysical research already done on these complexes. It is no wonder that material and inorganic chemistry are still today a source of novel photocatalysts. This is also the case for PXX (*peri*-xanthenoxanthene), the *O*-doped analogue of anthanthrene (**Figure 6a**). Substituted PXX derivatives show excellent carrier-transport and injection properties, easy processability, chemical inertness and thermal stability.[119] This made them a good choice for applications as organic semiconductors in transistors[120–123] or as conducting polymers.[124] The Bonifazi group has also been interested in these compounds,[119,125] and they have recently tested their use as photocatalysts in organic synthesis.[23]

PXX itself is a bright yellow solid, a simple molecule showing absorption in the UV and visible spectrum, with a lower energy peak at 439 nm (blue light) in acetonitrile; other photophysical data are summarised in **Figure 6** and **Table 14**.

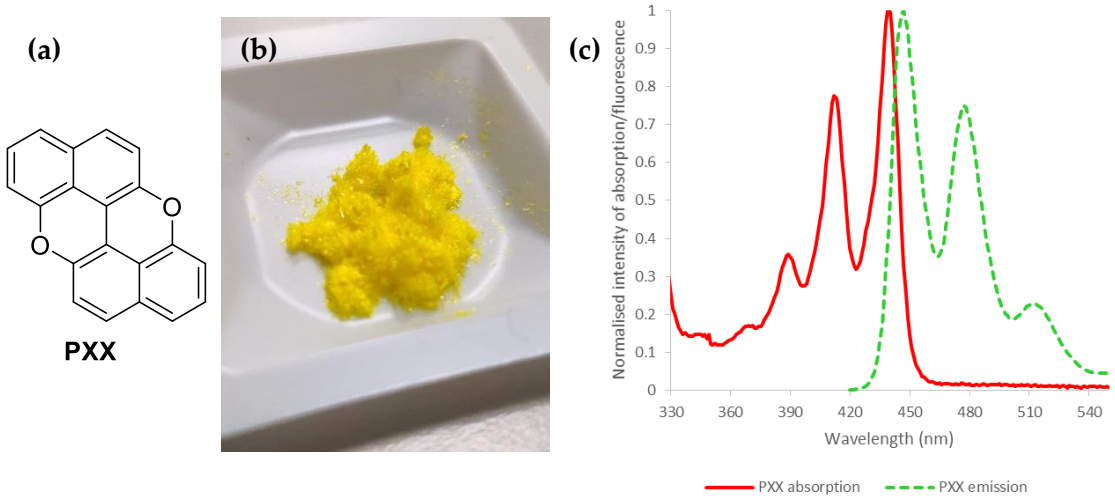

Figure 6
PXX's structure **(a)**, appearance **(b)** and absorption/emission spectra in acetonitrile **(c)**.

Table 14

Photophysical and electrochemical characterisation of PXX.[a]

Absorption λ (nm)	439
Emission λ (nm)	447
τ (ns)	5.1
Φ	0.60
$E^{1/2}(PXX^{\cdot+}/PXX)$	+ 0.77 V
$E^{1/2}(PXX^{\cdot+}/PXX^{*})$	- 2.00 V
$E^{1/2}(PXX/PXX^{\cdot-})$	- 2.16 V
$E^{1/2}(PXX^{*}/PXX^{\cdot-})$	+ 0.61 V

[a] Photophysical data determined in acetonitrile. Electrochemical data determined in acetonitrile *vs* SCE.[23]

Besides visible light absorption, of uttermost interest are the electrochemical properties of both ground state and excited state PXX. In the excited state a remarkable reduction potential of -2.00 V has been calculated,[23] suggesting the possibility of efficient SET reduction of a number of organic substrates (**Figure 7**). The resulting PXX radical cation will have a discrete potential (+0.77 V), allowing turnover of the photocatalytic cycle *via* oxidation of electron-rich reagents. The opposite catalytic cycle with initial oxidation of a substrate from the excited state PXX is also possible, but the lower redox potential (+0.61 V) and evidence from quenching studies in the following suggest this is a minor possible pathway.[23]

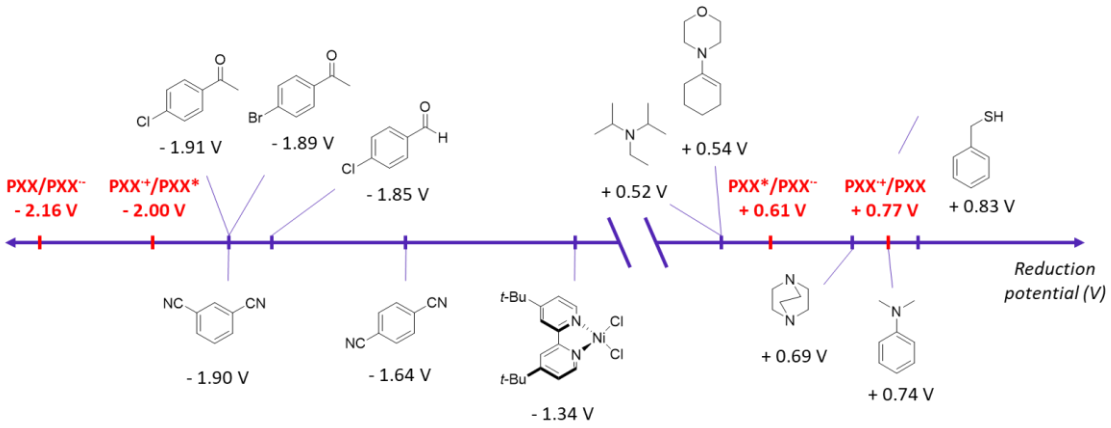

Figure 7

Reduction potentials of various organic compounds compared to the excited state reduction potential of PXX (-2.00 V) and the reduction potential of PXX radical cation (+0.77 V). Values give in acetonitrile *vs* SCE.[8,126]

The photophysical properties suggest using PXX as an alternative to the more common *fac*-[Ir(ppy)$_3$] described in **Section 3.1.1**, possessing a lower reduction potential in the

excited state (-2.00 V for PXX,[23] -1.73 V for *fac*-Ir(ppy)$_3$)[7] at a fraction of the cost.[XIII] Structural simplicity and low cost would also make it convenient when compared to the more structurally complex dyes described in **Section 3.1.1**.

The Bonifazi group carried out some preliminary tests of reactivity: the dehalogenation of organic halides, a benchmark reaction as described in the previous section, was thus chosen.[23] In the presence of DIPEA as electron donor, some electron-poor alkyl and aryl bromides were successfully converted into the corresponding hydrocarbons, in some cases with quantitative conversions (**Scheme 51**).

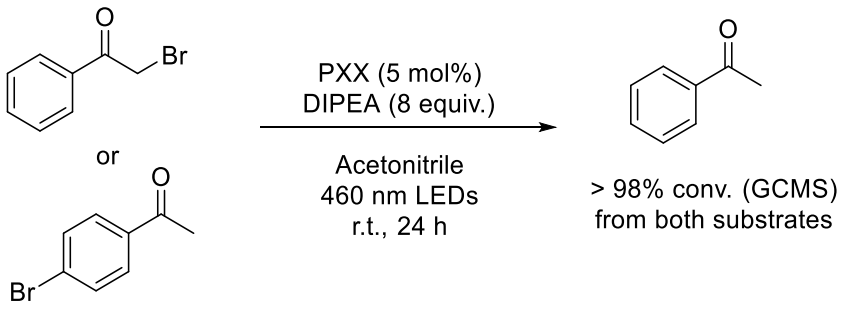

Scheme 51

Bonifazi's procedure for the debromination of organic bromides with PXX as photocatalyst.[23]

The mechanism of dehalogenation of aryl bromides was probed *via* fluorescence quenching studies. As mentioned above, a photoreductive mechanism resulted the most probable (**Scheme 52**), with initial reduction of the aryl bromide to its radical anion **27**, and subsequent expulsion of bromide to leave aryl radical **28**. The radical cation of PXX, formed after reduction of the bromide, can then oxidise DIPEA to its radical cation **29**, prone of HAT from radical **28**, delivering the product and oxidised DIPEA.

Electron paramagnetic resonance (EPR) experiments were also carried out on the reaction with 4-bromobenzaldehyde. A radical trap (*N-tert*-Butyl-α-phenylnitrone, PBN) was used to intercept organic radicals formed during the reaction. The nitroxide resulting from the addition of the aryl radical to PBN was detected and characterised (**Scheme 53**), confirming the formation of aryl radicals such as **28** in the reaction mixture.

[XIII] The cost of PXX, taking into consideration only raw materials, have been estimated as £ 4.01/mmol. If the same calculation is run for *fac*-[Ir(ppy)$_3$], for example, the cost rises to £ 48.75/mmol (while it is sold at £ 655/mmol). See **Section 6.3** for details. Other Ir photocatalysts, bearing more complex ligands, are even more expensive to produce.

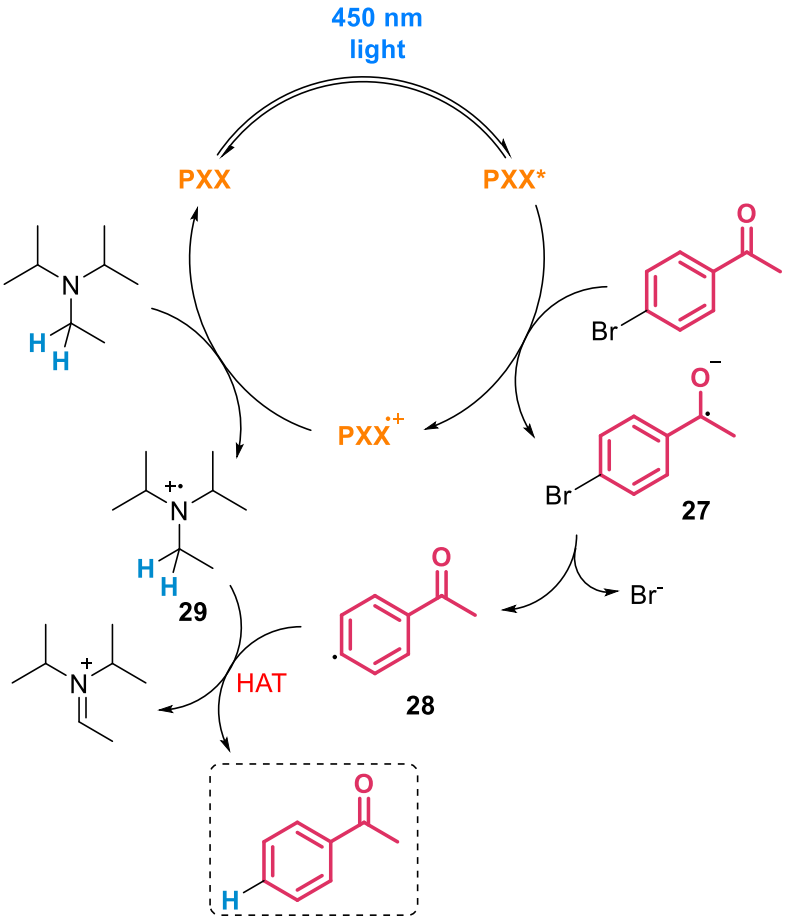

Scheme 52

Postulated mechanism for PXX-catalysed aryl bromide dehalogenation reaction.[23]

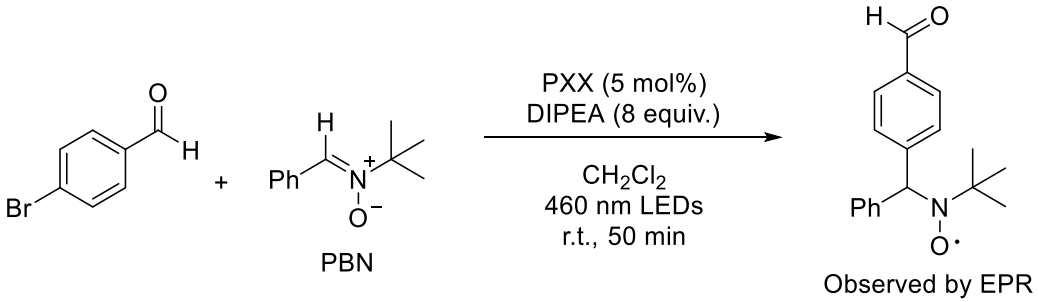

Scheme 53

EPR studies on the dehalogenation of 4-bromobenzaldehyde with PXX.[23]

These results confirmed the initial hypothesis that PXX could work effectively as a highly reducing photocatalyst, and called for further experiments to demonstrate broader reactivity, such as for the formation of carbon-carbon and carbon-heteroatom bonds, and coupling PXX photocatalysis with other catalytic manifolds.[XIV]

[XIV] During the preparation of this thesis and the upcoming manuscript, Dilman and co-workers reported using PXX as photocatalyst for a iododifluoromethylation reaction of alkenes.[260]

3.3 Aim of the project

In the constant development of highly reducing fully organic photocatalytic systems, it's interesting that a simple molecule such as PXX could rival bigger, more complex and more expensive photocatalysts in terms of photoredox properties. While most of the systems presented before have been employed on benchmark reactions, namely dehalogenations and additions to radical traps, such systems, and PXX in particular, should be ideal photocatalysts for more complex transformations. With this project simple and complex radical reactivity triggered by the reducing abilities of the excited state of PXX are demonstrated. The first attempts focused on the above mentioned benchmark transformations; however, looking at the use of more common Ir(III) photocatalysts, dual catalytic systems where the photoredox cycle is coupled to a second catalytic cycle (being from an organocatalyst or metallocatalyst) are next examined.

3.4 Activation of organic (pseudo)halides and addition to radical traps

While the dehalogenation reaction of electron-poor aryl halides had already been demonstrated by the Bonifazi group,[23] the next step involved the use of PXX as a photocatalyst for the formation of C–C bonds by introducing a radical trap.

3.4.1 Activation of aryl halides: addition to benzene

As initial test, 4'-bromoacetophenone was chosen as known substrate for reduction by PXX*, along with a large excess of benzene as radical trap (**Table 15**). Acetonitrile was used as solvent as it was found to be the best in the dehalogenation reactions,[23] and different bases were then examined. Initial results were promising as low to modest yields of coupled product **30a** were obtained (entries 1-7); in particular, DBU afforded 35% NMR yield (entry 3). Debromination byproduct **31** was omnipresent however, often in a similar yield to **30a**: this results suggest addition to benzene or the turnover of the photoredox cycle is a slow step, with which HAT can compete. It is not surprising that DIPEA, particularly prone to HAT, affords mostly **31** as main product (entry 6). Changes in base loading (entry 8), concentration (entry 9) or PXX loading (entry 10) did not provide improved yield of **30a**. Solvents were then screened: a range of polar solvent provided product with efficiencies close or inferior to acetonitrile (entries 11-13), while CH_2Cl_2 quenches reactivity (entry 14). When the reaction is run in neat benzene however,

a pleasing increase in yield (42%) is observed, along with reduced amount of byproduct (**30a**:**31** about 5:1). If the same reaction is run at 25 °C (with efficient fan cooling) the yield drops drammatically (19%, entry 16), suggesting the need for an increased temperature for this reaction to work. When run longer (40 h, entry 17) there is no change besides some development of **31**. If at this point an additional batch of PXX (2 mol%) is added (entry 18), the reaction provides 53% yield after a total of 64 h (entry 18).

Table 15

Screening and optimisation for the arylation of 4'-bromoacetophenone with benzene.

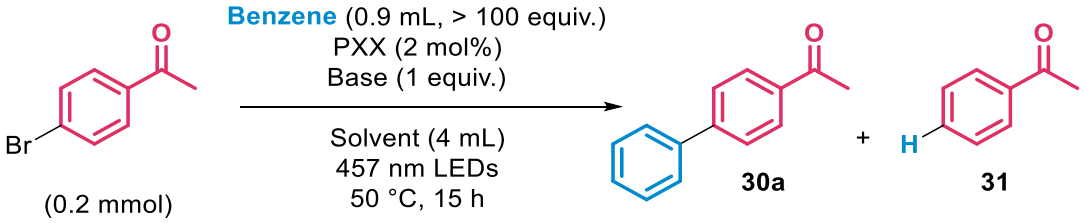

Entry	Base	Solvent	Other modif.	30a (%)[a]	Conversion (%)[a]	31 (%)[a]
1	none	Acetonitrile	-	5	30	5
2	DABCO	Acetonitrile	-	18	38	12
3	DBU	Acetonitrile	-	35	78	37
4	TMG	Acetonitrile	-	17	40	18
5	Cs_2CO_3	Acetonitrile	-	17	35	12
6	DIPEA	Acetonitrile	-	9	75	31
7	*t*-BuOK	Acetonitrile	-	18	95	6
8	DBU	Acetonitrile	2 equiv. DBU	30	96	40
9	DBU	Acetonitrile	2 mL ACN	37	80	31
10	DBU	Acetonitrile	5 mol% PXX	31	83	66
11	DBU	DMSO	-	38	92	30
12	DBU	DMF	-	11	86	31
13	DBU	Acetone	-	29	79	38
14	DBU	DCM	-	< 5	14	6
15	DBU	Benzene	-	42	54	8
16	DBU	Benzene	Run at 25 °C	19	26	< 5
17	DBU	Benzene	Run for 40 h	40	60	17
18	DBU	Benzene	Run for 64 h[b]	53	75	18

[a] Determined by ^{1}H NMR analysis of reaction mixtures, using 1,3,5-trimethoxybenzene or nitromethane as internal standard. [b] Additional 2 mol% PXX added after 40 h.

3.4.2 Activation of aryl halides: addition to pyrroles and other traps

Since little improvement was obtained with the reaction with benzene, it appeared wise turning to electron-rich systems, which should be able to capture the aryl radical more efficiently. The same reaction with *N*-methylpyrrole was thus tested (**Table 16**). Indeed, this reaction is overall more efficient, and better yields of **30b** were obtained. Bases (entries 1-6) and solvents (entries 8-10) have been examined, and the best combination resulted the use of Cs_2CO_3 in acetonitrile (entry 6, 82% NMR yield), even though other combinations are also possible, giving similar outcomes (entries 1, 2, 9, 10).

Table 16

Screening and optimisation for the arylation of 4'-bromoacetophenone with *N*-methylpyrrole.

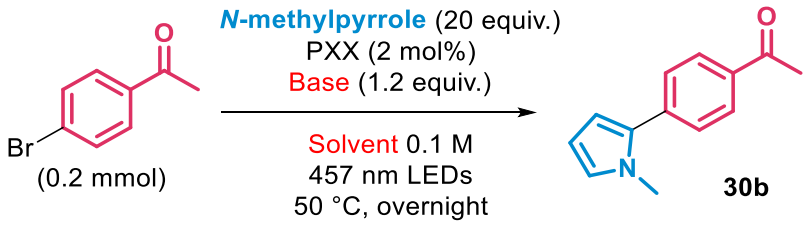

Entry	Base	Solvent	Yield (%)[a]	Conv. (%)[a]
1	DBU	Acetonitrile	76	100
2	BTMG	Acetonitrile	79	100
3	DIPEA	Acetonitrile	57	100
4	TEA	Acetonitrile	56	89
5	DABCO	Acetonitrile	35	43
6	Cs_2CO_3	Acetonitrile	82 (71)	> 95
7	Cs_2CO_3	DMF	46	100
8	Cs_2CO_3	DMA	48	100
9	Cs_2CO_3	DMSO	77	> 95
10	Cs_2CO_3	Acetone	76	> 95

[a] Determined by ^{1}H NMR analysis of crude products, using nitromethane as internal standard. Isolated yields in parentheses.

The newly found conditions were then applied to different aryl bromides (**Scheme 54**). While the ketone and aldehyde-containing derivative **30b** and **30c**, respectively, were obtained in good isolated yields (> 70%), the reactivity resulted poor with all other compounds starting from the corresponding ester (**30d**) and nitrile (**30e**). The reaction with bromopentafluorobenzene to compound **30f** also gave an overall 19% NMR yield of the two arylated isomers,[127] while benzimidazole **30g** was observed in only traces amounts.

Inspired by the results obtained and during her work on other dyes, Oliwia Matuszewska (PhD candidate in the Bonifazi group) found that by applying conditions analogous to those reported by König and co-workers[115] while using PXX, a wider range of aryl halides (chlorides in particular) could be functionalised. These conditions involve the use of DIPEA as base in DMSO as solvent, at room temperature. Pleasingly, limited amounts of dehalogenation were usually observed despite the use of DIPEA as base. Using these conditions a scope for the transformation was defined (**Scheme 55**). While the efficiency of this method with the acetophenone derivative **30b** is modest (53% yield), ester **30d**, nitriles **30e** and **30h** and pentafluorophenyl derivative **30f** are all obtained in

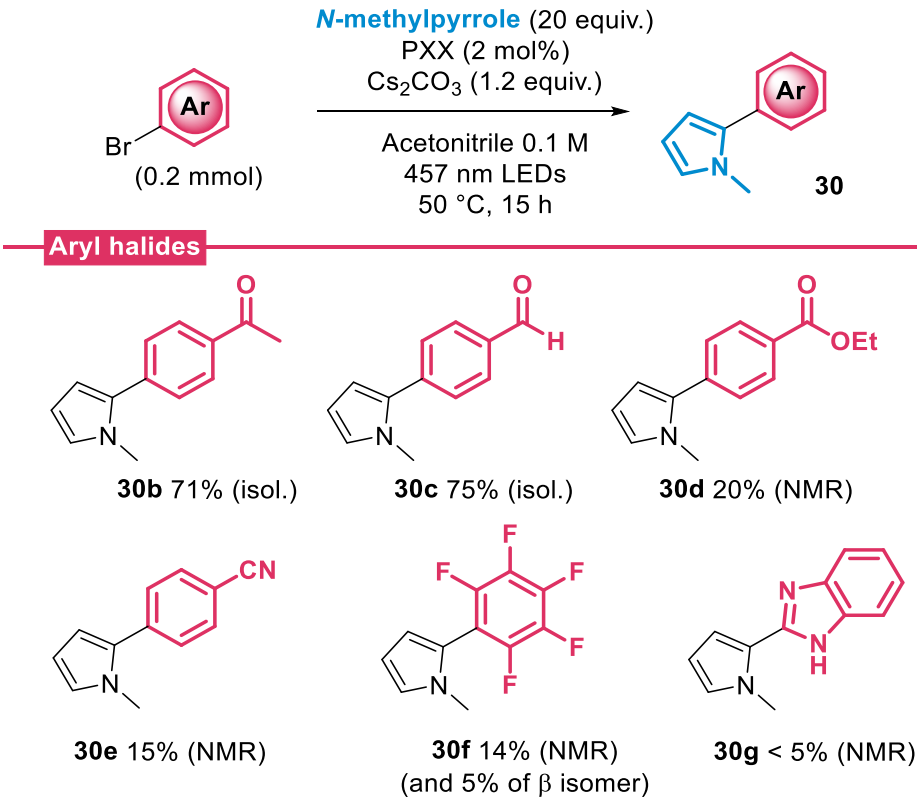

Scheme 54

Attempted scope of aryl bromides for the arylation with *N*-methylpyrrole. NMR or isolated yields are reported as specified.

good yields (53-69%). Unfortunately, heterocycle-containing **30g** and **30i** are obtained in low NMR yields. Other radical traps were tested using these conditions. Electron-rich aromatics gave mixed results: while poor reactivity was obtained with thiophene (to compound **30j**), a good reactivity was found with 1,3,5-trimethoxybenzene (**30k**, 58% yield). Pleasingly, the photo-Arbuzov reaction[108] worked well, and in the reaction with triethylphosphite compound **30l** was obtained in 66% yield. On the other hand, the reaction with bis(pinacol)diboron to compound **30m** proved difficult; inspired by the literature on this specific example,[128,129] Oliwia tried some slightly different sets of conditions but no improvement was obtained.

Mechanistically, the most likely pathway is outlined in **Scheme 56**.[95] In this mechanistic scenario, after reduction of the aryl halide and formation of the aryl radical, this can attack suitable unsaturated systems (radical traps) to form the new desired bond. The oxidation of the resulting radical adduct by PXX radical cation closes the catalytic cycle. This hypothesis is supported by the redox potentials and quenching experiments reported in **Table 17**. The excited state of PXX is capable of reducing all the aryl halide

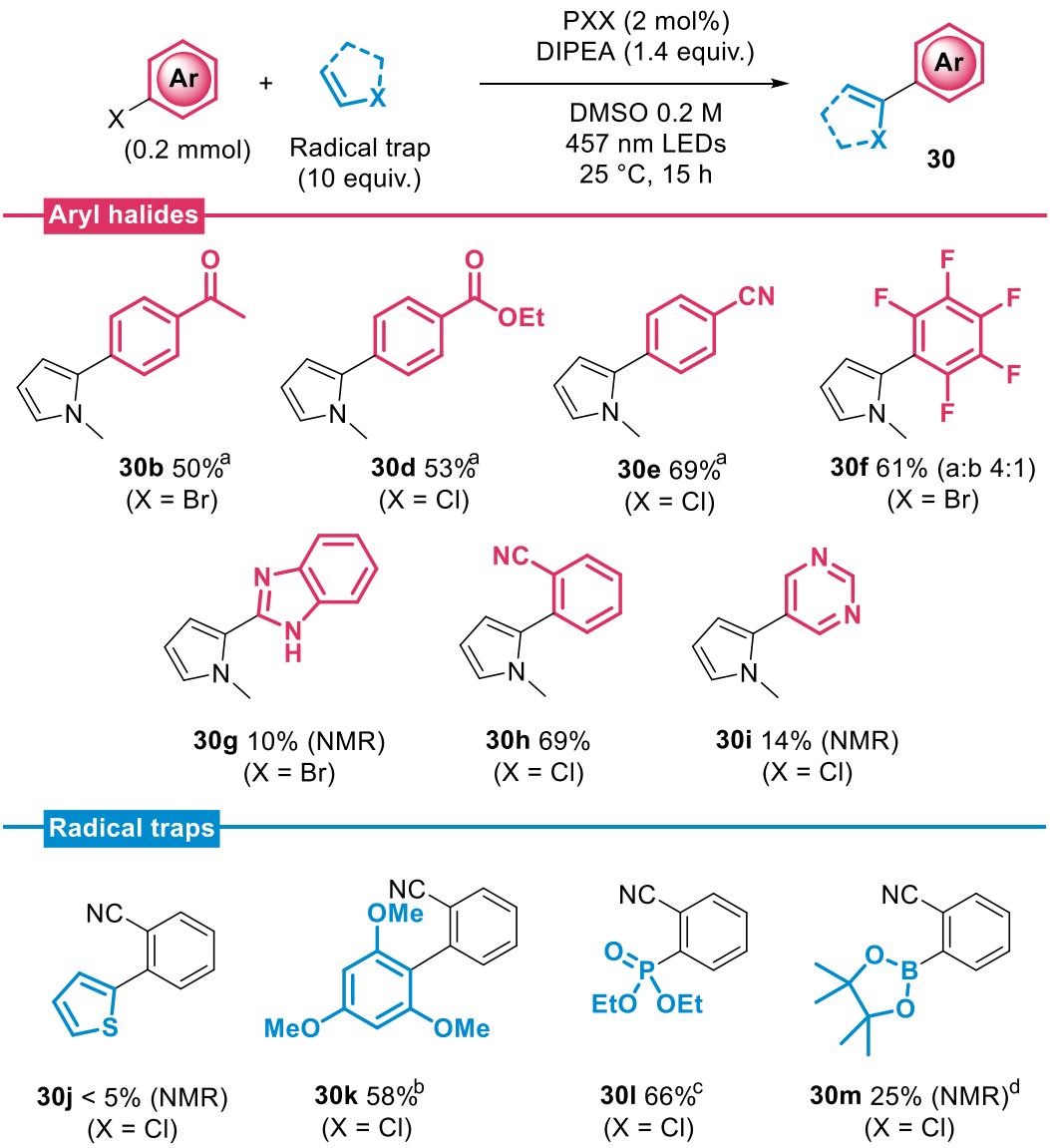

Scheme 55

Scope of aryl halides and radical traps using the second method for aryl halide arylation and other functionalisations. Isolated yields are reported unless otherwise stated. Notes: [a] Experiment performed by Oliwia Matuszewska, Cardiff University. [b] 20 equiv. of 1,3,5-trimethoxybenzene were used. [c] 5 equiv. of triethyl phosphite were used. [d] 3 equiv. of B_2pin_2 used, along with a DMSO:H_2O 9:1 solvent system.

substrates analysed, as suggested by their higher reduction potential compared to that of PXX* (- 2.00 V *vs* SCE). PXX* could have enough oxidising power (+0.61 V *vs* SCE) to oxidise DIPEA (+0.52 V *vs* SCE, entry 5), but not *N*-methypyrrole (+1.04 V *vs* SCE, entry 6). Quenching constants for the aryl halides (entries 1-4) are one to three orders of magnitude higher than those for DIPEA (entry 5) or *N*-methylpyrrole, for which quenching was not observed (entry 6).

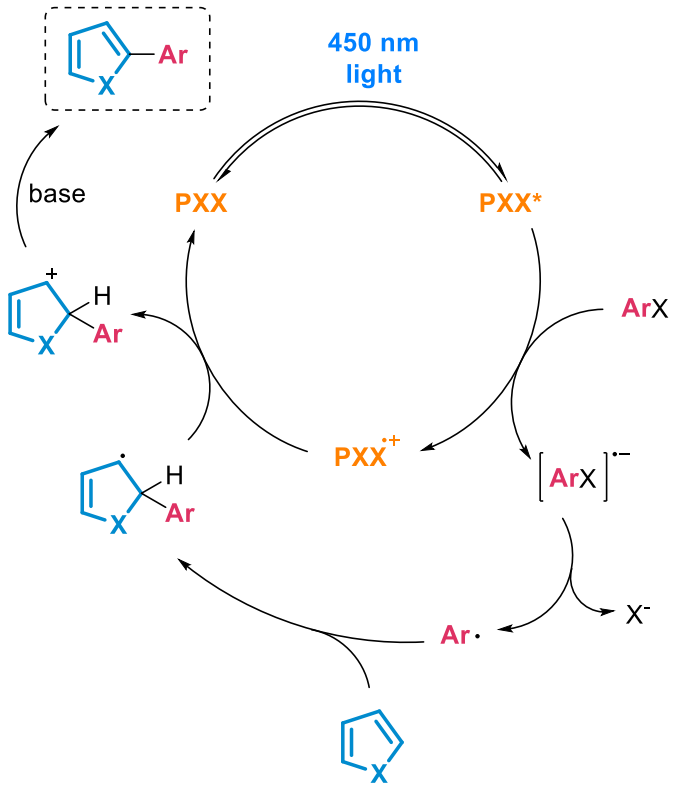

Scheme 56

Postulated mechanism for the PXX-photocatalysed addition of aryl radicals to radical traps (in this case, a 5-membered heterocycle).

Table 17

Redox potentials and quenching studies on PXX ($4 \cdot 10^{-5}$ M in acetonitrile, intensity of fluorescence recorded at 466 nm).

Entry	Quencher	E_{red} (V *vs* SCE)[a]	k_Q ($M^{-1}s^{-1}$)[b]
1	4'-Bromoacetophenone	-1.89 (r)	$1.3 \cdot 10^{10}$
2	4'-Chloroacetophenone	-1.91 (r)	$1.1 \cdot 10^{10}$
3	4-Bromobenzaldehyde	-1.76 (r)	$1.8 \cdot 10^{10}$
4	2-Chlorobenzonitrile	-1.80 (r)	$3.2 \cdot 10^{8}$
5	DIPEA	+0.52 (o)	$3.5 \cdot 10^{7}$
6	*N*-Methylpyrrole	+1.04 (o)	No quenching

[a] Determined in DMF (entry 4) or acetonitrile (other entries); (r) refers to a reduction of the quencher, (o) to an oxidation of the quencher. Obtained from references [8] (entries 1-3, 5-6) and [130] (entry 4). [b] Entries 1, 3, 5: obtained from reference [23]. Entries 2, 4, 6: calculated from Stern Volmer plots as $k_Q = K_{SV}/\tau_0$ where τ_0 is the lifetime of PXX* without quencher (5.1 ns in acetonitrile);[23] see **Section 6.11**.

3.4.3 Activation of alkyl and perfluoroalkyl (pseudo)halides

In a similar fashion as with aryl radicals, activated alkyl radicals have also been subjected to reactions with electron-rich arenes.[131] As a proof of concept, the conditions developed by the Stephenson group for the alkylation of heteroarenes using halomalonates were replicated: diethyl 2-bromo-2-methylmalonate was reacted with an excess of indole as

radical trap, along with PXX as photocatalyst and lutidine as base (**Scheme 57**). The coupled product **32** was obtained with good yield, demonstrating the ability of PXX to promote the reaction of activated alkyl halides as well.

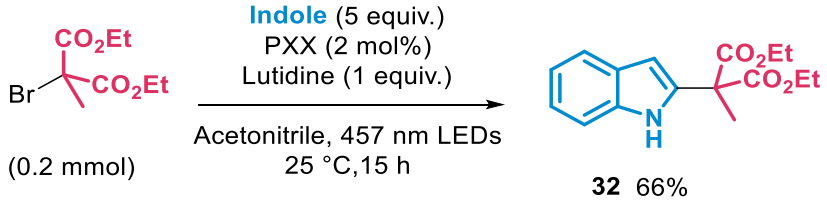

Scheme 57

Reaction of a bromomalonate substrate with indole as radical trap.

Perfluoroalkyl (pseudo)halides are another class of compounds that was taken into consideration as a mean to introduce perfluoroalkyl groups in organic molecules. The trifluoromethyl group in particular has found wide applications in the pharmaceutical industry for the electronic and steric properties it imparts on the molecules it is inserted into.[132,133] The reduction of perfluoroalkyl (pseudo)halides generates perfluoroalkyl radicals, particularly prone to attack on electron-rich systems. Inspired by the work of the MacMillan group on arene trifluoromethylations,[134] we tested the use of triflyl chloride with two different heteroarenes (**Scheme 58**). In both cases, trifluoromethylated products were readily obtained. In the reaction with *N*-methylpyrrole both mono- and bis-trifluoromethylation were observed: **33a** in 33% yield and **33b** in 57% yield, respectively. Only ^{19}F NMR yields are provided for this entry due to volatility of these products. With 3-methylbenzofuran product **33c** was obtained in 59% yield (by NMR) but some was lost during purification due to volatility. Pleasingly, when the same conditions were applied to the reaction with 3-methylbenzofuran and perfluorohexyl iodide, an 82% yield of coupled product **33d** was obtained.

3.5 Merging with organocatalysis: β-arylation of carbonyl compounds

The merging of photoredox catalysis with organocatalysis has been among the initiators of the growing interest in this field, starting with the early work on aldehyde α-alkylations from Nicewicz and MacMillan.[4] Typical organocatalysis intermediates such as enamines and iminium ions can readily participate in redox and radical reactions, both photocatalytic and from their intrinsic photoreactivity as well, as will be discussed in **Chapter 4**.[14]

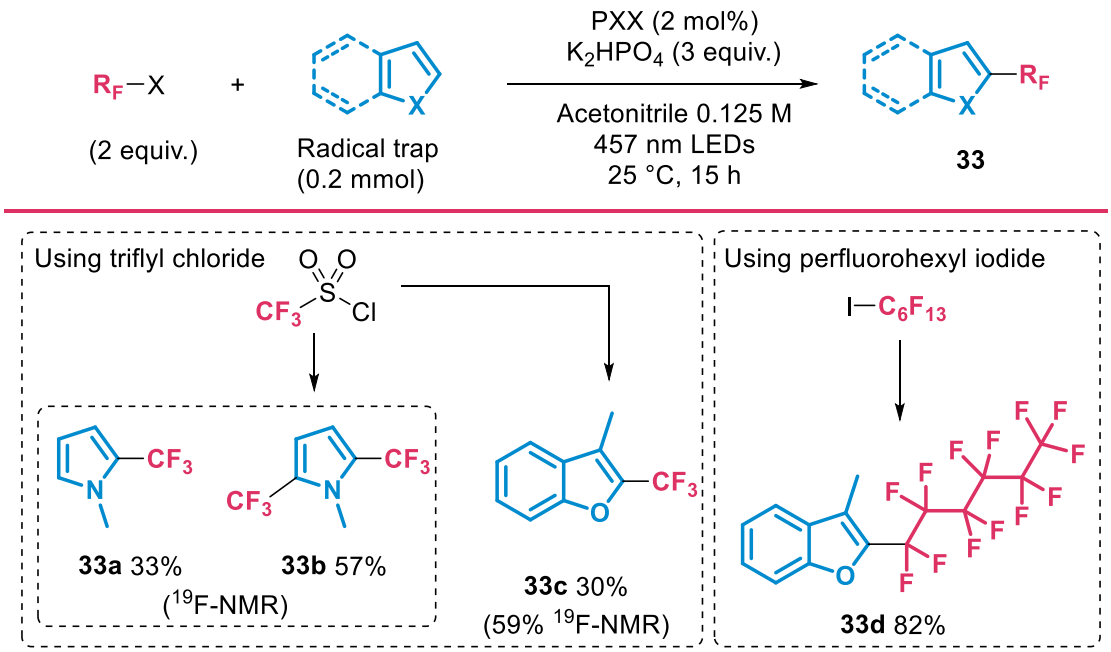

Scheme 58

PXX-catalysed perfluoroalkylation of heteroarenes. ^{19}F NMR yields determined using C_6D_6 as internal standard.

3.5.1 Scope of the transformation

In 2013-2015 the MacMillan group reported a series of interesting β-functionalisations of saturated carbonyl compounds (aldehydes and cyclic ketones). While the α position of carbonyl derivatives is easily accessible from the formation of enolate or enamine intermediates, limited examples were reported for the functionalisation of β positions without using α,β-unsaturated compounds in the first place. Arylation,[92] Giese addition,[135] aldol[93] and Mannich[136] reactions were thus described, all relying on similar mechanistic hypotheses. The arylation reaction in particular was carried out with *fac*-[Ir(ppy)$_3$] as photocatalyst and electron-poor benzonitriles as reaction partners. When the reaction with PXX was tested on 1,4-dicyanobenzene (**Scheme 59**), a good reactivity was found (79% yield) even if long reaction times (64 h) were necessary for complete conversion into coupled product **34a**. Applying the reaction conditions to other ketones good yields (60-79%) where obtained with different cyclohexanone derivatives (**34a-c**). Cyclopentanone **34d** was also obtained in 54% yield, while cycloheptanone **34e** could not be recovered in good amounts (less than 10% yield by NMR). When turning to other cyanoarenes only 4-cyanophthalide afforded **34g** in a modest 35% yield. Other substrates

provided limited or no conversion (**34f**, **34i**) or complex reaction mixtures (**34h**). Careful tuning of the reaction conditions (for example the organocatalyst) might be necessary to allow specific substrates to work in this reaction.

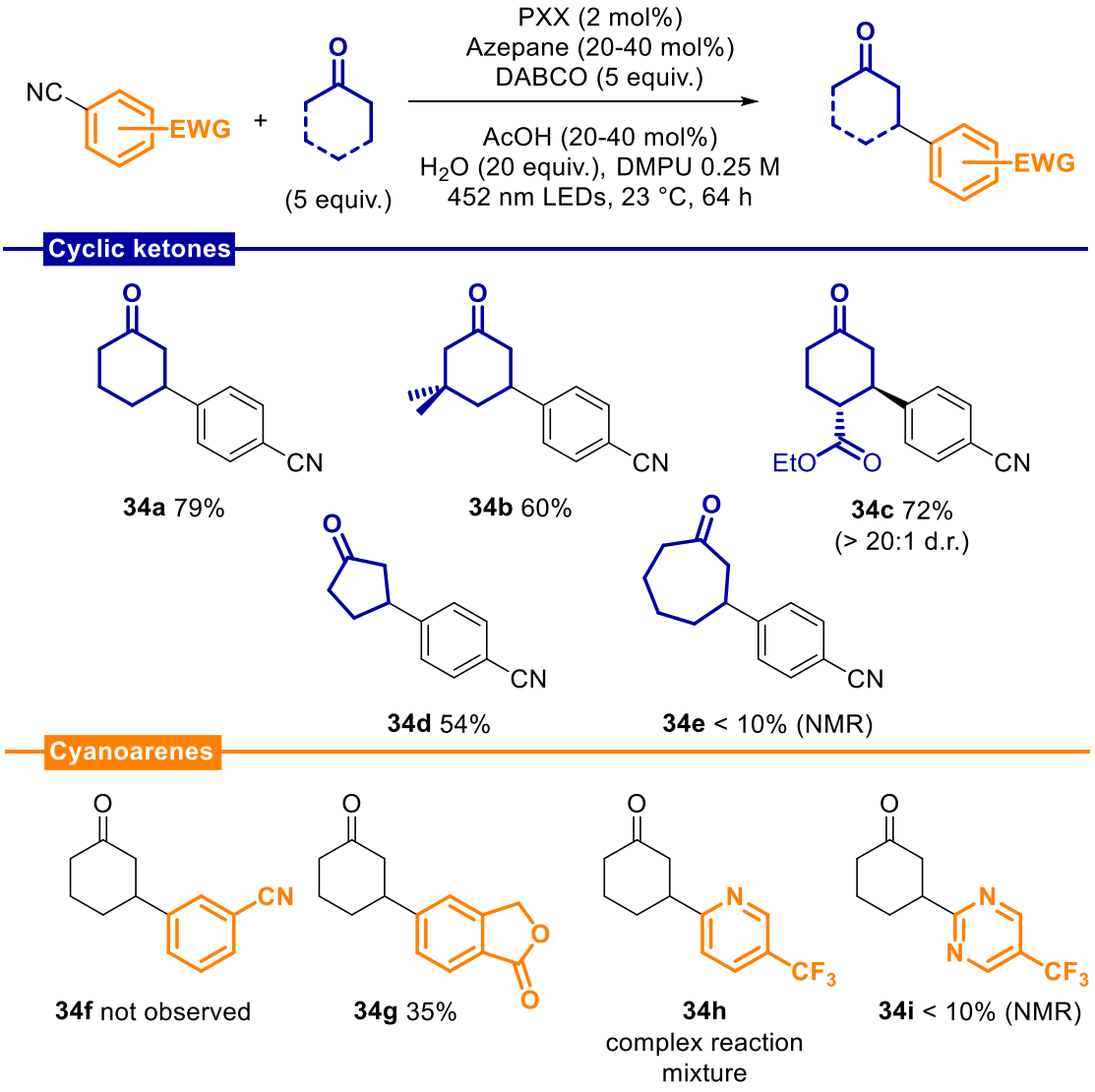

Scheme 59
Scope of the β-arylation of cyclic ketones with cyanoarenes.

When the same reaction, with slightly different conditions, was attempted on saturated aldehydes (**Scheme 60**) good results were initially obtained (50-75% yield depending on reaction times); however, later attempts consistently afforded reduced yield (less than 40%) and it was not possible to quickly identify the source of this difference. The suspect lies on the organocatalytic cycle, as the photocatalyst batch is the same as used for the β-arylation of cyclic ketones.

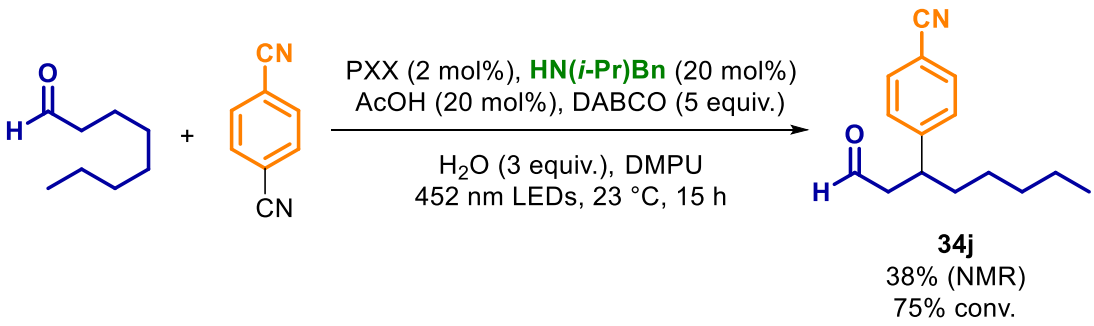

Scheme 60
Results on the β-arylation of octanal with 1,4-dicyanobenzene.

3.5.2 Mechanistic considerations

The commonly accepted mechanistic hypothesis, based on thermodynamic considerations, is reported in **Scheme 61**.[92] Initial reduction of an electron-poor benzonitrile by the excited state photocatalyst allows formation of persistent radical anion **35**.[137] The other half of the photoredox cycle is thought to proceed through oxidation of enamine **36** to the corresponding radical cation **37a**. While oxidation of **36** by the oxidised state of the photocatalyst is reported, later studies suggest the intervention of DABCO as redox mediator is also possible.[136] In intermediate **37a** the allylic protons have increased acidity due to the presence of the radical cation, and extraction of one of these protons by DABCO (as base) forms 5π species **38a**, which can then react through radical-radical coupling with **35** to afford the new C–C bond in intermediate **39**. Expulsion of cyanide and hydrolysis of the resulting **40** allows formation of the final product and turnover of the organocatalytic cycle.

The feasibility of this reaction with PXX was checked *via* electrochemical and fluorescence quenching experiments (**Table 18**). Four possible substrates (**41a-d**) all show reduction potentials higher than that of PXX* (-2.00 V *vs* SCE) and high quenching constants (entries 1-4).[XV] Other reaction components (entries 5-9) show either no quenching or quenching constants at least two orders of magnitude lower. For entries 7-9, this would involve oxidation of the quencher by PXX*, which has a low oxidation potential (+ 0.5 V *vs* SCE). Some degree of oxidation was shown for DABCO (entry 9) and the combination of cyclohexanone, acid and azepane (entry 8). ^{1}H NMR analysis of

[XV] Since quenching studies show similar results for all the substrates examined, it is possible that the lack of reactivity found for substrates **41b-d** (**Scheme 59**) derives from a non-optimised organocatalytic system.

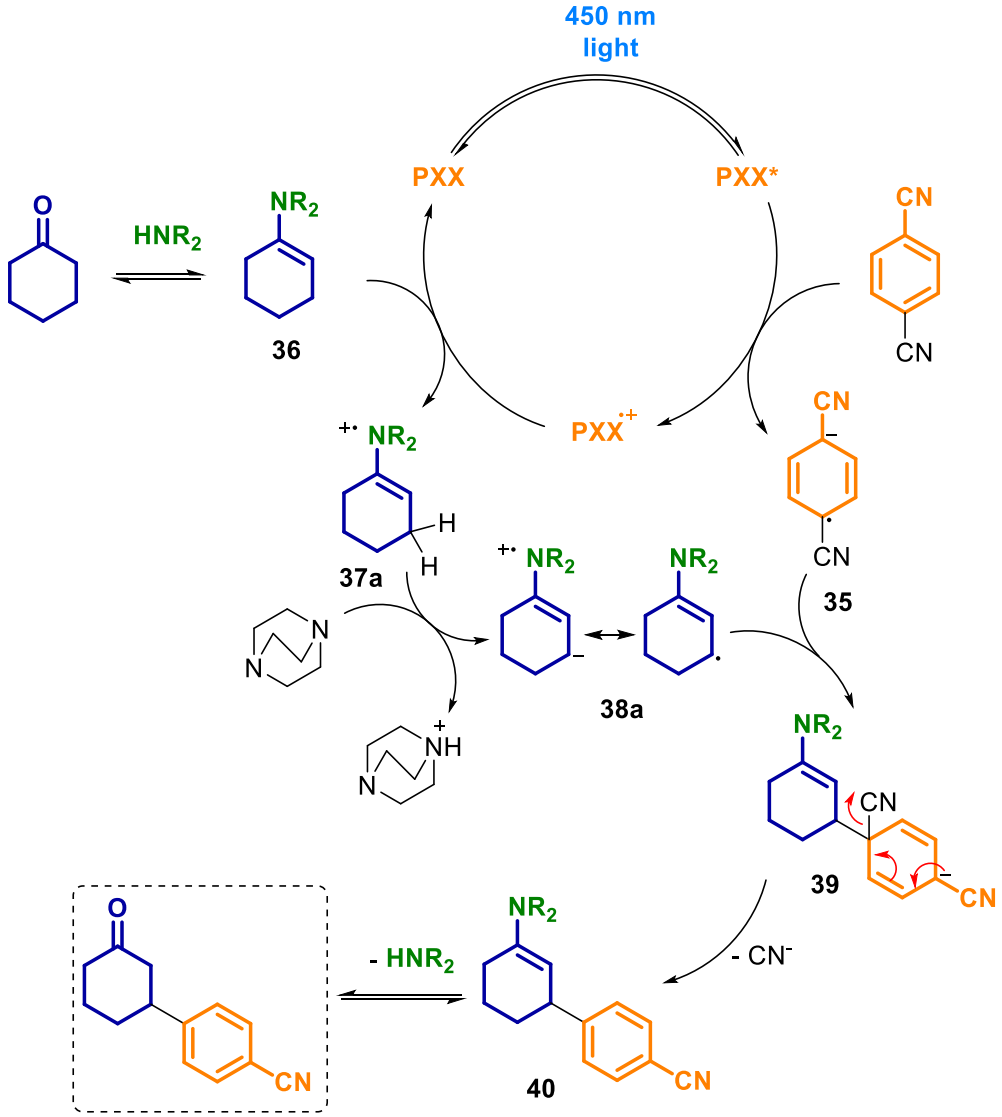

Scheme 61

Postulated mechanism for the photo-organocatalysed β-arylation of carbonyl compounds (in this case, cyclic ketones).[92]

the combination of reagents in entry 8 show minimal formation (< 5%) of enamine **36**, which is considered to be the species responsible of the quenching observed: due to the amounts formed the actual quenching constant might be at least 20 times higher (> $8 \cdot 10^8$ $M^{-1}s^{-1}$). In any case, the higher oxidation potential of PXX radical cation (+0.77 V *vs* SCE) should be sufficient to oxidise both the enamine and DABCO more efficiently. These results tend to support the mechanism detailed above.

Table 18

Redox potentials and quenching studies on PXX ($4 \cdot 10^{-5}$ M in acetonitrile, intensity of fluorescence recorded at 466 nm).

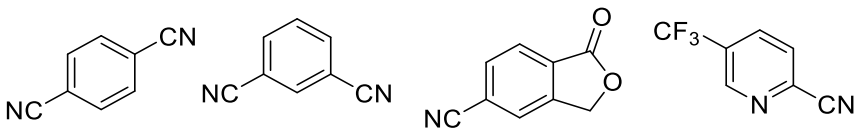

41a **41b** **41c** **41d**

Entry	Quencher	E_{red} (V *vs* SCE)[a]	k_Q ($M^{-1}s^{-1}$)[d]
1	1,4-dicyanobenzene **41a**	-1.64 (r)	$1.6 \cdot 10^{10}$
2	1,3-dicyanobenzene **41b**	-1.90 (r)	$1.2 \cdot 10^{10}$
3	4-cyanophthalide **41c**	-1.59 (r)	$1.6 \cdot 10^{10}$
4	Substrate **41d**	-1.53 (r)	$1.5 \cdot 10^{10}$
5	Cyclohexanone	-2.33 (r)	No quench
6	Cyclohexanone + AcOH	-	No quench
7	Azepane	≅ +0.9 (o)[b]	No quench
8	Cyclohexanone + AcOH + Azepane	+0.3 - +0.5 (o)[c]	$4.1 \cdot 10^{7}$
9	DABCO	+ 0.69 (o)	$2.2 \cdot 10^{8}$

[a] Determined in acetonitrile; (r) refers to a reduction of the quencher, (o) to an oxidation of the quencher. Entries 3, 4: experimentally determined (see **Section 6.10**). Other entries: obtained from reference [8]. [b] Typical values for cyclic secondary amines. [c] Typical values for enamines of cyclic secondary amines. [d] Calculated from Stern Volmer plots as $k_Q = K_{SV}/\tau_0$ where τ_0 is the lifetime of PXX* without quencher (5.1 ns in acetonitrile);[23] see **Section 6.11**.

Further mechanistic studies on the reaction of cyclohexanone with 1,4-dicyanobenzene were carried out by means of EPR spectroscopy (**Table 19**) with the collaboration of Dr Andrea Folli (Cardiff University). The reaction mixture was simplified by exclusion of water, replacement of DMPU with acetonitrile as solvent and use of stoichiometric amounts of azepane: these conditions were found to be productive, affording 85% NMR yield of product **34a** in 64 h. A radical trap (*N*-*tert*-butyl-α-phenylnitrone, PBN) was used to intercept organic radicals formed during the reaction. Upon irradiation at 450 nm, a signal featuring a distorted triplet of doublets (**Signal 1**, **Figure 8a**) appeared when the full reaction mixture was analysed in the presence of PBN (entry 1). The same signal was also observed when **41a** was excluded from the reaction mixture (entry 3). The spectral features are typical of a nitroxide resulting from addition of a radical species to PBN. Simulations of the spectra revealed **Signal 1** to be the superimposition of two triplets of doublets with the following coupling constants: a_N = 15.2 G and a_H = 1.89 G for the first signal, a_N = 14.7 G and a_H = 2.83 G for the second signal. The values found for the latter are comparable to those reported for some alkyl radicals: for example, for the trapping of *n*-butyl radicals in acetonitrile a_N = 14.88 G and a_H = 3.05 G, while for the trapping of

cyclohexyl radicals in cyclohexane a_N = 14.5 G and a_H = 2.2 G.[138] The formation of alkyl radical adducts such as **37b** or **38b** is thus suggested, deriving from radicals **37a** and **38a** respectively (**Scheme 62**). DFT calculations are ongoing to confirm the identity of the two adducts, as experimental values have not been reported yet. The fact that **Signal 1** is observed even in the absence of **41a** (entry 3) excludes observation of an adduct from addition of **35** to PBN. A singlet signal (**Signal 2**, **Figure 8b**) was obtained when the full reaction mixture was analysed in the absence of PBN (entry 2). The lack of spectral features made it difficult to track the source of this signal, but current hypotheses focus on the formation of solvated electrons in the acetonitrile medium.[139,140]

Table 19

Results of the EPR studies on the reaction of cyclohexanone and 1,4-dicyanobenzene with 450 nm light irradiation.[a]

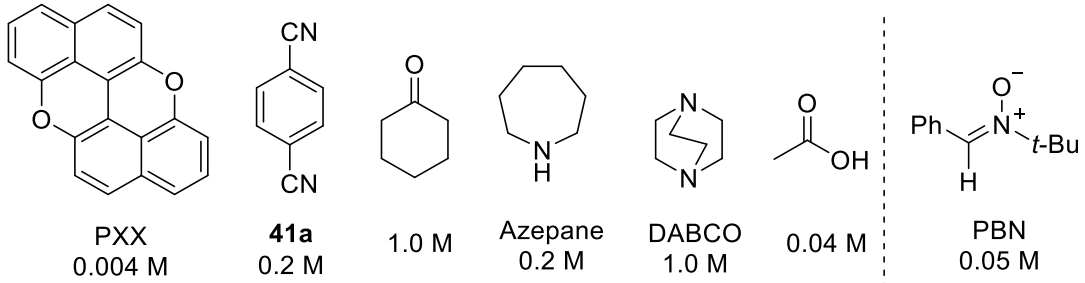

Solvent: acetonitrile

Entry	Reaction components						Outcome
	PXX	**41a**	Cyclohexanone	Azepane	DABCO	PBN	
1	y	y	y	y	y	y	**Signal 1**
2	y	y	y	y	y	n	**Signal 2**
3	y	n	y	y	y	y	**Signal 1**
4	y	n	y	y	y	n	No signal
5	y	y	n	n	y	y	No signal
6	y	y	n	n	n	y	No signal

[a] Labeled "y" when reaction component is present, "n" when it is absent. [b] The solution of the reaction mixture was diluted 1:1 with a 0.05 M solution of PBN: concentrations are thus halved for all components in the samples with PBN present.

While these studies have been helpful in suggesting the formation of radicals **37a** and/or **38a**, necessary for the formation of the C–C bond, it is puzzling that it was not possible to observe radical anion **35** (entry 2), which is considered a persistent radical[137] and was thought to be able to accumulate in the reaction mixture.[92] This intermediate does not react with PBN, as the adduct was also not observed. Moreover, if the identity of the adducts in **Signal 1** is confirmed, the formation of **37b** and/or **38b** would provide further

evidence that enamine **36** can be oxidised by the excited state of PXX, as suggested by the quenching studies (**Table 18**, entry 8). In an attempt to justify the lack of signal originating from **35** the possibility of back electron transfer (BET) with the photocatalyst was considered. For example, it was reported that when photoinduced SET occurs between **41a** and pyrene as photocatalyst, the so-formed **35** can engage in BET with pyrene radical cation dimer with a mechanism that was shown to involve the formation of a radical anion dimer of acetonitrile, a species in equilibrium with solvated electrons (**Scheme 63**).[139,140]

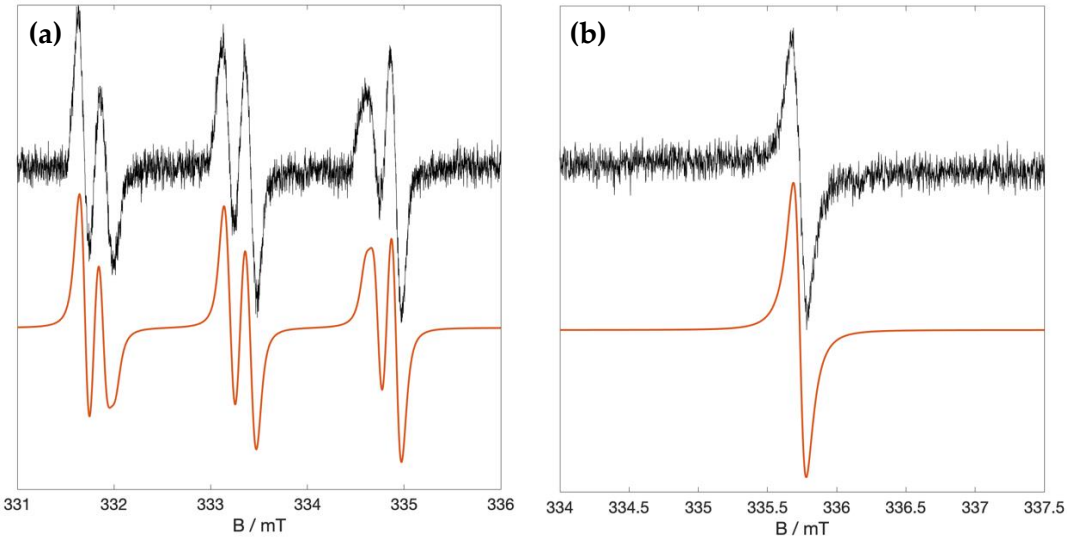

Figure 8
Signal 1 (a) and **Signal 2 (b)** observed during EPR studies with 450 nm light irradiation: experimental spectra in black, above; simulations in orange, below.

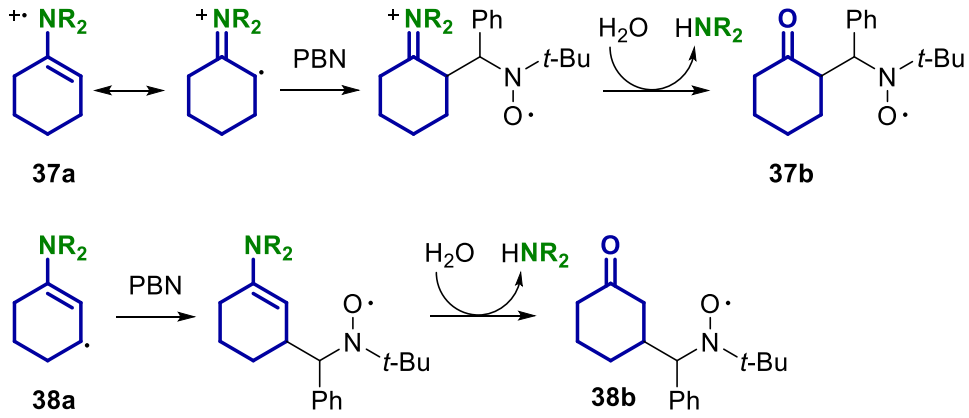

Scheme 62
Formation of α-adduct **37b** and β-adduct **38b** from addition of **37a** and **38a** to PBN, respectively.

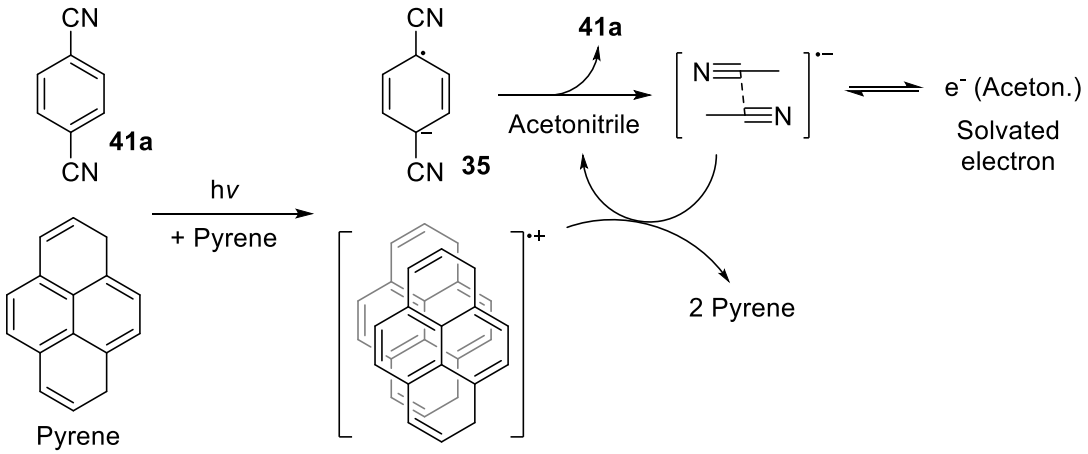

Scheme 63

Postulated mechanism for the back electron transfer between photogenerated **35** and pyrene radical cation dimer.[139]

It is possible a similar BET occurs with PXX, and that this happens fast enough for **35** to be short-lived in the reaction mixture. The formation of solvated electrons would also clarify the lack of multiplicity in **Signal 2**. In this case, the oxidative quenching mechanism presented before would be mostly unproductive for the formation of the product (**Scheme 64**).

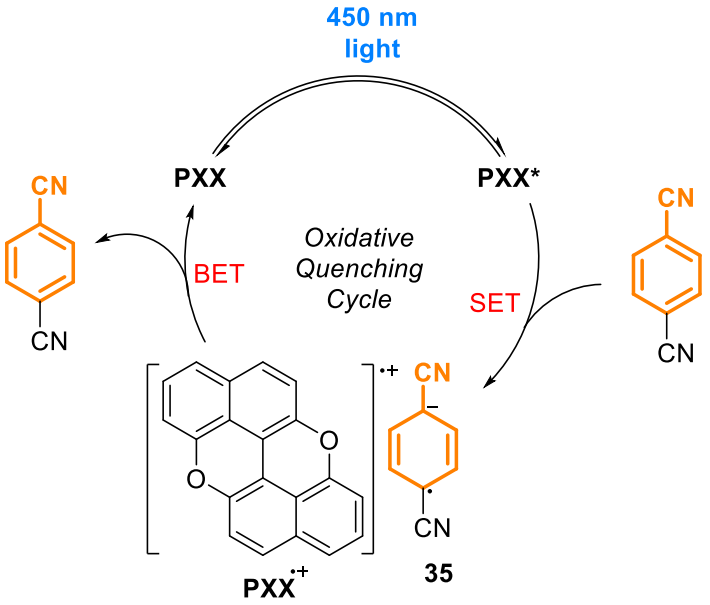

Scheme 64

Hypothetical unproductive SET-BET cycle for the photoreduction of **41a** by PXX excited state.

Combining this hypothesis with the awaited confirmation that enamine **36** can be oxidised by the excited state of PXX even in the absence of **41a** leads to postulating an alternative mechanism based on a reductive quenching cycle (**Scheme 65**). While enamine **36** follows the already discussed pathway to **38a**, the resulting PXX radical

anion can reduce **41a** to **35**; in this scenario BET is not possible, as it would involve neutral PXX. As **35** is now in solution, it can react with **38a** to deliver **39**, from which the product. While this alternative hypothesis is based on results from fluorescence quenching and EPR studies, further experiments such as transient spectroscopy measurements are being planned to better reveal the nature and reactivity of the species involved, so to confirm or challenge any of the mechanisms here discussed.

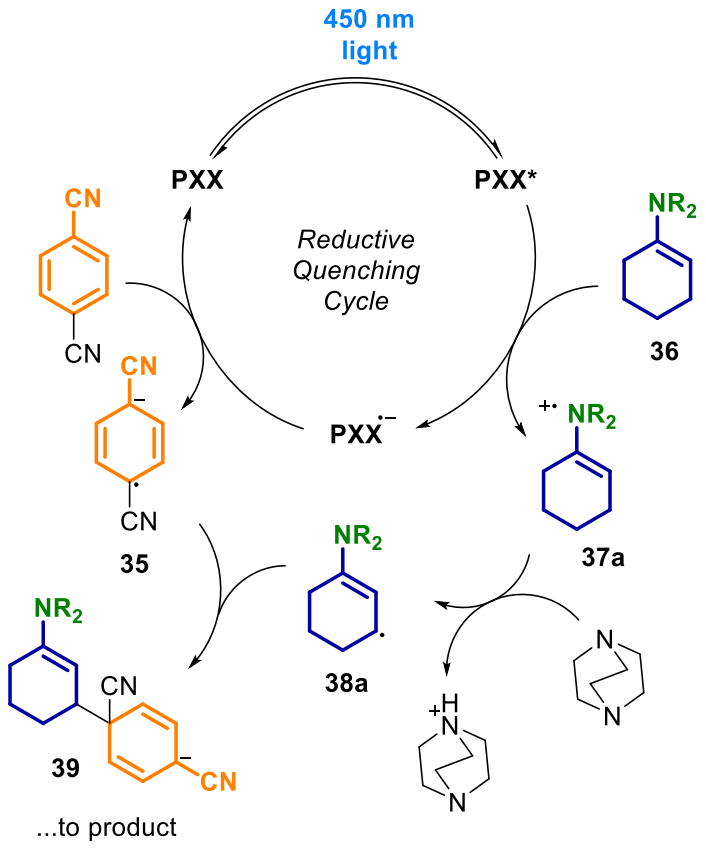

Scheme 65
Alternative mechanism for the organocatalysed β-arylation of ketones with PXX as photocatalyst, based on a reductive quenching cycle.

3.6 Merging with Ni catalysis: cross-coupling reactions

In **Chapter 2** the merging of photocatalysis and Ni catalysis was discussed, highlighting its importance in providing new and complementary routes towards C–C bond-forming cross-coupling reactions. As classical transition metal catalysis also encompasses the formation of different C–heteroatom bonds (the Buchwald-Hartwig amination being the most popular),[141,142] so has the field of Ni-photoredox catalysis.[143] In recent years, different works have reported the formation of C–N,[100,144–146] C–S,[100,147,148] C–O[149,150] and C–P bonds.[151]

3.6.1 On the mechanism of the Ni-photoredox amination reaction

In usual Ni(II)/Ni(0) catalysis the reductive elimination of carbon-heteroatom bonds is particularly difficult:[144,149] the role of the photocatalyst is typically considered to be centred on the modulation of the reactivity of key Ni intermediates, helping overcoming these limitations *via* a change of oxidation state or energy transfer.

The conditions and mechanism for the C–N bond-forming cross-coupling with an Ir photocatalyst in ligand-less conditions are reported in **Scheme 66**.[144] A similar version of this mechanism was initially proposed by the authors and more recently computational work from Ma and co-workers provided further details on the specific steps and the role of the photocatalyst.[152] In some preliminary steps (not reported here) the initial Ni(II) pre-catalyst is reduced to a Ni(0) complex **42a** by action of pyrrolidine, DABCO and the Ir photocatalyst. Once the aryl bromide is bound oxidative addition can occur, forming Ni(II) complex **42b**. The oxidation of this intermediate to the corresponding Ni(III) complex **42c** by the excited state photocatalyst eventually allows reductive elimination, after intermediate steps of bound amine deprotonation to **42d** and ligand exchange to **42e**. After reductive elimination the product is expelled and a new molecule of aryl bromide can bind the so-formed Ni(I) complex **42f**. Finally, the Ni catalytic cycle is turned over by reduction of Ni(I) to Ni(0) by the reduced state of the photocatalyst (Ir(II)), restoring the initial **42a**. Overall, the photocatalyst acts in three steps in modulating the oxidation state of Ni: (i) initial reduction of the Ni(II) salt to **42a**; (ii) oxidation of Ni(II) to Ni(III) (**42b** to **42c**), allowing easier reductive elimination later on; (iii) reduction of the final complex **42f** back to **42a**.

As already mentioned in **Section 3.1.1**, Miyake's group was the first to report the use of an organic photocatalyst for the formation of C–N and C–S bonds through Ni-photoredox catalysis (**Scheme 41**).[100] In that case, conditions similar to those mentioned above were employed for the C–N coupling while using photocatalysts **19** and **20**. Subsequent studies revealed that if irradiation is carried out at 365 nm the photocatalyst can be omitted, suggesting Ni photoactivity to be responsible for the cross-coupling.[153] Extensive photophysical and electrochemical studies using $[Ru(bpy)_3]Cl_2$

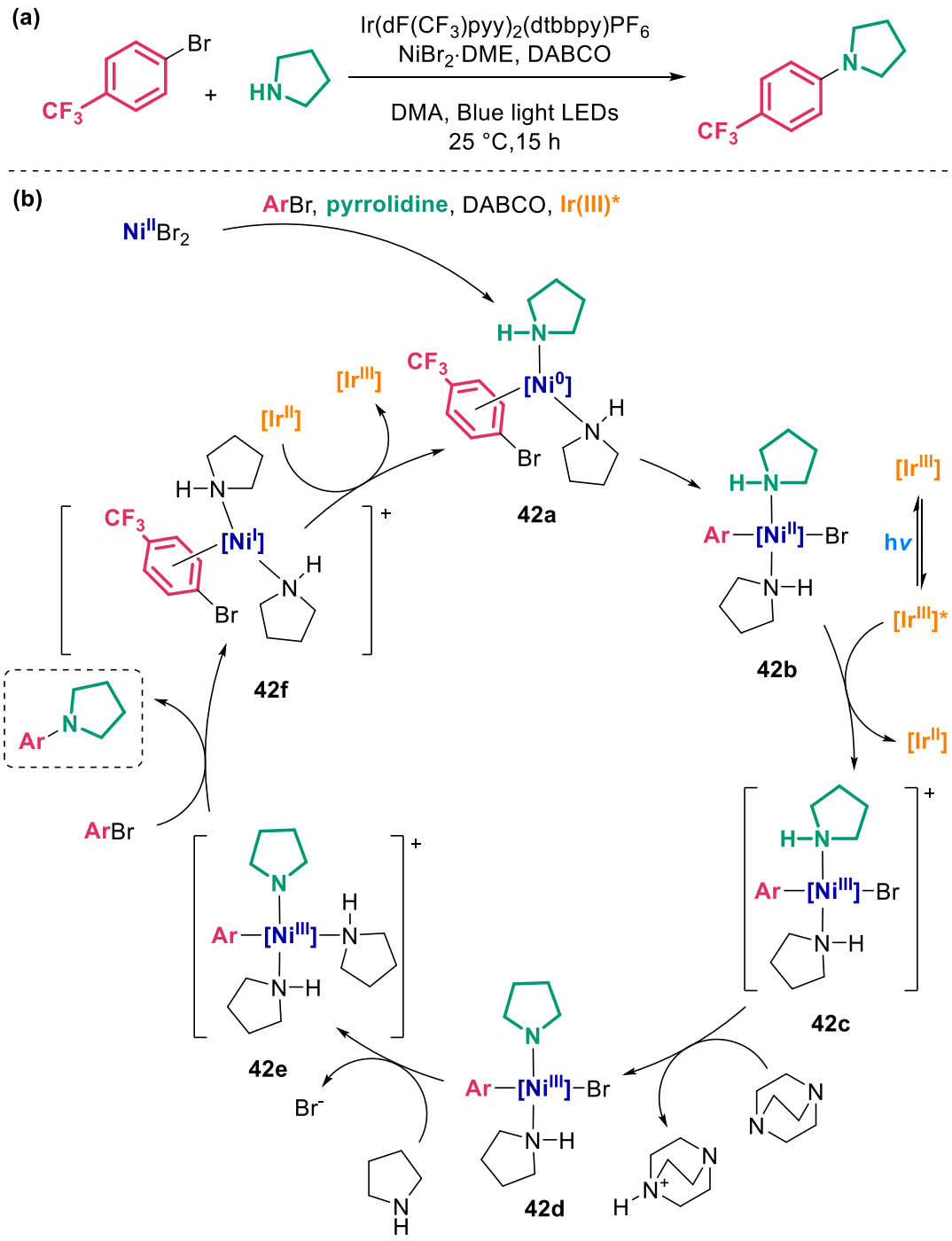

Scheme 66

General conditions **(a)**[144] and calculated mechanism **(b)**[152] for the Ni-photoredox C–N cross-coupling using the Buchwald and MacMillan's conditions.

and **20** as photocatalysts prompted the authors to propose a mechanism based on energy transfer (EnT) rather than electron transfer (**Scheme 67**),[101] an alternative already hypothesised for the Ni-photoredox cross-coupling of sulfonamides[146] and carboxylates[150] with aryl bromides. Coordination of morpholine to the initial Ni salt would form complex **43a** which, upon energy transfer from the excited state

photocatalyst, is sensitised to excited state **43b**. They then hypothesise an internal SET step forming amine radical cation **44a** and Ni(I) complex **43c**. Deprotonation from an additional morpholine will deliver aminyl radical **44b** and Ni(I) complex **43d**. Interaction with the aryl bromide through SET or proper oxidative addition will eventually lead to the final product (these steps were not discussed in detail). From these studies, they rationalised the use of **20** (**Scheme 41**) as photocatalyst: while the original $[Ir(dF(CF_3)ppy)_2(dtbbpy)]PF_6$ complex (**Scheme 66**) is a good photo-oxidant, **20** is the opposite, a good photoreductant, but in an EnT mechanism the overlap between the emission energy of the photocatalyst and the absorption of the Ni complex is more important, which is best with **20** rather than with $[Ru(bpy)_3]Cl_2$ (the Ir photocatalyst was not discussed).

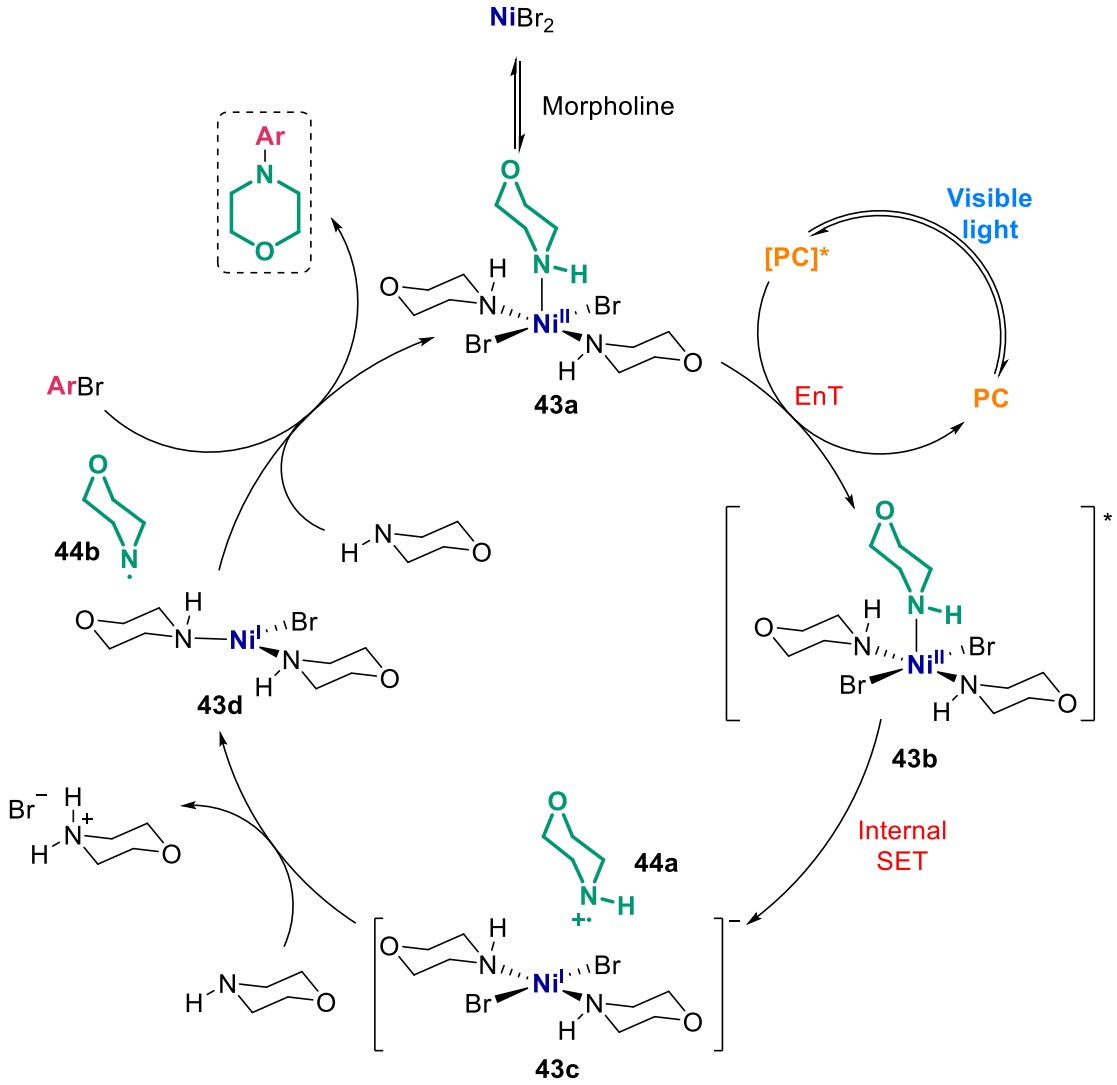

Scheme 67

Mechanism of the Ni-photoredox C–N cross-coupling based on energy transfer (EnT) as proposed by Miyake's group.[101]

3.6.2 C–N bond-forming cross-coupling

With either of the mechanisms described above, PXX had a chance to behave as a suitable photocatalyst for this transformation. In the case of an ET mechanism (**Scheme 66**), the reduction potential of Ni-morpholino complex **43a** was determined to be -1.27 V *vs* SCE,[101] well in the range of the excited state PXX. In the case of an EnT mechanism (**Scheme 67**), the photophysical properties of PXX are similar to those of **20** (for example, emission in the range 420-550 nm, see **Figure 6**). Indeed, applying the standard conditions, along with minor variations, and using PXX as photocatalyst revealed a very efficient reaction, providing quantitative yields in the reaction of pyrrolidine with an electron-poor aryl bromide (**Table 20**). For example, the PXX loading could be reduced from 2 mol% to 0.1 mol% without losses in efficiency (entries 1-6). Similarly, Ni loading can also be reduced to 1 mol% with only a minor reduction in yield (entry 8). Alternative Ni salts and solvents also provide efficient reactions (entries 9-10) with the exception being acetonitrile, still providing 79% yield (entry 11). Lastly, in absence of PXX only minor reactivity is observed (13% yield, entry 12), in line with the hypothesis of background photoactivity of the Ni complexes.[153]

Table 20

Screening of conditions for the Ni-photoredox C–N bond cross-coupling.

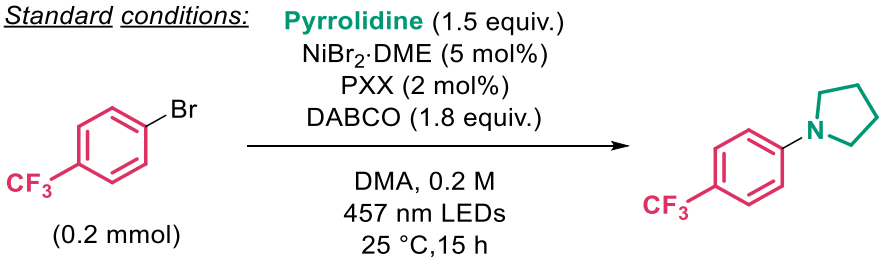

Entry	Modification from conditions	Yield (%)[a]	Conv. (%)[a]
1	4 mol% PXX	97	100
2	none (2 mol% PXX)	94	100
3	1 mol% of PXX	99	100
4	0.5 mol% of PXX	99	100
5	0.2 mol% of PXX	99 (87)	100
6	0.1 mol% of PXX	96	100
7	0.2 mol% PXX, 10 mol% Ni	99	100
8	0.2 mol% PXX, 1 mol% Ni	96	97
9	$NiCl_2$ DME as Ni source	95	100
10	DMF as solvent	95	100
11	Acetonitrile as solvent	79	98
12	No PXX	13	13

[a] Determined by ^1H NMR analysis of crude products, using 1,3,5-trimethoxybenzene as internal standard. Isolated yield in parentheses.

The conditions found above were thus applied to a range of aryl halides and amine reaction partners (**Scheme 68**). Secondary amines efficiently deliver coupled products **45a-c** (79-87% yield), with reactions almost devoid of impurities. Unfortunately, primary amines showed only limited reactivity (**45d-e**, 20% yield by NMR), and every attempt to increase the yield (for example, by heating the reaction mixture to 50 °C) did not provide any improvement. Pleasingly, benzophenone hydrazone is also a competent substrate, and derivative **45f** was obtained in 72% yield. To the best of our knowledge, this reaction has not been reported within current photoredox strategies,[154,155] except for a recent patent where a boron-dipyrromethene photocatalyst is used.[156] Guanidine derivative **45g** was obtained in limited yields (11% by NMR), and also in this case attempts to improve them were not fruitful. Examining other aryl bromides, electron-poor derivatives provide products in good yields (**45h-i**, 69-77% yield), while for electron-rich

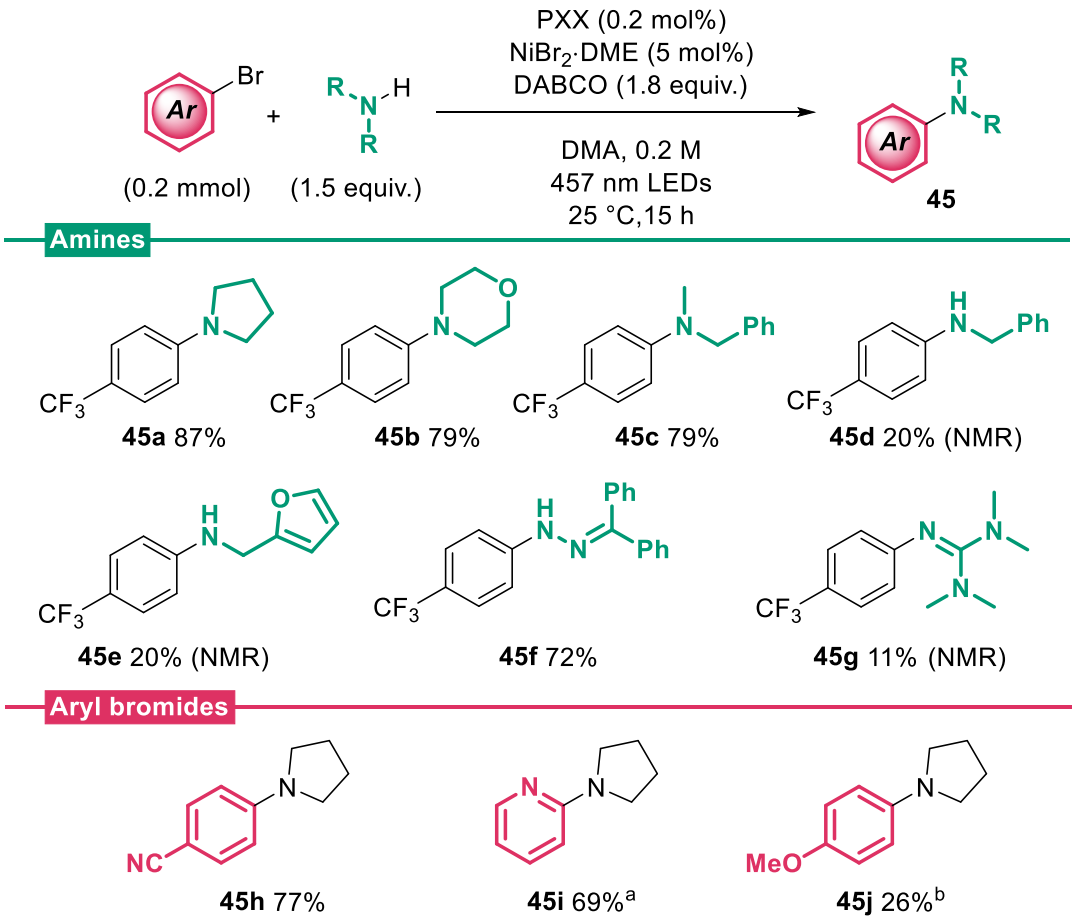

Scheme 68

Scope of the Ni-photoredox C–N cross-coupling. Isolated yields are reported, unless otherwise stated. ^{1}H NMR yields are determined using 1,3,5-trimethoxybenzene as internal standard. Notes: [a] Reaction time: 64 h. [b] 4-Anisyliodide used as substrate.

ones the reaction is more difficult, and **45j** was obtained in 26% yield only by using 4-anisyl iodide as reaction partner in place of the bromide.

The good reactivity found with benzophenone hydrazone was particularly intriguing. Products such as **45f** can be regarded as masked hydrazines, substrates for the formation of indole rings through a Fisher indole synthesis reaction.[154] When coupling conditions were applied to 4-iodofluorobenzene and benzophenone hydrazone, *N*-arylhydrazone **45k** was obtained with 95% NMR yield (**Scheme 69**). While **45k** was found to be prone to hydrolysis (both through aqueous washings and column chromatography on silica gel), the reaction mixture after evaporation of the solvent can be directly subjected to Fisher indole synthesis conditions[154] with an enolisable ketone to form indole **46** in 68% yield (over two steps). Compound **46** is an intermediate for the investigational drug Setipiprant, under study for treating asthma and scalp hair loss.[157] In this way, a quick and easy route to access this compound was demonstrated: an alternative to using the expensive and toxic 4-fluorophenylhydrazine as substrate.[XVI] Moreover, this reaction was performed on a synthetically useful 1 mmol scale, demonstrating the possibility to scale this reaction up in a laboratory setting.

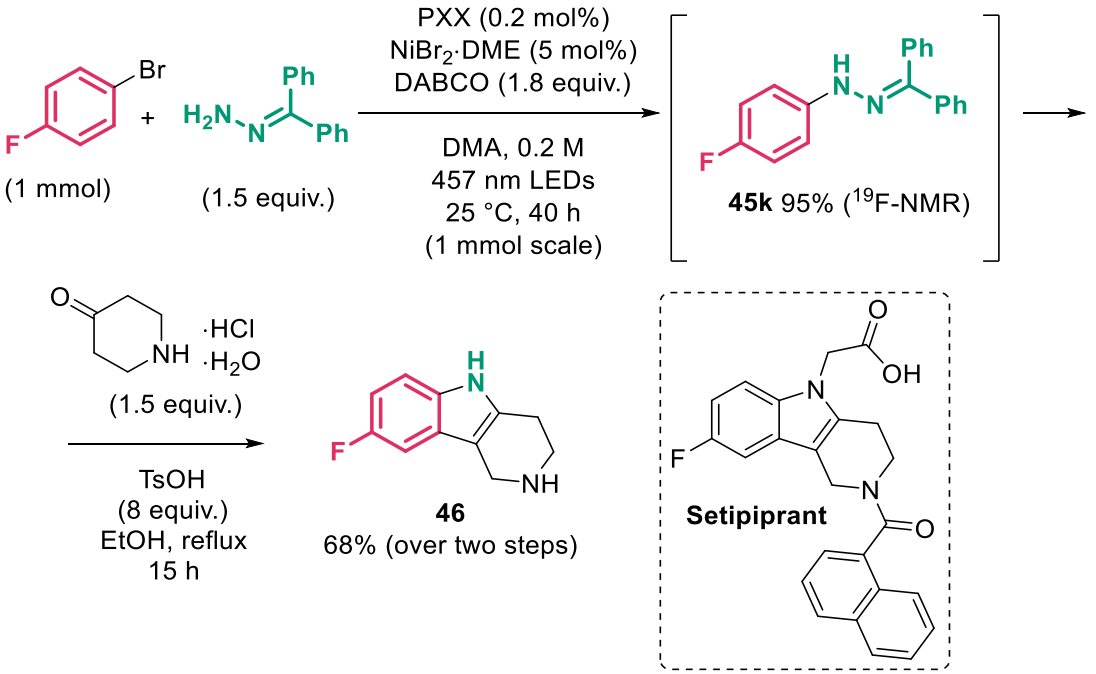

Scheme 69

Application of the Ni-photoredox C–N cross-coupling to a synthetic intermediate of Setipiprant.

[XVI] As of 30th January 2020, on the Merck website (www.sigmaaldrich.com) the price of 4-fluorophenyl hydrazine hydrochloride is £ 510/mol, while the price of 4-fluorobromobenzene is £ 26/mol and that of benzophenone hydrazone is £ 37/mol.

3.6.3 C–S and C–O bond-forming cross-couplings

The attention was then turned to the C–S bond-forming cross-coupling reaction. Conditions were replicated from the original work from Oderinde and co-workers.[147] Under these conditions, the reaction between 4-tolylbromide and octanethiol was found to be difficult (**Table 21**, entries 1-2); however, by replacing the former with 4-tolyl iodide the reactivity changed dramatically, and the coupled product **47a** was obtained quantitatively (entry 3). It was possible to reduce the loading of PXX and Ni pre-catalyst to 0.2 mol% and 5 mol% respectively (entries 4-6). Changes in Ni pre-catalyst or solvent (DMF, Acetonitrile) did not provide any loss in reactivity (entries 7-9). In the absence of PXX, the reaction does not proceed at all (entry 10).

Table 21

Screening of conditions for the Ni-photoredox C–N bond cross-coupling.

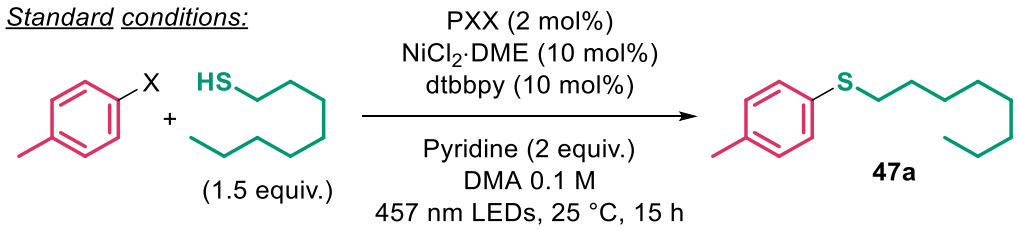

Entry	X	Modification from standard conditions	Yield (%)[a]
1	Br	none	23
2	Br	0.2 mol% PXX	0
3	I	none	> 99
4	I	0.4 mol% PXX	> 99
5	I	0.2 mol% PXX	98
6	I	0.2 mol% PXX, 5 mol% Ni and dtbbpy	> 99 (93)
7	I	$NiBr_2$ DME as Ni source (10 mol%)	99
8	I	DMF as solvent	> 99
9	I	Acetonitrile as solvent	> 99
10	I	No PXX	0

[a] Determined by ^1H NMR analysis of crude products, using 1,3,5-trimethoxybenzene as internal standard. Isolated yield in parentheses.

With the conditions found in entry 6, a brief scope of the transformation was examined (**Scheme 70**). Aryl iodides bearing elecron-rich groups work well (**47a-b**, 93-98% yield) and in the case of an electron-poor system the aryl bromide could be used as substrate: this is the case of benzonitrile **47c**, obtained in 93% yield. Examining other thiols, a more complex system as found in a protected cysteine is still amenable to reaction, even though a 85% yield of **47d** was obtained with 40 h reaction time. An aryl thiol in thiophenol is also a viable substrate, and **47e** is obtained in 92% yield.

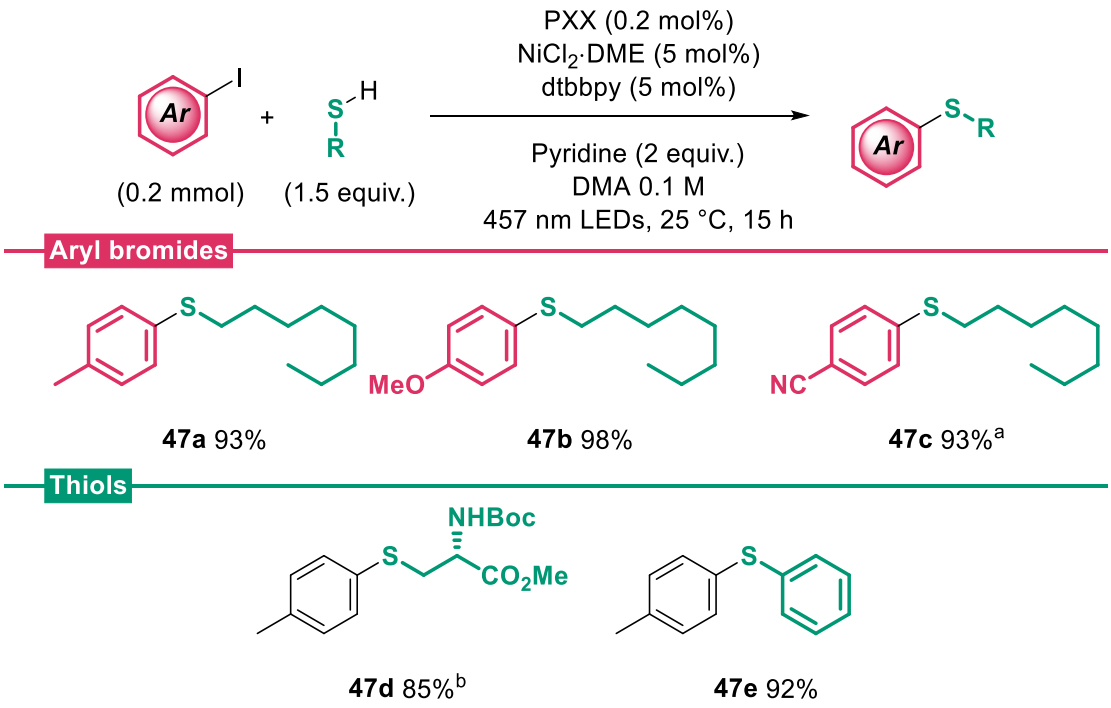

Scheme 70

Scope of the Ni-photoredox C–S cross-coupling. Isolated yields are reported. Notes: [a] 4-Bromobenzonitrile used as substrate. [b] Reaction time: 40 h.

A similar C–O bond-forming cross-coupling, developed by the MacMillan group,[149] was also attempted using PXX as photocatalyst. In these conditions, only the use of quinuclidine as base provided the formation of very limited amounts of ether **48** (**Scheme 71**). Further optimisation was not attempted in this case.

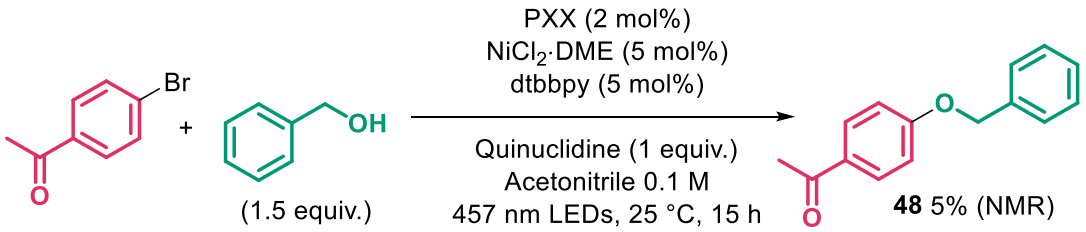

Scheme 71

Attempted Ni-photoredox C–O cross-coupling.

3.6.4 C–C bond-forming cross-coupling

Having demonstrated both the C–N and the C–S bond-forming cross-coupling, it was clear that PXX has the ability to interact with Ni centres at various oxidation states, promoting coupling reactions through different SET or EnT steps along the catalytic cycles. We then wondered whether similar processes might occur also in a C–C cross-coupling. The problem in this case is that, as seen in **Chapter 2**, alkyl radical precursors typically have quite high oxidation potentials: for instance, the cesium salt of **11a** has an

oxidation potential of + 0.90 V *vs* SCE in acetonitrile. PXX radical cation, obtained after initial oxidation of the excited state of PXX, has a relatively low oxidation potential (+ 0.77 V *vs* SCE in acetonitrile),[23] which could preclude some reactivity.

Indeed, when standard cross-coupling conditions (see **Chapter 2**) were applied to substrate **11h**, only 18% of coupled product **12h** was observed by ^{1}H NMR analysis (**Scheme 72a**). Minor amounts of dimer **49a** and decarboxylated byproduct **49b** were detected by NMR and LCMS (see **Section 2.7**). This result suggests that, despite thermodynamically not favorable, the activation of carboxylate substrates by PXX radical cation is still possible. Turning to trifluoroborate salt **10b**, no coupled product **9a** was observed under the same conditions.

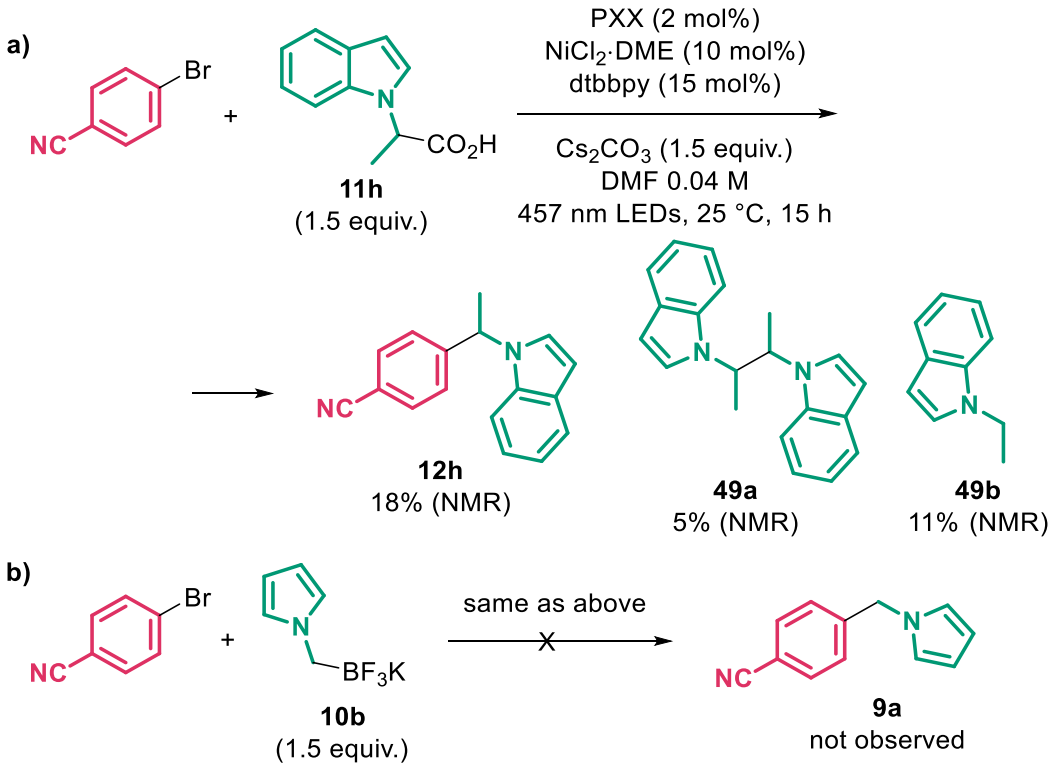

Scheme 72

Attempted Ni-photoredox C–C cross-couplings with **11h** and **10b**.

Having a more suitable radical source, whose oxidation potential does not exceed that of PXX radical cation, would make a C–C cross-coupling possible also with PXX as photocatalyst. For this reason the coupling of alkylated anilines such as *N*,*N*-dimethylaniline with aryl halides was examined.[34,48] In this case, *N*,*N*-dimethylaniline has a reported oxidation potential of +0.74 V *vs* SCE in acetonitrile,[8] much closer in value to +0.77 for PXX radical cation. Indeed, when conditions from the original work were applied using PXX as photocatalyst, a 71% NMR

yield could be obtained when 4-bromobenzonitrile was used as reaction partner (**Table 22**, entry 3). Unfortunately, loss of efficiency or even no coupling at all was observed when using other halide or tolyl derivatives as substrates (entries 1-2, 4-5). In this reaction the key radical species **50b** is probably formed through initial oxidation of the aniline to radical cation **50a**, and subsequent deprotonation of the α position.[91,158] After this, a classical cross-coupling pathway is envisaged (**Scheme 5**).

Table 22

Results on the Ni-photoredox C–C cross-coupling with *N*,*N*-dimethylaniline as substrate.

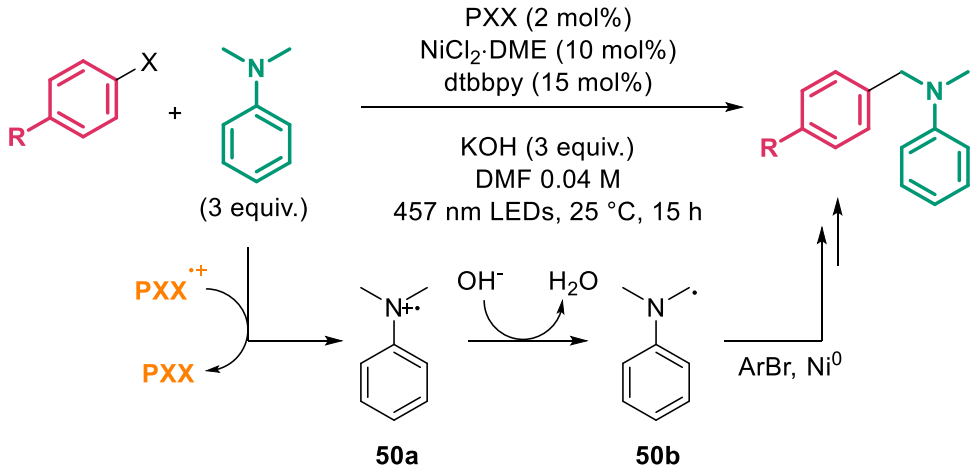

Entry	R	X	Yield (%)[a]	Conv. (%)[a]
1	Me	Br	0	0
2	Me	I	35	72
3	CN	Br	71	> 95
4	CN	I	< 40	n.d.
5	CN	Cl	0	0

[a] Determined by ^{1}H NMR analysis of crude products, using 1,3,5-trimethoxybenzene as internal standard.

3.7 Conclusions

In conclusion, the ability of PXX as photocatalyst to promote a wide variety of radical reactivities was demonstrated, in particular in reactions typical of the more common yet expensive Ir(III) complexes. The relatively high reduction potential of its excited state allows reduction of aryl, alkyl and perfluoroalkyl halides (and chlorides in particular); the resulting organic radicals can then add to suitable radical traps to form new C–C bonds. The efficiency of this process highly depends on the exact substrates and conditions. Turning the attention to more complex catalytic manifolds, PXX photocatalysis has been successfully coupled with both organocatalysis and metallocatalysis. In the first instance, a β-arylation of cyclic ketones with cyanoarenes

was shown to be productive; substrate scope needs improvement, and a more in-depth optimisation of the reaction components might allow access to other cyanoarenes. To demonstrate coupling with metallocatalysis, some Ni-catalysed cross-couplings were promoted by PXX photocatalysis, allowing the formation of C–N, C–S and, in special cases, C–C bonds from aryl halides. To the best of our knowledge, this work is one of the few examples of wide demonstrations of reactivity for a new highly reducing organic photocatalyst, adding another precious tool to the array of photocatalysts to be chosen from for promoting photoredox reactions. Compared to other photocatalysts, especially those listed in **Section 3.1**, PXX stands out for its very low reduction potential (-2.0 V *vs* SCE) coupled to structural simplicity, low cost and ease of preparation (see **Section 6.3**). Further studies are underway to expand the application of PXX photocatalysis to the preparation of specific classes of compounds.

Chapter 4
Photomediated asymmetric β-alkylation of enals

In this chapter, a novel strategy for the asymmetric introduction of sp^3 carbon groups at the β position of enals is presented. Common methods relying on organocatalysis or 1,4-addition of metal nucleophiles are plagued by competing 1,2-addition or low enantioselectivity. Visible light excitation of chiral iminium ions turns them into strong oxidants, capable of oxidising suitable radical precursors and thus trigger a stereocontrolled radical pathway that affords enantioenriched β-substituted aldehydes bearing a variety of alkyl fragments.

The work described in this chapter has been carried during a 4-month secondment (June-September 2017) in the Melchiorre group at the Institute of Chemical Research of Catalonia (ICIQ). During this period I joined the existing project on the β-alkylation of enals, working closely with Nurtalya Alandini, Phototrain PhD candidate, on the scope of the transformation. Our work is reported in ***Section 4.5****, and Nurtalya's contributions are acknowledged in the text and schemes.* ***Section 4.4*** *describes initial screening and optimisation, which were performed in different moments by other researchers in the Melchiorre group, among which Dr Charlie Verrier, Mauro Moliterno and Dr Hamish Hepburn. Since it's not part of my personal work, a very limited overview will be given in order to provide context.*

4.1 On the asymmetric 1,4-alkylation of enals

The conjugate addition of carbon nucleophiles to α,β-unsaturated carbonyl compounds is an efficient method for creating new C–C bonds in an enantioselective fashion.[159] Numerous catalytic processes have been reported using organometallic reagents, particularly in combination with copper additives, allowing the formation of new sp^3 centres with a variety of Michael acceptors. Difficulties arise when this same strategy is applied to α,β-unsaturated aldehydes. The higher reactivity of the aldehyde moiety leads to competition between 1,2- and 1,4- addition, as initially observed by the Bräse group.[160,161] The catalytic addition of diethyl zinc to enals proceeds with high stereocontrol but poor regioselectivity when a [2.2]paracyclophane-type ligand **51** is

employed: a ratio of approximately 2:1 between 1,4-addition product **52a** and 1,2-addition product **52b** was obtained with cinnamaldehyde as substrate (**Scheme 73**).

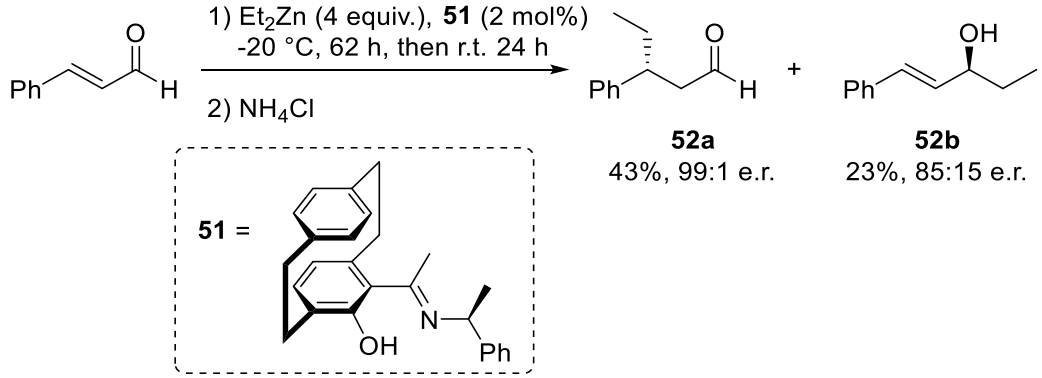

Scheme 73

Bräse's procedure for the enantioselective addition of diethyl zinc to enals.[160]

Later efforts from Alexakis and co-workers showed the role of copper along with a chiral biaryl-based ligand in promoting the addition of organozinc and Grignard reagents to enals.[162] With the formers good 1,4-:1,2-addition ratios (up to 100:0) are typically found, while enantioselectivity is often poor. With the latters, reduced regio- and chemoselectivity is observed, as mixtures of 1,4- and 1,2-adducts along with aldol products are obtained, the former though with overall better enantioselectivity. In a later work an improved ligand system allowed better enantiocontrol to be obtained with dialkylzinc compounds as organometallic reagents along with perfect regioselectivity with a range of alkylic enals (**Scheme 74**).[163] In this case cinnamaldehyde was not a good susbtrate, providing low e.r. and competition with aldol pathways.

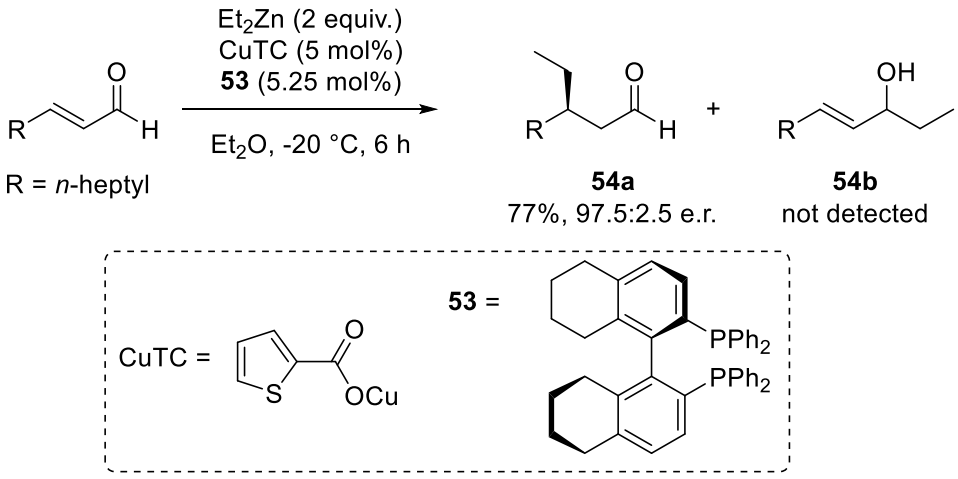

Scheme 74

Alexakis' improved conditions for the enantioselective addition of diethylzinc to enals.[163]

Another strategy for the β-functionalisation of enals relies on the use of chiral organocatalysts for the formation of electron-poor iminium ions: numerous applications have appeared focused on the stereoselective addition of soft nucleophiles to enals in this fashion.[164] The application of this same strategy for the installation of simple alkyl fragments is still underdeveloped. Córdova and co-workers reported the combination of organocatalysis and Cu catalysis for the β-alkylation of cinnamaldehydes (**Scheme 75**).[165] In this procedure the achiral organometallic reagent reacts with the *in situ*-formed chiral iminium ion **56**. While the enantioselectivity is often good, the scope is limited to the use of diethyl- and dimethylzinc, and 1,2-addition to the aldehyde is competing.

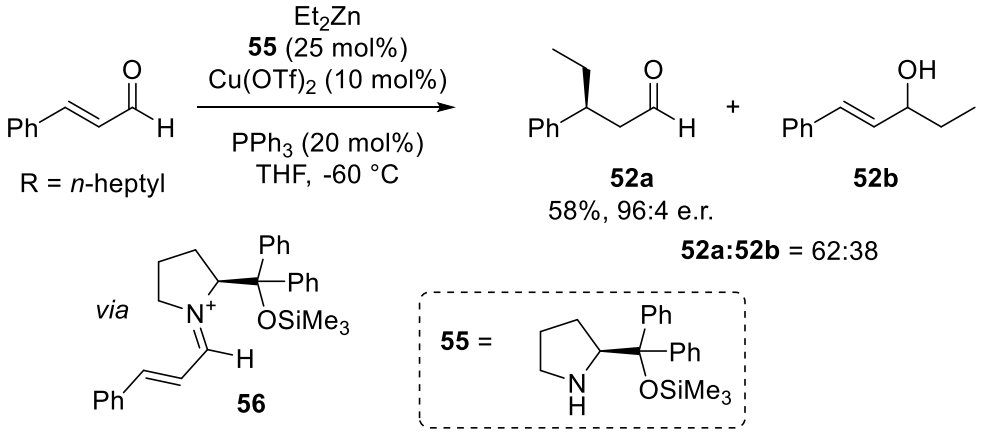

Scheme 75
Córdova's procedure for the combined organocatalytic and Cu-catalytic procedure for the enantioselective addition of diethyl zinc to cinnamaldehydes.[165]

The problems encountered in the current methods for the 1,4-addition of carbon nucleophiles to enals (or their iminium ions) suggest that a different mechanistic perspective might be necessary to obtain an efficient and selective reaction.

4.2 Organic intermediates as photoredox-active species

As mentioned in **Section 3.5**, the merging of organocatalysis and photoredox catalysis has been of extreme importance in promoting the development of these two fields, the latter in particular.[2,14] While a wide range of successful organocatalytic transformations, most of them enantioselective, had been found from the early 2000s,[166,167] some goals could not be achieved through the polar pathways that characterise enamine- or iminium ion-mediated catalysis.[XVII] This was the case of the catalytic enantioselective

[XVII] The modes of activation typical of organocatalysis also include hydrogen bonding, ion pairing and SOMO activation,[166] but these are not part of this discussion.

α-alkylation of carbonyls with alkyl halides: while the reaction with stoichiometric enamine had been reported in the 1960s,[168] the corresponding catalytic version eluded synthetic chemists for long.[169] This was due to complications in the classical S_N2 pathway, among which *N*-alkylation of the organocatalyst and competing aldol reactions. To overcome these problems, a new mechanistic perspective was necessary. In 2008 the MacMillan group recognised that radical reactivity could provide this change in perspective: alkyl halides could be used as sources of alkyl radicals, which could be promptly captured by an electron-rich alkene such as an organocatalytically-formed enamine. The application of $[Ru(bpy)_3]Cl_2$ as photocatalyst allowed the required redox activation and turnover (**Scheme 76**).[4] In the initially proposed mechanistic scenario, the carbonyl compound condenses with the organocatalyst **57** to form enamine **58a.** At the beginning, a sacrificial amount of **58a** is oxidised by the excited state Ru(II) photocatalyst to obtain an highly reducing Ru(I) complex, capable of reducing the electron-deficient alkyl bromide to the corresponding radical **59**. Enamine **58a** can efficiently trap **59** leading to the formation of adduct **58b**, whose oxidation to **58c** closes the photoredox cycle. Hydrolysis to the product releases the organocatalyst and allows turnover. With this strategy, enantioselectivities in some cases higher than 99:1 e.r. could be obtained with alkylic aldehydes and a range of activated alkyl bromides, in good to excellent yields (63-93%). Later mechanistic studies demonstrated that a radical chain mechanism is most probably in place (**Scheme 76c**): intermediate **58b** can reduce the alkyl bromide forming directly **58c** and radical **59** in the propagation step without further intervention from the photocatalyst, whose role is reduced to that of an initiator.[9]

When the Melchiorre group started studying a similar transformation with organocatalyst **60a** and activated alkyl bromides (**Scheme 77a**), control experiments revealed that the stereoselective reaction was promoted by light but there was no need of the photocatalyst. When electron-deficient benzyl bromides or phenacyl bromides were used, the group recognised the formation in solution of an Electron Donor-Acceptor (EDA) complex between the organocatalytically-formed enamine and the alkyl bromide in the ground state (**Scheme 77b**, Path A).[170] Visible light irradiation of the colored EDA complex induces SET, where the enamine reduces the alkyl bromide leading, after C-Br bond scission, to the formation of an alkyl radical **61a**. This radical is

part of a radical chain reaction with the ground state enamine **62a**, with the same type of intermediates discussed above (**Scheme 77c**).[171] Another mechanistic scenario has been demonstrated when bromomalonates are used as alkyl bromides.[172] In these conditions the intrinsic photoreactivity of the enamine intermediate is recognised to be responsible for SET: enamines such as **62a** can asborb visible light (mainly below 420 nm) and their excited state is a powerful reducing species, with a calculated reduction

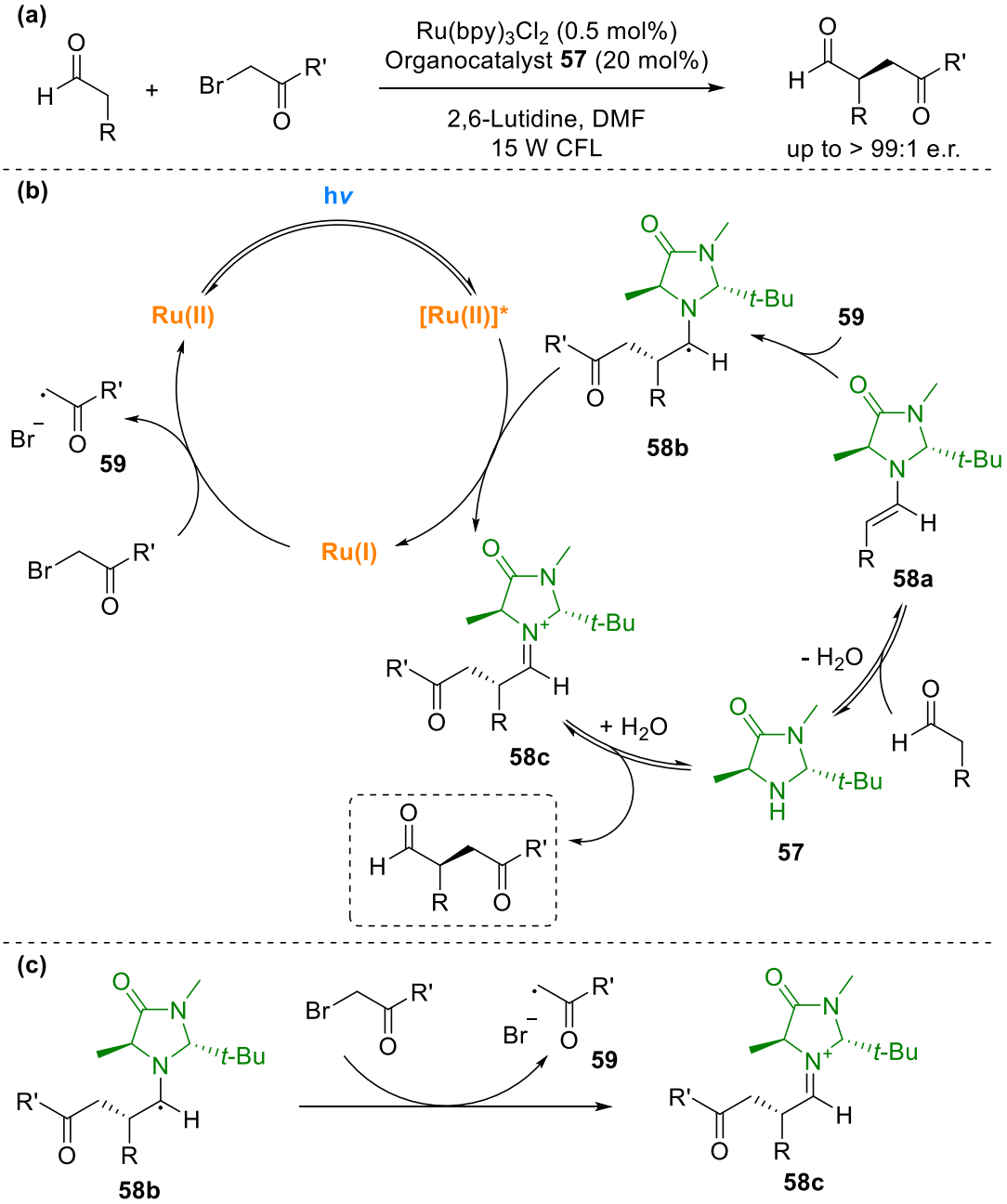

Scheme 76

General conditions **(a)** and proposed mechanism **(b)** for MacMillan's organo-photoredox enantioselective α-alkylation of carbonyl compounds.[4] The propagation step of a revised radical chain mechanism is reported in **(c)**.[9]

potential of -2.50 V *vs* SCE. The excited state of the enamine can thus reduce the bromomalonate leading to the formation of alkyl radical **61b** (**Scheme 77b**, Path B). From

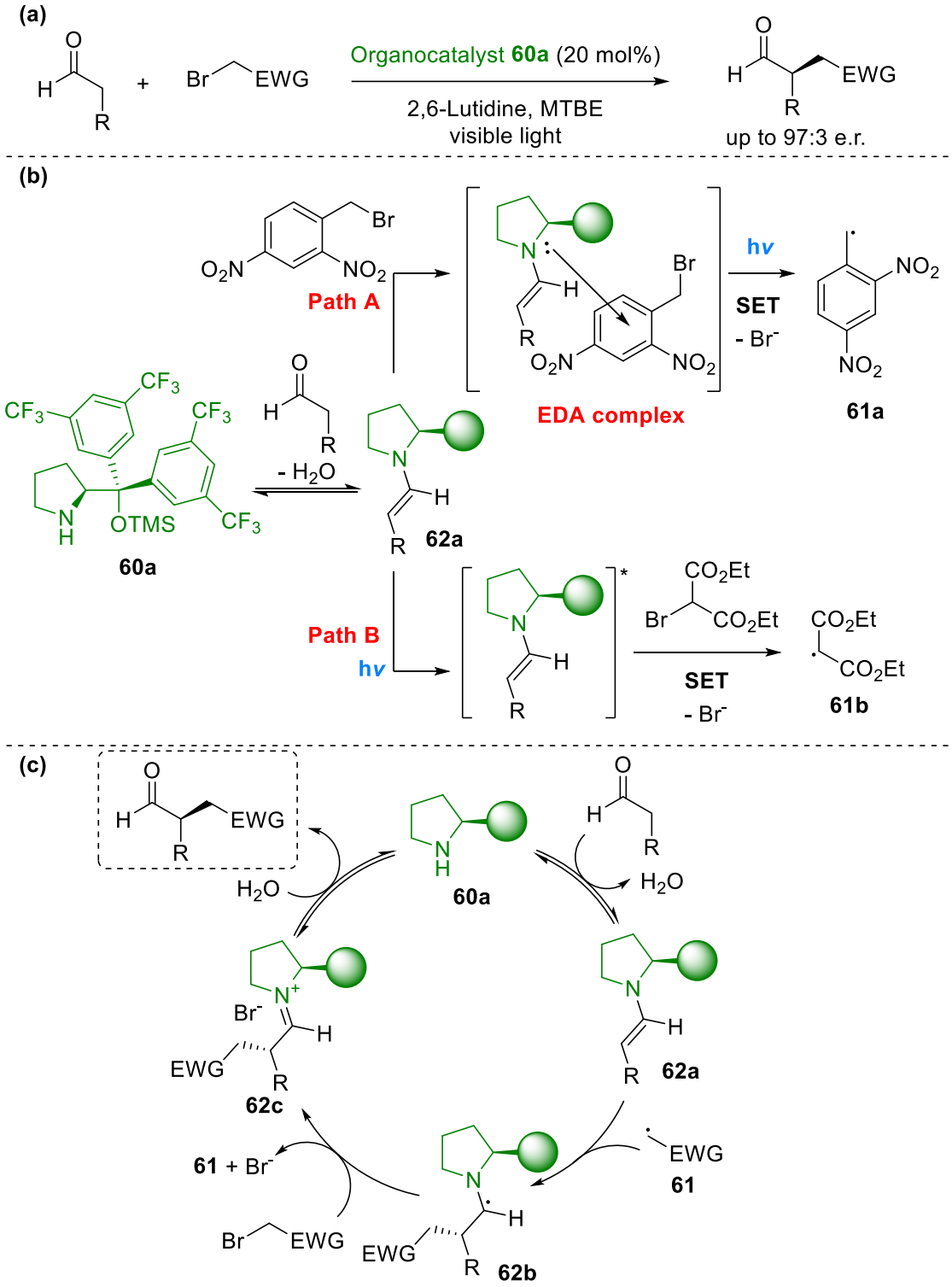

Scheme 77

General conditions **(a)**, proposed initiation mechanisms **(b)**[167,169] and proposed radical chain mechanism **(c)**[171] for Melchiorre's enantioselective α-alkylation of aldehydes in the absence of photocatalyst.

this point, the same radical chain reaction mechanism can take place.[171] This work is a remarkable example of how the different reactivity of the ground and excited state of an organic intermediate can be exploited for successful reactions: while the excited state of the enamine is a reductant involved in the initiation of the radical process through SET, the ground state enamine behaves as a nucleophile and provides asymmetric induction in the formation of the C–C bond.

The discovery of the excited state reactivity of enamine intermediates prompted further studies into exploiting the photochemistry of other organic species.[44,173] This has been the case for another typical intermediate in organocatalysis: when cinnamaldehydes condense with secondary amine organocatalysts, iminium ions such as **64a** can be formed. These are typically electrophilic species, prone to addition of soft nucleophiles on the β position, as already seen in **Scheme 75**. In this case, **64a** can absorb visible light (below 440 nm) and the excited state has been demonstrated having oxidising character: an oxidation potential of +2.4 V *vs* SCE was calculated for this species. These considerations led to the development of a photomediated enantioselective β-alkylation of enals with benzyl silanes (**Scheme 78a**).[174] In this mechanistic scenario, the excited state iminium ion is capable of oxidising benzyl silanes: this leads to the formation of a 5π species **64b** (the same type of intermediate encountered in **Section 3.5.2**) and a radical cation **65a** (**Scheme 78b**). Fragmentation of **65a** into benzyl radical **65b** and a formal trimethylsilylium unit (most likely captured by solvent) drives the reaction and prevents back electron transfer (BET). Radical-radical coupling between chiral intermediate **64b** and **65b** leads to the stereoselective formation of the new C–C bond. Hydrolysis of **64c** provides the product and releases the organocatalyst, allowing turnover. Silanes bearing α-heteroatoms (N, O, S) are also good substrates for this transformation. It is also worth noting that in the structure of the organocatalyst **63b**, the *gem*-difluoro substitution was introduced during catalyst design to improve lifetime. The high oxidising power of the iminium ion (E = +2.4 V *vs* SCE) can affect the organocatalyst itself, leading to oxidation to the corresponding amine radical cation and subsequent degradation. For example, the TDS-substituted equivalent of **60a** (**60b** in the following) has E = +1.57 V *vs* SCE. The incorporation of electron-withdrawing fluorine atoms moved the oxidation potential to +2.40 V *vs* SCE, increasing the lifetime of the organocatalyst and providing a much more efficient reaction. With the bulkier perfluoroisopropyl substituents on the benzene rings

a better enantioselectivity was obtained compared to the same catalyst with trifluoromethyl groups (**63a**).

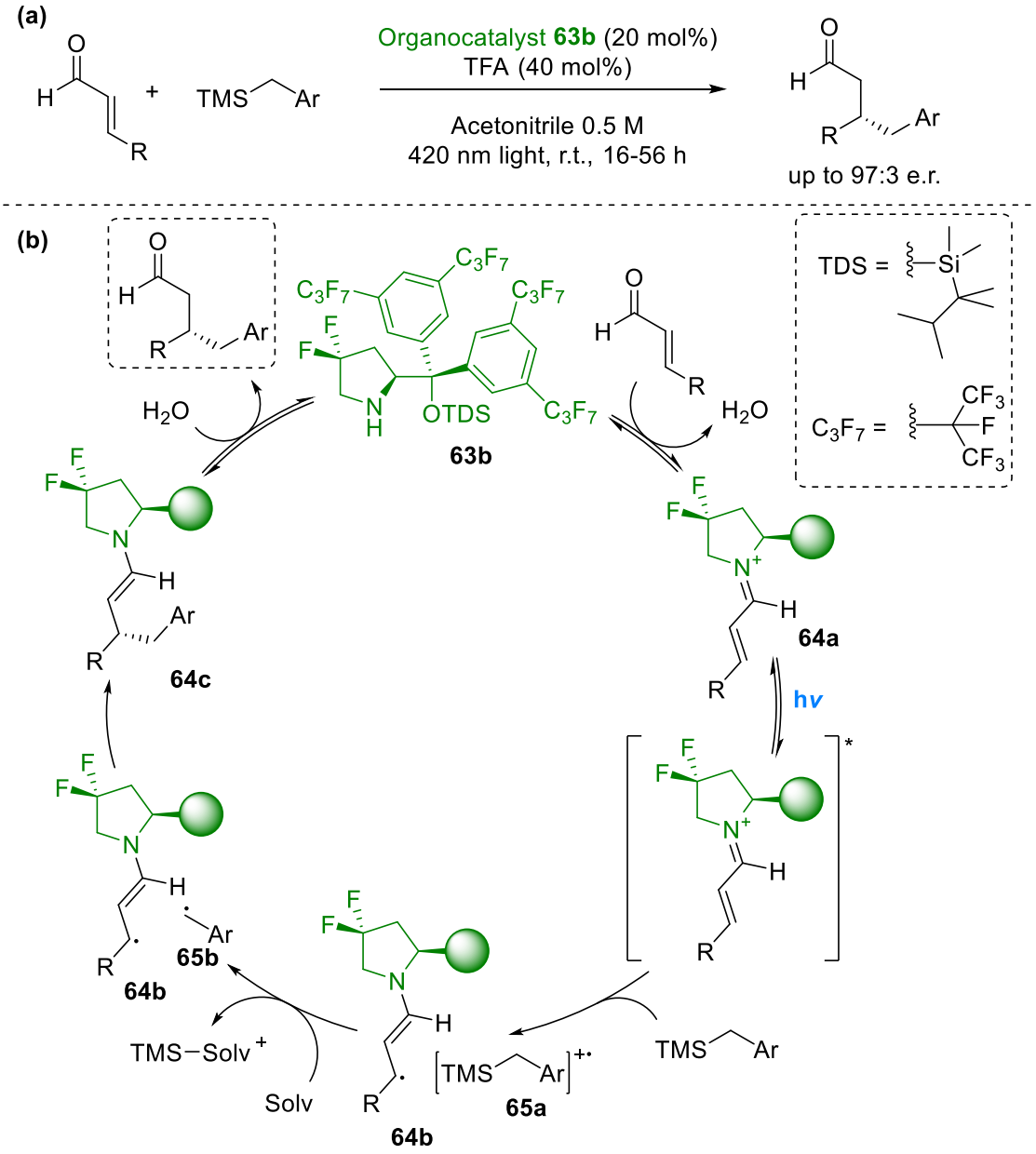

Scheme 78

General conditions **(a)** and proposed mechanism **(b)** for Melchiorre's photomediated β-alkylation of enals with benzyl silanes.[174]

4.3 Aim of the project

The photomediated benzylation of enals disclosed by the Melchiorre group offers a novel strategy for the β-functionalisation of carbonyl compounds. The group wondered then whether the use of suitable alkyl radical precursors would similarly allow the introduction of simple non-stabilised alkyl groups in a stereoselective fashion (**Scheme 79**). This method would allow an alternative pathway towards the so-far limited

asymmetric 1,4-addition of alkyl groups to enals. The main purpose of this project is thus to verify this hypothesis and explore scope and limitations of the methodology.

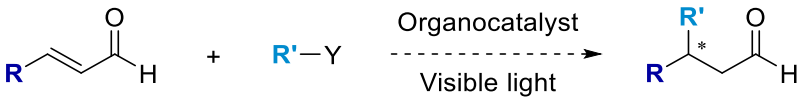

Scheme 79
Postulated photomediated β-alkylation of enals.

4.4 Summary of initial results and optimisation

Initial efforts of the group focused on potassium alkyltrifluoroborate salts such as **66a** as radical precursors.[27] Oxidation potentials usually between + 1.1-1.5 V *vs* SCE put them well in the range of oxidation by the excited iminium ion (+ 2.2-2.4 V *vs* SCE). Positive initial results showed modest yields obtained with three of the organocatalysts typically used in the group (**60b**, **63a-b**, **Table 23**, entries 1-3). **63a** and **63b** in particular, bearing a difluorinated proline moiety (see **Section 4.2**), showed the best reactivity along with promising enantioselectivity (from 82:18 to 85:15, entries 2-3). A first round of optimisation involved mainly the simpler and easier to synthesise organocatalyst **63a**. Improved results were obtained by diluting the reaction mixture (from 0.5 M to 0.2 M) and reducing the temperature (from 25 to -10 °C), as shown in entry 4: yield improves to 55% and enantioselectivity to 89:11 e.r.; however, the reaction proved sometimes difficult to reproduce, which had been found was due to the low solubility of **66a**. A cation exchange from K^+ to tetrabutylammonium (TBA^+) made derivative **66b** much more soluble and the reaction more reproducible (entry 5). Further attempts at optimisation of this reaction did not lead to significant improvements. A turning point in the reaction development was a test performed with dihydropyridine (DHP) **67a** as radical precursor in the same conditions: yield increased to 70% mantaining the same e.r. (entry 6). Dihydropyridines also possess accessible oxidation potentials (+ 1.1-1.9 V *vs* SCE) and have recently been introduced as convenient radical precursors, as already mentioned in **Section 2.1.1**.[40,41] The yield could be improved to 91% by increasing the loading of TFA to 80 mol% (entry 7). It was then observed that **63b** could provide product with increased stereocontrol (93:7 e.r.) even if in a reduced 59% yield (entry 8); in this case perfluorohexane was added to the solvent mixture in order to properly solubilise the fluorine-rich organocatalyst. A final round of optimisation saw the concentration

increased to 0.33 M and the loading of TFA increased to 1 equiv., leading to 88% yield and 93:7 e.r. (entries 9-10).

Table 23

Summary of the optimisation of the photomediated β-alkylation of enals with alkyltrifluoroborate salts and dihydropyridine precursors.

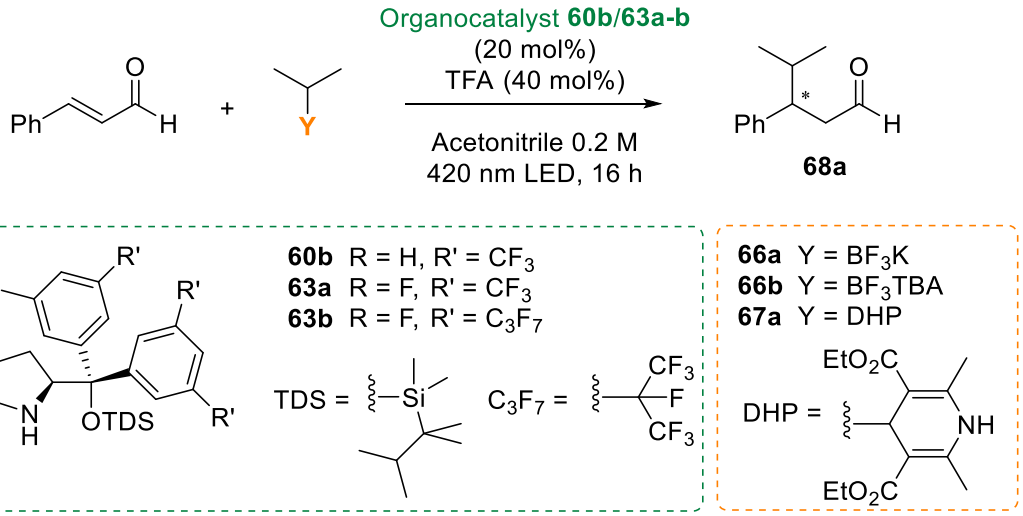

Entry	Catalyst	Radical precursor	TFA (mol%)	Temp. (°C)	Yield (%)[a]	e.r.[b]
1[c]	**60b**	**66a**	40	25	35	-
2[c]	**63a**	**66a**	40	25	44	82:18
3[c]	**63b**	**66a**	40	25	40	85:15
4	**63a**	**66a**	40	-10	55	89:11
5	**63a**	**66b**	40	-10	58	90:10
6	**63a**	**67a**	40	-10	70	90:10
7	**63a**	**67a**	80	-10	91	90:10
8[d]	**63a**	**67a**	80	-10	59	93:7
9[d]	**63b**	**67a**	100	-10	67	93:7
10[e]	**63b**	**67a**	100	-10	88 (83)	93:7

[a] Determined by ^{1}H NMR analysis of crude products using 1,3,5-trimethoxybenzene or trichloroethylene as internal standard. Isolated yield in parentheses. [b] Determined by chiral HPLC analysis. [c] Performed in solution of concentration 0.5 M. [d] Performed in 4:1 acetonitrile:perfluorohexane solvent mixture. [e] Performed in 2:1 acetonitrile:perfluorohexane solvent mixture, concentration 0.33 M.

It is worth mentioning that one advantage of using DHPs as radical precursors is the possibility to access the aldehyde feedstock,[41] as they are typically derived from the corresponding alkylic aldehydes through construction of the heterocyclic core (**Scheme 80**). This also includes alcohols and other acyl derivatives, easily transformed into the corresponding aldehydes, and a wide range of natural products.

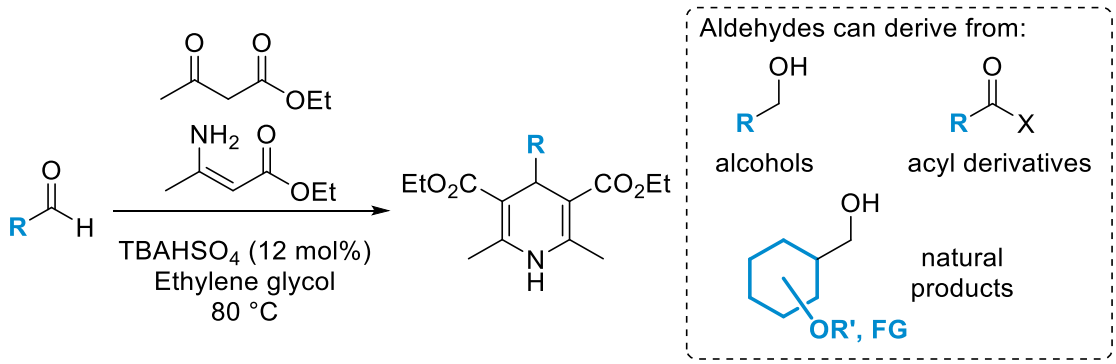

Scheme 80

Typical conditions for the preparation of DHPs: exploitation of the aldehyde feedstock.[41]

4.5 Scope of the transformation

With optimised conditions in hand,[XVIII] the scope of the transformation was then evaluated. A range of simple alkyl groups was examined (**Scheme 81**). Products containing secondary groups such as isopropyl (**68a**), 3-pentyl (**68b**), cyclohexyl (**68c**) and cyclopentyl (**68d**) were all obtained in good yields (64-83%) and enantioselectivities (from 92:8 to 97:3). Unfortunately, cyclobutyl derivative **68e** could not be obtained using the corresponding DHP as radical precursor; when the TBA trifluoroborate was used instead, this unusual compound was obtained in 29% yield with 86:14 e.r. A DHP precursor to a primary alkyl (non-benzylic) radical is not active in the reaction, thus product **68f** was not observed. While it was not possible to obtain the DHP derivative substituted with a *tert*-butyl group, the corresponding TBA trifluoroborate afforded **68g** in 60% yield and 87:13 e.r.. A benzyl group was also tested, and while the reaction works, yield and enantioselectivity of **68h** (44%, 86:14 e.r.) are inferior compared to those obtained previously using the trimethylsilane derivatives (87% yield, 94:6 e.r.).[174] Other secondary groups were then tested. Looking at heterocyclic derivatives, tetrahydropyran **68i** was obtained in 63% yield and 93:7 e.r., while Boc-piperidine **68j** proved to be a difficult substrate: a slightly different set of conditions (**63a** as organocatalyst, 1 equiv. of TFA and CH_2Cl_2 in the solvent system) were necessary to obtain a modest 35% yield, along with 86:14 e.r. Systems bearing already a non-defined stereocentre were then examined: it was found that the organocatalyst has no control over this second stereocentre, and compounds **68k-o** were all obtained with no or very

[XVIII] Preliminary results showed that 80 mol% of TFA with concentration 0.2 M was actually better for the majority of entries.

low diastereoselectivity (from 1:1 to 1.4:1 d.r.); however, yields are good (47-74%) and, taking every diastereoisomer individually, enantioselectivity is as well (from 91:9 to 96:4 e.r.).

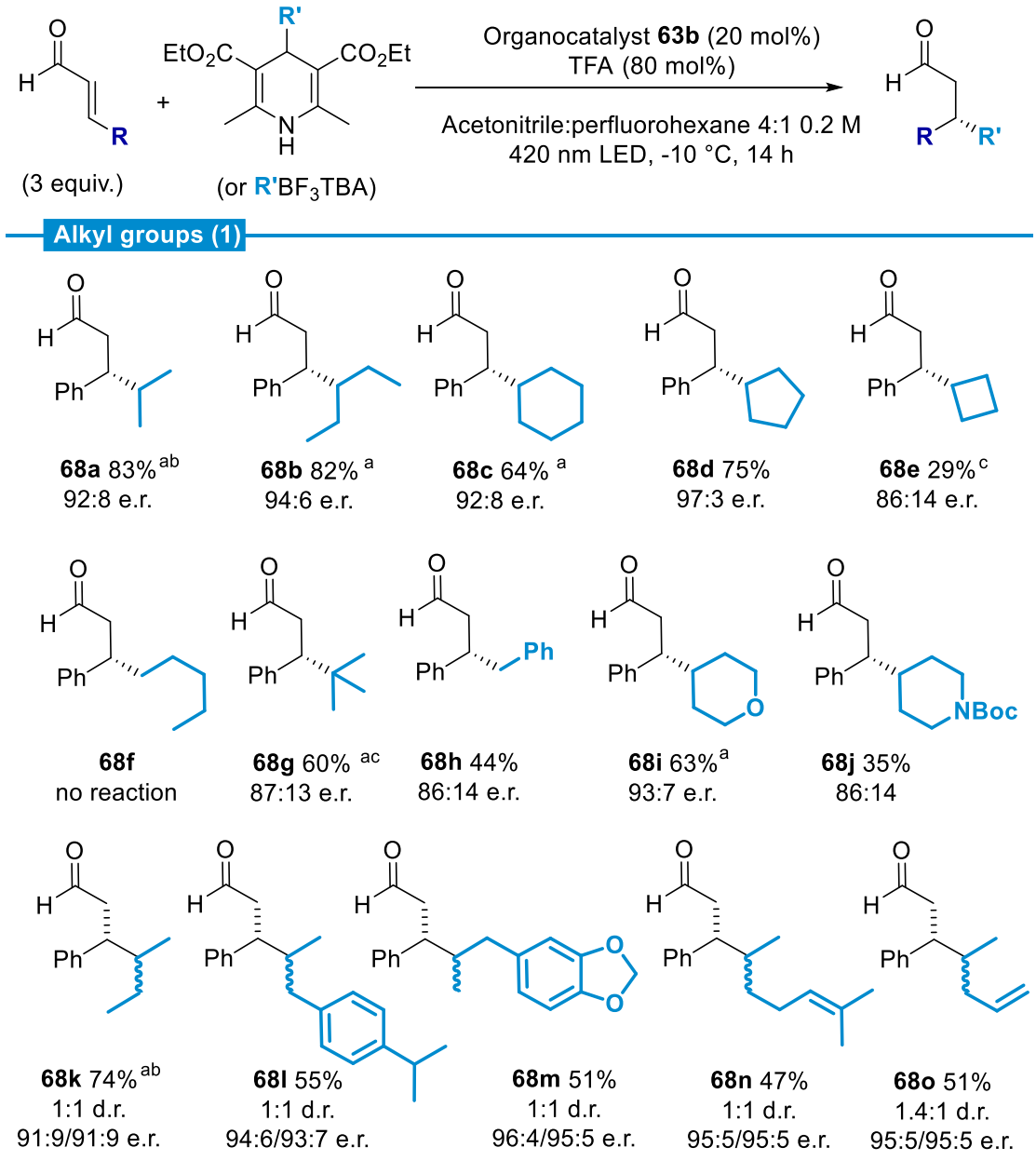

Scheme 81

Scope of simple alkyl groups for the photomediated β-alkylation of enals. Notes: [a] Experiment performed by Nurtalya Alandini, ICIQ. [b] Performed using 100 mol% TFA in acetonitrile:perfluorohexane 2:1, concentration 0.33 M. [c] Performed using the corresponding TBA trifluoroborate salt as radical precursor. [d] Performed using **63a** (20 mol%) as organocatalyst, 1 equiv. of TFA in CH_2Cl_2:perfluorohexane 4:1.

Alkyl groups bearing stabilising α-oxygen substituents were then examined (**Scheme 82**). Simple ester substituents afforded products **68p** and **68q** in 38% yield, 92:8 e.r. and 47% yield, 88:12 e.r., respectively. As mentioned in the previous section, DHP radical precursors can be obtained from the corresponding aldehydes. If the aldehyde derives

from a sugar compound bearing a primary alcohol, this route provides easy access to saccharide-type radical precursors.[42,43] Indeed, if a DHP derived from a protected galactose is used in this reaction, upon slight changes of conditions, including using **63a** as organocatalyst, product **68r** is obtained in 53% yield and good diastereoselectivity (19:1 d.r.).[XIX] If the enantiomer of the organocatalyst is used (***ent*-63a**), the diastereoisomer **68s** is obtained (54% yield) with 9:1 d.r.. This result indicates that the organocatalyst controls the stereoselectivity of the process, and can overcome the stereochemical information already present in the chiral substrate. In a similar fashion, uridine-derived **68t** was obtained in 59% yield as a mixture of three diastereoisomers (1:1.5:7 d.r.). Unfortunately, it was not possible to conclusively determine the stereochemistry of the main diastereoisomer, but the result is still interesting in

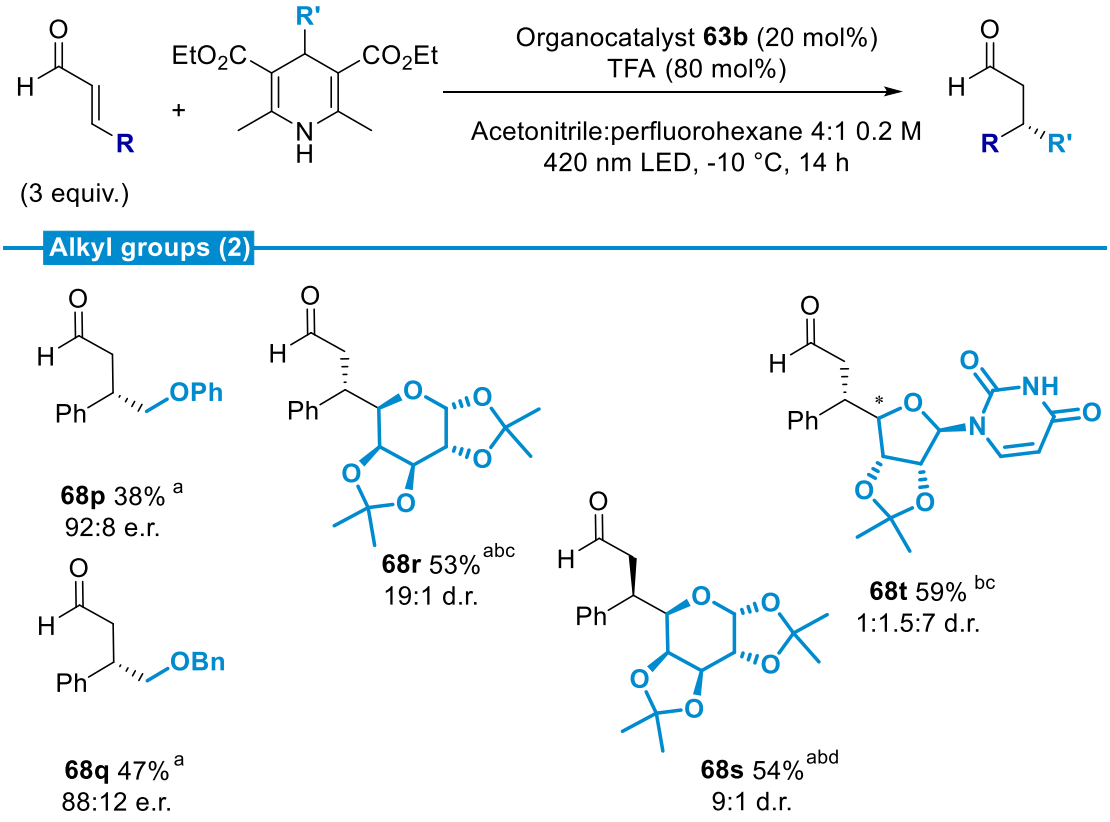

Scheme 82

Scope of α-oxygen alkyl groups for the photomediated β-alkylation of enals. Notes: [a] Experiment performed by Nurtalya Alandini, ICIQ. [b] Experiment performed in CH_2Cl_2 0.25 M. [c] Experiment performed with **63a** (20 mol%) as organocatalyst. [d] Experiment performed with ***ent*-63a** (20 mol%) as organocatalyst.

[XIX] The stereochemistry of **68r** was confirmed by X-Ray analysis performed by Nurtalya Alandini, ICIQ.

highlighting the level of structural complexity it is possible to introduce with this strategy.

Lastly, variation in the structure of the enal were also addressed (**Scheme 83**). Different substitutions on the phenyl ring can be accomodated: modest to good yields (39-69%) and e.r. between 80:20 and 91:9 are obtained for compounds **68u-68aa**, with no particular pattern regarding steric hindrance or electronic properties of the substituents. A furan ring (**68ab**) is not well tolerated, and an alkyl fragment in β position (**68ac**) shuts the reaction down completely. Most probably, these substitutions modify the photophysical properties of the iminium ion.

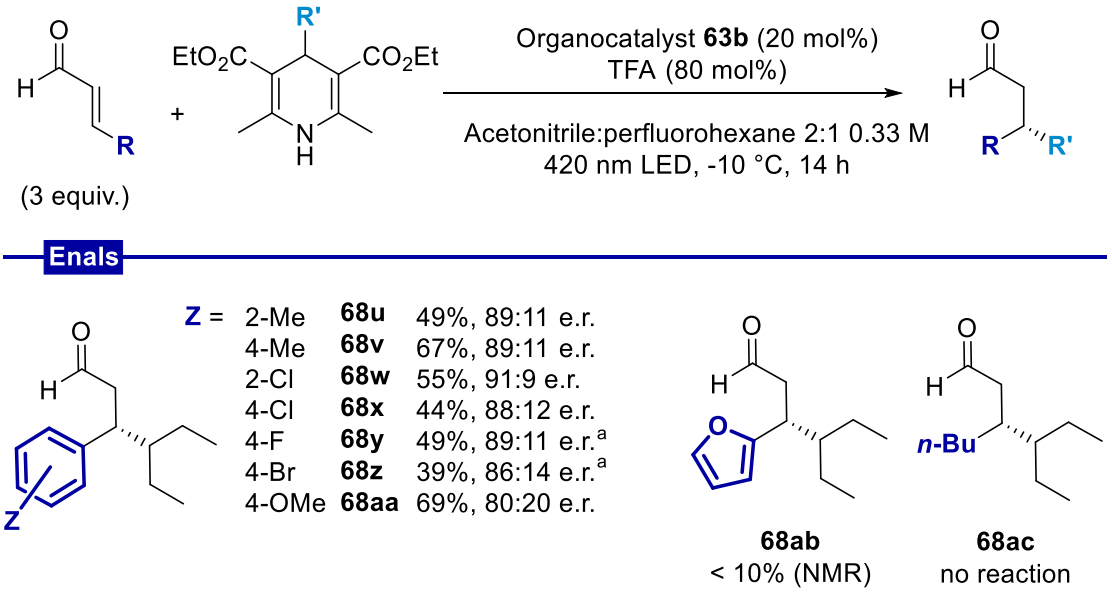

Scheme 83

Scope of enals for the photomediated β-alkylation of enals. Notes: [a] Experiment performed by Nurtalya Alandini, ICIQ.

4.6 Conclusions

In conclusion, a novel method for the asymmetric β-alkylation of enals has been developed. Instead of relying on classical organometallic reactivity, this chemistry is based on the visible light excitation of an *in situ* formed iminium ion: in the excited state, this is a strong oxidant, capable of generating alkyl radicals from readily available dihydropyridine (DHP) precursors. The explored scope was broad, and limitations were found in the use of alkylic enals, primary alkyl groups and in some particular substitution patterns. Sugar-derived DHPs were good substrates for the formation of unusual C–C bonds. This work complements the reactivity previously found by the group with activated alkylsilane precursors[174] while subsequent projects have enlarged

even more the synthetic potential of the excited state iminium ion: enantioselective reactions involving the oxidation of cyclopropanols, toluene derivatives, alkenes and allenes have been demonstrated.[175–178]

Chapter 5
Other attempted transformations

In this chapter, a brief overview of two attempted transformations will be given. The aim is to report some interesting findings in spite of the reactivity being not what was initially looked for. The first project (**Section 5.1**) centres on early attempts to obtain a photo-organocatalytic β-fluorination of aldehydes. The second (**Section 5.2**) is a brief overview of the efforts to obtain an API-like structure through a C−C cross-coupling that revealed a possibly convenient yet undeveloped method for the *N*-alkylation of azoles. For reasons of confidentiality, general structures only are shown in this second section.

5.1 On the β-fluorination of aldehydes

The formation of C−F bonds is of particular interest to the synthetic chemist, due to the important properties in pharmaceuticals, agrochemicals, and performance materials that the introduction of fluorine atoms can have on organic molecules.[132,133] Numerous efforts in the past decades have been directed to the synthesis of aryl and alkyl fluorides alike.[179,180] The reactivity of carbonyl compounds in this direction has also been exploited: α- and γ-fluorinations of enol-type derivatives with electrophilic fluorine sources are now common methodologies, even in enantioselective catalytic versions.[180] Direct fluorinations of carbonyl compounds in β position seem to be missing. The only example of conjugate addition of HF was reported for acrylic acid.[181] Other methods require additional features on the substrate molecule, relying on decarboxylative pathways,[182] the presence of benzylic positions,[183] leaving groups or directing groups.[184]

5.1.1 Mechanistic hypothesis

Inspiration for this project came from the work of the MacMillan group on the dual photo- and organocatalytic β-functionalisation of aldehydes.[92,93,135,136] This chemistry has been discussed already in **Section 3.5.2** about the PXX-catalysed β-arylation of cyclic ketones. In a similar mechanistic scenario (**Scheme 84**), the working hypothesis was that after photoredox oxidation of enamine **69a** to radical cation **69b** and deprotonation to they key 5π intermediate **69c**, this could abstract a fluorine atom from a suitable

fluorinating agent. The so-formed fluorinated enamine **69d** could then hydrolyse delivering the product. Radical **70**, formed after fluorine abstraction, could then be reduced by the photocatalyst in order to turnover the photocatalytic cycle. This hypothesis is based on different reports of alkyl radicals abstracting fluorine from electrophilic fluorinating agents such as those reported in **Scheme 84c**.[185]

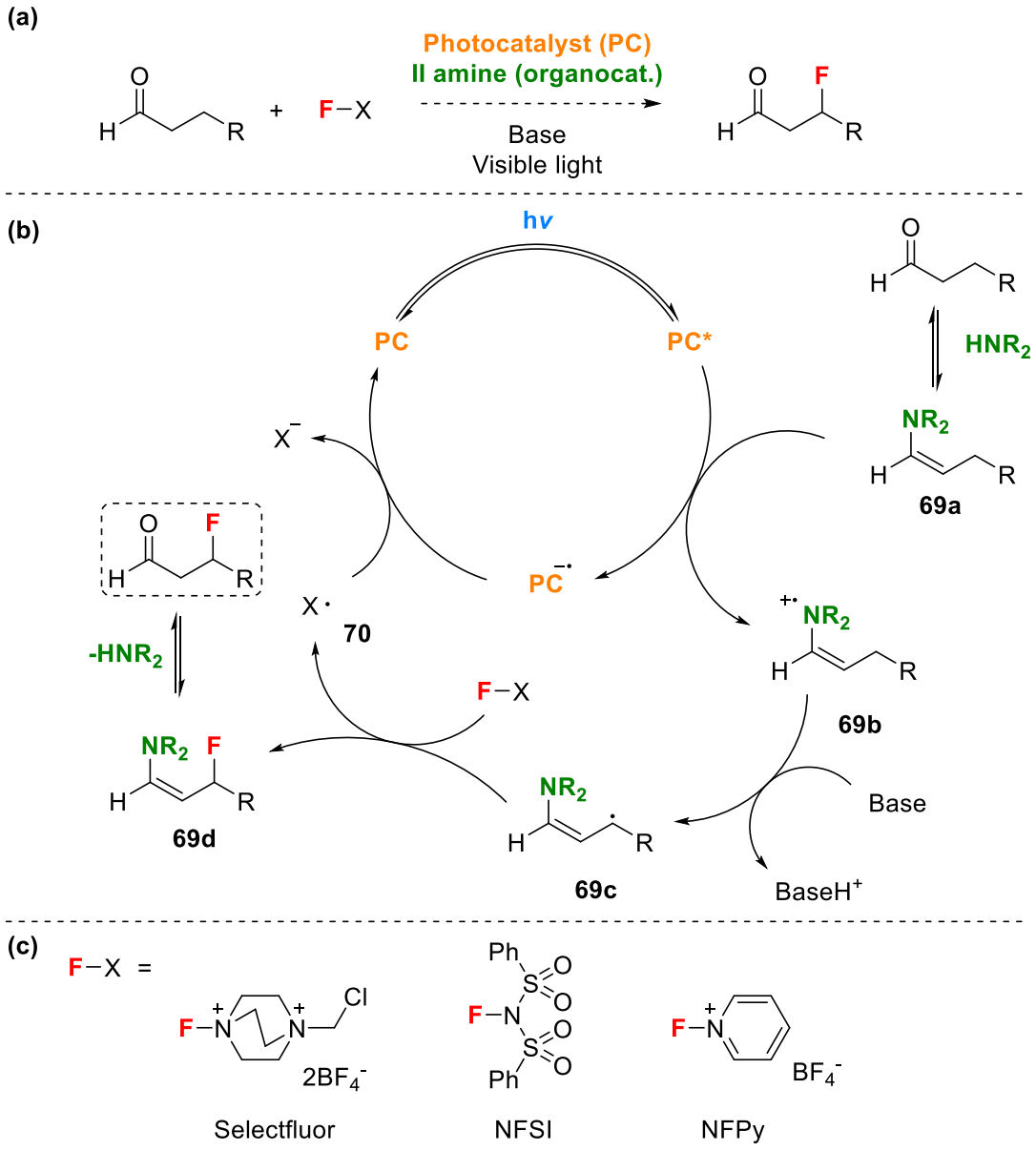

Scheme 84

General conditions **(a)**, mechanistic hypothesis **(b)** and electrophilic fluorinating agents **(c)** for the attempted β-fluorination of aldehydes.

5.1.2 Screening attempts and compatibility issues

The investigation started with a simple screening of the standard conditions employed by the MacMillan group for β-functionalisations, [92,93,135,136] looking for a proof of concept. Hexanal was chosen as saturated aldehyde, along with Selectfluor and NFSI as

fluorinating agents and dicyclohexylamine as organocatalyst. For the first trials, $[Ru(bpy)_3](PF_6)_2$ and $[Ru(bpz)_3](PF_6)_2$ were chosen as photocatalysts, along with some organic photocatalysts. TFA and water were initially excluded, since the MacMillan group reports them to be useful for reaction acceleration, but not indispensable. A collection of results is reported in **Table 24**. Unfortunately, no desired reactivity was obtained. The conditions employing Selectfluor usually lead to complete degradation of the starting material (SM), while in the reactions with NFSI some of it is still present in the reaction mixture. In entry 6, eosin Y was completely degradated to colorless byproducts upon contact with Selectfluor. A typical byproduct of these reactions, characterised by NMR and GCMS, was revealed to be α-methylenated compound **71**. It seemed reasonable it could be generated by attack of the enamine on the chloromethyl moiety of Selectfluor; however, the same reaction was later observed with NFSI as well, making the formation of **71** still puzzling. In the absence of light, it was still possible to observe its formation, suggesting a mechanism following a polar pathway.

Table 24

First attempts in the β-fluorination of aldehydes.

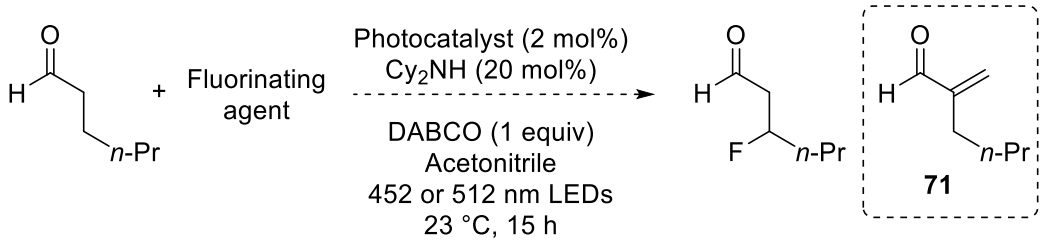

Entry	Photocatalyst	Fluorinating agent	Notes	Outcome[a]
1	$[Ru(bpy)_3](PF_6)_2$	Selectfluor	2:1 ACN:H_2O	SM
2	$[Ru(bpy)_3](PF_6)_2$	Selectfluor	-	BP
3	$[Ru(bpy)_3](PF_6)_2$	NFSI	-	BP + SM
4	$[Ru(bpz)_3](PF_6)_2$	Selectfluor	-	BP
5	$[Ru(bpz)_3](PF_6)_2$	NFSI	-	BP + SM
6	Eosin Y	Selectfluor	-	no PC
7	Eosin Y	NFSI	-	BP + SM

[a] SM = Starting material recovered, BP = Byproducts, no PC = degradation of photocatalyst.

A useful observation was that, upon addition of the reaction mixture (containing DABCO) to NFSI, a solid formed within minutes. The solid was isolated and the ^1H- and ^{19}F NMR spectra in D_2O suggest the formation of an adduct between NFSI and DABCO (**Scheme 85**). In this way, these two reagents are removed from the reaction mixture preventing any useful reaction.

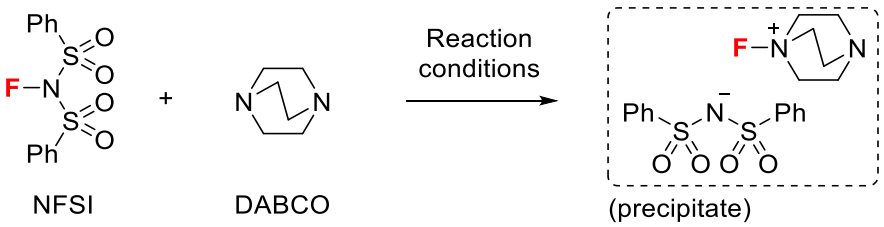

Scheme 85

Degradation of NFSI by DABCO, based on NMR experiments.

Further experimentation led to discovering that the fluorinating agents are often not compatible with nitrogen bases, DABCO above all.[186–189] This is unfortunate, DABCO being the favoured base in these β-functionalisation reactions. A small table of compatibilities was thus drawn (**Table 25**); the reactions between the fluorinating agents and the bases were monitored by ^{1}H and ^{19}F NMR. A number of cases showed compatibility of the two species (for example, pyridine or lutidine as base), while in the case of quinuclidine a neat transfer of fluorine to the base was observed. Partial degradation was observed in many other cases.

Table 25

Table of compatibilities between bases and fluorinating agents in acetonitrile.[a]

Base	**Fluorinating agent**		
	Selectfluor	NFSI	NFPy
DABCO	×	×	×
Quinuclidine	√ [b]	√ [b]	
Pyridine	√	√	
2,6-Lutidine	?	√	
2,4,6-Collidine	×	√	
DMAP		?	?
DBU		?	?
K_2CO_3	×		
TBAF (THF)		×	
KF	√		
TEA		?	
DIPEA		?	

[a] × = Degradation or formation of insoluble material; ? = Unclear of partial degradation; √ = Compatible. [b] Fluorine transfer to quinuclidine is observed; the resulting species is soluble.

Later experiments also showed lack of compatibility with the organocatalyst: reaction of dicyclohexylamine with NFSI in acetonitrile provides in 1 h partial conversion to the corresponding fluorinated amine (**Scheme 86**).[190]

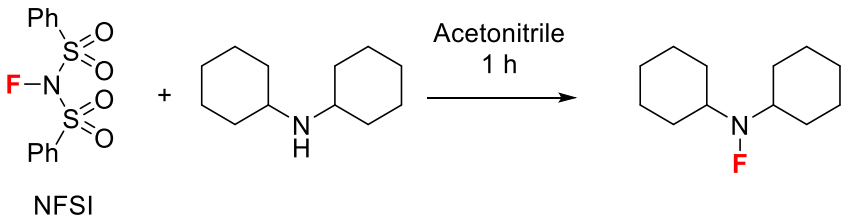

Scheme 86
Reaction of NFSI with dicyclohexylamine (organocatalyst).

From this point on, further attempts were made to obtain the desired chemistry. Screening bases, changing solvent (from acetonitrile to THF, DME and DMPU), organocatalyst (from dicyclohexylamine to morpholine and proline) and carrying out the reaction under air provided similar results, and no product was ever detected. Without DABCO as base the reaction mixtures look much cleaner (by ^{1}H NMR) and the starting material can usually be recovered. Some minor ^{19}F signals from alkyl C–F groups were detected in the reaction employing NFSI and collidine as base; however, it was not possible to identify the product. Some last attempts using cinnamaldehyde and cyclohexanone as substrates also proved fruitless.

5.1.3 Conclusions

In conclusion, it was not possible to observe any β-fluorination product in this project. Nonetheless, the instability of the most common electrophilic fluorinating reagents and their lack of compatibility with different bases, especially amines, was found. These issues should be considered by anyone attempting this transformation again.

5.2 From a C–C cross-coupling to a method for the *N*-alkylation of azoles

This small project focused on finding alternative strategies for the preparation of the pharmaceutically-relevant synthetic intermediate **72**, bearing an imidazole-type unit with an α-heteroatom substituent in position 2 on the ring. The most ideal disconnection involved breaking the C–C bond between the imidazole C2 and the rest of the molecule (**Scheme 87**), resulting in an simple heteroatom-substituted alkane **73** and an imidazole derivative, either halogenated (**74b-c**) or not (**74a**), depending on the conditions chosen. A photoredox HAT-based catalytic system, through the generation of radical **75**, was considered as a possible strategy in promoting such coupling.

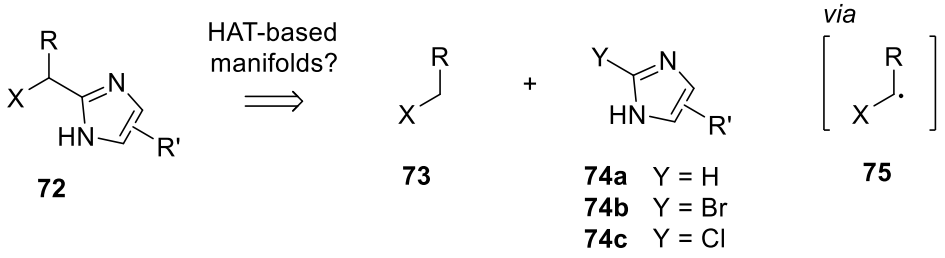

Scheme 87
Hypothetical convenient disconnection towards intermediate **72**.

5.2.1 Ni-photoredox HAT-based strategy

The first attempt focused on applying the MacMillan group's conditions for HAT-mediated Ni-photoredox cross-coupling to **73** and **74b**.[49] It is the same type of coupling described in **Section 2.1.2**, even though in a different setting. In the standard conditions (**Scheme 88**) no product was detected: 38% yield of adduct **76** was observed (and its structure postulated based on NMR and LCMS data), along with partial debromination of the imidazole substrate **74b** to **74a**.

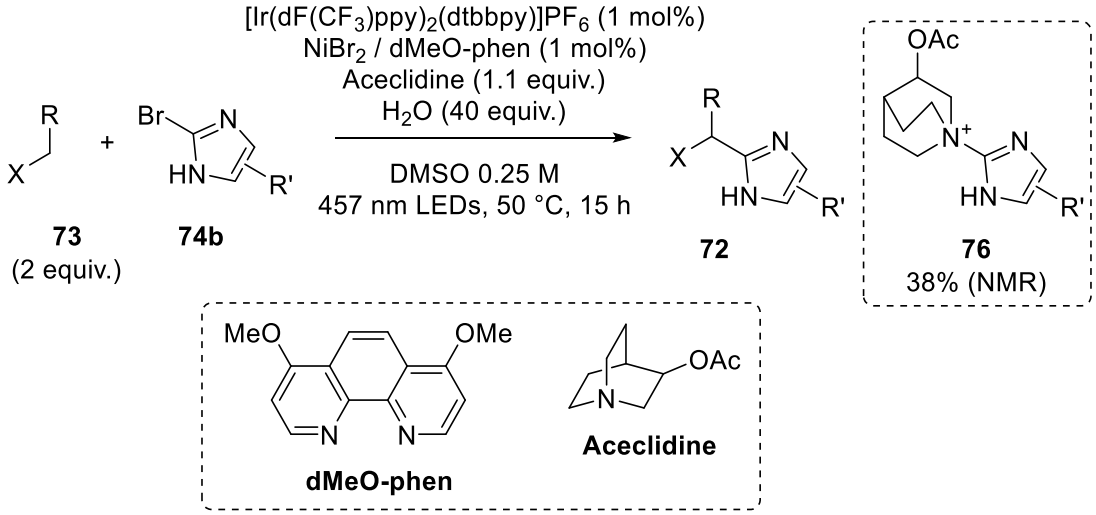

Scheme 88
Attempted HAT-mediate Ni-photoredox cross-coupling towards **72**.

Similar results were obtained when 4CzIPN was used as photocatalyst, or when the *N*-tosyl derivative of **74b** was used instead. Control experiments were performed with known substrates: the reaction of **74b** with tetramethylurea afforded 13% NMR yield of coupling product, while in the reaction of 4'-bromoacetophenone with **73** no coupling product was observed by NMR, and only minor amounts were detected by LCMS. These results suggest both **73** and **74b** to be difficult substrates in this reaction, and the coupling between the two is thus unlikely unless an intensive screening and optimisation effort is made.

5.2.2 Eosin Y HAT-based strategy

A second attempt was made employing a totally different setup. In this case, neutral eosin Y was used as photocatalyst and HAT reagent, according to the work of Wu and coworkers (**Scheme 89**).[191] Upon formation of radical **75** *via* HAT, a Minisci-type addition to **74b-c** would form the new C–C bond. Reduction of the so-formed species and expulsion of HY would deliver **72**. Unfortunately, no product was found, and the reaction mixture contained only unreacted starting material. Similar attempts provided the same results.

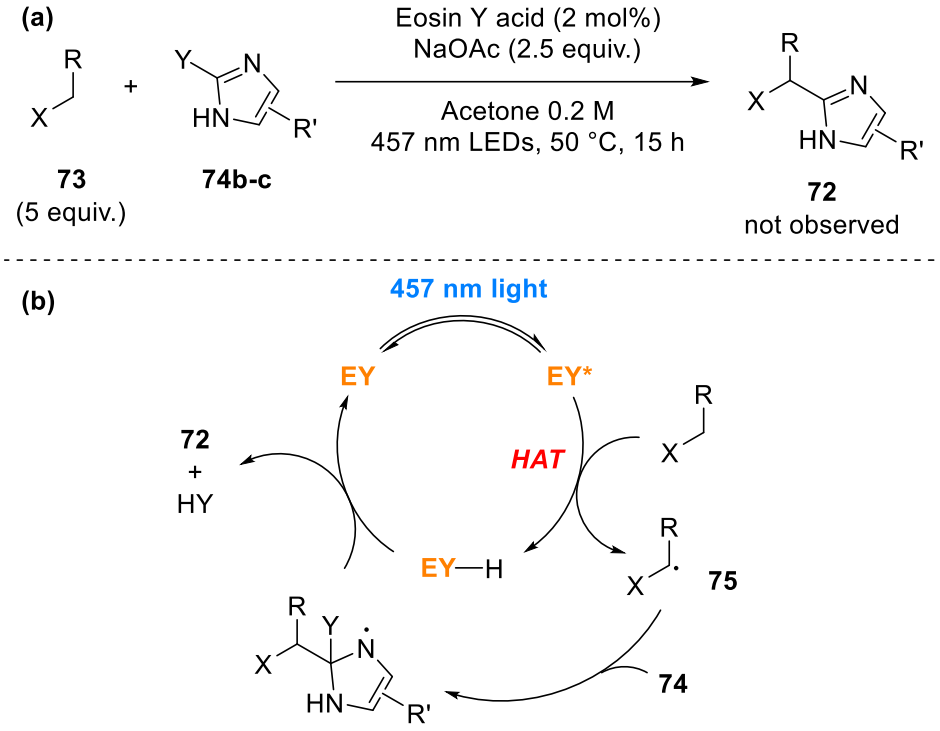

Scheme 89

Attempted reaction **(a)** and hypothetical mechanism **(b)** for the EosinY-HAT transfer coupling towards **72**.

5.2.3 Peracetate-based strategy and a method for the *N*-alkylation of azoles

A similar transformation had been reported by Wang and co-workers: they described a cross-dehydrogenative coupling between 5-membered heterocycles and protected amines (and other "hydrogen donors") using *tert*-butyl peracetate (tBPA) as stoichiometric oxidant (**Scheme 90**).[192] In these conditions, an Ir(III) photocatalyst is used to reduce tBPA for the release of a *tert*-butoxy radical. TFA is needed in the reaction to activate tBPA towards reduction through proton coupled electron transfer or PCET (as the process is thermodynamically disfavoured, E = - 1.56 V *vs* SCE for tBPA, E = - 0.89 V *vs* SCE for Ir(III)*). Once the *tert*-butoxy radical is generated, it can perform HAT on

the substrate, forming the alkyl radical that is now amenable for Minisci addition on the heterocycle.

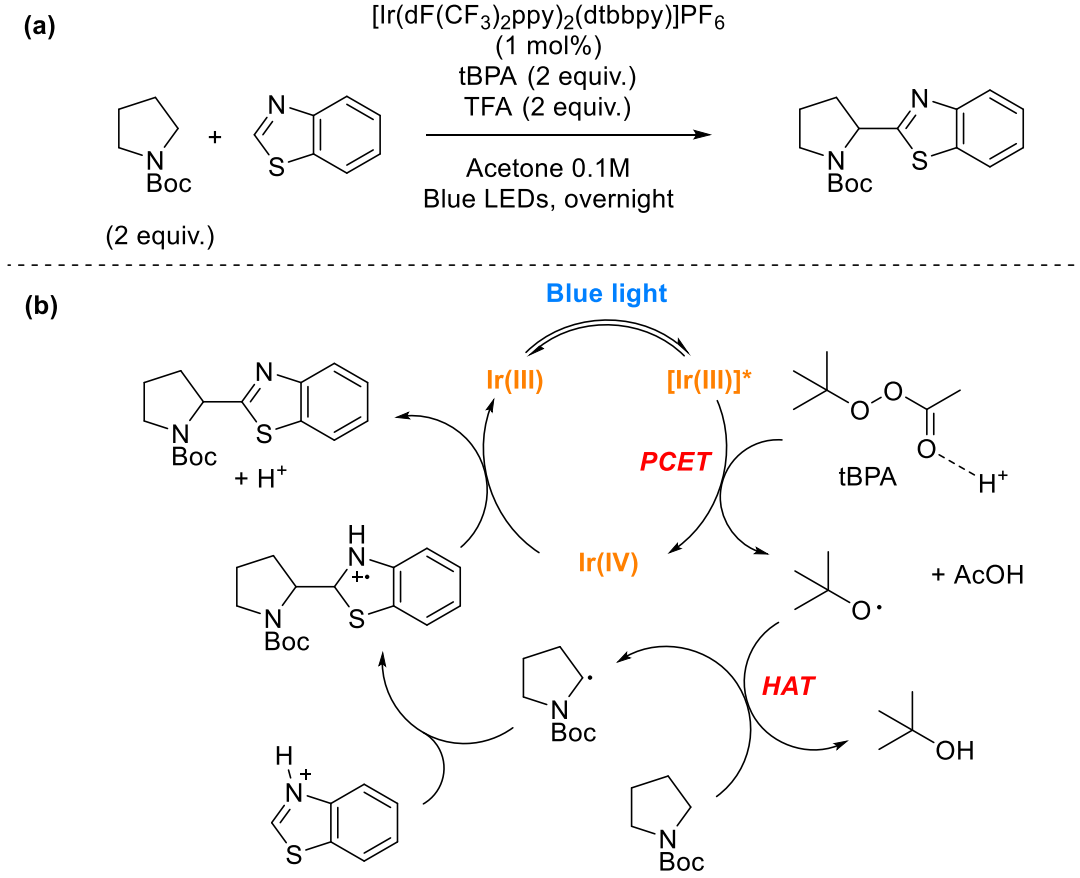

Scheme 90

Conditions **(a)** and proposed mechanism **(b)** for Wang's cross-dehydrogenative coupling of amines with heterocycles.[192]

When these conditions were tested on the system of interest (**Scheme 91**), again no product was found. Extensive reaction of **73** was observed and at least three over-oxidation products of **73** were characterised. This result suggests that α-oxidation of **73** is possible in these conditions, but the reaction deviates from the desired pathway to yield very different products.

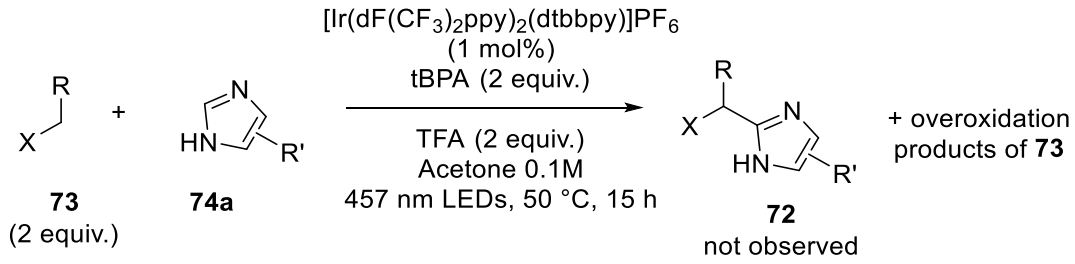

Scheme 91

Results in applying Wang's conditions for the synthesis of **72**.

As mentioned above, TFA is thought to help reduction of tBPA by the photocatalyst. It seemed reasonable that in the presence of *fac*-Ir(ppy)$_3$ as photocatalyst reduction of tBPA should happen without the need of TFA (E = -1.73 V *vs* SCE in its excited state).[7] If these modified conditions are applied, again no product was detected, but a 66% yield of a new coupled species was found (**Scheme 92**). Through NMR and LCMS analysis of an isolated sample, this product was concluded to have structure **77**: a plausible explanation is that, in these conditions, oxidation of **73** to the corresponding α-heteroatom carbocation can occur, which can then be attacked by the nucleophilic azole.

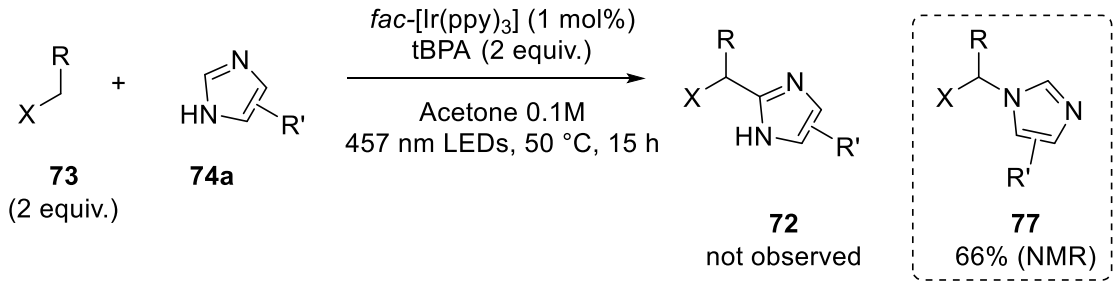

Scheme 92

Results in applying modified tBPA conditions for the synthesis of **72**.

While the desired reactivity was not found, this reaction seems an interesting way to activate an α-heteroatom position and introduce a *N*-azole unit, forming an (hemi)aminal-type species. A literature survey revealed that these transformations have been already reported employing iron catalysis,[193,194] ruthenium catalysis,[195] iodide catalysis,[196] hypervalent iodine reagents,[197,198] or rely on halogen bonding.[199] Only one other example involved a photocatalytic system, based on Mes-Acr-Me as photocatalyst, but was limited to pyrazoles and triazoles as azoles and THF as coupling partner.[200]

As a proof of concept, the same conditions were applied to the reaction of benzimidazole with THF and *N*-Boc pyrrolidine in acetone (**Scheme 93**): in both cases a modest yield (30-45%) of the *N*-coupled product was obtained.

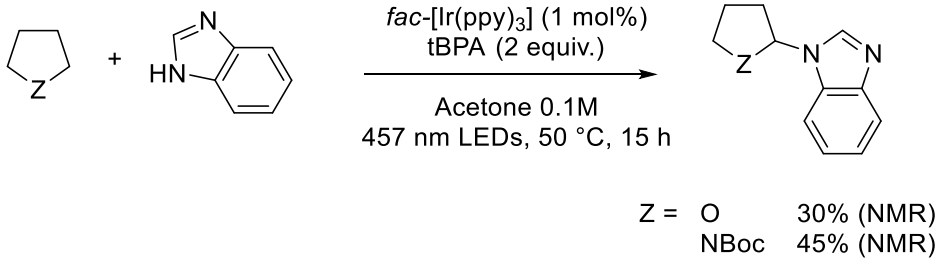

Scheme 93

Results in applying modified tBPA conditions to simpler substrates.

5.2.4 Conclusions

In conclusion, different cross-coupling strategies were tested in order to obtain pharmaceutically-relevant synthetic intermediate **72**. Ranging from Ni-photoredox to activation with tBPA, none of the strategies provided the desired product. During the investigation, it was found that the use of *fac*-[Ir(ppy)$_3$] as photocatalyst and tBPA as oxidant afforded *N*-alkylation instead of *C2*-alkylation of the azole moiety. When these conditions were applied to simpler substrates, modest but interesting yields (30-45%) were obtained, suggesting that further optimisation of conditions might furnish a simple photocatalytic strategy for the *N*-alkylation of azoles.

Chapter 6
Experimental section

6.1 General remarks

Procedures

Unless otherwise stated, all reactions were carried out under N_2 employing standard Schlenk techniques. When relevant, degassing of the solvent was performed by freeze-pump-thaw procedure: the flask was immersed in liquid nitrogen, and once the liquid was frozen (3 min.) it was put under high vacuum for 5 min., the flask was then closed and the liquid thawed in a water bath before being immersed in liquid nitrogen again. The procedure was repeated three times before refilling with nitrogen. Glassware was dried under vacuum with a heatgun before use unless experiments involved the use of water. Reagents and solvent were purchased from commercial suppliers (Sigma-Aldrich, Alfa Aesar, Acros Organics, TCI or Fluorochem) and used as received. When deemed necessary, purification of liquid reagents was performed by distillation under reduced pressure. Dry acetone was purchased from Acros Organics and used as received after degassing by N_2 sparging. Other dry solvents were purchased from Sigma-Aldrich and used as received after degassing by N_2 sparging. Deuterated solvents were purchased from Cambridge Isotope Laboratories or Sigma-Aldrich and used as received. Thin layer chromatography (TLC) analyses were performed on Macherey-Nagel pre-coated TLC-sheets POLYGRAM SIL G/UV_{254} with fluorescent indicator. Visualisation was performed with UV light, or alternatively using basic aqueous potassium permanganate, ceric molybdate or phosphomolibdic acid solutions and heat as developing agents. Purification by flash column chromatography was performed on a Teledyne ISCO Combi Flash R_f+ automated system or manually using Sigma-Aldrich high purity grade silica gel (pore size 60 Å, 440 mesh particle size, 35-75 μm particle size), as specified in each instance. For final products, yields were adjusted if traces of solvents are still present in the sample.

Differences in standard procedures in ICIQ: Unless otherwise stated, all reactions were carried out under Ar employing standard Schlenk techniques. Dry solvents were

obtained from a commercial SPS solvent dispenser. TLC analyses were performed on Merck precoated TLC plates (silica gel 60 GF_{254}, 0.25 mm).

General analytics

NMR spectra were recorded on Bruker spectrometers at 300, 400 or 500 MHz for ^{1}H nuclei at room temperature in the specified deuterated solvent. Chemical shifts are given in ppm relative to tetramethylsilane as standard (when $CDCl_3$ is used as solvent) or to residual non-deuterated signals as reference. Coupling constants (*J*) are given in hertz (Hz). Multiplicity is indicated with the following abbreviations: s, singlet; d, doublet; dd, doublet of doublets; ddd, doublet of doublets of doublets; t, triplet; dt, doublet of triplets; td, triplet of doublets; tt, triplet of triplets; q, quartet; dq, double of quartets; m, multiplet (multiplicity and *J* constants not easily determined); br s, broad signal. FT-IR analyses were conducted on a Shimadzu IRAffinity-1S Fourier transform infrared spectrophotometer. Spectra are reported as characteristic bands (cm^{-1}). High-resolution ESI mass spectra (HRMS) were performed on a Waters LCT HR TOF mass spectrometer by the analytical team in Cardiff University, or on a MicroTOF Focus and Maxis Impact (Bruker Daltonics) with ESI by the analytical team in ICIQ. UV-Vis measurements (absorption and fluorescence experiments) were performed on a Molecular Devices SpectraMax M5 spectrofluorimeter (DRL), an Agilent Cary Series UV-Vis-NIR Spectrophotometer (Cardiff) or an Agilent Cary Eclipse Fluorescence Spectrophotometer (Cardiff). Optical rotations were measured on a Perkin Elmer Polarimeter 341 (DRL) or a Jasco P-1030 Polarimeter (ICIQ) and reported for products with e.r. > 60:40 as follows: $[\alpha]_D^{Temp.}$ (*c* concentration in g per 100 mL, solvent). Melting points were measured in capillary tubes on a Electrothermal 9200 apparatus and are uncorrected. Internal temperature of reaction mixtures was measured with a Digitron TM-22D differential digital thermometer. Cyclic voltammetry (CV) experiments were conducted on a Metrohm Autolab PGSTAT204 potentiostat. The working electrode used was a glassy carbon electrode, the counter electrode was a platinum spiral and the quasi-reference electrode a silver wire. Tetrabutylammonium hexafluorophosphate ($TBAPF_6$) was added to the acetonitrile solution of the analyte as supporting electrolyte (concentration 0.1 M). For irreversible processes, the half-peak potential ($E^{p/2}$), corresponding to the potential at half the maximum current of the peak, was used as an estimation of the

reduction potential of the compound.[8] X-band (*ca.* 9.5 GHz) continuous wave electron paramagnetic resonance (EPR) experiments were performed at room temperature on a Bruker EMX spectrometer equipped with a Bruker ER4122-SHQE resonator. Irradiation was performed at 450 nm using a Sciencetech Tunable Light Source TLS-55-X300 operating a Xe lamp (maximum power 300 W) with a 300-1800 nm spectral range (0.2 nm resolution at 300-700 nm and 0.4 nm resolution at 700-1800 nm). The solutions for EPR analysis were degassed by freeze-pump-thaw technique, transferred to a glove-box, and samples prepared and sealed inside the glove-box. Spectra were simulated using the EasySpin[201] package operating within the Mathworks Matlab environment.

Determination of enantiomeric ratios

Chapter 2: Chiral SFC analysis was performed on a Waters Aquity UPC² instrument using a YMC CHIRAL ART Amylose-SA, YMC CHIRAL ART Cellulose-C, Lux i-Amylose-3 or Lux Cellulose-4 chiral column. Exact conditions of analysis for each compound are specified in the characterisation section. SFC traces were compared to those of racemic samples, prepared by running the cross-coupling reactions in DMF with bpy as achiral ligand.

Chapter 4: Chiral HPLC analysis was performed on an Agilent 1200 series HPLC, using a Daicel Chiralpak IC-3 column with hexane:*i*-PrOH as eluent. Chiral SFC analysis was performed on a Waters Aquity UPC² instrument using a CEL1, CEL2, ID3 or IE3 chiral column. Exact conditions of analysis for each compound are specified in the characterisation section. HPLC and SFC traces were compared to those of racemic samples, prepared by running the photomediated reaction with racemic 2-*tert*-butyl-3-methyl-5-benzyl-4-imidazolidinone as organocatalyst.

6.2 Photochemical reactors

DRL and Cardiff University: Photocatalytic reactions are carried out in a home-made photochemical reactor composed of an LED strip wrapped tightly around a clear 250 mL beaker (**Figure 9**). Reactions mixtures were prepared in 10 mL Schlenk flasks and fitted inside the beaker at a distance of about 2 cm from the strips. Unless otherwise stated, a fan was used to avoid overheating of the system and to maintain an internal temperature of 23-25 °C inside the reaction flasks. For the work described in **Chapter 2** and

Section 5.1, an ALED LIGHT RGB LED strip (5050 SMD RGB LEDs, 60 LEDs/meter), from here named ***LED strip 1***, was used: its emission is compared to the absorption of the photocatalyst 4CzIPN in **Figure 10a**. For the work described in **Chapter 3** and **Section 5.2**, an UltraLEDs Blue 120 high intensity, from here named ***LED strip 2*** was used: see **Figure 10b** for emission and comparison to the absorption of the photocatalyst PXX.

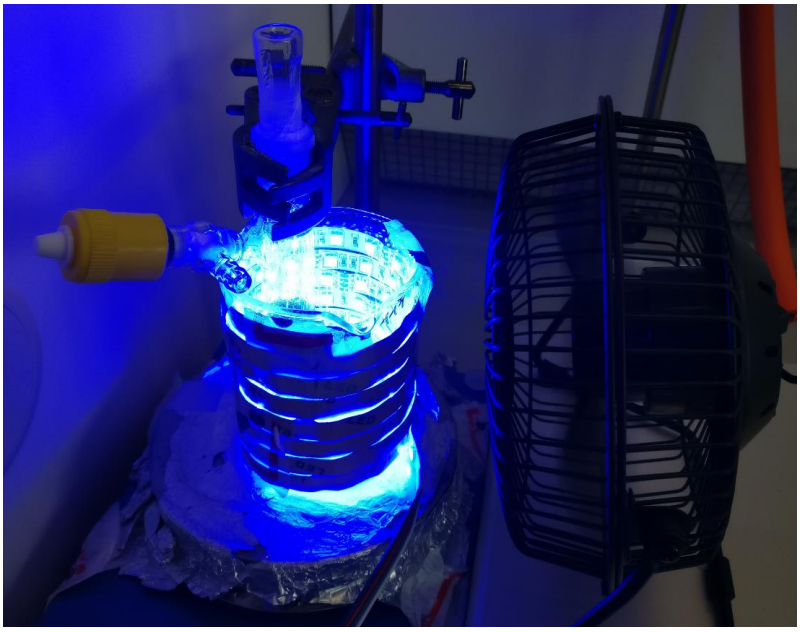

Figure 9
Photo of a typical photocatalytic setup in DRL.

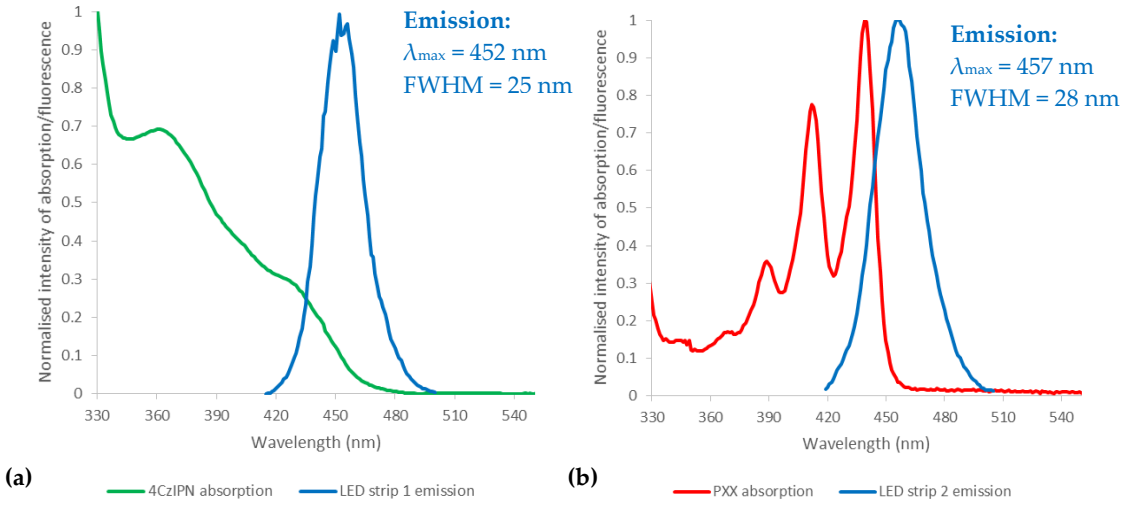

Figure 10
(a) Emission of ***LED strip 1*** compared to the absorbance of 4CzIPN (acetone). **(b)** Emission of ***LED strip 2*** compared to the absorbance of PXX (acetonitrile).

ICIQ: For the work described in **Chapter 4**, photomediated reactions were carried out in a home-made photochemical reactor composed of a single 420 nm high power (HP) LED. Reaction mixtures were prepared in 5 mL vials and accomodated above the LED into an aluminium block on a 3D-printed holder (**Figure 11**). Cooling liquid was let circulate in the block to allow for temperature control. The irradiance was fixed at 40 ± 2 mW/cm^2 as controlled by an external power supply and measured using a photodiode light detector. This setup ensured reproducible irradiation keeping a distance of 1 cm between light source and reaction vessel.

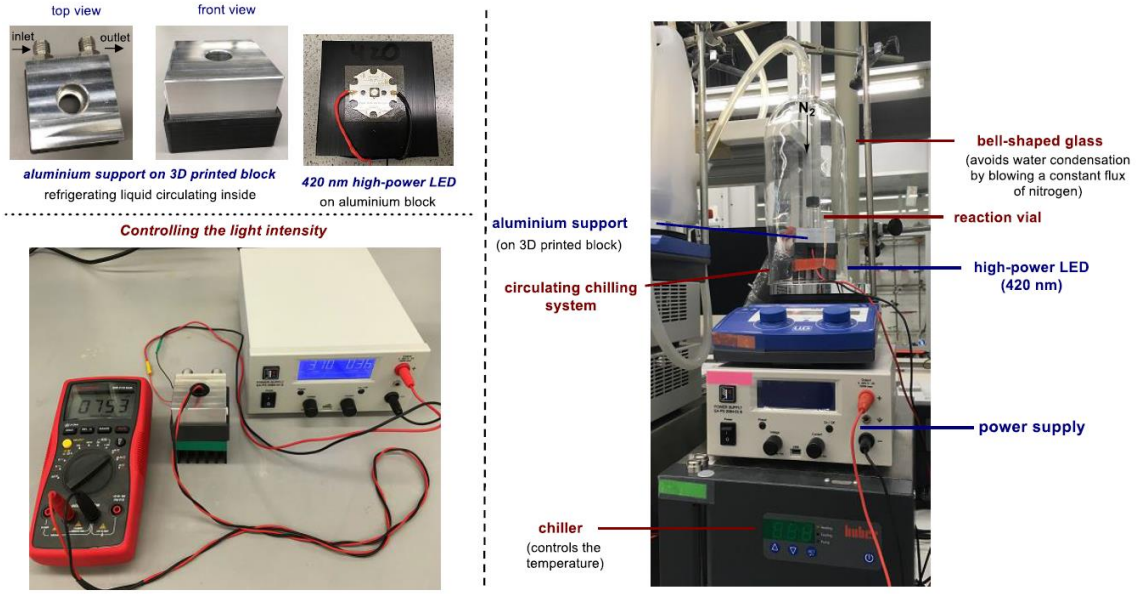

Figure 11

Depiction of the photochemical reactor used in ICIQ. Image taken from own paper.[22]

Actinometry

The light output of the reactors used in DRL was estimated with standard ferrioxalate actinometry.[9,202] A 0.15 M solution of ferrioxalate was prepared with 7.37 g of potassium ferrioxalate hydrate in 100 mL of 0.05 M H_2SO_4. A buffer solution was prepared with phenanthroline (100 mg) and sodium acetate (22.5 g) in 100 mL of 0.05 M H_2SO_4. For photon flux determination, 2 mL of the ferrioxalate solution were transferred in a 10 mL Schlenk flask (same as used for the photocatalytic reactions) and irradiated for 3 seconds. After irradiation, 4 mL of the phenanthroline solution were added, and the resulting solution stirred at room temperature for 1 h with no exposure to light. 1 mL of the solution was diluted 1/10 with 0.05 M H_2SO_4 in a volumetric flask, and the absorbance of the resulting solution recorded at 510 nm. A non-irradiated sample, subjected to the same procedure, was used as reference.

The following equation was used to determine conversion to Fe^{2+} ions:

$$n_{Fe^{2+}} = \frac{V \cdot \mathrm{A}}{l \cdot \varepsilon} \cdot 10$$

V is the initial volume of solution (0.006 L), A the absorbance at 510 nm of the irradiated solution (referenced to the non-irradiated one), l the path length (1 cm) and ε the molar absorbivity at 510 nm (11,100 L mol^{-1} cm^{-1})[202]. The factor of 10 is used to consider dilution.

The photon flux was then calculated as:

$$photon\ flux = \frac{n_{Fe^{2+}}}{\Phi \cdot t \cdot f}$$

where Φ is the quantum yield of the ferrioxalate actinometer (a value of 0.85 was used for a 0.15 M solution at 458 nm)[203], t the time (3 s) and f the fraction of light absorbed at 452 nm (maximum of emission of the LED strips). The last parameter was estimated based on the absorbance of the ferrioxalate solution at 452 nm:

$$f = 1 - 10^{-A_{452\ nm}}$$

Results are reported in **Table 26** for ***LED strip 1*** and ***LED strip 2***.

Table 26

Estimating the light output of our home-made photoreactors through standard actinometry.[a]

LED strip #	Exp #	Measured absorbance	n Fe^{2+} (mol)	Photon flux (mol/s)	Photon flux avg. (mol/s)
1	1	0.209	$1.13 \cdot 10^{-6}$	$4.57 \cdot 10^{-7}$	$4.63 \cdot 10^{-7}$
	2	0.209	$1.13 \cdot 10^{-6}$	$4.57 \cdot 10^{-7}$	
	3	0.217	$1.17 \cdot 10^{-6}$	$4.75 \cdot 10^{-7}$	
2	4	0.683	$3.69 \cdot 10^{-6}$	$1.49 \cdot 10^{-6}$	$1.55 \cdot 10^{-6}$
	5	0.752	$4.06 \cdot 10^{-6}$	$1.65 \cdot 10^{-6}$	
	6	0.688	$3.72 \cdot 10^{-6}$	$1.51 \cdot 10^{-6}$	

[a] Irradiation time: 3 s.

Low temperature reactor (Chapter 2)

In order to obtain data on the effect of temperature (**Table 10**), a slightly different reactor was used. The LED strips used (UltraLEDs Blue 120 high intensity, as in ***LED strip 2***) were thus wrapped around a 25 mL two-necked jacketed round bottomed flask. Reaction mixtures were prepared as usual with the exclusion of base (Cs_2CO_3), degassed by three cycles of freeze-pump-thaw, filled with N_2, and then transferred by syringe to the flask already containing the base. Irradiation was then started, with the jacket liquid set to the proper temperature. In the case of the 10 °C and 0 °C experiments, the reactor was setup

inside a glove bag with a continuous flow of dry N_2, in order to avoid condensation on the walls of the flask, and thus on the LEDs.

6.3 Preparation of photocatalysts

2,4,5,6-Tetra(carbazol-9-yl)isophthalonitrile (4CzIPN)

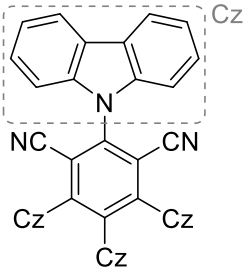

Following a reported procedure,[20] a 250 mL multi-necked round bottomed flask was charged with carbazole (1.67 g, 10 mmol, 5 equiv.) and put under N_2. THF (40 mL) was added to make a solution, to which NaH (600 mg of a 60% dispersion in mineral oil, 15 mmol, 7.5 equiv.) was added in portions. After 30 min of stirring at room temperature, tetrafluoroisophthalonitrile (400 mg, 2 mmol) was added, and the mixture stirred for 15 h. The reaction was quenched with water and the solvent evaporated. The resulting solid was washed with water and ethanol, before being re-crystallized from acetone/chloroform. A second re-crystallisation of the mother liquors afforded more solid. Title compound: bright yellow solid (1.15 g, 73% yield). **m.p.** 366-368 °C [Lit.[20] 354-356 °C]. **^{1}H NMR** (400 MHz, DMSO-d_6): δ 8.40 (d, *J* = 7.8 Hz, 2H), 8.24 (d, *J* = 8.2 Hz, 2H), 7.91 (d, *J* = 7.3 Hz, 4H), 7.82-7.76 (m, 6H), 7.61-7.48 (m, 6H), 7.22-7.12 (m, 8H), 6.85 (t, *J* = 7.3 Hz, 2H), 6.75 (t, *J* = 7.8 Hz, 2H). The spectral data are in good agreement with those previously reported.[20]

***Peri*-xanthenoxanthene (PXX)**

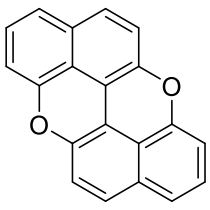

Following a reported procedure,[204] a 100 mL round bottomed flask was charged with [1,1'-binaphthalene]-2,2'-diol (573 mg, 2 mmol), CuI (1.14 g, 6 mmol, 3 equiv.) and pivalic acid (409 mg, 4 mmol, 2 equiv.), to which DMSO (25 mL) was added. The reaction mixture was stirred in open air at 140 °C for 8 h, until complete consumption of the starting material as verified by TLC. The mixture was diluted with CH_2Cl_2 and extracted with NH_4OH 30% solution (x3), then the aqueous phases were pooled and washed with CH_2Cl_2 (x3). Organics were pooled, washed with brine, dried ($MgSO_4$) and the solvent evaporated. The crude material was purified by flash column chromatography (eluent gradient from pure heptane to heptane:CH_2Cl_2 7:3) to give the corresponding product as a bright yellow solid (359 mg, 64% yield). **^{1}H NMR** (400 MHz, C_6D_6): δ 6.88 (d, *J* = 9.0 Hz,

2H), 6.84-6.79 (m, 4H), 6.69 (d, J = 9.0 Hz, 2H), 6.59-6.54 (m, 2H). **^{13}C NMR** (101 MHz, C_6D_6): δ 153.1, 144.6, 131.7, 127.4, 126.5, 122.1, 120.3, 117.5, 112.0, 108.9. The spectral data are in good agreement with those previously reported.[204]

Cost estimation for PXX and *fac*-Ir(ppy)$_3$

In this section a rough estimation of the cost per mmol of both PXX (**Table 27**) and *fac*-Ir(ppy)$_3$ (**Table 28**) are carried out. The best price found on Merck (www.sigmaaldrich.com) as of 27th January 2020 for a ≥ 99% purity compound (if possible) is used. The procedure for the preparation of *fac*-Ir(ppy)$_3$ was found in the literature.[205]

Table 27

Calculation of the approximate cost of PXX per mmol.

Chemical	Equivalents	Mass or Volume	Cost	Total cost
Binaphthol	1	286 mg	£ 3.14 /g	£ 0.90
CuI	3	571 mg	£ 1.23 /g	£ 0.70
Pivalic acid	2	0.23 mL	£ 41.9 /L	£ 0.10
DMSO	13 mL/mmol	13 mL	£ 67.2 /L	£ 0.87
TOTAL (100% y)[a]				£ 2.57 / mmol
TOTAL (64% y)[b]				£ 4.01 / mmol

[a] Cost if the yield was 100%. [b] Actual cost taking into account a 64% yield.

Table 28

Calculation of the approximate cost of *fac*-[Ir(ppy)$_3$] per mmol.

Chemical	Equivalents	Mass or Volume	Cost	Total cost
$IrCl_3$	1	299 mg	£ 136 /g	£ 40.66
2-Phenylpyridine	3.3	512 mg	£ 4.16 / g	£ 2.13
n-Butyllithium[a]	3.3	2.1 mL	£ 51.5 / L	£ 0.11
TOTAL (100% y)[b]				£ 42.90 / mmol
TOTAL (88% y)[c]				£ 48.75 / mmol
Sold as such[d]				£ 655 / mmol

[a] 1.6 M solution in hexane. [b] Cost if the yield was 100%. [c] Actual cost taking into account a 88% yield, as reported in the reference. [d] Cost of *fac*-[Ir(ppy)$_3$] as sold on the Merck website.

6.4 Preparation of chiral ligands

Ligands not mentioned in this section were obtained commercially or as part of the ligand collection in Dr. Reddy's Laboratories, Cambridge.

(*S*)-*tert*-Leucinol

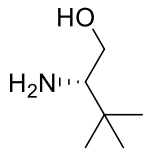

Following a reported procedure,[206] a 500 mL three necked round bottomed flask equipped with reflux condenser and addition funnel was charged with (*S*)-*tert*-leucine (5.25 g, 40 mmol) and put under N_2. THF (105 mL) was added to make a fine suspension, cooled in an ice bath. $NaBH_4$ (3.78 g, 100 mmol, 2.5 equiv.) was added in one portion. The addition funnel was charged with a solution of I_2 (10.15 g, 40 mmol, 1 equiv.) in THF (28 mL), which was then added dropwise over 30 min. The reaction mixture was heated to reflux, stirred for 15 h, cooled to room temperature and MeOH was added slowly until a clear solution formed, then stirred 30 min. The solution was concentrated, and the obtained semi-solid washed with 20% aqueous KOH (80 mL, 40 mmol, 1 equiv.) and stirred for 5 h. The aqueous phase was extracted with CH_2Cl_2, dried ($MgSO_4$) and the solvent evaporated to afford the desired product as a clear oil (3.6 g, 77% yield) that solidifies as white crystals in the fridge (5 °C). The product was used as such without further purification. **^{1}H NMR** (400 MHz, $CDCl_3$): δ 3.71 (dd, *J* = 10.2, 3.8 Hz, 1H), 3.21 (t, *J* = 10.2 Hz, 1H), 2.51 (dd, *J* = 10.2, 3.8 Hz, 1H), 1.99 (br s, 3H), 0.90 (s, 9H). **^{13}C NMR** (101 MHz, $CDCl_3$): δ 62.3, 61.8, 33.2, 26.3. The spectral data are in good agreement with those previously reported.[207]

(*S*)-4-(*tert*-Butyl)-2-(3-methylpyridin-2-yl)-4,5-dihydrooxazole (L3)

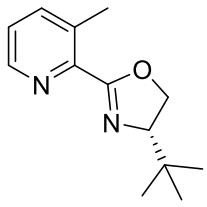

Following a reported procedure,[208] a 100 mL two-necked round bottomed flask equipped with reflux condenser was charged with zinc triflate (436 mg, 1.2 mmol, 20 mol%). The flask was put under vacuum and heated to 90 °C for 1 h. After cooling to room temperature, a previously prepared mixture of 2-cyano-3-methylpyridine (709 mg, 6 mmol) and (*S*)-*tert*-leucinol (703 mg, 6 mmol, 1 equiv.) in toluene (20 mL) was added. The reaction mixture was heated to reflux and stirred over 64 h, allowed to cool to room temperature, diluted with EtOAc and washed with a sat. aqueous $NaHCO_3$ solution. The aqueous phase was back-extracted with EtOAc twice, organics pooled, dried ($MgSO_4$) and solvent evaporated. The crude material was purified by automated flash column chromatography (eluent gradient: from pure heptane to heptane:EtOAc 1:1) to give the corresponding product as a colorless liquid (648 mg, 49% yield). The liquid solidifies to a white solid during storage in the fridge (5 °C). $[\alpha]_D^{20}$ = -53.5° (*c* 0.5, THF),

$[\alpha]_{365}^{20}$ = -202.4° (*c* 0.5, THF) [Lit.[208] $[\alpha]_{365}^{25}$ = -212.7° (*c* 0.1, THF)]. **m.p.** 65-66 °C. **^{1}H NMR** (400 MHz, $CDCl_3$): δ 8.53 (d, *J* = 4.7 Hz, 1H), 7.60 (d, *J* = 7.8 Hz, 1H), 7.27 (dd, *J* = 7.8, 4.7 Hz, 1H), 4.41 (dd, *J* = 9.9, 8.3 Hz, 1H), 4.26-4.15 (m, 2H), 0.99 (s, 9H). **^{13}C NMR** (101 MHz, $CDCl_3$): δ 161.1, 146.8, 145.8, 139.2, 135.0, 124.6, 77.2, 68.1, 33.9, 26.0, 20.7. The spectral data are in good agreement with those previously reported.[208]

(*S*)-4-(*tert*-Butyl)-2-(4-methylpyridin-2-yl)-4,5-dihydrooxazole (L4)

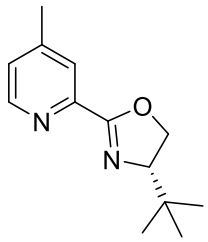

Following a reported procedure,[208] a 50 mL two-necked round bottomed flask equipped with reflux condenser was charged with zinc triflate (218 mg, 0.6 mmol, 20 mol%). The flask was put under vacuum and heated to 90 °C for 1 h. After cooling to room temperature, a previously prepared mixture of 2-cyano-4-methylpyridine (354 mg, 3 mmol) and (*S*)-*tert*-leucinol (352 mg, 3 mmol, 1 equiv.) in toluene (10 mL) was added. The reaction mixture was heated to reflux and stirred over 24 h, allowed to cool to room temperature, diluted with EtOAc and washed with a sat. aqueous $NaHCO_3$ solution. The aqueous phase was back-extracted with EtOAc twice, organics pooled, dried ($MgSO_4$) and solvent evaporated. The crude material was purified by automated flash column chromatography (eluent gradient: from pure heptane to heptane:EtOAc 1:1) to give the corresponding product as a light yellow oil (457 mg, 70% yield). The oil solidifies to a light yellow solid during storage in the fridge (5 °C). $[\alpha]_D^{20}$ = -84.7° (*c* 1.2, $CHCl_3$) [Lit.[209] $[\alpha]_D^{20}$ = -78° (*c* 0.24, $CHCl_3$]. **m.p.** 43-44 °C. **^{1}H NMR** (400 MHz, $CDCl_3$): δ 8.55 (d, *J* = 5.0 Hz, 1H), 7.93 (s, 1H), 7.20 (d, *J* = 5.0 Hz, 1H), 4.45 (dd, *J* = 10.2, 8.5 Hz, 1H), 4.31 (t, *J* = 8.5 Hz, 1H), 4.12 (dd, *J* = 10.2, 8.5 Hz, 1H), 2.41 (s, 3H), 0.98 (s, 9H). **^{13}C NMR** (101 MHz, $CDCl_3$): δ 162.3, 149.5, 147.9, 146.7, 126.4, 124.8, 76.5, 69.2, 34.0, 26.0, 21.0. The spectral data are in good agreement with those previously reported.[209]

(*S*)-4-(*tert*-Butyl)-2-(6-methylpyridin-2-yl)-4,5-dihydrooxazole (L5)

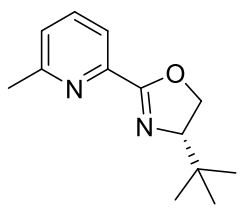

Inspired by a reported procedure,[210] a 50 mL two-necked round bottomed flask was charged with sodium methoxide (32 mg, 0.6 mmol, 20 mol%) and 2-cyano-6-methylpyridine (354 mg, 3 mmol) and put under N_2. MeOH (10 mL) was then added, and the reaction mixture stirred for 15 h. The solvent was evaporated to leave a yellow residue,

which was dissolved in EtOAc, washed with brine, dried ($MgSO_4$) and evaporated to leave the methyl carboximidate as a yellow oil. The flask was flushed with N_2, toluene (6 mL) added followed by (*S*)-*tert*-leucinol (387 mg, 3.3 mmol, 1.1 equiv.) and *p*-toluenesulfonic acid monohydrate (57 mg, 0.3 mmol, 10 mol%). The resulting solution was heated to 80 °C and stirred for 1 h, allowed to cool and quenched with water before extracting with EtOAc three times. Organics were pooled, dried ($MgSO_4$) and solvent evaporated. The crude material was purified by flash column chromatography (eluent gradient: from pure heptane to heptane:EtOAc 6:4) to give the corresponding product as a colorless oil that turns to a white solid upon standing (181 mg, 28% yield). $[\alpha]_D^{20}$ = -89.5° (*c* 0.5, $CHCl_3$) [Lit.[211] $[\alpha]_D^{20}$ = -83° (*c* 0.262, $CHCl_3$)]. **m.p.** 67-69 °C [Lit.[211] 71 °C]. **^{1}H NMR** (400 MHz, $CDCl_3$): δ 7.95 (d, *J* = 7.8 Hz, 1H), 7.65 (t, *J* = 7.8 Hz, 1H), 7.25 (d, *J* = 7.8 Hz, 1H), 4.46 (dd, *J* = 10.3, 8.5 Hz, 1H), 4.32 (t, *J* = 8.5 Hz, 1H), 4.11 (dd, *J* = 10.3, 8.5 Hz, 1H), 2.64 (s, 3H), 0.97 (s, 9H). **^{13}C NMR** (101 MHz, $CDCl_3$): δ 162.6, 158.6, 146.4, 136.7, 125.2, 121.3, 76.3, 69.4, 34.0, 26.0, 24.7. The spectral data are in good agreement with those previously reported.[212]

(*S*)-4-(*tert*-Butyl)-2-(5-(trifluoromethyl)pyridine-2-yl)-4,5-dihydrooxazole (L6)

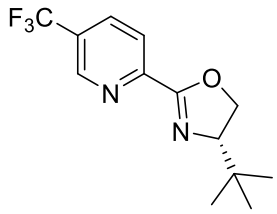

Following a reported procedure,[208] a 50 mL two-necked round bottomed flask equipped with reflux condenser was charged with zinc triflate (218 mg, 0.6 mmol, 20 mol%). The flask was put under vacuum and heated to 90 °C for 1 h. After cooling to room temperature, a previously prepared mixture of 2-cyano-5-(trifluoromethyl)pyridine (516 mg, 3 mmol) and (*S*)-*tert*-leucinol (352 mg, 3 mmol, 1 equiv.) in toluene (10 mL) was added. The reaction mixture was heated to reflux and stirred over 24 h, allowed to cool to room temperature, diluted with EtOAc and washed with a sat. aqueous $NaHCO_3$ solution. The aqueous phase was back-extracted with EtOAc twice, organics pooled, dried ($MgSO_4$) and solvent evaporated. The crude material was purified by flash column chromatography (eluent gradient: from pure heptane to heptane:EtOAc 8:2) to give the corresponding product as a white solid (584 mg, 71% yield). $[\alpha]_D^{20}$ = -68.5° (*c* 0.6, $CHCl_3$) [Lit.[213] $[\alpha]_D^{20}$ = -73° (*c* 0.1, $CHCl_3$)]. **m.p.** 106-107 °C. **^{1}H NMR** (400 MHz, $CDCl_3$): δ 8.96 (s, 1H), 8.23 (d, *J* = 8.3 Hz, 1H), 8.02 (d, *J* = 8.3 Hz, 1H), 4.49 (d, *J* = 10.3, 8.6 Hz, 1H), 4.35 (t, *J* = 8.6 Hz, 1H), 4.17 (dd, *J* = 10.3, 8.6 Hz, 1H), 0.99 (s, 9H). **^{19}F NMR** (376 MHz, $CDCl_3$):

δ -62.56. **^{13}C NMR** (101 MHz, $CDCl_3$): δ 161.4, 150.0, 146.6 (q, J_{CF} = 4.0 Hz), 133.9 (q, J_{CF} = 3.6 Hz), 127.9 (q, J_{CF} = 33.3 Hz), 123.7, 123.2 (q, J_{CF} = 272.2 Hz), 77.2, 69.6, 34.0, 25.9. The spectral data are in good agreement with those previously reported.[213]

(*S*)-2-(4-(*tert*-Butyl)-4,5-dihydrooxazol-2-yl)pyridine-3-ol (L7)

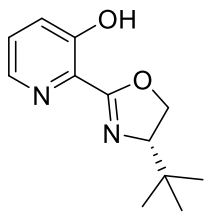

Following a reported procedure,[208] a 50 mL two-necked round bottomed flask equipped with reflux condenser was charged with zinc triflate (218 mg, 0.6 mmol, 20 mol%). The flask was put under vacuum and heated to 90 °C for 1 h. After cooling to room temperature, a previously prepared mixture of 2-cyano-3-hydroxypyridine (360 mg, 3 mmol) and (*S*)-*tert*-leucinol (352 mg, 3 mmol, 1 equiv.) in toluene (10 mL) was added. The reaction mixture was heated to reflux and stirred over 24 h, allowed to cool to room temperature, diluted with EtOAc and washed with a sat. aqueous $NaHCO_3$ solution. The aqueous phase was back-extracted with EtOAc twice, organics pooled, dried ($MgSO_4$) and solvent evaporated. The crude material was purified by flash column chromatography (eluent gradient: from pure heptane to heptane:EtOAc 7:3) to give the corresponding product as a colorless oil (515 mg, 78% yield). The oil solidifies to a white solid during storage in the fridge (5 °C). $[\alpha]_D^{20}$ = -23.9° (*c* 0.6, $CHCl_3$). **m.p.** 44-45 °C. **^{1}H NMR** (400 MHz, $CDCl_3$): δ 12.39 (s, 1H), 8.23 (dd, *J* = 4.3, 1.6 Hz, 1H), 7.37 (dd, *J* = 8.5, 1.6 Hz, 1H), 7.32 (dd, *J* = 8.5, 4.3 Hz, 1H), 4.48 (dd, *J* = 10.2, 8.9 Hz, 1H), 4.34 (dd, *J* = 8.9, 8.1 Hz, 1H), 4.20 (dd, *J* = 10.2, 8.1 Hz, 1H), 0.97 (s, 9H). **^{13}C NMR** (101 MHz, $CDCl_3$): δ 164.9, 157.2, 140.7, 129.7, 127.4, 124.6, 75.1, 68.7, 33.8, 25.8. **FT-IR**: ν (cm^{-1}) 2965, 2866, 2685, 2623, 2363, 1631, 1473, 1443, 1342, 1323, 13002, 1275, 1260, 1246, 1196, 1084, 1057, 1030, 1007. **HRMS (ESI)**: Exact mass calculated for $C_{12}H_{17}N_2O_2$ $[M+H]^+$: 221.1290, found 221.1297.

(*S*)-4-(*tert*-Butyl)-2-(pyrimidin-2-yl)-4,5-dihydrooxazole (L8)

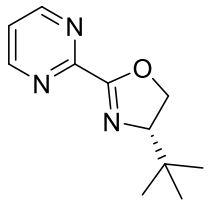

Following a reported procedure,[208] a 50 mL two-necked round bottomed flask equipped with reflux condenser was charged with zinc triflate (218 mg, 0.6 mmol, 20 mol%). The flask was put under vacuum and heated to 90 °C for 1 h. After cooling to room temperature, a previously prepared mixture of pyrimidine-2-carbonitrile (315 mg, 3 mmol) and (*S*)-*tert*-leucinol (352 mg, 3 mmol, 1 equiv.) in toluene (10 mL) was added. The reaction

mixture was heated to reflux and stirred over 24 h, allowed to cool to room temperature, diluted with EtOAc and washed with a sat. aqueous $NaHCO_3$ solution. The aqueous phase was back-extracted with EtOAc twice, organics pooled, dried ($MgSO_4$) and solvent evaporated. The crude material was purified by flash column chromatography (eluent gradient: from pure CH_2Cl_2 to CH_2Cl_2:MeOH 100:2) to give the corresponding product as a white solid (190 mg, 31% yield). $[\alpha]_D^{20}$ = -67.7° (*c* 0.6, $CHCl_3$) [Lit.[214] $[\alpha]_D^{24}$ = -56.5° (*c* 1.4, $CHCl_3$)]. **m.p.** 60-61 °C. **^{1}H NMR** (400 MHz, DMSO-d_6): δ 8.94 (d, *J* = 4.9 Hz, 2H), 7.66 (t, *J* = 4.9 Hz, 1H), 4.44 (dd, *J* = 10.4, 8.7 Hz, 1H), 4.29 (t, *J* = 8.7 Hz, 1H), 4.10 (dd, *J* = 10.4, 8.7 Hz, 1H), 0.90 (s, 9H). **^{13}C NMR** (101 MHz, DMSO-d_6): δ 106.1, 157.7, 155.5, 122.6, 75.8, 68.6, 33.5, 25.6. The spectral data are in good agreement with those previously reported.[214]

(*S*)-4-(*tert*-Butyl)-2-(isoquinol-1-yl)-4,5-dihydrooxazole (L10)

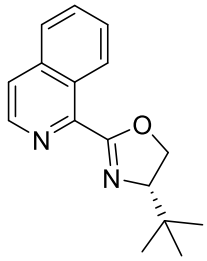

Following a reported procedure,[208] a 50 mL two-necked round bottomed flask equipped with reflux condenser was charged with zinc triflate (218 mg, 0.6 mmol, 20 mol%). The flask was put under vacuum and heated to 90 °C for 1 h. After cooling to room temperature, a previously prepared mixture of isoquinoline-1-carbonitrile (462 mg, 3 mmol) and (*S*)-*tert*-leucinol (352 mg, 3 mmol, 1 equiv.) in toluene (10 mL) was added. The reaction mixture was heated to reflux and stirred over 24 h, allowed to cool to room temperature, diluted with EtOAc and washed with a sat. aqueous $NaHCO_3$ solution. The aqueous phase was back-extracted with EtOAc twice, organics pooled, dried ($MgSO_4$) and solvent evaporated. The crude material was purified by flash column chromatography (eluent gradient: from pure heptane to heptane:EtOAc 6:4) to give the corresponding product as a white solid (492 mg, 64% yield). $[\alpha]_D^{20}$ = -77.8° (*c* 0.7, $CHCl_3$) [Lit.[215] $[\alpha]_D^{24}$ = -84.4 (*c* 1.0, $CHCl_3$)]. **m.p.** 92-93 °C. **^{1}H NMR** (400 MHz, $CDCl_3$): δ 9.32 (d, *J* = 7.8 Hz, 1H), 8.64 (d, *J* = 5.6 Hz, 1H), 7.88-7.85 (m, 1H), 7.77 (d, *J* = 5.6 Hz, 1H), 7.75-7.67 (m, 2H), 4.54-4.46 (m, 1H), 4.37-4.28 (m, 2H), 1.07 (s, 9H). **^{13}C NMR** (101 MHz, $CDCl_3$): δ 161.8, 146.4, 141.7, 136.7, 130.3, 128.5, 127.5, 127.4, 127.0, 123.3, 77.5, 68.2, 34.1, 26.1. The spectral data are in good agreement with those previously reported.[215]

(*S*)-4-Phenyl-2-(pyridin-2-yl)-4,5-dihydrooxazole (L11)

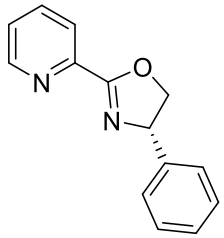

Following a reported procedure,[208] a 50 mL two-necked round bottomed flask equipped with reflux condenser was charged with zinc triflate (218 mg, 0.6 mmol, 20 mol%). The flask was put under vacuum and heated to 90 °C for 1 h. After cooling to room temperature, a previously prepared mixture of 2-cyanopyridine (312 mg, 3 mmol) and (*S*)-phenylglycinol (412 mg, 3 mmol, 1 equiv.) in toluene (10 mL) was added. The reaction mixture was heated to reflux and stirred over 24 h, allowed to cool to room temperature, diluted with EtOAc and washed with a sat. aqueous $NaHCO_3$ solution. The aqueous phase was back-extracted with EtOAc twice, organics pooled, dried ($MgSO_4$) and solvent evaporated. The crude material was purified by flash column chromatography (eluent gradient: from pure CH_2Cl_2 to CH_2Cl_2:MeOH 100:3) to give the corresponding product as a light yellow oil (61.7 mg, 9% yield). Further fractions from the chromatographic column contained the product but were not isolated due to impurities. **^{1}H NMR** (400 MHz, $CDCl_3$): δ 8.75 (ddd, *J* = 4.8, 1.8, 1.0, 1H), 8.18 (dt, *J* = 7.8, 1.0 Hz, 1H), 7.81 (td, *J* = 7.8, 1.8 Hz, 1H), 7.43 (ddd, *J* = 7.8, 4.8, 1.0 Hz, 1H), 7.39-7.27 (m, 5H), 5.47 (dd, *J* = 10.2, 8.6 Hz, 1H), 4.91 (dd, *J* = 10.2, 8.6 Hz, 1H), 4.40 (t, *J* = 8.6 Hz, 1H). The spectral data are in good agreement with those previously reported.[216]

(4*S*,5*R*)-4,5-Diphenyl-2-(pyridin-2-yl)-4,5-dihydrooxazole (L12)

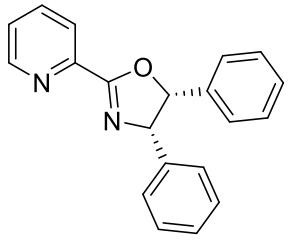

Following a reported procedure,[208] a 50 mL two-necked round bottomed flask equipped with reflux condenser was charged with zinc triflate (218 mg, 0.6 mmol, 20 mol%). The flask was put under vacuum and heated to 90 °C for 1 h. After cooling to room temperature, a previously prepared mixture of 2-cyanopyridine (312 mg, 3 mmol) and (1*R*,2*S*)-2-amino-1,2-diphenylethan-1-ol (640 mg, 3 mmol, 1 equiv.) in toluene (10 mL) was added. The reaction mixture was heated to reflux and stirred over 24 h, allowed to cool to room temperature, diluted with EtOAc and washed with a sat. aqueous $NaHCO_3$ solution. The aqueous phase was back-extracted with EtOAc twice, organics pooled, dried ($MgSO_4$) and solvent evaporated. The crude material was purified by automated flash column chromatography (eluent gradient: from pure heptane to pure EtOAc) to give the corresponding product as a colorless wax

(427 mg, 47% yield). $[\alpha]_D^{20}$ = -164.1° (*c* 0.4, $CHCl_3$) [Lit.[217] $[\alpha]_D^{20}$ = -194° (*c* 0.2, $CHCl_3$) reported for the enantiomer[XX]]. **^{1}H NMR** (400 MHz, $CDCl_3$): δ 8.82 (ddd, *J* = 4.8, 1.8, 1.0 Hz, 1H), 8.28 (dt, *J* = 7.8, 1.0 Hz, 1H), 7.87 (td, *J* = 7.8, 1.8 Hz, 1H), 7.49 (ddd, *J* = 7.8, 4.8, 1.0 Hz, 1H), 7.08-6.94 (m, 10H), 6.12 (d, *J* = 10.3 Hz, 1H), 5.83 (d, *J* = 10.3 Hz, 1H). **^{13}C NMR** (101 MHz, $CDCl_3$): δ 164.2, 150.0, 146.6, 137.2, 136.8, 136.1, 127.9, 127.7, 127.6, 127.4, 127.0, 126.5, 125.9, 124.3, 86.0, 74.6. The spectral data are in good agreement with those previously reported.[217]

(3a*S*,8a*R*)-2-(Pyridin-2-yl)-3a,8a-dihydro-8*H*-indeno[1,2-*d*]oxazole (L13)

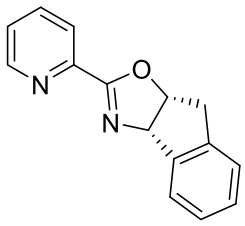

Inspired by a reported procedure,[210] a 50 mL two-necked round bottomed flask was charged with sodium methoxide (16 mg, 0.3 mmol, 10 mol%) and 2-cyanopyridine (312 mg, 3 mmol) and put under N_2. MeOH (10 mL) was then added, and the reaction mixture stirred for 15 h. The solvent was evaporated to leave a yellow residue, which was dissolved in EtOAc, washed with brine, dried ($MgSO_4$) and evaporated to leave the methyl carboximidate as a yellow oil. The flask was flushed with N_2, toluene (6 mL) added followed by (1*S*,2*R*)-*cis*-1-Amino-2-indanol (492 mg, 3.3 mmol, 1.1 equiv.) and *p*-toluenesulfonic acid monohydrate (57 mg, 0.3 mmol, 10 mol%). The resulting solution was heated to 80 °C and stirred for 1 h, allowed to cool to room temperature, quenched with water and extracted with EtOAc three times. Organics were pooled, dried ($MgSO_4$) and solvent evaporated. The crude material was purified by flash column chromatography (eluent gradient: from pure heptane to pure EtOAc) to give the corresponding product as a light yellow oil that turns to a light yellow solid upon standing (347 mg, 49% yield). $[\alpha]_D^{20}$ = -205.0° (*c* 0.5, $CHCl_3$). **m.p.** 115-116 °C [Lit.[218] 110-112 °C]. **^{1}H NMR** (400 MHz, $CDCl_3$): δ 8.68 (ddd, *J* = 4.8, 1.8, 1.0 Hz, 1H), 8.04 (dt, *J* = 7.8, 1.0 Hz, 1H), 7.74 (td, *J* = 7.8, 1.8 Hz, 1H), 7.61-7.56 (m, 1H), 7.35 (ddd, *J* = 7.8, 4.8, 1.0 Hz, 1H), 7.29-7.25 (m, 3H), 5.81 (d, *J* = 7.9 Hz, 1H), 5.58 (ddd, *J* = 7.9, 6.2, 2.4 Hz, 1H), 3.54 (dd, *J* = 18.0, 6.2 Hz, 1H), 3.47 (dd, *J* = 18.0, 2.4 Hz, 1H). **^{13}C NMR** (101 MHz, $CDCl_3$): δ 163.2, 149.6, 146.8, 141.5, 139.8, 136.5, 128.6, 127.5, 125.7, 125.5, 125.3, 124.1, 83.9, 77.1, 39.7. The spectral data are in good agreement with those previously reported.[218]

[XX] However, the stereochemistry of the aminoalcohol precursor used was confirmed as (1*R*,2*S*) by comparison of its optical rotation with literature values.

(*S*)-1-Amino-2-methyl-1-phenylpropan-2-ol

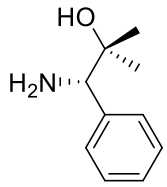

Following a reported procedure,[219] to a solution of methylmagnesium bromide (43 mL of a 1.4 M solution in toluene:THF 75:25, 60 mmol, 6 equiv.) in diethyl ether (30 mL) under N_2 was added (*S*)-phenylglycine methyl ester hydrochloride (2.0 g, 10 mmol) in portions over 1 h. The reaction mixture was stirred at room temperature for 15 h, then quenched by addition of saturated aqueous NH_4Cl solution dropwise. Water was added, the phases separated, and the aqueous phase extracted with EtOAc three times. The organic phases were pooled, dried ($MgSO_4$) and solvent evaporated. The crude material was purified by automated flash column chromatography (eluent gradient: from pure EtOAc to EtOAc:MeOH 80:20) to give the corresponding product as a light yellow oil (850 mg, 51% yield). The oil turned to a light yellow solid once in the fridge (5 °C). **m.p.** 52-53 °C [Lit.[220] 47-50 °C]. **^{1}H NMR** (400 MHz, $CDCl_3$): δ 7.35-7.25 (m, 5H), 3.80 (s, 1H), 2.03 (br s, 2H), 1.22 (s, 3H), 1.04 (s, 3H). **^{13}C NMR** (101 MHz, $CDCl_3$): δ 142.5, 128.1, 127.8, 127.3, 72.2, 64.5, 27.6, 24.8. The spectral data are in good agreement with those previously reported.[220]

(*S*)-5,5-Dimethyl-4-phenyl-2-(pyridin-2-yl)-4,5-dihydrooxazole (L14)

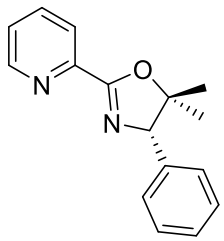

Following a reported procedure,[208] a 25 mL two-necked round bottomed flask equipped with reflux condenser was charged with zinc triflate (36 mg, 0.1 mmol, 10 mol%). The flask was put under vacuum and heated to 90 °C for 1 h. After cooling to room temperature, a previously prepared mixture of 2-cyanopyridine (104 mg, 1 mmol) and (S)-1-amino-2-methyl-1-phenylpropan-2-ol (165 mg, 1 mmol, 1 equiv.) in toluene (4 mL) was added. The reaction mixture was heated to reflux and stirred over 24 h, allowed to cool to room temperature, diluted with EtOAc and washed with a sat. aqueous $NaHCO_3$ solution. The aqueous phase was back-extracted with EtOAc twice, organics pooled, dried ($MgSO_4$) and solvent evaporated. The crude material was purified by automated flash column chromatography (eluent gradient: from pure CH_2Cl_2 to CH_2Cl_2:MeOH 95:5) to give the corresponding product as a yellow oil (427 mg, 47% yield). $[\alpha]_D^{20}$ = +35° (*c* 0.3, $CHCl_3$). **^{1}H NMR** (400 MHz, $CDCl_3$): δ 8.77

(ddd, *J* = 4.8, 1.7, 1.0 Hz, 1H), 8.23 (dt, *J* = 7.8, 1.0 Hz, 1H), 7.82 (td, *J* = 7.8, 1.8 Hz, 1H), 7.43 (ddd, *J* = 7.8, 4.8, 1.0 Hz, 1H), 7.37-7.25 (m, 5H), 5.12 (s, 1H), 1.73 (s, 3H), 1.01 (s, 3H). **^{13}C NMR** (101 MHz, $CDCl_3$): 162.9, 149.8, 147.3, 138.5, 136.6, 128.3, 127.6, 127.2, 125.6, 124.1, 88.4, 78.6, 29.2, 23.9. **FT-IR**: ν (cm^{-1}) 3060, 3030, 2976, 2930, 2868, 2318, 1636, 1570, 1350, 1283, 1090, 1043. **HRMS (ESI)**: Exact mass calculated for $C_{16}H_{17}N_2O$ $[M+H]^+$: 253.1341, found 253.1349.

2-((3a*S*,8a*R*)-3a,8a-Dihydro-8*H*-indeno[1,2-*d*]oxazol-2-yl)-2-((3a*S*,8a*R*)-3,3a,8,8a-tetrahydro-2*H*-indeno[1,2-*d*]oxazol-2-ylidene)acetonitrile (L16)

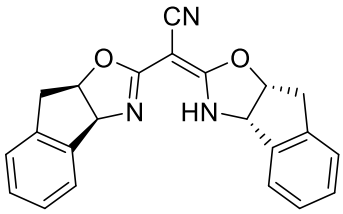

Following a reported procedure,[221] a dried 25 mL flask was charged with the corresponding bis-oxazoline (bis((3a*S*,8a*R*)-3a,8a-dihydro-8*H*-indeno[1,2-*d*]oxazol-2-yl)methane) (250 mg, 0.76 mmol), put under N_2, and a solution was made with 5 mL THF. This solution was cooled to -78 °C and *n*-BuLi (363 μL of 2.5 M solution in hexanes, 0.91 mmol, 1.2 equiv.) was added slowly, followed by TMEDA (136 μL, 0.91 mmol, 1.2 equiv.). The mixture was stirred at -78 °C for 1 h, then 0 °C for 30 min, then cooled to -78 °C again. *p*-Toluenesulfonyl cyanide (164 mg, 0.91 mmol, 1.2 equiv.) was added, the mixture was allowed to warm to room temperature and stirred for 15 h. Saturated aqueous NH_4Cl solution was added to quench the reaction and stirred for 5 min, before EtOAc was added and the mixture filtered. The resulting solid is a first batch of the title compound. The phases of the filtered mixture were separated and aqueous phase extracted with further EtOAc, organics pooled, dried ($MgSO_4$) and solvent evaporated to afford a second batch of the title compound. The desired product was obtained as a light yellow solid (184 mg, 68% yield). $[\alpha]_D^{20}$ = +202° (*c* 0.2, $CHCl_3$). **m.p.** not observed: decomposition above 280 °C. **^{1}H NMR** (400 MHz, $CDCl_3$): δ 7.49-7.44 (m, 2H), 7.34-7.26 (m, 6H), 5.51-5.43 (m, 4H), 3.42 (d, *J* = 3.8 Hz, 4H). **^{13}C NMR** (101 MHz, $CDCl_3$): δ 166.8, 140.7, 139.6, 129.1, 127.7, 125.6, 125.0, 84.9, 70.2, 38.8. The spectral data are in good agreement with those previously reported.[221]

2-((*S*)-4-(*tert*-Butyl)-4,5-dihydrooxazol-2-yl)-2-((*S*)-4-(*tert*-butyl)oxazolidin-2-ylidene)acetonitrile (L17)

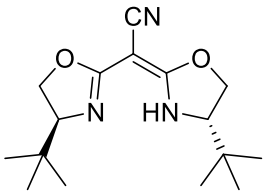

Following a reported procedure,[221] a dried 25 mL flask was charged with the corresponding bis-oxazoline (bis((*S*)-4-(*tert*-butyl)-4,5-dihydrooxazol-2-yl)methane) (201 mg, 0.76 mmol), put under N_2, and a solution was made with 5 mL THF. This solution was cooled to -78 °C and *n*-BuLi (363 μL of 2.5 M solution in hexanes, 0.91 mmol, 1.2 equiv.) was added slowly, followed by TMEDA (136 μL, 0.91 mmol, 1.2 equiv.). The mixture was stirred at -78 °C for 1 h, then 0 °C for 30 min, then cooled to -78 °C again. *p*-Toluenesulfonyl cyanide (164 mg, 0.91 mmol, 1.2 equiv.) was then added, the mixture was allowed to warm to room temperature and stirred for 15 h. Saturated aqueous NH_4Cl solution was added to quench the reaction and stirred for 5 min, then extracted with EtOAc three times. The organic phases were pooled, washed with brine, dried ($MgSO_4$) and solvent evaporated. The crude material was purified by flash column chromatography (eluent gradient: from pure heptane to heptane:EtOAc 6:4) to give the corresponding product as a white solid (181 mg, 82% yield). $[\alpha]_D^{20}$ = +62.5° (*c* 0.6, $CHCl_3$). **m.p.** 179-180 °C. **^{1}H NMR** (400 MHz, $CDCl_3$): δ 4.42 (t, *J* = 9.2 Hz, 2H), 4.27 (dd, *J* = 9.2, 6.8 Hz, 2H), 3.87 (dd, *J* = 9.2, 6.8 Hz, 2H), 0.90 (s, 18H). **^{13}C NMR** (101 MHz, $CDCl_3$): δ 167.1, 70.2, 70.0, 49.6, 33.6, 25.3. The spectral data are in good agreement with those previously reported.[221]

Retrosynthetic sequence to ligand L18:

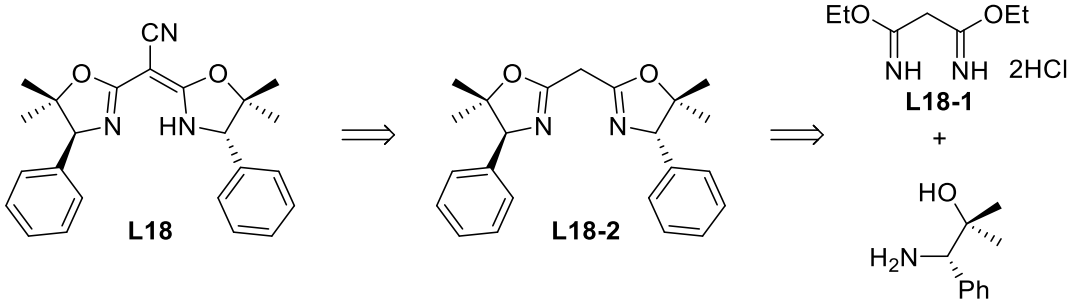

Diethyl malonimidate dihydrochloride (L18-1)

Partly following a reported procedure,[222] a 250 mL multi-necked round bottomed flask was charged with malononitrile (198 mg, 3 mmol) and put under N_2. A solution was made with dioxane (2 mL) and ethanol (363 μL, 6.15 mmol, 2.05 equiv.). Hydrogen chloride (37.5 mL of 4 M solution in dioxane, 150 mmol, 50 equiv.) was added dropwise

through an addition funnel. White precipitation was observed. The mixture was stirred at room temperature over three days, then filtered and the solid washed with dry diethyl ether and dried under vacuum. Title compound: white solid (397 mg, 57%). The product was used as such without further purification. **^{1}H NMR** (400 MHz, DMSO-d_6): δ 8.30 (br s, 3H), 7.34 (t, *J* = 50.8 Hz, 5H), 5.44 (br s, 4H), 4.42 (s, 1H), 4.21 (br s, 4H), 1.31 (t, *J* = 7.0 Hz, 6H). Additional protons are reported, probably belonging to excess HCl or H_2O. The spectral data are in good agreement with those previously reported.[223]

Bis((*S*)-5,5-dimethyl-4-phenyl-4,5-dihydrooxazol-2-yl)methane (L18-2)

Following a reported procedure,[222] a 50 mL two-necked round bottomed flask equipped with reflux condenser was charged with diethyl malonimidate dihydrochloride (**L18-1**) (231 mg, 1 mmol) and (*S*)-1-amino-2-methyl-1-phenylpropan-2-ol (330 mg, 2 mmol, 2 equiv.) and put under N_2. Dry CH_2Cl_2 (6 mL) was added, the mixture heated to vigorous reflux and stirred for 15 h. The resulting milky suspension was allowed to cool to room temperature and quenched with H_2O, then extracted with CH_2Cl_2 three times. Organics were pooled, washed with brine, dried (Na_2SO_4) and the solvent evaporated. The crude material was purified by automated flash column chromatography (eluent gradient: from pure heptane to pure EtOAc) to give the corresponding product as a yellow oil (245 mg, 67% yield). **^{1}H NMR** (400 MHz, $CDCl_3$): δ 7.35-7.24 (m, 10H), 4.90 (s, 2H), 3.53 (t, *J* = 1.2 Hz, 2H), 1.60 (s, 6H), 0.88 (s, 6H). The spectral data are in good agreement with those previously reported.[224]

2-((*S*)-5,5-Dimethyl-4-phenyl-4,5-dihydrooxazol-2-yl)-2-((*S*)-5,5-dimethyl-4-phenyloxazolidin-2-ylidene)acetonitrile (L18)

Following a reported procedure,[221] a dried 25 mL flask was charged with the corresponding bis-oxazoline **L18-2** (243 mg, 0.67 mmol), put under N_2, and a solution was made with 5 mL THF. This solution was cooled to -78 °C and *n*-BuLi (322 μL of 2.5 M solution in hexanes, 0.8 mmol, 1.2 equiv.) was added slowly, followed by TMEDA (121 μL, 0.8 mmol, 1.2 equiv.). The mixture was stirred at -78 °C for 1 h, then 0 °C for 30 min, then cooled to -78 °C again. *p*-Toluenesulfonyl cyanide (146 mg, 0.8 mmol, 1.2 equiv.) was then added, the reaction mixture was allowed to warm to room temperature and stirred for 15 h. Saturated aqueous NH_4Cl solution was added to

quench the reaction and stirred for 5 min, then extracted with EtOAc three times. The organic phases were pooled, washed with brine, dried ($MgSO_4$) and solvent evaporated. The crude material was purified by automated flash column chromatography (eluent gradient: from pure heptane to heptane:EtOAc 6:4) to give the corresponding product as a cream solid (198 mg, 76% yield). $[\alpha]_D^{20}$ = +342.9° (*c* 0.6, $CHCl_3$). **m.p.** 227-228 °C. **^{1}H NMR** (400 MHz, $CDCl_3$): δ 7.37-7.27 (m, 6H), 7.21-7.17 (m, 4H), 4.84 (s, 2H), 1.67 (s, 6H), 0.95 (s, 6H). **^{13}C NMR** (101 MHz, $CDCl_3$): 166.9, 137.8, 128.6, 128.2, 126.8, 117.4, 89.2, 73.0, 50.9, 28.2, 23.5. **FT-IR**: ν (cm^{-1}) 3065, 2992, 2972, 2928, 2202, 1642, 1589, 1554, 1500, 1458, 1379, 1356, 1308, 1240, 1192, 1064. **HRMS (ESI)**: Exact mass calculated for $C_{24}H_{26}N_3O_2$ $[M+H]^+$: 388.2025, found 388.2031.

6.5 Preparation of *α*-heterocyclic acid substrates

(*S*)-2-(1*H*-Pyrrol-1-yl)propanoic acid (11a)

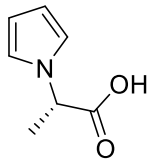

Following a reported procedure,[225] a 250 mL three-necked round bottomed flask equipped with reflux condenser was charged with NaOAc (4.1 g, 50 mmol, 1 equiv.) and *L*-alanine (4.45 g, 50 mmol). The flask was put under N_2, degassed water (22.5 mL), acetic acid (7.5 mL) and 1,2-dichloroethane (30 mL) were added, and the mixture brought to 90 °C. To the colorless solution, 2,5-dimethoxytetrahydrofuran (6.5 mL, 50 mmol, 1 equiv.) was added, and the mixture stirred at the same temperature for 15 h, cooled to room temperature and the phases separated. The aqueous phase was washed with CH_2Cl_2 twice, organics were pooled, dried ($MgSO_4$) and solvent evaporated. The resulting brown oil was purified by flash column chromatography (eluent heptane:EtOAc 8:2) to afford the desired product as a light yellow oil that solidified upon standing (6.96 g, 59% yield). $[\alpha]_D^{20}$ = +11.2° (*c* 1.1, MeOH) [Lit.[69] $[\alpha]_D^{28}$ = +19.0° (*c* 1.2, MeOH)]. **m.p.** 80-81 °C [Lit.[69] 79-80 °C]. **^{1}H NMR** (400 MHz, $CDCl_3$): δ 11.10 (br s, 1H), 6.75 (t, *J* = 2.2 Hz, 2H), 6.21 (t, *J* = 2.2 Hz, 2H), 4.80 (q, *J* = 7.4 Hz, 1H), 1.77 (d, *J* = 7.4 Hz, 3H). **^{13}C NMR** (101 MHz, $CDCl_3$): δ 177.0, 119.8, 108.9, 56.6, 18.0. The spectral data are in good agreement with those previously reported.[69]

2-(2-Acetyl-1*H*-pyrrol-1-yl)propanoic acid (11b)

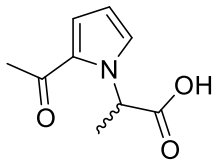

A dried 100 mL two-necked round bottomed flask was charged with 2-acetyl-1*H*-pyrrole (1.64 g, 15 mmol) and put under N_2. DMF (20 mL) was added to make a solution, which was then immersed in an ice bath. NaH (1.5 g, 60% in mineral oil, 37.5 mmol, 2.5 equiv.) was added in portions, and the mixture stirred in ice bath for 30 min. 2-bromopropionic acid (1.42 mL, 15.75 mmol, 1.05 equiv.) was added dropwise, the ice bath removed and the mixture stirred at room temperature for 15 h, slowly quenched with water. The aqueous phase was washed with heptane and EtOAc, then acidified with 10% aqueous HCl solution until pH < 1 and extracted with EtOAc three times, organics were pooled, dried ($MgSO_4$) and solvent evaporated. The crude material was purified by automated flash column chromatography (eluent gradient: from pure heptane to heptane:EtOAc 4:6) to give the corresponding product as a cream solid (1.01 g, 37% yield). **m.p.** 121-122 °C [Lit.[226] 114-116 °C]. **^{1}H NMR** (400 MHz, $CDCl_3$): δ 10.80 (br s, 1H), 7.11 (dd, *J* = 2.7, 1.6 Hz, 1H), 7.06 (dd, *J* = 4.1, 1.6 Hz, 1H), 6.25 (dd, *J* = 4.1, 2.7 Hz, 1H), 5.78 (q, *J* = 7.3 Hz, 1H), 2.45 (s, 3H), 1.76 (d, *J* = 7.3 Hz, 3H). **^{13}C NMR** (101 MHz, $CDCl_3$): δ 189.6, 175.5, 130.5, 127.7, 121.4, 109.2, 55.7, 27.1, 17.4. The spectral data are in good agreement with those previously reported.[226]

2-(2-(Methoxycarbonyl)-1*H*-pyrrol-1-yl)propanoic acid (11c)

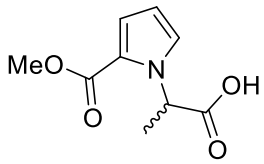

A dried 100 mL two-necked round bottomed flask was charged with methyl 1*H*-pyrrole-2-carboxylate (1.77 g, 15 mmol) and put under N_2. DMF (20 mL) was added to make a solution, which was then immersed in an ice bath. NaH (1.5 g, 60% in mineral oil, 37.5 mmol, 2.5 equiv.) was added in portions, and the mixture stirred in ice bath for 30 min. 2-bromopropionic acid (1.42 mL, 15.75 mmol, 1.05 equiv.) was added dropwise, the ice bath removed and the mixture stirred at room temperature 2 days. The mixture was slowly quenched with water, the aqueous phase washed with heptane and EtOAc, and then acidified with 10% aqueous HCl solution until pH < 1, extracted with EtOAc three times, organics were pooled, dried ($MgSO_4$) and solvent evaporated. The crude material was purified by automated flash column chromatography (eluent gradient: from pure heptane to heptane:EtOAc 6:4) to give the corresponding product as a cream solid (875 mg, 30%

yield). **m.p.** 120-121 °C. **^{1}H NMR** (400 MHz, $CDCl_3$): δ 11.01 (br s, 1H), 7.04 (dd, *J* = 2.7, 1.8 Hz, 1H), 7.01 (dd, *J* = 3.9, 1.8 Hz, 1H), 6.22 (dd, *J* = 3.9, 2.7 Hz, 1H), 5.85 (dd, *J* = 7.3 Hz, 1H), 3.80 (s, 3H), 1.79 (d, *J* = 7.3 Hz, 3H). **^{13}C NMR** (101 MHz, $CDCl_3$): δ 177.0, 162.0, 125.8, 122.2, 118.7, 108.9, 55.0, 51.3, 17.5. **FT-IR**: ν (cm^{-1}) 3119, 2995, 2550 (br), 1953, 1717, 1682, 1527, 1437, 1414, 1341, 1283, 1207, 1119, 1107, 1084, 1065, 1007. **HRMS (EI)**: Exact mass calculated for $C_9H_{11}NO_4$ $[M]^+$: 197.0688, found 197.0688.

2-(2-(Dimethylcarbamoyl)-1*H*-pyrrol-1-yl)propanoic acid (11d)

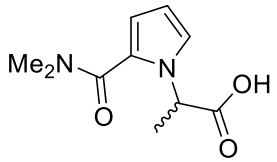

A dried 50 mL two-necked round bottomed flask was charged with *N*,*N*-dimethyl-1*H*-pyrrole-2-carboxamide (500 mg, 3.62 mmol) and put under N_2. DMF (5 mL) was added to make a solution, which was then immersed in an ice bath. NaH (360 mg, 60% in mineral oil, 9.05 mmol, 2.5 equiv.) was added in portions, and the mixture stirred in ice bath for 30 min. 2-bromopropionic acid (0.34 mL, 3.8 mmol, 1.05 equiv.) was added dropwise, the ice bath removed and the mixture stirred at room temperature for 15 h. The mixture was slowly quenched with water, the aqueous phase washed with heptane and EtOAc, and then acidified with 10% HCl solution until pH < 1, extracted with EtOAc seven times, organics were pooled, dried ($MgSO_4$) and solvent evaporated. The crude material was purified by flash column chromatography (eluent gradient: from pure CH_2Cl_2 to CH_2Cl_2:EtOAc 100:6) to give the corresponding product as a yellow oil that solidifies upon standing (418 mg, 55% yield). **m.p.** 111-112 °C. **^{1}H NMR** (400 MHz, $CDCl_3$): δ 13.57 (br s, 1H), 6.97 (dd, *J* = 2.8, 1.6 Hz, 1H), 6.49 (dd, *J* = 3.9, 1.6 Hz, 1H), 6.22 (dd, *J* = 3.9, 2.8 Hz, 1H), 5.13 (q, *J* = 7.2 Hz, 1H), 3.33 (s, 3H), 3.13 (s, 3H), 1.68 (d, *J* = 7.2 Hz, 3H). **^{13}C NMR** (101 MHz, $CDCl_3$): δ 170.7, 165.0, 123.6, 123.1, 115.2, 109.1, 55.0, 40.2, 36.2, 16.7. **FT-IR**: ν (cm^{-1}) 3140, 2997, 2974, 2951, 2400 (br), 1751, 1541, 1434, 1337, 1304, 1279, 1256, 1223, 1213, 1179, 1124, 1093, 1078, 1057, 1003. **HRMS (ESI)**: Exact mass calculated for $C_{10}H_{15}N_2O_3$ $[M+H]^+$: 211.1083, found 211.1092.

Benzyl 2-bromopropanoate

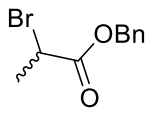

Following a reported procedure,[227] a 500 mL three-necked round bottomed flask equipped with addition funnel was charged with DCC (12.4 g, 60 mmol, 1.2 equiv.) and put under N_2. 150 mL of diethyl ether were

added, followed by 2-bromopropionic acid (4.5 mL, 50 mmol). The addition funnel was charged with a previously prepared solution of benzyl alcohol (6.2 mL, 60 mmol, 1.2 equiv.), DMAP (366 mg, 3 mmol, 6 mol%) in 30 mL of diethyl ether, added dropwise. White precipitate formed during addition. The reaction mixture was stirred at room temperature for 5 h, before being diluted with hexane (200 mL), filtered and evaporated. The crude material was purified by flash column chromatography (eluent gradient: from pure heptane to heptane:CH_2Cl_2 85:15) to give the corresponding product as a colorless liquid (12.15 g, 77% yield). **^{1}H NMR** (400 MHz, $CDCl_3$): δ 7.39-7.32 (m, 5H), 5.24-5.17 (m, 2H), 4.41 (q, *J* = 6.9 Hz, 1H), 1.84 (d, *J* = 6.9 Hz, 3H). **^{13}C NMR** (101 MHz, $CDCl_3$): δ 170.1, 135.2, 128.6, 128.5, 128.2, 67.6, 40.0, 21.7. The spectral data are in good agreement with those previously reported.[227]

Retrosynthetic sequence to substrate 11e:

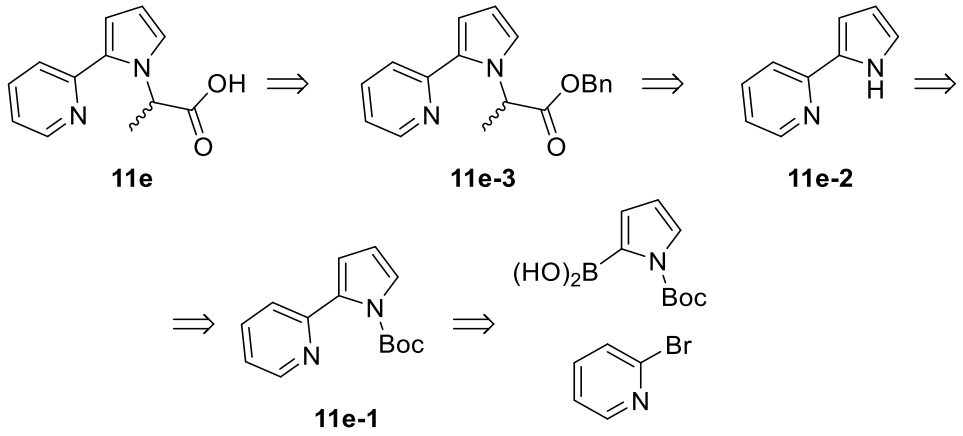

2-(*N*-Boc-1*H*-Pyrrol-2-yl)pyridine (11e-1)

Following a reported procedure,[228] a 250 mL three-necked round bottomed flask was charged with $Pd(PPh_3)_4$ (1.0 g, 0.9 mmol, 10 mol%) and put under N_2. A solution prepared with (*N*-Boc-1*H*-pyrrol-2-yl)boronic acid (1.9 g, 9 mmol), 2-bromopyridine (1.4 g, 9 mmol, 1 equiv.) and THF (75 mL) was then added, followed by aqueous K_2CO_3 (23 mL, 1.2 M, 27 mmol, 2 equiv.). The biphasic mixture was stirred vigorously, heated to 100 °C and kept at this temperature for 15 h, cooled to room temperature, water added and the aqueous phase extracted with CH_2Cl_2 four times. Organic extracts were combined, dried ($MgSO_4$) and solvent evaporated. The crude material was purified by flash column chromatography (eluent gradient: from pure heptane to heptane:EtOAc 8:2) to give the corresponding product as a light yellow oil (1.54 g, 70% yield). **^{1}H NMR**

(400 MHz, $CDCl_3$): δ 8.63-8.60 (m, 1H), 7.68 (td, *J* = 7.8, 1.8 Hz, 1H), 7.39 (dt, *J* = 7.8, 1.1 Hz, 1H), 7.36 (dd, *J* = 3.3, 1.8 Hz, 1H), 7.22-7.18 (m, 1H), 6.41 (dd, *J* = 3.3, 1.8 Hz, 1H), 6.24 (t, *J* = 3.3 Hz, 1H), 1.35 (s, 9H). **^{13}C NMR** (101 MHz, $CDCl_3$): δ 153.0, 149.3, 148.8, 135.7, 134.1, 123.5, 121.7, 115.6, 110.5, 83.6, 27.6. The spectral data are in good agreement with those previously reported.[229]

2-(1*H*-Pyrrol-2-yl)pyridine (11e-2)

Following a reported procedure,[228] compound **11e-1** (1.5 g, 6.12 mmol) was dissolved in CH_2Cl_2 (30 mL) and aqueous HCl (33 mL, 3 M, 98 mmol, 16 equiv.) was added dropwise while in ice bath. The biphasic mixture was stirred vigorously at room temperature for 15 h. The phases where separated, and the aqueous phase basified to pH 12 with aqueous Na_2CO_3, before being extracted with CH_2Cl_2. Organic phases dried ($MgSO_4$) and solvent evaporated. The crude material was purified by flash column chromatography (pure CH_2Cl_2 as eluent) to give the corresponding product as a white solid (882 mg, 79% yield). **m.p.** 88-89 °C [Lit.[230] 90-91 °C]. **^{1}H NMR** (400 MHz, $CDCl_3$): δ 9.93 (br s), 8.47-8.45 (m, 1H), 7.62 (td, *J* = 7.7, 1.8 Hz, 1H), 7.55 (dt, *J* = 8.1, 1.1 Hz, 1H), 7.05-7.01 (m, 1H), 6.91-6.89 (m, 1H), 6.73-6.70 (m, 1H), 6.31-6.28 (m, 1H). **^{13}C NMR** (101 MHz, $CDCl_3$): δ 150.6, 148.8, 136.5, 131.5, 120.5, 119.9, 118.2, 110.2, 107.1. The spectral data are in good agreement with those previously reported.[231]

Benzyl 2-(2-(pyridin-2-yl)-1*H*-pyrrol-1-yl)propanoate (11e-3)

A dried 100 mL two-necked round bottomed flask was charged with compound **11e-2** (432 mg, 3 mmol) and put under N_2. DMF (5 mL) was added and the resulting solution immersed in an ice bath. NaH (300 mg, 60% in mineral oil, 7.5 mmol, 2.5 equiv.) was added in portions, and the mixture stirred in ice bath for 30 min. Benzyl 2-bromopropionate (766 mg, 3.15 mmol, 1.05 equiv.) was added dropwise, the ice bath removed and the mixture stirred at room temperature for 5 h, slowly quenched with sat. aqueous NH_4Cl solution, then water, and extracted with EtOAc twice. Organics were pooled, washed with brine, dried ($MgSO_4$), solvent evaporated. The crude material was purified by flash column chromatography (first purification with pure CH_2Cl_2 as eluent, second purification with eluent gradient from pure heptane to heptane:EtOAc 8:2) to give the corresponding product as a light orange oil (919 mg, 32% yield). **^{1}H NMR**

(400 MHz, $CDCl_3$): δ 8.30 (d, *J* = 4.9 Hz, 1H), 7.58 (m, 1H), 7.52 (d, *J* = 8.1 Hz, 1H), 7.33-7.27 (m, 3H), 7.25-7.21 (m, 2H), 7.00-6.96 (m, 2H), 6.65 (dd, *J* = 3.7, 1.7 Hz, 1H), 6.27 (dd, *J* = 3.3 Hz, 1H), 6.13 (q, *J* = 7.4 Hz, 1H), 5.15 (d, *J* = 12.4 Hz, 1H), 5.09 (d, *J* = 12.4 Hz, 1H), 1.79 (d, *J* = 7.4 Hz, 3H). **^{13}C NMR** (101 MHz, $CDCl_3$): δ 172.3, 152.2, 148.0, 136.3, 135.9, 131.9, 128.4, 128.0, 127.9, 122.5, 121.2, 120.2, 111.2, 108.5, 66.6, 55.8, 18.0. **FT-IR**: ν (cm^{-1}) 3034, 2953, 2918, 1849, 1740, 1587, 1481, 1560, 1545, 1481, 1441, 1377, 1339, 1308, 1290, 1271, 1213, 1171, 1092, 1065, 1024. **HRMS (ESI)**: Exact mass calculated for $C_{19}H_{19}N_2O_2$ $[M+H]^+$: 307.1447, found 307.1454.

2-(2-(Pyridin-2-yl)-1*H*-pyrrol-1-yl)propanoic acid (11e)

A 25 mL round-bottomed flask was charged with Pd/C (92 mg, 5% weight of Pd, 0.044 mmol, 5 mol%) and put under N_2. A solution of compound **11e-3** (266.5 mg, 0.87 mmol) in MeOH (5 mL) was added. The mixture was sparged with H_2 through a needle connected to a filled balloon for 10 min. The needle was removed from the solution but left in the flask, and the mixture was stirred for 4 h. When complete conversion was verified by TLC, it was filtered over celite and the solvent evaporated. The crude material was purified by flash column chromatography (heptane:EtOAc 1:1 as eluent) to give the corresponding product as a bright red solid (125 mg, 66% yield). **m.p.** 147-148 °C. **^{1}H NMR** (400 MHz, $CDCl_3$): δ 8.50 (d, *J* = 5.2 Hz, 1H), 7.90 (td, *J* = 7.8, 1.7 Hz, 1H), 7.68 (dt, *J* = 8.1, 1.0 Hz, 1H), 7.34-7.30 (m, 1H), 7.08 (dd, *J* = 2.9, 1.7 Hz, 1H), 6.58 (dd, *J* = 3.8, 1.7 Hz, 1H), 6.31 (dd, *J* = 3.8, 2.9 Hz, 1H), 5.16 (q, *J* = 7.1 Hz, 1H), 1.72 (d, *J* = 7.1 Hz, 3H). **^{13}C NMR** (101 MHz, $CDCl_3$): δ 171.3, 150.3, 145.9, 139.4, 130.2, 123.7, 122.5, 121.7, 113.1, 109.9, 54.4, 16.9. **FT-IR**: ν (cm^{-1}) 3143, 3119, 2992, 2967, 2945, 2922, 2851, 2450 (br), 1923, 1744, 1595, 1566, 1543, 1445, 1396, 1373, 1352, 1329, 1288, 1273, 1233, 1209, 1179, 1146, 1119, 1070, 1053, 1011. **HRMS (ESI)**: Exact mass calculated for $C_{12}H_{13}N_2O_2$ $[M+H]^+$: 217.0977, found 217.0985.

Retrosynthetic sequence to substrate 11f:

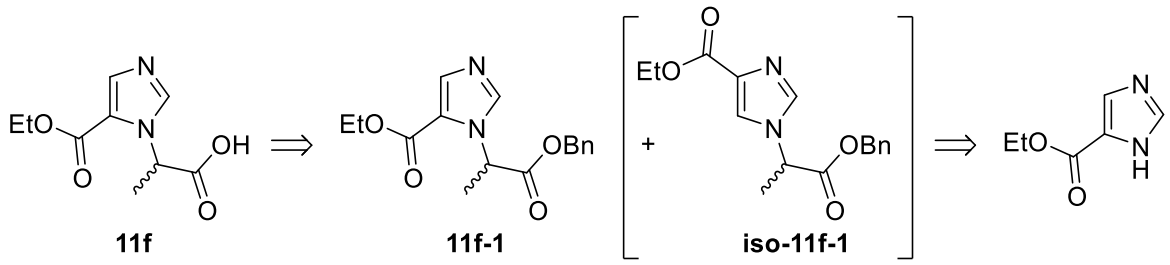

Ethyl 1-(1-(benzyloxy)-1-oxopropan-2-yl)-1*H*-imidazole-5-carboxylate (11f-1) & ethyl 1-(1-(benzyloxy)-1-oxopropan-2-yl)-1*H*-imidazole-5-carboxylate (iso-11f-1)

A dried 100 mL two-necked round bottomed flask was charged with ethyl 1*H*-imidazole-5-carboxylate (708 mg, 5.05 mmol) and Cs_2CO_3 (2.0 g, 6.06 mmol, 1.2 equiv.) and put under N_2. DMF (20 mL) was added, followed by slow addition of benzyl 2-bromopropionate (910 mg, 5.05 mmol, 1 equiv.). The resulting mixture was stirred at room temperature for 2 h until completion (judged by TLC), diluted with EtOAc and washed with aqueous $NaHCO_3$. The aqueous phase was back-extracted with EtOAc. Organics were pooled, dried ($MgSO_4$) and solvent evaporated. The crude material was purified by flash column chromatography (eluent gradient: from heptane:EtOAc 5:5 to 2:8) to give the two isomers in distinct groups of fractions. Compound **11f-1** was in the first group fractions and was isolated as a light yellow oil (375 mg, 25% yield). Compound **iso-11f-1** was in the second group of fractions and was isolated as a colourless viscous oil (780 mg, 51% yield). The nature of the two isolated isomers was confirmed by 2D-NMR experiments (HSQC, HMBC). ***Characterisation of 11f-1:*** **^{1}H NMR** (400 MHz, $CDCl_3$): δ 7.77 (s, 2H), 7.38-7.27 (m, 5H), 5.70 (q, *J* = 7.4 Hz, 1H), 5.21 (d, *J* = 12.3 Hz, 1H), 5.16 (d, *J* = 12.3 Hz, 1H), 4.24 (q, *J* = 7.1 Hz, 2H), 1.83 (d, *J* = 7.4 Hz, 3H), 1.32 (t, *J* = 7.1 Hz, 3H). **^{13}C NMR** (101 MHz, $CDCl_3$): δ 170.2, 160.4, 140.1, 137.8, 135.1, 128.6, 128.4, 128.2, 122.7, 67.5, 60.6, 54.6, 17.8, 14.2. **FT-IR**: ν (cm^{-1}) 3132, 3065, 3032, 2982, 2987, 1748, 1707, 1541, 1375, 1352, 1302, 1224, 1132, 1069, 1020. **HRMS (ESI)**: Exact mass calculated for $C_{16}H_{19}N_2O_4$ $[M+H]^+$: 303.1345, found 303.1355. ***Characterisation of iso-11f-1:*** **^{1}H NMR** (400 MHz, $CDCl_3$): δ 7.72 (d, *J* = 1.4 Hz, 1H), 7.58 (d, *J* = 1.4 Hz, 1H), 7.40-7.28 (m, 5H), 5.20 (d, *J* = 12.2 Hz, 1H), 5.16 (d, *J* = 12.2. Hz, 1H), 4.92 (q, *J* = 7.3 Hz, 1H), 4.37 (q, *J* = 7.1 Hz, 2H), 1.78 (d, *J* = 7.3 Hz, 3H), 1.38 (t, *J* = 7.1 Hz, 3H). **^{13}C NMR** (101 MHz, $CDCl_3$): δ 169.2, 162.7, 137.2, 134.6, 134.3, 128.8, 128.7, 128.4, 124.1, 68.0, 60.6,

55.5, 18.5, 14.4. **FT-IR**: ν (cm^{-1}) 3119, 3063, 3034, 2982, 2941, 2905, 1742, 1719, 1545, 1497, 1456, 1381, 1314, 1275, 1211, 1177, 1126, 1082, 1045, 1022. **HRMS (ESI)**: Exact mass calculated for $C_{16}H_{19}N_2O_4$ $[M+H]^+$: 303.1345, found 303.1355.

2-(5-(Ethoxycarbonyl)-1*H*-imidazol-1-yl)propanoic acid (11f)

A 100 mL round-bottomed flask was charged with compound **11f-1** (357 mg, 1.18 mmol), Pd/C (130 mg, 5% weight of Pd, 0.059 mmol, 5 mol%) and put under N_2. EtOH (20 mL) was added, and the mixture was sparged with H_2 through a needle connected to a filled balloon for 10 min. The needle was removed from the solution but left in the flask, and the mixture was stirred for 2 h. When complete conversion was verified by TLC, the mixture was filtered over celite and the solvent evaporated to afford the title compound as a white solid (230 mg, 91% yield). **m.p.** 126-128 °C. **^{1}H NMR** (400 MHz, D_2O): δ 8.86 (br s, 1H), 8.12 (d, *J* = 1.4 Hz, 1H), 5.40 (q, *J* = 7.4 Hz, 1H), 4.35 (q, *J* = 7.1 Hz, 2H), 1.81 (d, *J* = 7.4 Hz, 3H), 1.31 (t, *J* = 7.1 Hz, 3H). **^{13}C NMR** (101 MHz, D_2O): δ 175.5, 159.0, 136.7, 126.9, 125.0, 63.0, 60.0, 16.5, 13.2. **FT-IR**: ν (cm^{-1}) 3144, 3007, 2968, 2977, 2423 (br), 1965 (br), 1697, 1595, 1545, 1476, 1456, 1443, 1395, 1373, 1346, 1319, 1277, 1161, 1028. **HRMS (ESI)**: Exact mass calculated for $C_9H_{13}N_2O_4$ $[M+H]^+$: 213.0875, found 213.0885.

Retrosynthetic sequence to substrate 11g:

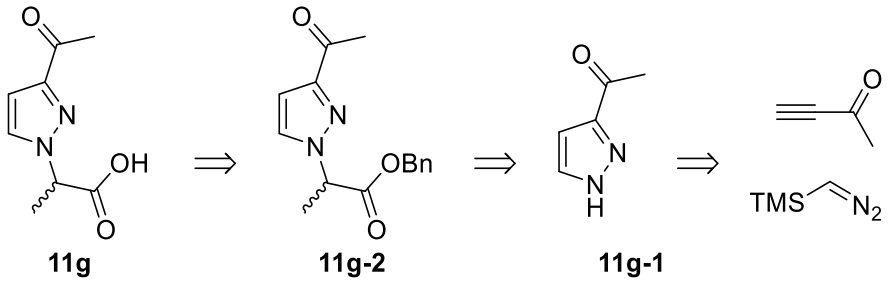

1-(1*H*-Pyrazol-3-yl)ethan-1-one (11g-1)

Following a reported procedure,[232] a 25 mL round bottomed flask under N_2 was charged with but-3-yn-2-one (0.70 mL, 9 mmol) and THF (7.5 mL). The flask was immersed in ice bath, and a solution of trimethylsilyldiazomethane (4.5 mL, 2 M in hexane, 9 mmol, 1 equiv.) was added dropwise. The bath was removed, and the mixture stirred at room temperature for 3 h. Water was added, and the mixture extracted with EtOAc. Organics were dried ($MgSO_4$) and solvent evaporated to afford the desired compound as a light

orange oil (979 mg, 99% yield), which was used in the next step without further purification. **^{1}H NMR** (400 MHz, $CDCl_3$): δ 12.26 (br s, 1H), 7.73 (d, *J* = 2.2 Hz, 1H), 6.86 (d, *J* = 2.2 Hz, 1H), 2.62 (s, 3H). The spectral data are in good agreement with those previously reported.[233]

Benzyl 2-(3-acetyl-1*H*-pyrazol-1-yl)propanoate (11g-2)

A 250 mL three-necked round bottomed flask was charged with K_2CO_3 (1.42 g, 10.3 mmol, 1.2 equiv.) and put under N_2. A solution of compound **11g-1** (945 mg, 8.6 mmol) in acetonitrile (65 mL) was added, followed by slow addition of a solution of 2-bromopropionate (2.50 g, 10.3 mmol, 1.2 equiv.) in acetonitrile (15 mL). The resulting mixture was left stir for 15 h, filtered over celite and the solvent evaporated. The crude material was purified by flash column chromatography (eluent gradient: from pure CH_2Cl_2 to CH_2Cl_2:acetone 100:4) to give the corresponding product as a light yellow oil (1.93 g, 82% yield). The reported connectivity was confirmed by 2D-NMR experiments (HSQC, HMBC). **^{1}H NMR** (400 MHz, $CDCl_3$): δ 7.54 (d, *J* = 2.5 Hz, 1H), 7.38-7.26 (m, 5H), 6.83 (d, *J* = 2.5 Hz, 1H), 5.22-5.16 (m, 3H), 2.56 (s, 3H), 1.83 (d, *J* = 7.3 Hz, 3H). **^{13}C NMR** (101 MHz, $CDCl_3$): δ 194.0, 169.8, 151.4, 134.9, 130.1, 128.7, 128.6, 128.1, 106.9, 67.6, 60.3, 26.5, 17.6. **FT-IR**: ν (cm^{-1}) 3123, 3067, 3034, 2997, 2947, 1744, 1684, 1499, 1474, 1456, 1418, 1302, 1248, 1223, 1126, 1082, 1049, 1028. **HRMS (ESI)**: Exact mass calculated for $C_{15}H_{16}N_2O_3Na$ $[M+Na]^+$: 295.1059, found 295.1064.

2-(3-Acetyl-1*H*-pyrazol-1-yl)propanoic acid (11g)

A 100 mL round-bottomed flask was charged with Pd/C (356 mg, 5% weight of Pd, 0.168 mmol, 5 mol%) and put under N_2. A solution of compound **11g-2** (912 mg, 3.35 mmol) in EtOAc (20 mL) was added. The mixture was sparged with H_2 through a needle connected to a filled balloon for 10 min. The needle was removed from the solution but left in the flask, and the mixture was stirred for 2 h. When complete conversion was verified by TLC, the mixture was filtered over celite and the solvent evaporated to afford the title compound as a white solid (600 mg, 98% yield). **m.p.** 105-106 °C. **^{1}H NMR** (400 MHz, $CDCl_3$): δ 7.78 (br s, 1H), 7.55 (d, *J* = 2.5 Hz, 1H), 6.85 (d, *J* = 2.5 Hz, 1H), 5.20 (q, *J* = 7.4 Hz, 1H), 2.58 (s, 3H), 1.88 (d, *J* = 7.4 Hz, 3H). **^{13}C NMR** (101 MHz, $CDCl_3$): δ 194.2, 174.1, 151.3, 130.4, 107.2, 56.0, 26.6, 17.5. **FT-IR**: ν (cm^{-1}) 3142,

3123, 2949 (br), 2787, 2692, 2592, 2504, 1748, 1684, 1645, 1476, 1387, 1350, 1300, 1242, 1225, 1188, 1105, 1057, 1034, 1016, 1001. **HRMS (ESI)**: Exact mass calculated for $C_8H_{11}N_2O_3$ $[M+H]^+$: 183.0770, found 183.0777.

2-(1*H*-Indol-1-yl)propanoic acid (11h)

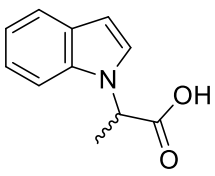

A dried 250 mL three-necked round bottomed flask was charged with indole (3.51 g, 30 mmol) and put under N_2. DMF (40 mL) was added and the resulting solution immersed in an ice bath. NaH (3.0 g, 60% in mineral oil, 75 mmol, 2.5 equiv.) was added in portions, and the mixture stirred in ice bath for 30 min. 2-bromopropionic acid (2.8 mL, 31.5 mmol, 1.05 equiv.) was added dropwise, the ice bath removed and the mixture stirred at room temperature for 15 h, then slowly quenched with water. The aqueous phase was washed with heptane and EtOAc, acidified with 10% aqueous HCl solution until pH < 1, extracted with EtOAc three times, organics were pooled, dried ($MgSO_4$) and solvent evaporated. The crude material was purified by automated flash column chromatography (eluent gradient: from pure heptane to heptane:EtOAc 6:4) to give the corresponding product as a light yellow solid (3.05 g, 54% yield). **m.p.** 115-116 °C [Lit.[234] 98-101 °C].[XXI] **^{1}H NMR** (400 MHz, $CDCl_3$): δ 10.74 (br s, 1H), 7.63 (d, *J* = 7.8 Hz, 1H), 7.29 (d, *J* = 8.3 Hz, 1H), 7.25-7.19 (m, 2H), 7.15-7.10 (m, 1H), 6.58 (dd, *J* = 3.4, 0.7 Hz, 1H), 5.16 (q, *J* = 7.4 Hz, 1H), 1.85 (d, *J* = 7.4 Hz, 3H). **^{13}C NMR** (101 MHz, $CDCl_3$): δ 177.7, 136.1, 128.6, 124.8, 122.0, 121.2, 120.1, 109.0, 102.8, 53.2, 17.3. The spectral data are in good agreement with those previously reported.[234]

2-(1*H*-Pyrrolo[2,3-*b*]pyridin-1-yl)propanoic acid (11i)

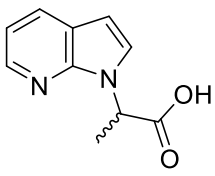

A dried 100 mL two-necked round bottomed flask was charged with 1*H*-pyrrolo[2,3-*b*]pyridine (1.77 g, 15 mmol) and put under N_2. DMF (20 mL) was added and the resulting solution was immersed in an ice bath. NaH (1.5 g, 60% in mineral oil, 37.5 mmol, 2.5 equiv.) was added in portions, and the mixture stirred in ice bath for 30 min. 2-bromopropionic acid (1.42 mL, 15.75 mmol, 1.05 equiv.) was added dropwise, the ice bath removed and the mixture stirred at room temperature for 5 h, then slowly quenched and diluted with

[XXI] Softening of the material, but not melting, is observed at 102-105 °C.

water, then washed with heptane and EtOAc. The aqueous phase was acidified with 10% aqueous HCl solution to pH 6, then extracted with EtOAc. Acidification continued, and extractions performed at pH 4, pH 2.5 and pH 1. TLC analysis showed material from the organic phases extracted at pH 6, 4 and 2.5, which were then pooled, dried ($MgSO_4$) and solvent evaporated. The crude material was purified by flash column chromatography (first purification with eluent gradient from pure CH_2Cl_2 to CH_2Cl_2:MeOH 100:4; second purification with eluent gradient from pure heptane to heptane:acetone 7:3) to give the corresponding product as a white solid (889 mg, 31% yield). **m.p.** 134-136 °C. **^{1}H NMR** (400 MHz, $CDCl_3$): δ 11.69 (br s, 1H), 8.33 (dd, *J* = 5.0, 1.4 Hz, 1H), 7.98 (dd, *J* = 7.8, 1.4 Hz, 1H), 7.40 (d, *J* = 3.7 Hz, 1H), 7.11 (dd, *J* = 7.8, 5.0 Hz, 1H), 6.56 (d, *J* = 3.7 Hz, 1H), 5.61 (q, *J* = 7.4 Hz, 1H), 1.89 (d, *J* = 7.4 Hz, 3H). **^{13}C NMR** (101 MHz, $CDCl_3$): δ 173.6, 146.2, 141.2, 130.6, 126.6, 122.0, 116.2, 100.9, 55.5, 17.4. **FT-IR**: ν (cm^{-1}) 3130, 3003, 2939, 2750, 1446 (br), 1869 (br), 1714, 1684, 1576, 1516, 1485, 1456, 1425, 1381, 1350, 1304, 1425, 1350, 1271, 1248, 1209, 1070, 1023. **HRMS (ESI)**: Exact mass calculated for $C_{10}H_{11}N_2O_2$ $[M+H]^+$: 191.0821, found 191.0830.

Retrosynthetic sequence to substrate 11j:

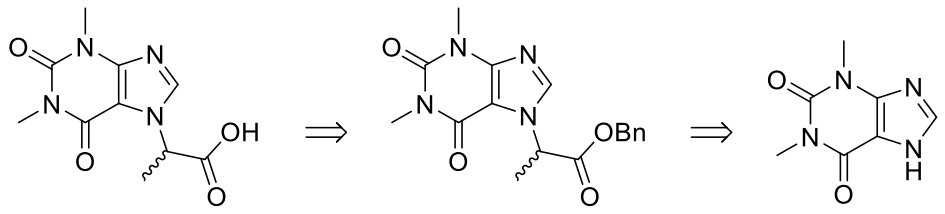

Benzyl 2-(1,3-dimethyl-2,6-dioxo-1,2,3,6-tetrahydro-7*H*-purin-7-yl)propanoate (11j-1)

A dried 100 mL two-necked round bottomed flask was charged with theophylline (910 mg, 5.05 mmol) and Cs_2CO_3 (2.0 g, 6.06 mmol, 1.2 equiv.) and put under N_2. DMF (20 mL) was added, followed by slow addition of benzyl 2-bromopropionate (910 mg, 5.05 mmol, 1 equiv.). The resulting mixture was stirred at room temperature for 2 h until completion (judged by TLC), diluted with EtOAc and washed with aqueous $NaHCO_3$. The aqueous phase was back-extracted with EtOAc. Organics were pooled, dried ($MgSO_4$) and solvent evaporated to afford the title compound as a white solid (1.73 g, 99% yield). The reported connectivity was confirmed by 2D-NMR experiments (HSQC, HMBC). **m.p.** 136-137 °C. **^{1}H NMR** (400 MHz, $CDCl_3$): δ 7.74 (s, 1H), 7.39-7.31 (m, 5H),

5.66 (q, *J* = 7.4 Hz, 1H), 5.24 (d, *J* = 12.2 Hz, 1H), 5.19 (d, *J* = 12.2 Hz, 1H), 3.60 (s, 3H), 3.38 (s, 3H), 1.86 (d, *J* = 7.4 Hz, 3H). **^{13}C NMR** (101 MHz, $CDCl_3$): δ 169.7, 155.2, 151.6, 148.7, 139.8, 134.8, 128.6, 128.6, 128.3, 106.9, 67.9, 54.8, 29.8, 28.0, 18.01. **FT-IR**: ν (cm^{-1}) 3142, 2954, 2895, 1734, 1701, 1653, 1541, 1474, 1456, 1429, 1399, 1375, 1331, 1294, 1248, 1101, 1038. **HRMS (ESI)**: Exact mass calculated for $C_{17}H_{19}N_4O_4$ $[M+H]^+$: 343.1406, found 343.1412.

2-(1,3-Dimethyl-2,6-dioxo-1,2,3,6-tetrahydro-7*H*-purin-7-yl)propanoic acid (11j)

A 50 mL round-bottomed flask was charged with compound **11j-1** (856 mg, 2.5 mmol), Pd/C (266 mg, 5% weight of Pd, 0.125 mmol, 5 mol%) and put under N_2. MeOH (10 mL) was added, and the mixture was sparged with H_2 through a needle connected to a filled balloon for 10 min. The needle was removed from the solution but left in the flask, and the mixture was stirred for 2 h. When complete conversion was verified by TLC, the mixture was filtered over celite and the solvent evaporated to afford the title compound as a white solid (574 mg, 91% yield). **m.p.** 176-177 °C. **^{1}H NMR** (400 MHz, DMSO-d_6): δ 13.29 (br s, 1H), 8.21 (s, 1H), 5.47 (q, *J* = 7.4 Hz, 1H), 3.45 (s, 3H), 3.22 (s, 3H), 1.76 (d, *J* = 7.4 Hz, 3H). **^{13}C NMR** (101 MHz, DMSO-d_6): δ 171.2, 154.3, 150.9, 148.3, 141.7, 106.1, 54.6, 29.4, 27.5, 17.1. The spectral data are in good agreement with those previously reported.[235]

2-(9*H*-Carbazol-9-yl)propanoic acid (11k)

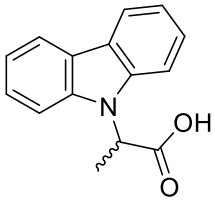

A dried 250 mL three-necked round bottomed flask was charged with carbazole (5.02 g, 30 mmol) and put under N_2. DMF (40 mL) was added and the resulting solution was immersed in an ice bath. NaH (3.0 g, 60% in mineral oil, 75 mmol, 2.5 equiv.) was added in portions, and the mixture stirred in ice bath for 30 min. 2-bromopropionic acid (2.8 mL, 31.5 mmol, 1.05 equiv.) was added dropwise, the ice bath removed at the end of the addition and the mixture stirred at room temperature for 15 h, slowly quenched with water, the aqueous phase washed with heptane and EtOAc, and then acidified with 10% aqueous HCl solution until pH < 1. The aqueous phase was then extracted with EtOAc three times, organics were pooled, dried ($MgSO_4$) and solvent evaporated. The crude material was purified by automated flash column chromatography (eluent gradient: from pure

heptane to heptane:EtOAc 7:3) to give the corresponding product as a light brown solid (7.18 g, 77% yield). **m.p.** 151-152 °C [Lit.[234] 149-151 °C]. **^{1}H NMR** (400 MHz, $CDCl_3$): δ 8.10 (d, *J* = 7.9 Hz, 2H), 7.47-7.42 (m, 2H), 7.38 (d, *J* = 8.2 Hz, 2H), 7.28-7.24 (m, 2H), 5.47 (q, *J* = 7.3 Hz, 1H), 1.85 (d, *J* = 7.3 Hz, 3H). **^{13}C NMR** (101 MHz, $CDCl_3$): δ 175.1, 139.4, 125.8, 123.5, 120.5, 119.6, 109.2, 51.8, 15.2. The spectral data are in good agreement with those previously reported.[234]

2-(1,3-Dioxoisoindolin-2-yl)propanoic acid (11l)

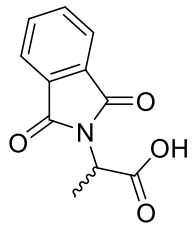

Following a reported procedure,[236] a mixture of phthalic anhydride (1.48 g, 10 mmol) and (±)-alanine (0.9 g, 10 mmol, 1 equiv.) in AcOH (22 mL) was refluxed under air for 2 h. The mixture was allowed to cool, and the solvent evaporated. The resulting white solid was re-crystallised from EtOH to afford the title compound (560 mg, 26% yield). Material present in the mother liquors was not recovered. **m.p.** 156-157 °C [Lit.[237] 160-163 °C]. **^{1}H NMR** (400 MHz, $CDCl_3$): δ 13.21 (br s, 1H), 7.94-7.85 (m, 4H), 4.87 (q, *J* = 7.3 Hz, 1H), 1.55 (d, *J* = 7.3 Hz, 3H). **^{13}C NMR** (101 MHz, $CDCl_3$): δ 171.0, 167.1, 134.7, 131.3, 123.2, 47.0, 14.8. The spectral data are in good agreement with those previously reported.[238]

2-(1*H*-Pyrrol-1-yl)hexanoic acid (11n)

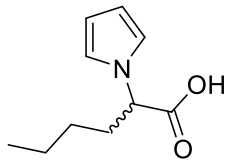

Following a reported procedure,[225] a 250 mL three-necked round bottomed flask equipped with reflux condenser was charged with NaOAc (2.87 g, 35 mmol, 1 equiv.) and (±)-norleucine (4.59 g, 35 mmol). The flask was put under N_2, degassed water (15 mL), acetic acid (5 mL) and 1,2-dichloroethane (21 mL) were added, and the mixture brought to 90 °C. To the colorless solution, 2,5-dimethoxytetrahydrofuran (4.5 mL, 35 mmol, 1 equiv.) was added, and the mixture stirred at the same temperature for 15 h, then cooled to room temperature and the phases separated. The aqueous phase was washed with CH_2Cl_2 twice, organics were pooled, dried ($MgSO_4$) and solvent evaporated. The resulting brown oil was purified by automated flash column chromatography (eluent gradient: from pure heptane to heptane:EtOAc 7:3) to afford the desired product as a light yellow oil (4.21 g, 67% yield). **^{1}H NMR** (400 MHz, $CDCl_3$): δ 11.65 (br s, 1H), 6.73 (t, *J* = 2.2 Hz,

2H), 6.20 (t, *J* = 2.2 Hz, 2H), 4.57 (dd, *J* = 9.8, 5.8 Hz, 1H), 2.20-1.97 (m, 2H), 1.42-1.14 (m, 4H), 0.88 (t, *J* = 7.0 Hz, 3H). **^{13}C NMR** (101 MHz, $CDCl_3$): δ 177.4, 120.1, 108.8, 61.7, 32.2, 28.0, 22.1, 13.8. **FT-IR**: ν (cm^{-1}) 3102, 2957, 2930, 2872, 2610 (br), 1717, 1558, 1541, 1489, 1277, 1211, 1090, 1069. **HRMS (ESI)**: Exact mass calculated for $C_{10}H_{16}NO_2$ $[M+H]^+$: 182.1181, found 182.1187.

3-Phenyl-2-(1*H*-pyrrol-1-yl)propanoic acid (11o)

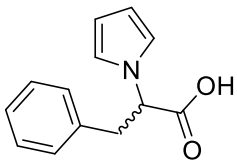

Following a reported procedure,[69] a 250 mL three-necked round bottomed flask equipped with reflux condenser was charged with (±)-phenylalanine (5.78 g, 35 mmol). Water (35 mL), acetic acid (18 mL) and 1,2-dichloroethane (55 mL) were added, followed by 2,5-dimethoxytetrahydrofuran (4.5 mL, 35 mmol, 1 equiv.). The mixture was heated to 80 °C and stirred for 45 min, then cooled to room temperature and the phases separated. The aqueous phase was washed with CH_2Cl_2 twice, organics were pooled, dried ($MgSO_4$) and solvent evaporated. The resulting brown oil was purified by flash column chromatography (eluent heptane:EtOAc 8:2) to afford the desired product as a grey solid (2.85 g, 38% yield). **m.p.** 97-99 °C [Lit.[234] 101-104 °C]. **^{1}H NMR** (400 MHz, $CDCl_3$): δ 10.86 (br s, 1H), 7.26-7.18 (m, 3H), 7.04-6.99 (m, 2H), 6.70 (t, *J* = 2.2 Hz, 2H), 6.16 (t, *J* = 2.2 Hz, 2H), 4.79 (dd, *J* = 9.2, 5.9 Hz, 1H), 3.44 (dd, *J* = 14.0, 5.9 Hz, 1H), 3.29 (dd, *J* = 14.0, 9.2 Hz, 1H). **^{13}C NMR** (101 MHz, $CDCl_3$): δ 175.7, 136.0, 128.8, 128.6, 127.2, 120.2, 109.0, 63.3, 39.0. The spectral data are in good agreement with those previously reported.[239]

3-Methyl-2-(1*H*-pyrrol-1-yl)butanoic acids (11p)

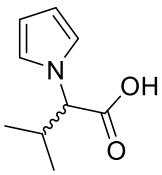

Following a reported procedure,[69] a 250 mL three-necked round bottomed flask equipped with reflux condenser was charged with (±)-valine (2.93 g, 25 mmol) and put under N_2. Acetic acid (50 mL) was added, followed by 2,5-dimethoxytetrahydrofuran (3.25 mL, 25 mmol, 1 equiv.). The mixture was heated to 80 °C and stirred for 30 min, then cooled to room temperature and the phases separated. The aqueous phase was washed with CH_2Cl_2 twice, organics were pooled, dried ($MgSO_4$) and solvent evaporated. The resulting brown oil was purified by flash column chromatography (eluent heptane:EtOAc 8:2) to afford the desired product as a cream solid (4.18 g, 48% yield). **m.p.** 84-85 °C. **^{1}H NMR**

(400 MHz, $CDCl_3$): δ 10.58 (br s, 1H), 6.77 (t, *J* = 2.1 Hz, 2H), 6.18 (t, *J* = 2.1 Hz, 2H), 4.15 (d, *J* = 10.0 Hz, 1H), 2.49-2.35 (m, 1H), 1.05 (d, *J* = 6.6 Hz, 3H), 0.79 (d, *J* = 6.6 Hz, 3H). **^{13}C NMR** (101 MHz, $CDCl_3$): δ 176.5, 120.5, 108.6, 68.7, 31.8, 19.4, 18.7. The spectral data are in good agreement with those previously reported.[239]

5-Methoxy-5-oxo-2-(1*H*-pyrrol-1-yl)pentanoic acid (11q)

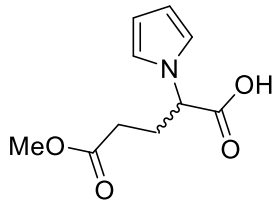

Following a reported procedure,[240] a 100 mL two-necked round bottomed flask equipped with reflux condenser was charged with (±)-glutamic acid δ-methyl ester (1.61 g, 10 mmol) and put under N_2. Water (15 mL), acetic acid (57 μL, 1 mmol, 10 mol%) and 1,2-dichloroethane (15 mL) were added, followed by 2,5-dimethoxytetrahydrofuran (1.4 mL, 11 mmol, 1.1 equiv.). The mixture was heated to reflux and stirred for 1 h, then cooled to room temperature and the phases separated. The aqueous phase was washed with CH_2Cl_2 twice, organics were pooled, dried ($MgSO_4$) and solvent evaporated. The resulting orange oil was purified by flash column chromatography (eluent gradient: from pure heptane to heptane:EtOAc 1:1) to afford the desired product as a light yellow oil (822 mg, 39% yield). **^{1}H NMR** (400 MHz, $CDCl_3$): δ 9.92 (br s, 1H), 6.70 (t, *J* = 2.1 Hz, 2H), 6.20 (t, *J* = 2.1 Hz, 2H), 4.79 (dd, *J* = 10.2, 5.3 Hz, 1H), 3.66 (s, 3H), 2.55-2.44 (m, 1H), 2.36-2.14 (m, 3H). **^{13}C NMR** (101 MHz, $CDCl_3$): δ 175.8, 172.8, 120.1, 109.2, 60.3, 51.9, 29.6, 27.6. The spectral data are in good agreement with those previously reported.[240]

2-(1*H*-Pyrrolo[2,3-*b*]pyridin-1-yl)hexanoic acid (11r)

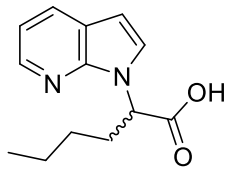

A dried 100 mL two-necked round bottomed flask was charged with 1*H*-pyrrolo[2,3-*b*]pyridine (1.77 g, 15 mmol) and put under N_2. DMF (20 mL) was added and the resulting solution was immersed in an ice bath. NaH (1.50 g, 60% in mineral oil, 37.5 mmol, 2.5 equiv.) was added in portions, and the mixture stirred in ice bath for 30 min. 2-bromohexanoic acid (2.24 mL, 15.8 mmol, 1.05 equiv.) was added dropwise, the ice bath removed at the end of the addition and the mixture stirred at room temperature for 15 h, then slowly quenched and diluted with water, and washed with heptane and EtOAc. The aqueous phase was acidified with 10% aqueous HCl solution until pH 5, at which point it was extracted with EtOAc. Acidification continued and extraction performed at pH 4.5 and

3. TLC analysis shows supposed product in the organic phases extracted at pH 5 and 4.5, which were then pooled, dried ($MgSO_4$) and solvent evaporated. The crude material was purified by automated flash column chromatography (eluent gradient: from pure heptane to heptane:EtOAc 7:3) to give the corresponding product as a cream solid (2.35 g, 67% yield). **m.p.** 99-100 °C. **^{1}H NMR** (400 MHz, $CDCl_3$): δ 12.73 (br s, 1H), 8.32 (dd, *J* = 4.9, 1.4 Hz, 1H), 8.00 (dd, *J* = 7.9, 1.4 Hz, 1H), 7.34 (d, *J* = 3.6 Hz, 1H), 7.14 (dd, *J* = 7.9, 4.9 Hz, 1H), 6.55 (d, *J* = 3.6 Hz, 1H), 5.35 (dd, *J* = 10.0, 5.7 Hz, 1H), 2.38-2.28 (m, 1H), 2.24-2.14 (m, 1H), 1.39-1.21 (m, 3H), 1.16-1.05 (m, 1H), 0.82 (t, *J* = 7.2 Hz, 3H). **^{13}C NMR** (101 MHz, $CDCl_3$): δ 173.6, 146.4, 141.1, 130.6, 127.3, 121.9, 116.1, 101.0, 57.8, 31.9, 28.1, 22.0, 13.7. **FT-IR**: ν (cm^{-1}) 2957, 2930, 2857, 2410 (br), 2365, 1734, 1701, 1655, 1600, 1580, 1514, 1433, 1356, 1201, 1101. **HRMS (ESI)**: Exact mass calculated for $C_{13}H_{17}N_2O_2$ $[M+H]^+$: 233.1290, found 233.1300.

6.6 Ni-photoredox enantioselective cross-couplings

General procedure

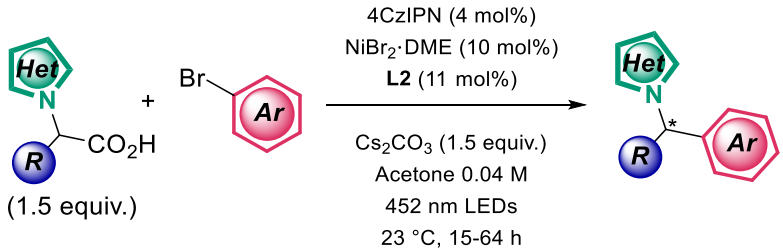

A 10 mL dried Schlenk flask was charged with $NiBr_2$ DME (6.2 mg, 0.02 mmol, 10 mol%) and ligand **L2** (4.8 mg, 0.022 mmol, 11 mol%). The flask was put under N_2, 2 mL of dry acetone were added, and the mixture stirred for 10 minutes to form a red, finely divided suspension. A second 10 mL dried Schlenk flask was charged with the aryl bromide (if solid, 0.2 mmol), carboxylic acid (0.3 mmol, 1.5 equiv.) and 4CzIPN (6.3 mg, 0.008 mmol, 4 mol%). The flask was put under N_2, 3 mL of dry acetone were added to form a yellow solution, which was then added to the previously prepared Ni solution. Finally, aryl bromide (if liquid, 0.2 mmol) and Cs_2CO_3 (97.7 mg, 0.3 mmol, 1.5 equiv.) were added directly. The flask was sealed, and three cycles of freeze-pump-thaw were performed before refilling with N_2. The flask was accommodated into our reactor (***LED strip 1***) and stirred for 15-64 h at 23 °C with fan cooling under blue light irradiation. After the defined reaction time, the reaction mixture was diluted with EtOAc or CH_2Cl_2 and filtered over

celite. The solution was evaporated to dryness, and the residue purified by flash column chromatography to obtain the desired compound.

(*S*)-4-(1-(1*H*-Pyrrol-1-yl)ethyl)benzonitrile (12a)

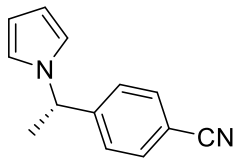

Prepared according to the general procedure using 4-bromobenzonitrile (36.4 mg, 0.2 mmol) and (*S*)-2-(1*H*-pyrrol-1-yl)propanoic acid (41.7 mg, 0.3 mmol, 1.5 equiv.), with reaction time of 15 h. The crude material was purified by flash column chromatography (heptane:EtOAc 95:5 as eluent) to give the corresponding product as a cream solid (31.4 mg, 80% yield). The enantiomeric ratio was determined by SFC analysis on a YMC CHIRAL ART Amylose-SA column (CO_2:MeOH 99:1 for 2 min, then gradient ramp to 95:5 over 6 min, ramp to 99:1 over 0.5 min, 99:1 for 1 min; flow rate 2 mL/min; λ = 225 nm); τ_{major} = 5.71 min, τ_{minor} = 5.97 min; e.r. 77:23. $[\alpha]_D^{20}$ = +7.1° (*c* 2.4, $CHCl_3$). **m.p.** 68-69 °C [Lit.[241] 64 °C]. **^{1}H NMR** (400 MHz, $CDCl_3$): δ 7.59 (d, *J* = 8.5 Hz, 2H), 7.12 (d, *J* = 8.5 Hz, 2H), 6.74 (t, *J* = 2.2 Hz, 2H), 6.23 (t, *J* = 2.2 Hz, 2H), 5.33 (q, *J* = 7.1 Hz, 1H), 1.85 (d, *J* = 7.1 Hz, 3H). **^{13}C NMR** (101 MHz, $CDCl_3$): δ 149.1, 132.6, 126.4, 119.4, 118.6, 111.4, 108.8, 57.7, 21.8. The spectral data are in good agreement with those previously reported.[241]

1 mmol scale reaction

Prepared according to the general procedure in a 30 mL Schlenk flask, using 4-bromobenzonitrile (182.0 mg, 1 mmol), (*S*)-2-(1*H*-pyrrol-1-yl)propanoic acid (158.6 mg, 1.14 mmol, 1.14 equiv.), 4CzIPN (31.6 mg, 0.04 mmol, 4 mol%), $NiBr_2$ DME (30.9 mg, 0.1 mmol, 10 mol%), **L2** (24.0 mg, 0.11 mmol, 11 mol%), Cs_2CO_3 (371.4 mg, 1.14 mmol, 1.14 equiv.) and acetone (25 mL). After degassing, the flask was accommodated into our reactor and stirred for 20 h at room temperature with fan cooling under blue light irradiation. After work-up, the crude material was purified by flash column chromatography (eluent gradient: from pure heptane to heptane:EtOAc 92:8) to give **12a** as a white solid (175.3 mg, 89% yield). The enantiomeric ratio was determined as detailed above: e.r. 77:23.

(*S*)-4-(1-(2-Acetyl-1*H*-pyrrol-1-yl)ethyl)benzonitrile (12b)

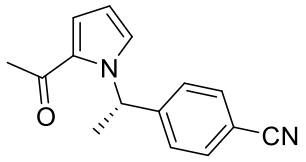

Prepared according to the general procedure using 4-bromobenzonitrile (36.4 mg, 0.2 mmol) and 2-(2-acetyl-1*H*-pyrrol-1-yl)propanoic acid (54.4 mg, 0.3 mmol, 1.5 equiv.), using 4CzIPN (12.6 mg, 0.016 mmol, 8 mol%) with reaction time of 64 h. The crude material was purified by flash column chromatography (pure CH_2Cl_2 as eluent) to give the corresponding product as a light yellow oil (23.8 mg, 50% yield). The enantiomeric ratio was determined by SFC analysis on a YMC CHIRAL ART Amylose-SA column (CO_2:MeOH 99:1 for 2 min, then gradient ramp to 95:5 over 6 min, ramp to 99:1 over 0.5 min, 99:1 for 1 min; flow rate 2 mL/min; λ = 225 nm); τ_{major} = 7.44 min, τ_{minor} = 6.95 min; e.r. 92:8. $[\alpha]_D^{20}$ = -60.3° (*c* 2.1, $CHCl_3$). **^{1}H NMR** (400 MHz, $CDCl_3$): δ 7.57 (d, *J* = 8.4 Hz, 2H), 7.17-7.12 (m, 3H), 7.06-7.04 (m, 1H), 6.68 (q, *J* = 7.2 Hz, 1H), 6.29-6.25 (m, 1H), 2.38 (s, 3H), 1.79 (d, *J* = 7.2 Hz, 3H). **^{13}C NMR** (101 MHz, $CDCl_3$): δ 188.5, 148.9, 132.4, 130.4, 126.6, 126.2, 121.2, 118.7, 111.0, 109.0, 55.7, 27.6, 21.9. **FT-IR**: ν (cm^{-1}) 3113, 2982, 2922, 2849, 2228, 1647, 1608, 1526, 1504, 1424, 1360, 1337, 1279, 1237, 1107, 1093, 1070, 1053, 1018. **HRMS (EI)**: Exact mass calculated for $C_{15}H_{14}N_2O$ $[M]^+$: 238.1106, found 238.1112.

Methyl (*S*)-1-(1-(4-cyanophenyl)ethyl)-1*H*-pyrrole-2-carboxylate (12c)

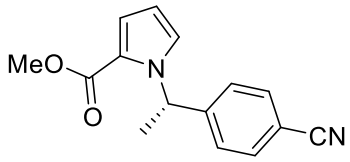

Prepared according to the general procedure using 4-bromobenzonitrile (36.4 mg, 0.2 mmol) and 2-(2-(methoxycarbonyl)-1*H*-pyrrol-1-yl)propanoic acid (59.2 mg, 0.3 mmol, 1.5 equiv.), with reaction time of 40 h. The crude material was purified by flash column chromatography (eluent gradient: from pure heptane to heptane:EtOAc 93:7) to give the corresponding product as a clear oil (34.1 mg, 67% yield). The enantiomeric ratio was determined by SFC analysis on a YMC CHIRAL ART Cellulose-C column (CO_2:MeOH 99:1 for 2 min, then gradient ramp to 95:5 over 6 min, ramp to 99:1 over 0.5 min, 99:1 for 1 min; flow rate 2 mL/min; λ = 225 nm); τ_{major} = 6.88 min, τ_{minor} = 6.31 min; e.r. 72:28. $[\alpha]_D^{20}$ = -26.9° (*c* 2.7, $CHCl_3$). **^{1}H NMR** (400 MHz, $CDCl_3$): δ 7.58 (d, *J* = 8.4 Hz, 2H), 7.14 (d, *J* = 8.4 Hz, 2H), 7.10-7.08 (m, 1H), 7.04-7.02 (m, 1H), 6.58 (q, *J* = 7.2 Hz, 1H), 6.27-6.24 (m, 1H), 3.73 (s, 3H), 1.82 (d, *J* = 7.2 Hz, 3H). **^{13}C NMR** (101 MHz, $CDCl_3$): δ 161.4, 148.9, 132.5, 126.5, 125.0, 122.2, 119.0, 118.7, 111.1, 109.0, 55.3, 51.1, 22.0. **FT-IR**: ν (cm^{-1}) 3115, 2986, 2949, 2228, 1697, 1609, 1530,

1504, 1437, 1412, 1379, 1340, 1283, 1237, 1209, 1112, 1065, 1051, 1018. **HRMS (EI)**: Exact mass calculated for $C_{15}H_{14}N_2O_2$ [M]$^+$: 254.1055, found 254.1059.

(*S*)-1-(1-(4-Cyanophenyl)ethyl)-*N*,*N*-dimethyl-1*H*-pyrrole-2-carboxamide (12d)

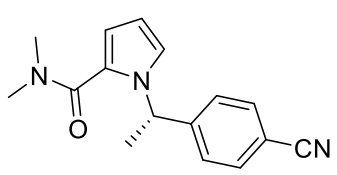

Prepared according to the general procedure using 4-bromobenzonitrile (36.4 mg, 0.2 mmol) and 2-(2-(dimethylcarbamoyl)-1*H*-pyrrol-1-yl)propanoic acid (63.1 mg, 0.3 mmol, 1.5 equiv.), with reaction time of 64 h. The crude material was purified by flash column chromatography (eluent gradient: from pure heptane to heptane:EtOAc 1:1) to give the corresponding product as a yellow oil (6.2 mg, 12% yield). The enantiomeric ratio was determined by SFC analysis on a YMC CHIRAL ART Cellulose-C column (CO_2:MeOH 99:1 for 2 min, then gradient ramp to 90:10 over 16 min, ramp to 99:1 over 0.5 min, 99:1 for 1 min; flow rate 2 mL/min; λ = 225 nm); τ_{major} = 13.74 min, τ_{minor} = 12.52 min; e.r. 91:9. $[\alpha]_D^{20}$ = -62.8° (*c* 0.4, $CHCl_3$). **^{1}H NMR** (400 MHz, $CDCl_3$): δ 7.57 (d, *J* = 8.4 Hz, 2H), 7.15 (d, *J* = 8.4 Hz, 2H), 6.92 (dd, *J* = 2.7, 1.6 Hz, 1H), 6.38 (dd, *J* = 3.7, 1.6 Hz, 1H), 6.19 (dd, *J* = 3.7, 2.7 Hz, 1H), 6.13 (q, *J* = 7.1 Hz, 1H), 2.95 (s, 6H), 1.80 (d, *J* = 7.1 Hz, 3H). **^{13}C NMR** (101 MHz, $CDCl_3$): δ 164.2, 149.3, 132.3, 126.7, 125.8, 121.3, 118.7, 113.5, 111.0, 107.6, 54.8, 21.5. The signal corresponding to the amide N-CH_3 groups is not visible. **FT-IR**: ν (cm^{-1}) 3107, 2976, 2922, 2851, 2228, 1616, 1535, 1418, 1389, 1285, 1086. **HRMS (EI)**: Exact mass calculated for $C_{16}H_{17}N_3O$ [M]$^+$: 267.1372, found 267.1372.

(*S*)-4-(1-(2-(Pyridin-2-yl)-1*H*-pyrrol-1-yl)ethyl)benzonitrile (12e)

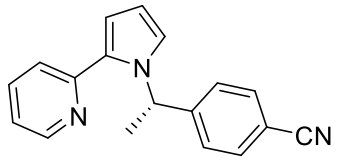

Prepared according to the general procedure using 4-bromobenzonitrile (36.4 mg, 0.2 mmol) and 2-(2-(pyridine-2-yl)-1*H*-pyrrol-1-yl)propanoic acid (47.6 mg, 0.22 mmol, 1.1 equiv.), with reaction time of 64 h. The crude material was purified by flash column chromatography (first column with eluent gradient: from pure heptane to heptane:EtOAc 85:15; second column with eluent gradient: from pure CH_2Cl_2 to CH_2Cl_2:EtOAc 100:1) to give the corresponding product as a yellow waxy solid (12.3 mg, 22% yield). The enantiomeric ratio was determined by SFC analysis on a Lux Cellulose-4 column (CO_2:MeOH 99:1 for 2 min, then gradient ramp to 82:18 over 26 min,

ramp to 99:1 over 0.5 min, 99:1 for 1 min; flow rate 2 mL/min; λ = 225 nm); τ_{major} = 17.49 min, τ_{minor} = 16.67 min; e.r. 85:15. $[\alpha]_D^{20}$ = -267.2° (*c* 0.8, $CHCl_3$). **^{1}H NMR** (400 MHz, $CDCl_3$): δ 8.48-8.45 (m, 1H), 7.58 (td, *J* = 7.9, 1.9 Hz, 1H), 7.50 (d, *J* = 8.4 Hz, 2H), 7.44 (dt, *J* = 7.9, 1.0 Hz, 1H), 7.10 (d, *J* = 8.4 Hz, 2H), 7.05-6.95 (m, 3H), 6.60 (dd, *J* = 3.6, 1.7 Hz, 1H), 6.29 (t, *J* = 3.6 Hz, 1H), 1.85 (d, *J* = 7.2 Hz, 3H). **^{13}C NMR** (101 MHz, $CDCl_3$): δ 152.5, 149.9, 148.3, 136.4, 132.4, 132.2, 126.7, 121.9, 121.4, 120.5, 118.9, 111.7, 110.6, 108.8, 54.6, 21.6. **FT-IR**: ν (cm^{-1}) 3102, 3048, 2978, 2934, 2876, 2849, 2228, 1607, 1585, 1560, 1541, 1505, 1479, 1447, 1412, 1377, 1321, 1290, 1269, 1233, 1153, 1078, 1065, 1043, 1018. **HRMS (ESI)**: Exact mass calculated for $C_{18}H_{16}N_3$ $[M+H]^+$: 274.1344, found 274.1354.

(*S*)-4-(1-(3-Acetyl-1*H*-pyrazol-1-yl)ethyl)benzonitrile (12g)

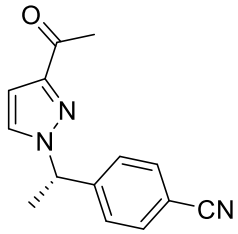

Prepared according to the general procedure using 4-bromobenzonitrile (36.4 mg, 0.2 mmol) and 2-(3-acetyl-1*H*-pyrazol-1-yl)propanoic acid (54.7 mg, 0.3 mmol, 1.5 equiv.), with reaction time of 64 h. The crude material was purified by flash column chromatography (eluent gradient: from pure CH_2Cl_2 to CH_2Cl_2:acetone 100:2) to give the corresponding product as a yellow oil (27.4 mg, 57% yield). The enantiomeric ratio was determined by SFC analysis on a Lux Cellulose-4 column (CO_2:MeOH 99:1 for 2 min, then gradient ramp to 88:12 over 26 min, ramp to 99:1 over 0.5 min, 99:1 for 1 min; flow rate 2 mL/min; λ = 225 nm); τ_{major} = 23.85 min, τ_{minor} = 24.68 min; e.r. 68:32. $[\alpha]_D^{20}$ = + 10.4° (*c* 2.1, $CHCl_3$). **^{1}H NMR** (400 MHz, $CDCl_3$): δ 7.64 (d, *J* = 8.4 Hz, 2H), 7.44 (d, *J* = 2.4 Hz, 1H), 7.29 (d, *J* = 8.4 Hz, 2H), 6.83 (d, *J* = 2.4 Hz, 1H), 5.62 (q, *J* = 7.1 Hz, 1H), 2.58 (s, 3H), 1.95 (d, *J* = 7.1 Hz, 3H). **^{13}C NMR** (101 MHz, $CDCl_3$): δ 194.0, 151.5, 146.4, 132.7, 129.8, 126.9, 118.4, 112.1, 107.0, 61.4, 26.5, 21.3. **FT-IR**: ν (cm^{-1}) 3119, 2988, 2938, 2230, 1680, 1608, 1506, 1474, 1416, 1360, 1252, 1215, 1124, 1045. **HRMS (EI)**: Exact mass calculated for $C_{14}H_{13}N_3O$ $[M]^+$: 239.1059, found 239.1056.

(*S*)-4-(1-(1*H*-Indol-1-yl)ethyl)benzonitrile (12h)

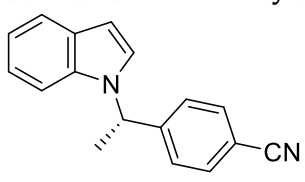

Prepared according to the general procedure using 4-bromobenzonitrile (36.4 mg, 0.2 mmol) and 2-(1*H*-indol-1-yl)propanoic acid (56.7 mg, 0.3 mmol, 1.5 equiv.), along with

L1 as ligand (6.1 mg, 0.03 mmol, 15 mol%) with reaction time of 15 h. The crude material was purified by flash column chromatography (eluent gradient: from pure heptane to heptane:EtOAc 9:1) to give the corresponding product as a yellow waxy solid (37.7 mg, 77% yield). The enantiomeric ratio was determined by SFC analysis on a YMC CHIRAL ART Amylose-SA column (CO_2:MeOH 99:1 for 2 min, then gradient ramp to 95:5 over 16 min, ramp to 99:1 over 0.5 min, 99:1 for 1 min; flow rate 2 mL/min; λ = 225 nm); τ_{major} = 13.61 min, τ_{minor} = 15.12 min; e.r. 71:29. $[\alpha]_D^{20}$ = -34.6° (*c* 2.9, $CHCl_3$). **^{1}H NMR** (400 MHz, $CDCl_3$): δ 7.67-7.64 (m, 1H), 7.57 (d, *J* = 8.4 Hz, 2H), 7.31 (d, *J* = 3.3 Hz, 1H), 7.16 (d, *J* = 8.4 Hz, 2H), 7.14-7.08 (m, 3H), 6.62 (d, *J* = 3.3 Hz, 1H), 5.70 (q, *J* = 7.1 Hz, 1H), 1.95 (d, *J* = 7.1 Hz, 3H). **^{13}C NMR** (101 MHz, $CDCl_3$): δ 148.3, 135.9, 132.6, 128.8, 126.5, 124.4, 121.8, 121.1, 120.0, 118.5, 111.4, 109.7, 102.2, 54.5, 21.6. **FT-IR**: ν (cm^{-1}) 3051, 2980, 2936, 2878, 2228, 1699, 1608, 1508, 1458, 1410, 1310, 1229, 1190, 1088, 1016. **HRMS (EI)**: Exact mass calculated for $C_{17}H_{14}N_2$ $[M]^+$: 246.1157, found 246.1158.

(*S*)-4-(1-(1*H*-Pyrrolo[2,3-*b*]pyridin-1-yl)ethyl)benzonitrile (12i)

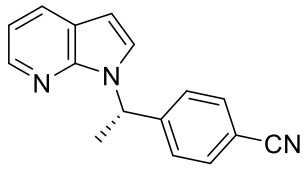

Prepared according to the general procedure using 4-bromobenzonitrile (36.4 mg, 0.2 mmol) and 2-(1*H*-pyrrolo[2,3-*b*]pyridin-1-yl)propanoic acid (57.1 mg, 0.3 mmol, 1.5 equiv.), with reaction time of 40 h. The crude material was purified by flash column chromatography (first column with eluent gradient: from pure CH_2Cl_2 to CH_2Cl_2:acetone 100:2; second column with eluent gradient: from pure heptane to heptane:EtOAc 8:2) to give the corresponding product as a colorless waxy solid (32.2 mg, 65% yield). The enantiomeric ratio was determined by SFC analysis on a YMC CHIRAL ART Amylose-SA column (CO_2:MeOH 99:1 for 2 min, then gradient ramp to 95:5 over 16 min, ramp to 99:1 over 0.5 min, 99:1 for 1 min; flow rate 2 mL/min; λ = 225 nm); τ_{major} = 14.88 min, τ_{minor} = 12.89 min; e.r. 83:17. $[\alpha]_D^{20}$ = -144.2° (*c* 2.5, $CHCl_3$). **^{1}H NMR** (400 MHz, $CDCl_3$): δ 8.30 (dd, *J* = 4.7, 1.5 Hz, 1H), 7.93 (dd, *J* = 7.8, 1.5 Hz, 1H), 7.57 (d, *J* = 8.5 Hz, 2H), 7.30-7.27 (m, 3H), 7.09 (dd, *J* = 7.8, 4.7 Hz, 1H), 6.55 (d, *J* = 3.6 Hz, 1H), 6.33 (q, *J* = 7.2 Hz, 1H), 1.93 (d, *J* = 7.2 Hz, 3H). **^{13}C NMR** (101 MHz, $CDCl_3$): δ 148.0, 147.4, 143.1, 132.5, 129.0, 126.9, 124.5, 120.6, 118.6, 116.3, 111.3, 100.7, 51.7, 20.7. **FT-IR**: ν (cm^{-1}) 3049, 2980, 2936, 2880, 2228, 1923, 1609, 1593, 1570, 1504,

1570, 1504, 1479, 1425, 1346, 1302, 1273, 1192, 1115, 1090, 1053, 1016. **HRMS (ESI)**: Exact mass calculated for $C_{16}H_{14}N_3$ [M+H]$^+$: 248.1188, found 248.1189.

(*S*)-4-(1-(1,3-Dimethyl-2,6-dioxo-1,2,3,6-tetrahydro-7*H*-purin-7-yl)ethyl)benzonitrile (12j)

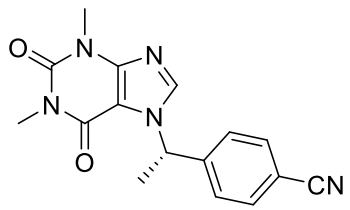

Prepared according to the general procedure using 4-bromobenzonitrile (36.4 mg, 0.2 mmol) and 2-(1,3-dimethyl-2,6-dioxo-1,2,3,6-tetrahydro-7*H*-purin-7-yl)propanoic acid (75.7 mg, 0.3 mmol, 1.5 equiv.), with reaction time of 64 h. The crude material was purified by flash column chromatography (first column with eluent gradient: from heptane:EtOAc 5:5 to 2:8; second column with eluent gradient: from pure CH_2Cl_2 to CH_2Cl_2:MeOH 100:2) to give the corresponding product as a light yellow solid (16.7 mg, 27% yield). The enantiomeric ratio was determined by SFC analysis on a Lux i-Amylose-3 column (CO_2:MeOH 99:1 for 2 min, then gradient ramp to 78:22 over 3 min, 78:22 for 22 min, ramp to 99:1 over 1.5 min, 99:1 for 1 min; flow rate 2 mL/min; λ = 225 nm); τ_{major} = 23.31 min, τ_{minor} = 19.98 min; e.r. 77:23. $[\alpha]_D^{20}$ = -21.2° (*c* 1.2, $CHCl_3$). **m.p.** 187-189 °C. **^{1}H NMR** (400 MHz, $CDCl_3$): δ 7.75 (s, 1H), 7.66 (d, *J* = 8.4 Hz, 2H), 7.37 (d, *J* = 8.4 Hz, 2H), 6.22 (q, *J* = 7.2 Hz, 1H), 3.60 (s, 3H), 3.35 (s, 3H), 1.95 (d, *J* = 7.2 Hz, 3H). **^{13}C NMR** (101 MHz, $CDCl_3$): δ 155.0, 151.5, 149.2, 145.5, 138.4, 132.9, 127.0, 118.2, 112.4, 106.8, 55.9, 29.8, 28.1, 21.1. **FT-IR**: ν (cm^{-1}) 3119, 3057, 2986, 2951, 2228, 1699, 1651, 1607, 1541, 1506, 1472, 1450, 1410, 1331, 1298, 1273, 1233, 1200, 1018. **HRMS (ESI)**: Exact mass calculated for $C_{16}H_{16}N_5O_2$ [M+H]$^+$: 310.1304, found 310.1311.

(*S*)-4-(1-(9*H*-Carbazol-9-yl)ethyl)benzonitrile (12k)

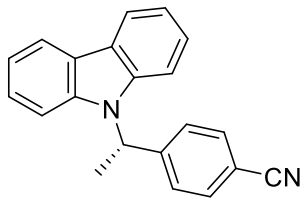

Prepared according to the general procedure using 4-bromobenzonitrile (36.4 mg, 0.2 mmol) and 2-(9*H*-carbazol-9-yl)propanoic acid (71.8 mg, 0.3 mmol, 1.5 equiv.), with reaction time of 15 h. The crude material was purified by flash column chromatography (eluent gradient: from pure heptane to heptane:EtOAc 92.5:7.5) to give the corresponding product as a white waxy solid (40.4 mg, 68% yield). The enantiomeric ratio was determined by SFC analysis on a Lux i-Amylose-3 column

(CO_2:MeOH: 99:1 for 2 min, then gradient ramp to 82:18 over 16 min, ramp to 99:1 over 0.5 min, 99:1 for 1 min; flow rate 2 mL/min; λ = 225 nm); τ_{major} = 12.97 min, τ_{minor} = 14.10 min; e.r. 57:43. **^{1}H NMR** (400 MHz, $CDCl_3$): δ 8.13 (d, *J* = 7.7 Hz, 2H), 7.60 (d, *J* = 8.4 Hz, 2H), 7.40-7.34 (m, 4H), 7.27-7.22 (m, 2H), 7.17 (d, *J* = 8.4 Hz, 2H), 6.07 (q, *J* = 7.2 Hz, 1H), 2.03 (d, *J* = 7.2 Hz, 3H). **^{13}C NMR** (101 MHz, $CDCl_3$): δ 146.3, 139.4, 132.5, 127.2, 125.7, 123.6, 120.5, 119.4, 118.6, 111.4, 109.8, 52.1, 17.4. **FT-IR**: ν (cm^{-1}) 3049, 2982, 2938, 2878, 2814, 2228, 1923, 1894, 1859, 1773, 1607, 1595, 1504, 1481, 1450, 1408, 1327, 1265, 1223, 1155, 1134, 1121, 1084, 1015, 1003. **HRMS (ESI)**: Exact mass calculated for $C_{21}H_{16}N_2Na$ $[M+Na]^+$: 319.1211, found 319.1210.

(*S*)-4-(1-(1*H*-Pyrrol-1-yl)pentyl)benzonitrile (12n)

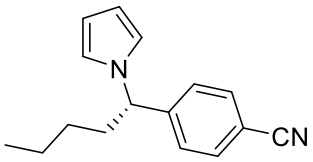

Prepared according to the general procedure using 4-bromobenzonitrile (36.4 mg, 0.2 mmol) and 2-(1*H*-pyrrol-1-yl)hexanoic acid (54.4 mg, 0.3 mmol, 1.5 equiv.), with reaction time of 15 h. The crude material was purified by flash column chromatography (eluent gradient: from pure heptane to heptane:EtOAc 95:5) to give the corresponding product as a light yellow oil (47.6 mg, 81% yield). The enantiomeric ratio was determined by SFC analysis on a YMC CHIRAL ART Cellulose-C column (CO_2:acetonitrile 99:1 for 2 min, then gradient ramp to 95:5 over 6 min, ramp to 99:1 over 0.5 min, 99:1 for 1 min; flow rate 2 mL/min; λ = 225 nm); τ_{major} = 7.05 min, τ_{minor} = 7.36 min; e.r. 77:23. $[\alpha]_D^{20}$ = +8.9° (*c* 3.0, $CHCl_3$). **^{1}H NMR** (400 MHz, $CDCl_3$): δ 7.59 (d, *J* = 8.5 Hz, 2H), 7.20 (d, *J* = 8.5 Hz, 2H), 6.73 (t, *J* = 2.1 Hz, 2H), 6.21 (t, *J* = 2.1 Hz, 2H), 5.06 (dd, *J* = 9.3, 6.1 Hz, 1H), 2.26-2.04 (m, 2H), 1.44-1.24 (m, 4H), 0.90 (t, *J* = 7.1 Hz, 3H). **^{13}C NMR** (101 MHz, $CDCl_3$): δ 148.0, 132.5, 126.9, 119.5, 118.6, 111.3, 108.7, 63.0, 35.1, 28.6, 22.4, 13.9. **FT-IR**: ν (cm^{-1}) 3100, 2955, 2930, 2862, 2228, 1609, 1504, 1487, 1466, 1414, 1323, 1271, 1088, 1067, 1018. **HRMS (ESI)**: Exact mass calculated for $C_{16}H_{19}N_2$ $[M+H]^+$: 239.1548, found 239.1554.

(S)-4-(2-Phenyl-1-(1*H*-pyrrol-1-yl)ethyl)benzonitrile (12o)

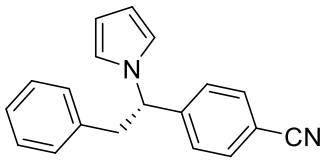

Prepared according to the general procedure using 4-bromobenzonitrile (36.4 mg, 0.2 mmol) and 3-phenyl-2-(1*H*-pyrrol-1-yl)propanoic acid (64.6 mg, 0.3 mmol,

1.5 equiv.), with reaction time of 15 h. The crude material was purified by flash column chromatography (eluent gradient: from pure heptane to heptane:EtOAc 95:5) to give the corresponding product as a pale waxy solid (47.5 mg, 87% yield). The enantiomeric ratio was determined by SFC analysis on a YMC CHIRAL ART Amylose-SA column (CO_2:MeOH 99:1 for 2 min, then gradient ramp to 95:5 over 16 min, ramp to 99:1 over 0.5 min, 99:1 for 1 min; flow rate 2 mL/min; λ = 225 nm); τ_{major} = 14.84 min, τ_{minor} = 13.71 min; e.r. 71:29. $[\alpha]_D^{20}$ = +44.3° (*c* 3.8, $CHCl_3$). **^{1}H NMR** (400 MHz, $CDCl_3$): δ 7.55 (d, *J* = 8.3 Hz, 2H), 7.26-7.18 (m, 3H), 7.14 (d, *J* = 8.3 Hz, 2H), 7.00-6.96 (m, 2H), 6.73 (t, *J* = 2.1 Hz, 2H), 6.19 (t, *J* = 2.1 Hz, 2H), 5.32 (t, *J* = 7.7 Hz, 1H), 3.58 (dd, *J* = 13.7, 7.7 Hz, 1H), 3.36 (dd, *J* = 13.7, 7.7 Hz, 1H). **^{13}C NMR** (101 MHz, $CDCl_3$): δ 146.8, 136.8, 132.4, 128.9, 128.6, 127.2, 127.0, 119.7, 118.6, 111.6, 108.9, 64.5, 41.8. **FT-IR**: ν (cm^{-1}) 3100, 3063, 3028, 2924, 2862, 2228, 1674, 1607, 1551, 1487, 1454, 1414, 1265, 1090, 1069, 1018. **HRMS (ESI)**: Exact mass calculated for $C_{19}H_{17}N_2$ $[M+H]^+$: 273.1392, found 273.1398.

(S)-4-(2-Methyl-1-(1*H*-pyrrol-1-yl)propyl)benzonitrile (12p)

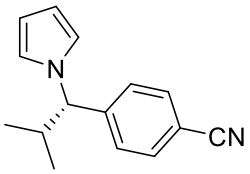

Prepared according to the general procedure using 4-bromobenzonitrile (36.4 mg, 0.2 mmol) and 3-methyl-2-(1*H*-pyrrol-1-yl)butanoic acid (50.2 mg, 0.3 mmol, 1.5 equiv.), with reaction time of 15 h. The crude material was purified by flash column chromatography (eluent gradient: from pure heptane to heptane:EtOAc 95:5) to give the corresponding product as a cream solid (28.1 mg, 63% yield). The enantiomeric ratio was determined by SFC analysis on a YMC CHIRAL ART Amylose-SA column (CO_2:MeOH 99:1 for 2 min, then gradient ramp to 95:5 over 6 min, ramp to 99:1 over 0.5 min, 99:1 for 1 min; flow rate 2 mL/min; λ = 225 nm); τ_{major} = 6.85 min, τ_{minor} = 7.27 min; e.r. 55:45. **m.p.** 78-79 °C. **^{1}H NMR** (400 MHz, $CDCl_3$): δ 7.61 (d, *J* = 8.4 Hz, 2H), 7.40 (d, *J* = 8.4 Hz, 2H), 6.75 (t, *J* = 2.1 Hz, 2H), 6.15 (t, *J* = 2.1 Hz, 2H), 4.54 (d, *J* = 10.4 Hz, 1H), 2.62-2.49 (m, 1H), 0.96 (d, *J* = 6.6 Hz, 3H), 0.85 (d, *J* = 6.6 Hz, 3H). **^{13}C NMR** (101 MHz, $CDCl_3$): δ 146.1, 132.5, 127.9, 119.4, 118.5, 111.6, 108.6, 70.7, 32.4, 20.4, 20.0. **FT-IR**: ν (cm^{-1}) 3132, 3105, 3053, 2974, 2926, 2872, 2226, 1608, 1548, 1504, 1487, 1467, 1420, 1385, 1368, 1269, 1180, 1132, 1086, 1070, 1020. **HRMS (ESI)**: Exact mass calculated for $C_{15}H_{17}N_2$ $[M+H]^+$: 225.1392, found 225.1399.

Methyl (*S*)-4-(4-cyanophenyl)-4-(1*H*-pyrrol-1-yl)butanoate (12q)

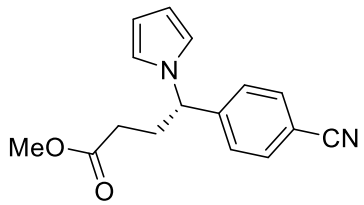

Prepared according to the general procedure using 4-bromobenzonitrile (36.4 mg, 0.2 mmol) and (*S*)-5-methoxy-5-oxo-2-(1*H*-pyrrol-1-yl)pentanoic acid (63.4 mg, 0.3 mmol, 1.5 equiv.), with reaction time of 40 h. The crude material was purified by flash column chromatography (pure CH_2Cl_2 as eluent) to give the corresponding product as a colourless waxy solid (46.4 mg, 86% yield). The enantiomeric ratio was determined by SFC analysis on a YMC CHIRAL ART Amylose-SA column (CO_2:MeOH 99:1 for 2 min, then gradient ramp to 95:5 over 16 min, ramp to 99:1 over 0.5 min, 99:1 for 1 min; flow rate 2 mL/min; λ = 225 nm); τ_{major} = 13.29 min, τ_{minor} = 12.25 min; e.r. 79:21. $[\alpha]_D^{20}$ = +8.4 (*c* 3.6, $CHCl_3$). **^{1}H NMR** (400 MHz, $CDCl_3$): δ 7.60 (d, *J* = 8.4 Hz, 2H), 7.22 (d, *J* = 8.4 Hz, 2H), 6.71 (t, *J* = 2.1 Hz, 2H), 6.22 (t, *J* = 2.1 Hz, 2H), 5.22 (dd, *J* = 9.9, 5.7 Hz, 1H), 3.68 (s, 3H), 2.55-2.26 (m, 4H). **^{13}C NMR** (101 MHz, $CDCl_3$): δ 173.0, 147.0, 132.6, 126.8, 119.5, 118.5, 111.6, 109.2, 61.6, 51.8, 30.4, 30.3. **FT-IR**: ν (cm^{-1}) 3127, 3100, 2951, 2924, 2849, 2228, 1730, 1608, 1504, 1487, 1437, 1416, 1369, 1312, 1198, 1090, 1018. **HRMS (ESI)**: Exact mass calculated for $C_{16}H_{16}N_2O_2Na$ $[M+Na]^+$: 291.1109, found 291.1110.

(*S*)-4-(1-(1*H*-Pyrrolo[2,3-*b*]pyridin-1-yl)pentyl)benzonitrile (12r)

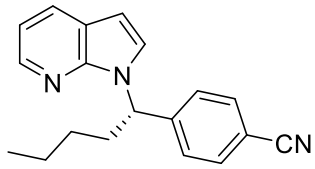

Prepared according to the general procedure using 4-bromobenzonitrile (36.4 mg, 0.2 mmol) and 2-(1*H*-pyrrolo[2,3-*b*]pyridin-1-yl)hexanoic acid (69.7 mg, 0.3 mmol, 1.5 equiv.), with reaction time of 64 h. The crude material was purified by flash column chromatography (eluent gradient: from pure heptane to heptane:EtOAc 9:1) to give the corresponding product as a yellow sticky solid (35.6 mg, 62% yield). The enantiomeric ratio was determined by SFC analysis on a YMC CHIRAL ART Amylose-SA column (CO_2:MeOH 99:1 for 2 min, then gradient ramp to 95:5 over 16 min, ramp to 99:1 over 0.5 min, 99:1 for 1 min; flow rate 2 mL/min; λ = 225 nm); τ_{major} = 13.32 min, τ_{minor} = 12.36 min; e.r. 82:18. $[\alpha]_D^{20}$ = -58.5° (*c* 1.6, $CHCl_3$). **^{1}H NMR** (400 MHz, $CDCl_3$): δ 8.30 (dd, *J* = 4.7, 1.5 Hz, 1H), 7.92 (dd, *J* = 7.8, 1.5 Hz, 1H), 7.57 (d, *J* = 8.5 Hz, 2H), 7.37 (d, *J* = 8.5 Hz, 2H), 7.32 (d, *J* = 3.6 Hz, 1H), 7.07 (dd, *J* = 7.8, 4.7 Hz, 1H), 6.55 (d, *J* = 3.6 Hz, 1H), 6.14 (dd, *J* = 9.5, 6.5 Hz, 1H), 2.36-2.22 (m, 2H), 1.44-1.19 (m, 4H), 0.86 (t, *J* = 7.1 Hz,

3H). **^{13}C NMR** (101 MHz, $CDCl_3$): δ 147.8, 147.3, 143.1, 132.4, 128.9, 127.4, 124.5, 120.5, 118.6, 116.2, 111.2, 100.8, 56.5, 34.4, 28.5, 22.3, 13.8. **FT-IR**: ν (cm^{-1}) 3049, 2954, 2930, 2228, 1608, 1593, 1570, 1506, 1481, 1425, 1346, 1310, 1271, 1115, 1020. **HRMS (ESI)**: Exact mass calculated for $C_{19}H_{20}N_3$ $[M+H]^+$: 290.1657, found 290.1655.

(*S*)-1-(4-(1-(1*H*-Pyrrol-1-yl)ethyl)phenyl)ethan-1-one (12s)

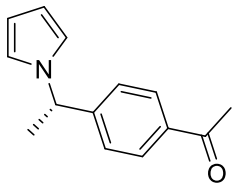

Prepared according to the general procedure using 4'-bromoacetophenone (39.8mg, 0.2 mmol) and (*S*)-2-(1*H*-pyrrol-1-yl)propanoic acid (41.7 mg, 0.3 mmol, 1.5 equiv.), with reaction time of 15 h. The crude material was purified by flash column chromatography (eluent gradient: from pure heptane to heptane:EtOAc 9:1) to give the corresponding product as a light yellow oil (37.5 mg, 88% yield). The enantiomeric ratio was determined by SFC analysis on a YMC CHIRAL ART Amylose-SA column (CO_2:MeOH 99:1 for 2 min, then gradient ramp to 95:5 over 6 min, ramp to 99:1 over 0.5 min, 99:1 for 1 min; flow rate 2 mL/min; λ = 225 nm); τ_{major} = 7.23 min, τ_{minor} = 7.63 min; e.r. 78:22. $[\alpha]_D^{20}$ = +11.2° (*c* 2.9, $CHCl_3$). **^{1}H NMR** (400 MHz, $CDCl_3$): δ 7.89 (d, *J* = 8.4 Hz, 2H), 7.14 (d, *J* = 8.4 Hz, 2H), 6.76 (t, *J* = 2.1 Hz, 2H), 6.22 (t, *J* = 2.1 Hz, 2H), 5.33 (q, *J* = 7.1 Hz, 1H), 2.57 (s, 3H), 1.85 (d, *J* = 7.1 Hz, 3H). **^{13}C NMR** (101 MHz, $CDCl_3$): δ 197.6, 148.9, 136.3, 128.8, 126.0, 119.5, 108.5, 57.9, 26.7, 21.9. **FT-IR**: ν (cm^{-1}) 3100, 2980, 2936, 2878, 1678, 1607, 1489, 1450, 1414, 1358, 1304, 1261, 1184, 1088, 1057, 1042, 1015. **HRMS (ESI)**: Exact mass calculated for $C_{14}H_{16}NO$ $[M+H]^+$: 214.1232, found 214.1237.

(*S*)-4-(1-(1*H*-Pyrrol-1-yl)ethyl)benzaldehyde (12t)

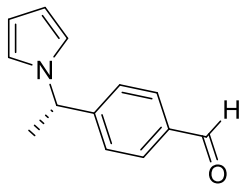

Prepared according to the general procedure using 4-bromobenzaldehyde (37.0 mg, 0.2 mmol) and (*S*)-2-(1*H*-pyrrol-1-yl)propanoic acid (41.7 mg, 0.3 mmol, 1.5 equiv.), with reaction time of 15 h. The crude material was purified by flash column chromatography (eluent gradient: from pure heptane to heptane:EtOAc 9:1) to give the corresponding product as a light yellow oil (32.4 mg, 81% yield). The enantiomeric ratio was determined by SFC analysis on a YMC CHIRAL ART Amylose-SA column (CO_2:MeOH 99:1 for 2 min, then gradient ramp to 95:5 over 6 min, ramp to 99:1 over 0.5 min, 99:1 for 1 min; flow rate 2 mL/min; λ = 225 nm); τ_{major} = 6.34 min, τ_{minor} = 6.86 min;

e.r. 79:21. $[\alpha]_D^{20}$ = +7.0° (*c* 2.5, $CHCl_3$). **^{1}H NMR** (400 MHz, $CDCl_3$): δ 9.98 (s, 1H), 7.82 (d, *J* = 8.3 Hz, 2H), 7.20 (d, *J* = 8.3 Hz, 2H), 6.76 (t, *J* = 2.1 Hz, 2H), 6.23 (t, *J* = 2.1 Hz, 2H), 5.36 (q, *J* = 7.1 Hz, 1H), 1.87 (d, *J* = 7.1 Hz, 3H). **^{13}C NMR** (101 MHz, $CDCl_3$): δ 191.7, 150.5, 135.6, 130.2, 126.3, 119.5, 108.6, 57.9, 21.9. **FT-IR**: ν (cm^{-1}) 3098, 2980, 2936, 2830, 2737, 1701, 1607, 1576, 1489, 1450, 1423, 1304, 1277, 1209, 1169, 1088, 1057, 1042, 1015. **HRMS (EI)**: Exact mass calculated for $C_{13}H_{13}NO$ $[M]^+$: 199.0997, found 199.1000.

(*S*)-2-(4-(1-(1*H*-Pyrrol-1-yl)ethyl)phenyl)benzo[*d*]thiazole (12u)

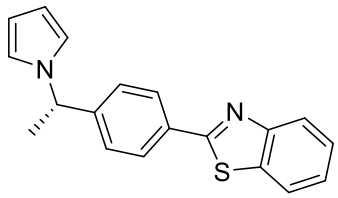

Prepared according to the general procedure using 2-(4-bromophenyl)benzo[*d*]thiazole (58.0 mg, 0.2 mmol) and (*S*)-2-(1*H*-pyrrol-1-yl)propanoic acid (41.7 mg, 0.3 mmol, 1.5 equiv.), with reaction time of 15 h. The crude material was purified by flash column chromatography (eluent gradient: from pure heptane to heptane:EtOAc 100:5) to give the corresponding product as a white solid (50.1 mg, 82% yield). The enantiomeric ratio was determined by SFC analysis on a YMC CHIRAL ART Amylose-SA column (CO_2:MeOH 99:1 for 2 min, then gradient ramp to 80:20 over 3 min, 80:20 for 22 min, ramp to 99:1 over 1.5 min, 99:1 for 1.5 min; flow rate 2 mL/min; λ = 225 nm); τ_{major} = 15.26 min, τ_{minor} = 20.58 min; e.r. 77:23. $[\alpha]_D^{20}$ = +0.9° (*c* 4.0, $CHCl_3$). **m.p.** 144-146 °C. **^{1}H NMR** (400 MHz, $CDCl_3$): δ 8.07 (d, *J* = 8.0 Hz, 1H), 8.03 (d, *J* = 8.4 Hz, 2H), 7.90 (d, *J* = 8.0 Hz, 1H), 7.52-7.47 (m, 1H), 7.41-7.37 (m, 1H), 7.19 (d, *J* = 8.4 Hz, 2H), 6.79 (t, *J* = 2.1 Hz, 2H), 6.23 (t, *J* = 2.1 Hz, 2H), 5.35 (q, *J* = 7.1 Hz, 1H), 1.88 (d, *J* = 7.1 Hz, 3H). **^{13}C NMR** (101 MHz, $CDCl_3$): δ 167.5, 154.1, 146.6, 135.0, 132.8, 127.9, 126.5, 126.4, 125.2, 123.2, 121.6, 119.5, 108.4, 57.9, 22.0. **FT-IR**: ν (cm^{-1}) 3117, 3088, 3059, 2998, 1666, 1605, 1557, 1508, 1479, 454, 1435, 1420, 1400, 1381, 1281, 1250, 1231, 1119, 1103, 1084, 1057, 1049, 1016, 1084. **HRMS (ESI)**: Exact mass calculated for $C_{19}H_{17}N_2S$ $[M+H]^+$: 305.1112, found 305.1115.

(*S*)-2-(4-(1-(1*H*-Pyrrol-1-yl)ethyl)phenyl)-1,3,4-oxadiazole (12v)

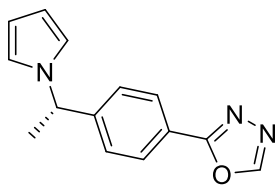

Prepared according to the general procedure using 2-(4-bromophenyl)-1,3,4-oxadiazole (45.0 mg, 0.2 mmol) and (*S*)-2-(1*H*-pyrrol-1-yl)propanoic acid (41.7 mg, 0.3 mmol, 1.5 equiv.), with reaction time of 15 h. The crude material was

purified by flash column chromatography (eluent gradient: from pure heptane to heptane:EtOAc 7:3) to give the corresponding product as a light yellow waxy solid (35.8 mg, 75% yield). The enantiomeric ratio was determined by SFC analysis on a YMC CHIRAL ART Amylose-SA column (CO_2:EtOH 99:1 for 2 min, then gradient ramp to 85:15 over 16 min, ramp to 99:1 over 0.5 min, 99:1 for 1 min; flow rate 2 mL/min; λ = 225 nm); τ_{major} = 14.93 min, τ_{minor} = 15.44 min; e.r. 76:24. $[\alpha]_D^{20}$ = +16.4° (*c* 2.6, $CHCl_3$). **^{1}H NMR** (400 MHz, $CDCl_3$): δ 8.45 (s, 1H), 8.02 (d, *J* = 8.4 z, 2H), 7.21 (d, *J* = 8.4 Hz, 2H), 6.77 (t, *J* = 2.1 Hz, 2H), 6.23 (t, *J* = 2.1 Hz, 2H), 5.36 (q, *J* = 7.1 Hz, 1H), 1.87 (d, *J* = 7.1 Hz, 3H). **^{13}C NMR** (101 MHz, $CDCl_3$): δ 164.4, 152.6, 147.9, 127.5, 126.5, 122.6, 119.5, 108.5, 57.8, 21.9. **FT-IR**: ν (cm^{-1}) 3120, 2980, 2936, 2880, 1683, 1618, 1585, 1557, 1514, 1491, 1450, 1420, 1302, 1277, 1088, 1067, 1016. **HRMS (ESI)**: Exact mass calculated for $C_{14}H_{14}N_3O$ $[M+H]^+$: 240.1137, found 240.1146.

(*S*)-2-(1-(1*H*-Pyrrol-1-yl)ethyl)benzonitrile (12w)

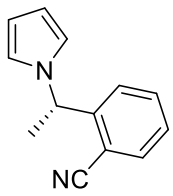

Prepared according to the general procedure using 2-bromobenzonitrile (36.4 mg, 0.2 mmol) and (*S*)-2-(1*H*-pyrrol-1-yl)propanoic acid (41.7 mg, 0.3 mmol, 1.5 equiv.), with reaction time of 15 h. The crude material was purified by flash column chromatography (eluent gradient: from pure heptane to heptane: CH_2Cl_2 6:4) to give the corresponding product as a light yellow oil (9.0 mg, 23% yield). The enantiomeric ratio was determined by SFC analysis on a Lux Cellulose-4 column (CO_2:acetonitrile 99:1 for 20 min; flow rate 2 mL/min; λ = 225 nm); τ_{major} = 16.17 min, τ_{minor} = 14.30 min; e.r. 78:22. $[\alpha]_D^{20}$ = +29.4° (*c* 0.7, $CHCl_3$). **^{1}H NMR** (400 MHz, $CDCl_3$): δ 7.66 (dd, *J* = 7.8, 1.2 Hz, 1H), 7.51 (td, *J* = 7.8, 1.2 Hz, 1H), 7.35 (td, *J* = 7.8, 1.2 Hz, 1H), 6.97 (d, *J* = 7.8 Hz, 1H), 6.81 (t, *J* = 2.1 Hz, 2H), 6.23 (t, *J* = 2.1 Hz, 2H), 5.70 (q, *J* = 7.1 Hz, 1H), 1.90 (d, *J* = 7.1 Hz, 3H). **^{13}C NMR** (101 MHz, $CDCl_3$): δ 147.6, 133.6, 132.9, 128.0, 125.8, 119.6, 117.3, 110.2, 108.7, 56.2, 21.4. **FT-IR**: 3134, 3100, 3065, 2984, 2934, 2851, 2224, 1599, 1489, 1449, 1300, 1277, 1099, 1057. **HRMS (ESI)**: Exact mass calculated for $C_{13}H_{13}N_2$ $[M+H]^+$: 197.1079, found 196.1084.

(*S*)-1-(1-(3,5-Bis(trifluoromethyl)phenyl)ethyl)-1*H*-pyrrole (12x)

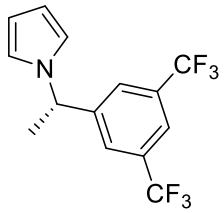

Prepared according to the general procedure using 1-bromo-3,5-bis(trifluoromethyl)benzene (35 μL, 0.2 mmol) and (*S*)-2-(1*H*-pyrrol-1-yl)propanoic acid (41.7 mg, 0.3 mmol, 1.5 equiv.), with reaction time of 15 h. The crude material was purified by flash column chromatography (eluent gradient: from pure pentane to pentane:Et_2O 100:1.5) to give the corresponding product as a colorless liquid (40.8 mg, 66% yield). The enantiomeric ratio was determined by SFC analysis on a YMC CHIRAL ART Cellulose-C column (CO_2:MeOH 99.7:0.3 for 2 min, then gradient ramp to 99:1 over 6 min, ramp to 99.7:0.3 over 0.5 min, 99.7:0.3 for 1 min; flow rate 2 mL/min; λ = 225 nm); τ_{major} = 1.66 min, τ_{minor} = 1.78 min; e.r. 64:36. $[\alpha]_D^{20}$ = +0.5° (*c* 2.3, $CHCl_3$). **^{1}H NMR** (400 MHz, $CDCl_3$): δ 7.77 (s, 1H), 7.45 (s, 2H), 6.75 (t, *J* = 2.1 Hz, 2H), 6.25 (t, *J* = 2.1 Hz, 2H), 5.39 (q, *J* = 7.1 Hz, 1H), 1.89 (d, *J* = 7.1 Hz, 3H). **^{19}F NMR** (376 MHz, $CDCl_3$): δ -62.9 (s). **^{13}C NMR** (101 MHz, $CDCl_3$): δ 146.4, 132.1 (q, J_{CF} = 33.4 Hz), 125.9, 123.1 (q, J_{CF} = 272.5 Hz), 121.7-121.5 (m), 119.3, 109.2, 57.4, 21.9. **FT-IR**: ν (cm^{-1}) 2918.3, 1506, 1489, 1375, 1279, 1132. **HRMS (EI)**: Exact mass calculated for $C_{14}H_{11}NF_6$ $[M]^+$: 307.0796, found 307.0791.

2-(1-(1*H*-Pyrrol-1-yl)ethyl)pyridine (12y)

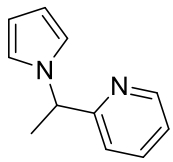

Prepared according to the general procedure using 2-bromopyridine (19 μL, 0.2 mmol) and (*S*)-2-(1*H*-pyrrol-1-yl)propanoic acid (41.7 mg, 0.3 mmol, 1.5 equiv.), with reaction time of 15 h. The crude material was purified by flash column chromatography (eluent gradient: from pure CH_2Cl_2 to CH_2Cl_2:acetone 100:2) to give the corresponding product as a colorless liquid (16.2 mg, 47% yield). The enantiomeric ratio was determined by SFC analysis on a YMC CHIRAL ART Amylose-SA column (CO_2:MeOH 99:1 for 2 min, then gradient ramp to 95:5 over 6 min, ramp to 99:1 over 0.5 min, 99:1 for 1 min; flow rate 2 mL/min; λ = 225 nm); τ_{major} = 3.27 min, τ_{minor} = 3.87 min; e.r. 59:41. **^{1}H NMR** (400 MHz, $CDCl_3$): δ 8.56 (ddd, *J* = 4.9, 1.8, 1.0 Hz, 1H), 7.58 (td, *J* = 7.8, 1.8 Hz, 1H), 7.15 (ddd, *J* = 7.8, 4.9, 1.0 Hz, 1H), 6.82 (t, *J* = 2.1 Hz, 2H), 6.72 (d, *J* = 7.8 Hz, 1H), 6.22 (t, *J* = 2.1 Hz, 2H), 5.37 (q, *J* = 7.1 Hz, 1H), 1.90 (d, *J* = 7.1 Hz, 3H). **^{13}C NMR** (101 MHz, $CDCl_3$): δ 162.5, 149.0, 137.1, 122.3, 120.0, 119.6, 108.4, 60.0, 20.6. **FT-IR**: ν (cm^{-1}) 3100, 3050, 2980, 2938, 2874, 1587, 1572,

1489, 1474, 1435, 1404, 1371, 1302, 1277, 1248, 1150, 1090, 1059, 1043. **HRMS (ESI)**: Exact mass calculated for $C_{11}H_{13}N_2$ $[M+H]^+$: 173.1079, found 173.1083.

(*S*)-1-(1-Phenylethyl)-1*H*-pyrrole (12z)

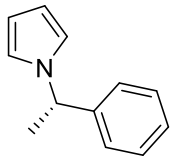

Prepared according to the general procedure using bromobenzene (21 μL, 0.2 mmol) and (*S*)-2-(1*H*-pyrrol-1-yl)propanoic acid (41.7 mg, 0.3 mmol, 1.5 equiv.), with reaction time of 64 h. The crude material was purified by flash column chromatography (eluent gradient: from pentane to pentane:Et_2O 100:7) to give the corresponding product as a colorless oil (3.3 mg, 10% yield). The enantiomeric ratio was determined by SFC analysis on a YMC CHIRAL ART Amylose-SA column (CO_2:MeOH 99:1 for 2 min, then gradient ramp to 95:5 over 6 min, ramp to 99:1 over 0.5 min, 99:1 for 1 min; flow rate 2 mL/min; λ = 225 nm); τ_{major} = 2.05 min, τ_{minor} = 2.32 min; e.r. 70:30. $[\alpha]_D^{20}$ = +9° (*c* 0.2, EtOH). Enantiopure **(*S*)-12z** was prepared from (*S*)-α-methylbenzylamine using a known procedure.[242] This yielded a single peak at 2.07 min on SFC analysis using the above method, and $[\alpha]_D^{20}$= +6.3° (*c* 1.0, $CHCl_3$), +10.0° (c 1.2, EtOH) [Lit.[243] $[\alpha]_D^{20}$ = + 6.8 (*c* 2.7, $CHCl_3$), Lit.[244] $[\alpha]_D^{25}$ = + 46.0 (*c* 0.9, EtOH)], confirming the major enantiomer to have *S* configuration. **^{1}H NMR** (400 MHz, $CDCl_3$): δ 7.33-7.28 (m, 2H), 7.27-7.23 (m, 1H), 7.11-7.07 (m, 2H), 6.76 (t, *J* = 2.1 Hz, 2H), 6.19 (t, *J* = 2.1 Hz, 2H), 5.29 (q, *J* = 7.1 Hz, 1H), 1.84 (d, *J* = 7.1 Hz, 3H). **^{13}C NMR** (101 MHz, $CDCl_3$): δ 143.6, 128.6, 127.4, 125.8, 119.5, 108.0, 58.1, 22.1. The spectral data are in good agreement with those previously reported.[242]

(*S*)-1-(4-(1-(2-Acetyl-1*H*-pyrrol-1-yl)ethyl)phenyl)ethan-1-one (12ab)

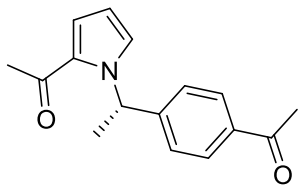

Prepared according to the general procedure using 4′-bromoacetophenone (39.8mg, 0.2 mmol) and (*S*)-2-(2-acetyl1*H*-pyrrol-1-yl)propanoic acid (54.4 mg, 0.3 mmol, 1.5 equiv.), with reaction time of 64 h. The crude material was purified by flash column chromatography (eluent gradient: from pure CH_2Cl_2 to CH_2Cl_2:acetone 100:2) to give the corresponding product as a yellow waxy solid (17.6 mg, 34% yield). The enantiomeric ratio was determined by SFC analysis on a Lux Cellulose-4 column (CO_2:acetonitrile 99:1 for 2 min, then gradient ramp to 55:15 over 18 min, 55:15 for 3 min, ramp to 99:1 over 1 min, 99:1 for 1 min; flow rate 2 mL/min;

λ = 225 nm); τ_{major} = 20.33 min, τ_{minor} = 19.77 min; e.r. 94:6. $[\alpha]_D^{20}$ = -69.2° (*c* 1.3, $CHCl_3$). **^{1}H NMR** (400 MHz, $CDCl_3$): δ 7.88 (d, *J* = 8.3 Hz, 2H), 7.16 (d, *J* = 8.3 Hz, 2H), 7.12 (dd, *J* = 2.7, 1.7 Hz, 1H), 7.04 (dd, *J* = 4.0, 1.7 Hz, 1H), 6.71 (q, *J* = 7.2 Hz, 1H), 6.24 (dd, *J* = 4.0, 2.7 Hz, 1H), 2.56 (s, 3H), 2.39 (s, 3H), 1.79 (d, *J* = 7.2 Hz, 3H). **^{13}C NMR** (101 MHz, $CDCl_3$): δ 197.6, 188.5, 148.7, 136.0, 130.5, 128.7, 126.4, 126.2, 121.0, 108.8, 55.8, 27.7, 26.6, 22.0. **FT-IR**: ν (cm^{-1}) 3115, 2980, 2924, 2878, 2851, 1682, 1649, 1609, 1574, 1524, 1458, 1408, 1358, 1335, 1267, 1236, 1204, 1094, 1015. **HRMS (ESI)**: Exact mass calculated for $C_{16}H_{18}NO_2$ $[M+H]^+$: 256.1338, found 256.1340.

6.7 PXX-photocatalysed reactions

General procedure for reaction of aryl halides with radical traps (Method A)

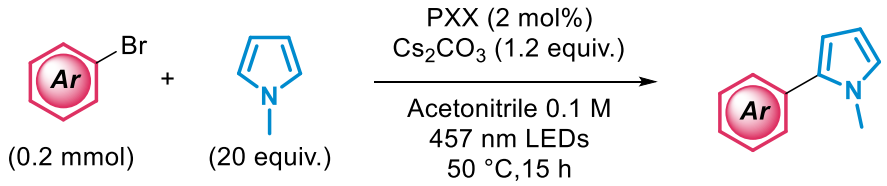

A 10 mL dried Schlenk flask was charged with aryl bromide (0.2 mmol), PXX (1.1 mg, 0.004 mmol, 2 mol%) and Cs_2CO_3 (78.2 mg, 0.24 mmol, 1.2 equiv.). The flask was put under N_2 and 2 mL of acetonitrile were added, followed by *N*-methylpyrrole (355 µL, 4 mmol, 20 equiv.). The flask was sealed, and three cycles of freeze-pump-thaw were performed before refilling with N_2. The flask was accommodated into our reactor (***LED strip* 2**) and stirred for 15 h at 50 °C with limited fan cooling under blue light irradiation. The reaction mixture was diluted with CH_2Cl_2 and filtered over celite. The solution was evaporated to dryness, and the residue purified by flash column chromatography to obtain the desired compound.

1-(4-(1-Methyl-1*H*-pyrrol-2-yl)phenyl)ethan-1-one (30b)

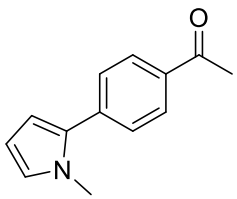

Prepared according to the general procedure (Method A) using 4'-bromoacetophenone (39.8 mg, 0.2 mmol). The crude material was purified by flash column chromatography (eluent gradient: from pure heptane to heptane:EtOAc 9:1) to give the corresponding product as a yellow oil (28.3 mg, 71% yield). **^{1}H NMR** (400 MHz, $CDCl_3$): δ 7.99 (dt, *J* = 8.5, 1.9 Hz, 2H), 7.50 (dt, *J* = 8.5, 1.9 Hz, 2H), 6.78-6.76 (m, 1H), 6.35 (dd, *J* = 1.8, 3.6 Hz,

1H), 6.23 (dd, *J* = 2.7, 3.6 Hz, 1H), 3.72 (s, 3H), 2.62 (s, 3H). **^{13}C NMR** (101 MHz, $CDCl_3$): δ 197.6, 137.9, 134.9, 133.4, 128.6, 128.0, 125.3, 110.2, 108.4, 35.4, 26.6. The spectral data are in good agreement with those previously reported.[115]

4-(1-Methyl-1*H*-pyrrol-2-yl)benzaldehyde (30c)

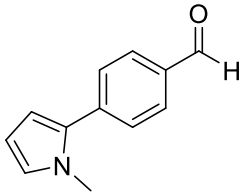

Prepared according to the general procedure (Method A) using 4-bromobenzaldehyde (37.0 mg, 0.2 mmol). The crude material was purified by flash column chromatography (eluent gradient: from pure heptane to heptane:EtOAc 9:1) to give the corresponding product as a yellow oil (27.7 mg, 75% yield). **^{1}H NMR** (400 MHz, $CDCl_3$): δ 10.02 (s, 1H), 7.90 (dt, *J* = 8.4, 1.8 Hz, 2H), 7.57 (dt, *J* = 8.4, 1.8 Hz, 2H), 6.80-6.78 (m, 1H), 6.39 (dd, *J* = 3.7, 1.8 Hz, 1H), 6.24 (dd, *J* = 3.7, 2.7 Hz, 1H), 3.75 (s, 3H). **^{13}C NMR** (101 MHz, $CDCl_3$): δ 191.8, 139.2, 134.2, 133.2, 130.0, 128.2, 125.8, 110.7, 108.5, 35.6. The spectral data are in good agreement with those previously reported.[115]

General procedure for reaction of aryl halides with radical traps (Method B)

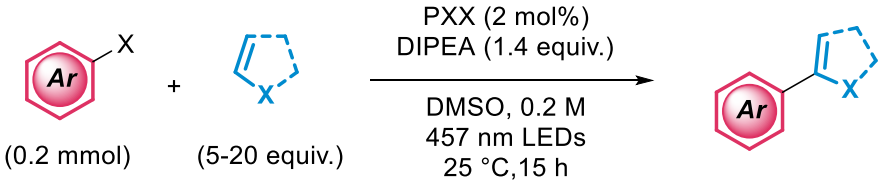

A 10 mL dried Schlenk flask was charged with aryl halide (0.2 mmol, if solid), radical trap (5-20 equiv., if solid) and PXX (1.1 mg, 0.004 mmol, 2 mol%). The flask was put under N_2 and 1 mL of DMSO was added, followed by aryl halide (0.2 mmol, if liquid), radical trap (5-20 equiv., if liquid) and DIPEA (49 μL, 0.28 mmol, 1.4 equiv.). The flask was sealed, and three cycles of freeze-pump-thaw were performed before refilling with N_2. The flask was accommodated into our reactor (***LED strip 2***) and stirred for 15 h at 25 °C with fan cooling under blue light irradiation. The reaction mixture was diluted with EtOAc and extracted with H_2O:brine 1:1 solution. The aqueous phase was extracted with EtOAc (x2), organics pooled and dried ($MgSO_4$). The solution was evaporated to dryness, and the residue purified by flash column chromatography to obtain the desired compound.

2-(1-Methyl-1*H*-pyrrol-2-yl)benzonitrile (30h)

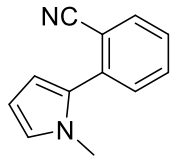

Prepared according to the general procedure (Method B) using 2-chlorobenzonitrile (27.5 mg, 0.2 mmol) and *N*-methylpyrrole (178 μL, 2 mmol, 10 equiv.). The crude material was purified by flash column chromatography (eluent gradient: from pure heptane to heptane:EtOAc 9:1) to give the corresponding product as a yellow oil (25.2 mg, 69% yield). **^{1}H NMR** (400 MHz, $CDCl_3$): δ 7.74 (ddd, *J* = 7.6, 1.4, 0.7 Hz, 1H), 7.61 (ddd, *J* = 8.0, 7.6, 1.4 Hz, 1H), 7.46-7.37 (m, 2H), 6.80 (dd, *J* = 2.7, 1.8 Hz, 1H), 6.41 (dd, *J* = 3.7, 1.8 Hz, 1H), 6.25 (dd, *J* = 3.7, 2.7 Hz, 1H), 3.62 (s, 3H). **^{13}C NMR** (101 MHz, $CDCl_3$): δ 136.9, 133.6, 132.4, 130.9, 129.9, 127.4, 124.8, 118.7, 112.8, 11.5, 108.3, 34.9. The spectral data are in good agreement with those previously reported.[115]

1-Methyl-2/3-(pentafluorophenyl)-1*H*-pyrrole (30f)

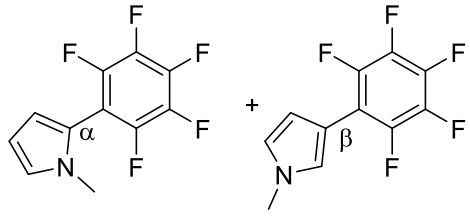

Prepared according to the general procedure (Method B) using bromopentafluorobenzene (25 μL, 0.2 mmol) and *N*-methylpyrrole (178 μL, 2 mmol, 10 equiv.). The crude material was purified by flash column chromatography (eluent pure petroleum ether) to give the corresponding product as a yellow oil (30.0 mg, 61% yield of the isomeric mixture of composition *α*:β 4:1 as determined by NMR). **Characterisation of the *α* isomer: ^{1}H NMR** (300 MHz, $CDCl_3$): δ 6.87-6.84 (m, 1H), 6.32 (dd, *J* = 3.7, 1.7 Hz, 1H), 6.28 (dd, *J* = 3.7, 2.7 Hz, 1H), 3.54 (t, *J* = 1.0 Hz, 3H). **^{19}F NMR** (101 MHz, $CDCl_3$): δ -139.5 (dd, *J* = 23.9, 8.3 Hz, 2F), -154.6 (t, *J* = 21.1 Hz, 1F), -162.11 (ddd, *J* = 23.9, 21.1, 8.3 Hz, 2F). **Characterisation of the β isomer: ^{1}H NMR** (400 MHz, $CDCl_3$): δ 7.13-7.09 (m, 1H), 6.70 (t, *J* = 2.5 Hz, 1H), 6.60-6.56 (m, 1H), 3.73 (s, 3H). **^{19}F NMR** (101 MHz, $CDCl_3$): δ -142.8 (dd, *J* = 21.6, 6.5 Hz, 2F), -161.1 (t, *J* = 21.6 Hz, 1F), -163.9 (td, *J* = 21.6, 6.5 Hz, 2F). The spectral data are in good agreement with those previously reported.[127]

2′,4′,6′-Trimethoxy-[1,1′-biphenyl]-2-carbonitrile (30k)

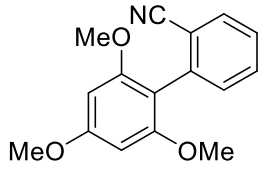

Prepared according to the general procedure (Method B) using 2-chlorobenzonitrile (27.5 mg, 0.2 mmol) and 1,3,5-trimethoxybenzene (673 mg, 4 mmol, 20 equiv.). The crude material was purified by flash column chromatography (eluent gradient: from pure petroleum ether to petroleum ether:EtOAc 85:15) to give the corresponding product as a yellow oil (31.0 mg, 58% yield). **^{1}H NMR** (400 MHz, $CDCl_3$): δ 7.70 (ddd, *J* = 7.7, 1.4, 0.7 Hz, 1H), 7.58 (td, *J* = 7.7, 1.4 Hz, 1H), 7.42-7.33 (m, 2H), 6.23 (s, 2H), 3.87 (s, 3H), 3.75 (s, 6H). **^{13}C NMR** (101 MHz, $CDCl_3$): δ 161.9, 158.3, 138.8, 132.6, 132.5, 131.9, 126.9, 119.0, 114.7, 108.5, 90.8, 55.8, 55.4. The spectral data are in good agreement with those previously reported.[115]

Diethyl (2-cyanophenyl)phosphonate (30l)

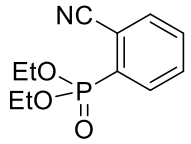

Prepared according to the general procedure (Method B) using 2-chlorobenzonitrile (27.5 mg, 0.2 mmol) and triethylphosphite (172 μL, 1 mmol, 5 equiv.). The crude material was purified by flash column chromatography (eluent gradient: from petroleum ether:EtOAc 8:2 to pure EtOAc) to give the corresponding product as a yellow oil (31.4 mg, 66% yield). **^{1}H NMR** (300 MHz, $CDCl_3$): δ 8.16-8.06 (m, 1H), 7.85-7.76 (m, 1H), 7.73-7.60 (m, 2H), 4.34-4.12 (m, 4H), 1.37 (t, *J* = 7.1 Hz, 6H). **^{31}P NMR** (162 MHz, $CDCl_3$): δ 12.6. **^{13}C NMR** (101 MHz, $CDCl_3$): δ 134.5 (d, J_{CP} = 6.8 Hz), 134.4 (d, J_{CP} = 9.4 Hz), 132.4 (d, J_{CP} = 2.6 Hz), 132.3 (d, J_{CP} = 189.0 Hz), 132.2 (d, J_{CP} = 14.0 Hz), 117.1 (d, J_{CP} = 6.0 Hz), 114.6 (d, J_{CP} = 4.8 Hz), 63.2 (d, J_{CP} = 6.0 Hz), 16.2 (d, J_{CP} = 6.3 Hz). The spectral data are in good agreement with those previously reported.[115]

Diethyl 2-(1*H*-indol-2-yl)-2-methylmalonate (32)

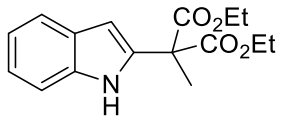

A 10 mL dried Schlenk flask was charged with indole (117.2 mg, 1 mmol, 5 equiv.) and PXX (1.1 mg, 0.004 mmol, 2 mol%). The flask was put under N_2 and 0.25 mL of acetonitrile were added, followed by diethyl 2-bromo-2-methylmalonate (38 μL, 0.2 mmol) and 2,6-lutidine (23 μL, 0.2 mmol, 1 equiv.). The flask was sealed, and three cycles of freeze-pump-thaw were performed before refilling with N_2. The flask was accommodated into our reactor

(***LED strip 2***) and stirred for 15 h at 25 °C with fan cooling under blue light irradiation. The reaction mixture was diluted with EtOAc and extracted with H_2O. The aqueous phase was extracted with EtOAc (x2), organics pooled, washed with brine and dried ($MgSO_4$). The solution was evaporated to dryness, and the residue purified by flash column chromatography (eluent gradient: from pure heptane to heptane:EtOAc 94:6) to give the corresponding product as a colorless oil that solidifies upon standing (38.0 mg, 66% yield). **m.p.** 60-61 °C. **^{1}H NMR** (400 MHz, $CDCl_3$): δ 9.09 (br, 1H), 7.58 (d, *J* = 7.9 Hz, 1H), 7.37 (d, *J* = 8.2 Hz, 1H), 7.18 (t, *J* = 7.7 Hz, 1H), 7.08 (t, *J* = 7.3 Hz, 1H), 6.48-6.46 (m, 1H), 4.24 (q, *J* = 7.1 Hz, 4H), 1.95 (s, 3H), 1.27 (t, *J* = 7.1 Hz, 6H). **^{13}C NMR** (101 MHz, $CDCl_3$): δ 170.4, 136.2, 134.8, 127.5, 122.2, 120.6, 119.8, 111.1, 101.4, 62.2, 54.4, 21.2, 14.0. The spectral data are in good agreement with those previously reported.[131]

General procedure for reaction of perfluoroalkyl (pseudo)halides with radical traps

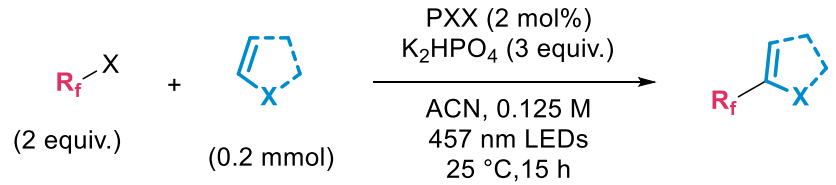

A 10 mL dried Schlenk flask was charged with K_2HPO_4 (104.5 mg, 0.6 mmol, 3 equiv.) and PXX (1.1 mg, 0.004 mmol, 2 mol%). The flask was put under N_2 and 1.6 mL of acetonitrile were added, followed by radical trap (0.2 mmol). The flask was sealed with a rubber septum, and three cycles of freeze-pump-thaw were performed before refilling with N_2. Perfluoroalkyl halide (0.4 mmol, 2 equiv.) was added with syringe *via* the septum. The flask was accommodated into our reactor (***LED strip 2***) and stirred for 15 h at 25 °C with fan cooling under blue light irradiation. The reaction mixture was diluted with CH_2Cl_2 and filtered over celite. The solution was carefully evaporated to dryness, and the residue purified by flash column chromatography to obtain the desired compound.

1-Methyl-2-(trifluoromethyl)pyrrole (33a) and

1-methyl-2,5-bis(trifluoromethyl)pyrrole (33b)

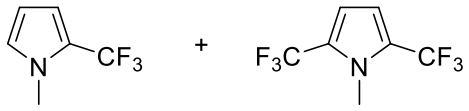

33a **33b**

Prepared according to the general procedure using *N*-methylpyrrole (18 μL, 0.2 mmol) and triflyl chloride (43 μL, 0.4 mmol, 2 equiv.). Due to volatility of the title compounds, the reaction was carried out in CD_3CN and analysed directly by ^{19}F NMR using C_6D_6 as internal standard: 33% **33a**, 57% **33b** (sum: 80% yield). **Characterisation of 33a: ^{1}H NMR** (400 MHz, CD_3CN): δ 6.85 (t, *J* = 2.1 Hz, 1H), 6.59-6.56 (m, 1H), 6.09 (t, *J* = 3.3 Hz, 1H), 3.71 (s, 3H). **^{19}F NMR** (376 MHz, CD_3CN): δ -59.3. The spectral data are in good agreement with those previously reported.[134] **Characterisation of 33b: ^{1}H NMR** (400 MHz, CD_3CN): δ 6.66 (s, 2H), 3.78 (s, 3H). **^{19}F NMR** (376 MHz, CD_3CN): δ -60.3. The spectral data are in good agreement with those previously reported.[245]

3-Methyl-2-(trifluoromethyl)benzofuran (33c)

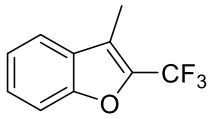

Prepared according to the general procedure using 3-methylbenzofuran (25 μL, 0.2 mmol) and triflyl chloride (43 μL, 0.4 mmol, 2 equiv.). The crude material (59% ^{19}F NMR yield using C_6D_6 as internal standard) was purified by flash column chromatography (eluent pure pentane) to give the corresponding product as a colorless oil (12.2 mg, 30% yield). Note: about 10% of a bis-trifluoromethylated impurity. **^{1}H NMR** (400 MHz, $CDCl_3$): δ 7.61 (d, *J* = 7.8 Hz, 1H), 7.52 (dt, *J* = 8.3, 0.8 Hz, 1H), 7.44 (td, *J* = 7.7, 1.2 Hz, 1H), 7.35-7.31 (m, 1H), 2.41 (q, J_{HF} = 2.0 Hz, 3H). **^{19}F NMR** (376 MHz, $CDCl_3$): δ -62.0 (q, J_{HF} = 2.0 Hz). The spectral data are in good agreement with those previously reported.[134]

3-Methyl-2-(perfluorohexyl)benzofuran (33d)

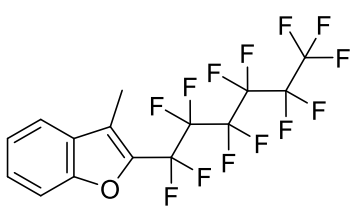

Prepared according to the general procedure using 3-methylbenzofuran (25 μL, 0.2 mmol) and perfluorohexyl iodide (87 μL, 0.4 mmol, 2 equiv.). The crude material was purified by flash column chromatography (eluent pure pentane) to give the corresponding product as a yellow oil (73.4 mg, 82% yield). **^{1}H NMR** (400 MHz, $CDCl_3$): δ 7.62 (d, *J* = 7.8 Hz, 1H), 7.53 (d, *J* = 8.3 Hz, 1H), 7.46-7.41 (m, 1H),

7.33 (t, J = 7.4 Hz, 1H), 2.41 (t, J_{HF} = 2.5 Hz, 3H). **^{19}F NMR** (376 MHz, $CDCl_3$): δ -80.8 (br s, 3F), -111.4 (t, J = 13.2 Hz, 2F), -122.2 (br, 2F), -122.8 (m, 4F), -126.2 (m, 2F). **^{13}C NMR** (101 MHz, $CDCl_3$): δ 154.6, 137.3 (t, J_{CF} = 30.6 Hz), 128.5, 127.0, 123.4, 121.1, 120.6, 118.6 (t, J_{CF} = 33.3 Hz), 115.8 (t, J_{CF} = 33.1 Hz), 111.9, 111.05 (t, J_{CF} = 31.6 Hz), 108.4, 7.8 (other signals not visible or superimposed). **FT-IR**: ν (cm^{-1}) 1616, 1454, 1392, 1375, 1362, 1296, 1232, 1194, 1142, 1090, 1069. **HRMS (ESI)**: Exact mass calculated for $C_{15}H_8OF_{13}$ $[M+H]^+$: 451.0362, found 451.0362.

General procedure for β-arylation of cyclic ketones

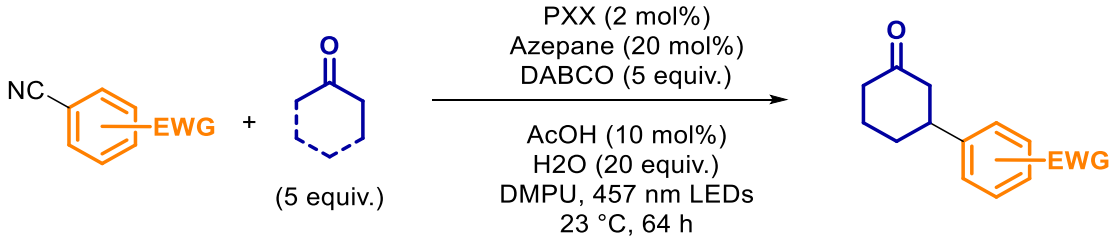

A 10 mL dried Schlenk flask was charged with cyanoarene (0.2 mmol), DABCO (112.2 mg, 1 mmol, 5 equiv.) and PXX (1.1 mg, 0.004 mmol, 2 mol%). The flask was put under N_2 and 0.4 mL of a previously prepared solution of azepane (0.1 M, 0.04 mmol, 20 mol%) and AcOH (0.1 M, 0.04 mmol, 20 mol%) was added, followed by 0.4 mL DMPU. Cyclic ketone (1 mmol, 5 equiv.) and H_2O (72 µL, 4 mmol, 20 equiv.) were added directly. The flask was sealed, and three cycles of freeze-pump-thaw were performed before refilling with N_2. The flask was accommodated into our reactor (***LED strip 1***) and stirred for 64 h at 23 °C with fan cooling under blue light irradiation. The reaction mixture was diluted with EtOAc and washed with NaOH 1 M solution. The aqueous phase was washed with EtOAc (x3), organics pooled, washed with brine, dried ($MgSO_4$). The solution was evaporated to dryness, and the residue purified by flash column chromatography to obtain the desired compound.

4-(3-Oxocyclohexyl)benzonitrile (34a)

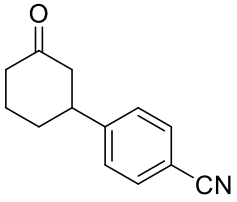

Prepared according to the general procedure using 1,4-dicyanobenzene (25.6 mg, 0.2 mmol) and cyclohexanone (104 µL, 1 mmol, 5 equiv.). The crude material was purified by flash column chromatography (eluent gradient: from pure heptane to heptane:EtOAc 7:3) to give the corresponding product as a colorless oil (31.4 mg, 79%

yield). The reported structure was verified by 2D-NMR experiments (COSY, HSQC). **^{1}H NMR** (400 MHz, $CDCl_3$): δ 7.64 (d, *J* = 8.2 Hz, 2H), 7.34 (d, *J* = 8.2 Hz, 2H), 3.08 (tt, *J* = 11.7, 3.8 Hz, 1H), 2.63-2.56 (m, 1H), 2.56-2.45 (m, 2H), 2.45-2.35 (m, 1H), 2.21-2.13 (m, 1H), 2.13-2.06 (m, 1H), 1.92-1.74 (m, 2H). **^{13}C NMR** (101 MHz, $CDCl_3$): δ 209.8, 149.5, 132.6, 127.5, 118.8, 110.7, 48.2, 44.6, 41.1, 32.3, 25.3. The spectral data are in good agreement with those previously reported.[246]

4-(3,3-Dimethyl-5-oxocyclohexyl)benzonitrile (34b)

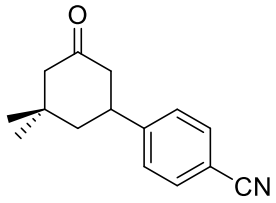

Prepared according to the general procedure using 1,4-dicyanobenzene (25.6 mg, 0.2 mmol) and 3,3-dimethylcyclohexanone (139 μL, 1 mmol, 5 equiv.), along with 40 mol% of both azepane and AcOH. The crude material was purified by flash column chromatography (eluent gradient: from pure heptane to heptane:EtOAc 8:2) to give the corresponding product as a colorless oil (27.1 mg, 60% yield). **^{1}H NMR** (400 MHz, $CDCl_3$): δ 7.64 (d, *J* = 8.3 Hz, 2H), 7.35 (d, *J* = 8.3 Hz, 2H), 3.21 (tt, *J* = 12.5, 4.4 Hz, 1H), 2.57-2.50 (m, 1H), 2.46-2.30 (m, 2H), 2.22 (dt, *J* = 13.5, 2.0 Hz, 1H), 1.88-1.75 (m, 2H), 1.15 (s, 3H), 1.02 (s, 3H). **^{13}C NMR** (101 MHz, $CDCl_3$): δ 209.8, 149.4, 132.6, 127.6, 118.8, 110.7, 54.2, 47.5, 45.8, 40.4, 35.5, 32.1, 25.7. The spectral data are in good agreement with those previously reported.[92]

Ethyl *trans*-2-(4-cyanophenyl)-4-oxocyclohexane-1-carboxylate (34c)

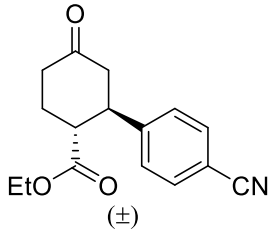

Prepared according to the general procedure using 1,4-dicyanobenzene (25.6 mg, 0.2 mmol) and ethyl 4-oxocyclohexane-1-carboxylate (159 μL, 1 mmol, 5 equiv.). The crude material was purified by flash column chromatography (eluent gradient: from pure heptane to heptane:EtOAc 6:4) to give the corresponding product as a yellor oil that solidifies on standing (39.0 mg, 72% yield, > 20:1 d.r. by NMR analysis). **m.p.** 113-114 °C. **^{1}H NMR** (400 MHz, $CDCl_3$): δ 7.63 (d, *J* = 8.4 Hz, 2H), 7.35 (d, *J* = 8.4 Hz, 2H), 3.98-3.91 (m, 2H), 3.37 (td, *J* = 11.5, 4.9 Hz, 1H), 3.00 (td, *J* = 11.5, 3.6 Hz, 1H), 2.64-2.45 (m, 4H), 2.38-2.30 (m, 1H), 2.11-1.99 (m, 1H), 1.01 (t, *J* = 7.1 Hz, 3H). **^{13}C NMR** (101 MHz, $CDCl_3$): δ 207.4, 172.9, 147.0, 132.6, 128.1, 118.6,

111.3, 60.8, 48.1, 47.2, 46.5, 39.8, 28.6, 14.0. The spectral data are in good agreement with those previously reported.[92]

4-(3-Oxocyclopentyl)benzonitrile (34d)

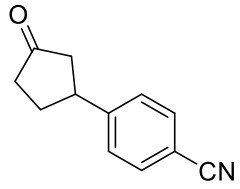

Prepared according to the general procedure using 1,4-dicyanobenzene (25.6 mg, 0.2 mmol) and cyclopentanone (89 μL, 1 mmol, 5 equiv.). The crude material was purified by flash column chromatography (eluent gradient: from pure heptane to heptane:EtOAc 7:3) to give the corresponding product as a yellow-orange oil (20.0 mg, 54% yield). **^{1}H NMR** (400 MHz, $CDCl_3$): δ 7.65 (dt, *J* = 8.3, 1.9 Hz, 2H), 7.38 (d, *J* = 8.3 Hz, 2H), 3.54-3.43 (m, 1H), 2.71 (dd, *J* = 17.9, 8.9 Hz, 1H), 2.55-2.44 (m, 2H), 2.40-2.28 (m, 2H), 2.05-1.93 (m, 1H). **^{13}C NMR** (101 MHz, $CDCl_3$): δ 216.8, 148.5, 132.6, 127.6, 118.8, 110.7, 45.3, 42.2, 38.7, 30.8. The spectral data are in good agreement with those previously reported.[30]

5-(3-Oxocyclohexyl)isobenzofuran-1(3*H*)-one (34g)

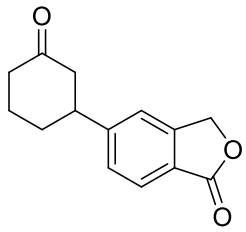

Prepared according to the general procedure using 4-cyanophthalide (31.8 mg, 0.2 mmol) and cyclohexanone (104 μL, 1 mmol, 5 equiv.), along with 40 mol% of both azepane and AcOH. The crude material was purified by flash column chromatography (eluent gradient: from pure heptane to heptane:EtOAc 1:1) to give the corresponding product as a yellow oil (16.1 mg, 35% yield). **^{1}H NMR** (400 MHz, $CDCl_3$): δ 7.89 (d, *J* = 8.0 Hz, 1H), 7.42 (d, *J* = 8.0 Hz, 1H), 7.35 (s, 1H), 5.31 (s, 2H), 3.17 (tt, *J* = 11.7, 4.0 Hz, 1H), 2.67-2.60 (m, 1H), 2.60-2.47 (m, 2H), 2.47-2.37 (m, 1H), 2.23-2.09 (m, 2H), 1.97-1.76 (m, 2H). **^{13}C NMR** (101 MHz, $CDCl_3$): δ 209.8, 170.8, 151.2, 147.4, 128.0, 126.2, 124.5, 120.2, 69.5, 48.5, 44.9, 41.1, 32.6, 25.3. **FT-IR**: ν (cm^{-1}) 2938, 2864, 1755, 1705, 1618, 1447, 1344, 1286, 1267, 1252, 1223, 1180, 1113, 1093, 1043, 1001. **HRMS (ESI)**: Exact mass calculated for $C_{14}H_{15}O_3$ $[M+H]^+$: 231.1016, found 231.1015.

General procedure for C–N cross coupling

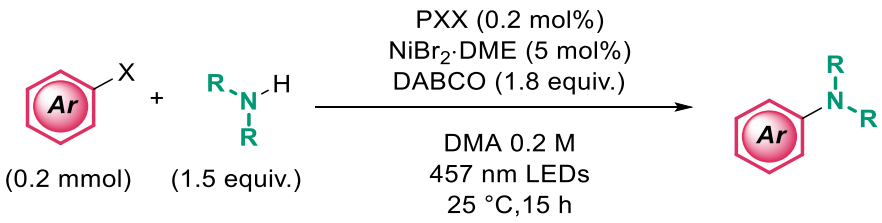

A 10 mL dried Schlenk flask was charged with $NiBr_2$·DME (3.1 mg, 0.01 mmol, 5 mol%), DABCO (40.4 mg, 0.36 mmol, 1.8 equiv.) and aryl halide (if solid, 0.2 mmol). The flask was put under N_2 and 1 mL of a previously prepared PXX solution (0.4 mM in DMA) was added. Aryl halide (if liquid, 0.2 mmol) and amine (0.3 mmol, 1.5 equiv.) were added directly. The flask was sealed, and three cycles of freeze-pump-thaw were performed before refilling with N_2. The flask was accommodated into our reactor (***LED strip* 2**) and stirred for 15-64 h at 25 °C with fan cooling under blue light irradiation. After the defined reaction time, the reaction mixture was diluted with EtOAc and washed with saturated aqueous $NaHCO_3$ solution, brine and dried ($MgSO_4$). The solution was evaporated to dryness, and the residue purified by flash column chromatography to obtain the desired compound.

1-(4-(Trifluoromethyl)phenyl)pyrrolidine (45a)

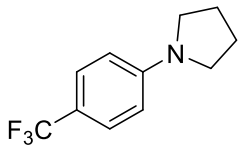

Prepared according to the general procedure using 1-bromo-4-trifluoromethylbenzene (28 µL, 0.2 mmol) and pyrrolidine (25 µL, 0.3 mmol, 1.5 equiv.), with reaction time of 15 h. The crude material was purified by flash column chromatography (eluent gradient: from pure heptane to heptane:EtOAc 100:2) to give the corresponding product as a light yellow solid (37.4 mg, 87% yield). **m.p.** 93-94 °C [Lit.[247] 96-97 °C]. **^{1}H NMR** (400 MHz, $CDCl_3$): δ 7.43 (d, *J* = 8.6 Hz, 2H), 6.54 (d, *J* = 8.6 Hz, 2H), 3.34-3.29 (m, 4H), 2.05-2.01 (m, 4H). **^{19}F NMR** (376 MHz, $CDCl_3$): δ -60.6. **^{13}C NMR** (101 MHz, $CDCl_3$): δ 149.7, 126.4 (q, J_{CF} = 3.7 Hz), 125.4 (q, J_{CF} = 270.0 Hz), 116.6 (q, J_{CF} = 32.5 Hz), 110.8, 47.5, 25.5. The spectral data are in good agreement with those previously reported.[144]

1-(4-(Trifluoromethyl)phenyl)morpholine (45b)

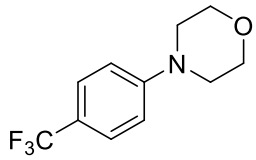

Prepared according to the general procedure using 1-bromo-4-trifluoromethylbenzene (28 μL, 0.2 mmol) and morpholine (26 μL, 0.3 mmol, 1.5 equiv.), with reaction time of 15 h. The crude material was purified by flash column chromatography (eluent gradient: from pure heptane to heptane:EtOAc 9:1) to give the corresponding product as a white solid (36.6 mg, 79% yield). **m.p.** 72-73 °C [Lit.[248] 66.7-67.0 °C]. **^{1}H NMR** (400 MHz, $CDCl_3$): δ 7.50 (d, *J* = 8.6 Hz, 2H), 6.92 (d, *J* = 8.6 Hz, 2H), 3.89-3.85 (m, 4H), 3.26-3.22 (m, 4H). **^{19}F NMR** (376 MHz, $CDCl_3$): δ -61.4. **^{13}C NMR** (101 MHz, $CDCl_3$): δ 153.3, 126.4 (m), 124.6 (q, J_{CF} = 270.8 Hz), 121.0 (q, J_{CF} = 32.6 Hz), 114.3, 66.6, 48.2. The spectral data are in good agreement with those previously reported.[144]

***N*-Benzyl-*N*-methyl-4-(trifluoromethyl)aniline (45c)**

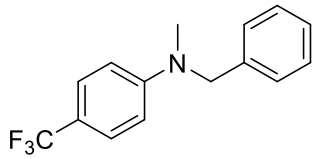

Prepared according to the general procedure using 1-bromo-4-trifluoromethylbenzene (28 μL, 0.2 mmol) and *N*-benzylmethylamine (26 μL, 0.3 mmol, 1.5 equiv.), with reaction time of 15 h. The crude material was purified by flash column chromatography (eluent gradient: from pure heptane to heptane:EtOAc 95:5) to give the corresponding product as a light yellow oil (41.9 mg, 79% yield). **^{1}H NMR** (400 MHz, $CDCl_3$): δ 7.42 (d, *J* = 8.7 Hz, 2H), 7.35-7.30 (m, 2H), 7.28-7.23 (m, 1H), 7.20-7.16 (m, 2H), 6.72 (d, *J* = 8.7 Hz, 2H), 4.59 (s, 2H), 3.09 (s, 3H). **^{19}F NMR** (376 MHz, $CDCl_3$): δ -60.8. **^{13}C NMR** (101 MHz, $CDCl_3$): δ 151.6, 137.9, 128.8, 127.2, 126.5 (m), 126.4, 125.2 (q, J_{CF} = 269.2 Hz), 117.8 (q, J_{CF} = 32.6 Hz), 111.2, 56.1, 38.8. The spectral data are in good agreement with those previously reported.[249]

4-(Pyrrolidin-1-yl)benzonitrile (45h)

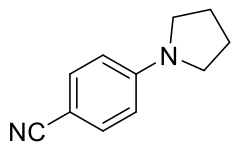

Prepared according to the general procedure using 4-bromobenzonitrile (36.4 mg, 0.2 mmol) and pyrrolidine (25 μL, 0.3 mmol, 1.5 equiv.), with reaction time of 15 h. The crude material was purified by flash column chromatography (heptane:EtOAc 9:1 as eluent) to give the corresponding product as a light yellow solid (26.4 mg, 77% yield). **m.p.** 85-86 °C [Lit.[250] 88-90 °C]. **^{1}H NMR** (400 MHz, $CDCl_3$): δ 7.44 (m, 2H), 6.50 (m, 2H), 3.34-3.30 (m, 4H),

2.07-2.01 (m, 4H). **^{13}C NMR** (101 MHz, $CDCl_3$): δ 150.0, 133.5, 121.0, 111.4, 96.5, 47.5, 25.4. The spectral data are in good agreement with those previously reported.[251]

2-(Pyrrolidin-1-yl)pyridine (45i)

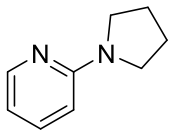

Prepared according to the general procedure using 2-bromopyridine (19 μL, 0.2 mmol) and pyrrolidine (25 μL, 0.3 mmol, 1.5 equiv.), with reaction time of 64 h. The crude material was purified by flash column chromatography (eluent gradient: from pure heptane to heptane:EtOAc 7:3) to give the corresponding product as a light yellow oil (20.3 mg, 69% yield). **^{1}H NMR** (400 MHz, $CDCl_3$): δ 8.16 (ddd, *J* = 5.0, 1.9, 0.8 Hz, 1H), 7.42 (ddd, *J* = 8.6, 7.1, 1.9 Hz, 1H), 6.50 (ddd, *J* = 7.1, 5.0, 0.8 Hz, 1H), 6.35 (d, *J* = 8.6 Hz, 1H), 3.48-3.42 (m, 4H), 2.05-1.97 (m, 4H). **^{13}C NMR** (101 MHz, $CDCl_3$): δ 157.3, 148.1, 136.9, 111.0, 106.5, 46.6, 25.6. The spectral data are in good agreement with those previously reported.[100]

1-(4-Methoxyphenyl)pyrrolidine (45j)

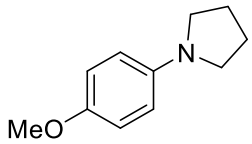

Prepared according to the general procedure using 4-iodoanisole (46.8 mg, 0.2 mmol) and pyrrolidine (25 μL, 0.3 mmol, 1.5 equiv.), with reaction time of 15 h. The crude material was purified by flash column chromatography (eluent gradient: from pure heptane to heptane:EtOAc 95:5) to give the corresponding product as a light yellow oil (9.2 mg, 26% yield). **^{1}H NMR** (400 MHz, $CDCl_3$): δ 6.87-6.82 (d, *J* = 9.0 Hz, 2H), 6.56-6.51 (m, 2H), 3.75 (s, 3H), 3.26-3.20 (m, 4H), 2.01-1.96 (m, 4H). **^{13}C NMR** (101 MHz, $CDCl_3$): δ 150.8, 143.2, 115.0, 112.6, 56.0, 48.3, 25.4. The spectral data are in good agreement with those previously reported.[100]

1-(Diphenylmethylene)-2-(4-(trifluoromethyl)phenyl)hydrazine (45f)

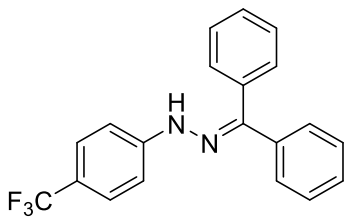

Prepared according to the general procedure using 1-bromo-4-trifluoromethylbenzene (28 μL, 0.2 mmol) and benzophenone hydrazone (58.9 mg, 0.3 mmol, 1.5 equiv.), with reaction time of 15 h. The crude material was purified by flash column chromatography (eluent gradient: from pure heptane to heptane:EtOAc 98:2) to give the corresponding product as a yellow oil (49.0 mg, 72% yield, mass corrected for 5% benzophenone due to partial hydrolysis on the column). **^{1}H NMR**

(400 MHz, $CDCl_3$): δ 7.66-7.52 (m, 6H), 7.47 (d, *J* = 8.6 Hz, 2H), 7.37-7.29 (m, 5H), 7.12 (d, *J* = 8.6 Hz, 2H). **^{19}F NMR** (376 MHz, $CDCl_3$): δ -61.2. **^{13}C NMR** (101 MHz, $CDCl_3$): δ 147.0, 146.2, 137.9, 132.3, 129.8, 129.6, 129.0, 128.6, 128.3, 126.7, 126.6, 121.7, 121.4, 112.4. The spectral data are in good agreement with those previously reported.[154,252]

1-(Diphenylmethylene)-2-(4-fluorophenyl)hydrazine (45k)

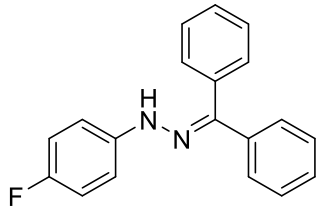

Prepared according to the general procedure using 1-bromo-4-fluorobenzene (110 μL, 1.0 mmol) and benzophenone hydrazone (294 mg, 1.5 mmol, 1.5 equiv.), with reaction time of 40 h. 95% conversion to product was obtained, according to ^{19}F NMR analysis. The reaction mixture was evaporated to dryness, affording an orange-brown solid. The crude material was used in the next step (indole synthesis to **46**) without further purification.

It is possible to purify this compound: another batch (1 mmol scale starting from 1-iodo-4-fluorobenzene) was subjected to the general procedure's work-up and flash column chromatography (eluent gradient: from pure heptane to heptane:EtOAc 97:3) to give the corresponding product as a light yellow oil (136.4 mg, 47% yield, mass corrected for 25% benzophenone due to partial hydrolysis on the column). **^{1}H NMR** (400 MHz, $CDCl_3$): δ 7.62-7.55 (m, 4H), 7.55-7.50 (m, 1H), 7.42 (s, 1H), 7.35-7.27 (m, 5H), 7.05-7.00 (m, 2H), 6.98-6.92 (m, 2H). **^{19}F NMR** (376 MHz, $CDCl_3$): δ -124.9 (m). The spectral data are in good agreement with those previously reported.[155]

7-Fluoro-2,3,4,5-tetrahydro-1*H*-pyrido[4,3-*b*]indole (46)

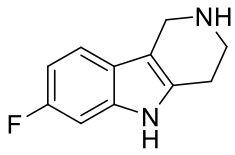

A 100 mL round-bottomed flask equipped with reflux condenser was charged with the crude reaction mixture of hydrazone **45k** (275.8 mg, 0.95 mmol), 4-piperidone monohydrate hydrochloride (218.9 mg, 1.43 mmol, 1.5 equiv.) and *p*-toluenesulfonic acid (1.45 g, 7.6 mmol, 8 equiv.). The flask was put under N_2 and degassed absolute ethanol (16 mL) was added. The resulting mixture was heated to reflux overnight, after which water and heptane are added. Phases were separated, and the aqueous phase washed further with heptane (x2) before being basified with NaOH 1 M aqueous solution to pH 14, then extracted with EtOAc (x4). Organics are dried (Na_2SO_4) and evaporated. The resulting material contains

product and residual *p*-toluenesulfonic acid. It is then redissolved in AcOEt and washed with NaOH 1 M (x3). The organic phase is dried (Na_2SO_4) and evaporated to afford the corresponding product as an orange-red solid (129.0 mg, 68% yield over two steps). Further purification was not attempted. **m.p.** not observed, decomposition at 173-174 °C. **^{1}H NMR** (400 MHz, DMSO-d_6): δ 10.82 (br s, 1H), 7.23 (dd, *J* = 8.8, 4.6 Hz, 1H), 7.06 (dd, *J* = 10.0, 2.5 Hz, 1H), 6.80 (td, *J* = 8.8, 2.5 Hz, 1H), 3.80 (s, 2H), 3.35 (br s, 1H), 3.00 (t, *J* = 5.7 Hz, 2H), 2.65 (t, *J* = 5.7 Hz, 2H). **^{19}F NMR** (376 MHz, DMSO-d_6): δ -125.9 (td, *J* = 10.0, 4.6 Hz). **^{13}C NMR** (101 MHz, DMSO-d_6): δ 155.6 (d, J_{CF} = 231.1 Hz), 135.7, 131.9, 125.8 (d, J_{CF} = 9.9 Hz), 111.3 (d, J_{CF} = 9.9 Hz), 108.7 (d, J_{CF} = 4.5 Hz), 107.6 (d, J_{CF} = 25.6 Hz), 102.0 (d, J_{CF} = 23.2 Hz), 42.9, 41.5, 24.2. **FT-IR**: ν (cm^{-1}) 3315, 3144, 3102, 3035, 2918, 2857, 2737 (br), 1626, 1589, 1506, 1473, 1454, 1429, 1364, 1327, 1232, 1177, 1128, 1109, 1082. **HRMS (EI)**: Exact mass calculated for $C_{11}H_{11}N_2F$ $[M]^+$: 190.0906, found 190.0910.

General procedure for C–S cross coupling

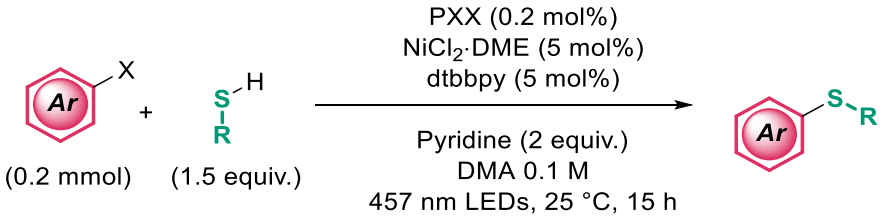

A 10 mL dried Schlenk flask was charged with $NiCl_2$·DME (2.2 mg, 0.01 mmol, 5 mol%), dtbbpy (2.7 mg, 0.01 mmol, 5 mol%) and aryl halide (if solid, 0.2 mmol). The flask was put under N_2 and 1 mL of a previously prepared PXX solution (0.4 mM in DMA) was added, followed by 1 mL DMA. Aryl halide (if liquid, 0.2 mmol), sulfide (0.3 mmol, 1.5 equiv.) and pyridine (32 μL, 0.4 mmol, 2 equiv.) were added directly. The flask was sealed, and three cycles of freeze-pump-thaw were performed before refilling with N_2. The flask was accommodated into our reactor (***LED strip 2***) and stirred for 15-40 h at 25 °C with fan cooling under blue light irradiation. After the defined reaction time, the reaction mixture was diluted with dichloromethane and washed with saturated aqueous $NaHCO_3$ solution, brine and dried ($MgSO_4$). The solution was evaporated to dryness, and the residue purified by flash column chromatography to obtain the desired compound.

Octyl(*p*-tolyl)sulfane (47a)

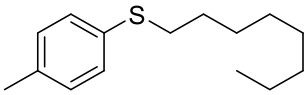

Prepared according to the general procedure using 4-iodotoluene (43.6 mg, 0.2 mmol) and octanethiol (52 μL, 0.3 mmol, 1.5 equiv.), with reaction time of 15 h. The crude material was purified by flash column chromatography (eluent gradient: from pure heptane to heptane:EtOAc 99:1) to give the corresponding product as a yellow oil (47.3 mg, 93% yield). **^{1}H NMR** (400 MHz, $CDCl_3$): δ 7.24 (d, *J* = 8.2 Hz, 2H), 7.09 (d, *J* = 8.2 Hz, 2H), 2.87 (t, *J* = 7.4 Hz, 2H), 2.31 (s, 3H), 1.61 (quintuplet, *J* = 7.4 Hz, 2H), 1.44-1.35 (m, 2H), 1.33-1.18 (m, 8H), 0.87 (t, *J* = 7.1 Hz, 3H). **^{13}C NMR** (101 MHz, $CDCl_3$): δ 135.8, 133.1, 129.7, 129.6, 34.3, 31.8, 29.3, 29.2, 29.1, 28.8, 22.7, 21.0, 14.1. The spectral data are in good agreement with those previously reported.[126]

(4-Methoxyphenyl)(octyl)sulfane (47b)

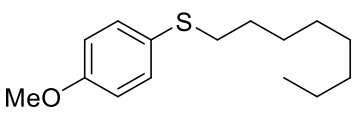

Prepared according to the general procedure using 4-iodoanisole (46.8 mg, 0.2 mmol) and octanethiol (52 μL, 0.3 mmol, 1.5 equiv.), with reaction time of 15 h. The crude material was purified by flash column chromatography (eluent heptane:EtOAc 98:2) to give the corresponding product as a dark yellow oil (49.5 mg, 98% yield). **^{1}H NMR** (400 MHz, $CDCl_3$): δ 7.33 (dt, *J* = 8.8, 2.6 Hz, 2H), 6.84 (dt, *J* = 8.8, 2.6 Hz, 2H), 3.79 (s, 3H), 2.81 (t, *J* = 7.4 Hz, 2H), 1.57 (quintuplet, *J* = 7.4 Hz, 2H), 1.43-1.34 (m, 2H), 1.31-1.20 (m, 8H), 0.87 (t, *J* = 7.0 Hz, 3H). **^{13}C NMR** (101 MHz, $CDCl_3$): δ 158.7, 132.9, 126.9, 114.5, 55.3, 35.8, 31.8, 29.4, 29.2, 29.2, 28.7, 22.7, 14.1. The spectral data are in good agreement with those previously reported.[253]

4-(Octylthio)benzonitrile (47c)

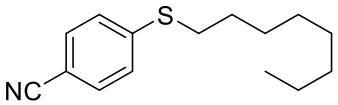

Prepared according to the general procedure using 4-bromobenzonitrile (36.4 mg, 0.2 mmol) and octanethiol (52 μL, 0.3 mmol, 1.5 equiv.), with reaction time of 15 h. The crude material was purified by flash column chromatography (eluent heptane:EtOAc 95:5) to give the corresponding product as a yellow oil (46.0 mg, 93% yield). **^{1}H NMR** (400 MHz, $CDCl_3$): δ 7.52 (dt, *J* = 8.6, 1.9 Hz, 2H), 7.28 (dt, *J* = 8.6, 1.9 Hz, 2H), 2.97 (t, *J* = 7.4 Hz, 2H), 1.69 (quintuplet, *J* = 7.4 Hz, 2H), 1.48-1.40 (m, 2H), 1.35-1.21 (m, 8H), 0.88 (t, *J* = 7.1 Hz, 3H). **^{13}C NMR** (101 MHz, $CDCl_3$): δ 145.4, 132.3, 126.7, 119.1, 107.9, 32.0,

31.9, 29.2, 29.2, 29.0, 28.7, 22.8, 14.2. The spectral data are in good agreement with those previously reported.[253]

Methyl *N*-(tert-butoxycarbonyl)-*S*-(p-tolyl)-L-cysteinate (47d)

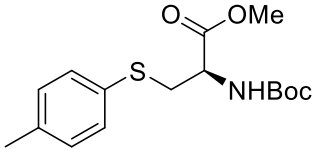

Prepared according to the general procedure using 4-iodotoluene (43.6 mg, 0.2 mmol) and methyl *N*-Boc cysteine (62 μL, 0.3 mmol, 1.5 equiv.), with reaction time of 40 h. The crude material was purified by flash column chromatography (eluent gradient: from pure toluene to toluene:EtOAc 95:5) to give the corresponding product as a colorless oil (55.4 mg, 85% yield). **^{1}H NMR** (400 MHz, $CDCl_3$): δ 7.32 (d, *J* = 8.1 Hz, 2H), 7.10 (d, *J* = 8.1 Hz, 2H), 5.33 (d, *J* = 7.7 Hz, 1H), 4.57-4.49 (m, 1H), 3.53 (s, 3H), 3.32 (d, *J* = 4.8 Hz, 2H), 2.31 (s, 3H), 1.42 (s, 9H). **^{13}C NMR** (101 MHz, $CDCl_3$): δ 171.1, 155.0, 137.3, 131.8, 130.9, 129.8, 80.0, 53.2, 52.3, 37.8, 28.3, 21.1. The spectral data are in good agreement with those previously reported.[126]

Phenyl(*p*-tolyl)sulfane (47e)

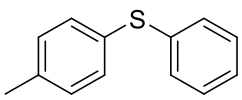

Prepared according to the general procedure using 4-iodotoluene (43.6 mg, 0.2 mmol) and thiophenol (31 μL, 0.3 mmol, 1.5 equiv.), with reaction time of 15 h. The crude material was purified by flash column chromatography (eluent pure heptane) to give the corresponding product as a yellow oil (36.8 mg, 92% yield). **^{1}H NMR** (400 MHz, $CDCl_3$): δ 7.30 (d, *J* = 8.2 Hz, 2H), 7.27-7.22 (m, 4H), 7.22-7.16 (m, 1H), 7.13 (d, *J* = 8.2 Hz, 2H), 2.34 (s, 3H). **^{13}C NMR** (101 MHz, $CDCl_3$): δ 137.6, 137.1, 132.3, 131.3, 130.1, 129.8, 129.1, 126.4, 21.2. The spectral data are in good agreement with those previously reported.[254]

6.8 Preparation of dihydropyridine precursors

Dihydropyridines and alkyltrifluoroborate salts not described in the following were prepared by other members of the Melchiorre group; please refer to the main publication.[22]

2-Methylpent-4-enal

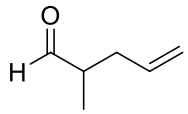

Following a reported procedure,[255] a 100 mL round bottomed flask was charged with ethyl 2-methylpent-4-enoate (1.42 g, 10 mmol), which was dissolved in CH_2Cl_2 (40 mL) and cooled to -78 °C in an acetone/dry ice bath. DIBAL solution (10 mL, 10 mmol, 1 M in hexane) was added dropwise, and the reaction mixture let stir for 1.5 h at the same temperature, before quenching with MeOH and saturated $NaHCO_3$ solution. The solution is let warm to room temperature and extracted with Et_2O (x3). Organics are pooled, dried (Na_2SO_4), the solvent evaporated. The crude material was purified by flash column chromatography (eluent pentane:Et_2O 100:2) to give the corresponding product as a colorless oil (473 mg, 48% yield, with about 20% residual ester starting material as impurity). **^{1}H NMR** (500 MHz, $CDCl_3$): δ 9.67 (d, *J* = 1.4 Hz, 1H), 5.84-5.69 (m, 1H), 5.14-5.00 (m, 2H), 2.55-2.37 (m, 2H), 2.24-2.09 (m, 1H), 1.12 (d, *J* = 7.0 Hz, 3H). The spectral data are in good agreement with those previously reported.[255]

5′-deoxy-2′,3′-*O*-(1-methylethylidene)uridine

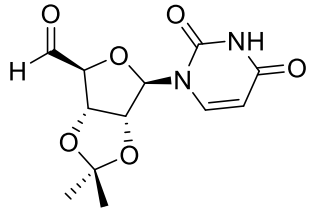

A 250 mL round bottomed flask was charged with 2′,3′-*O*-(1-methylethylidene)uridine (1.5 g, 5.28 mmol), which was dissolved in acetonitrile (80 mL). Dess-Martin periodinane (2.69 g, 6.33 mmol, 1.2 equiv.) was added to the solution in portions. The resulting white suspension was stirred at room temperature for 45 min, and then filtered. After evaporating the solvent, the crude material was dry-loaded directly and purified by flash column chromatography (eluent gradient: from hexane:AcOEt 4:6 to 1:9) to give the corresponding product as a white solid (1.09 g, 73% yield). **^{1}H NMR** (500 MHz, $CDCl_3$): δ 9.44 (s, 1H), 9.13 (br s, 1H), 7.26 (d, *J* = 8.0 Hz, 1H), 5.77 (d, *J* = 8.0 Hz, 1H), 5.50 (s, 1H), 5.22 (dd, *J* = 6.3, 1.6 Hz, 1H), 5.11 (d, *J* = 6.3 Hz, 1H), 4.56 (d, *J* = 1.5 Hz, 1H), 1.54 (s, 3H), 1.37 (s, 3H). The spectral data are in good agreement with those previously reported.[256]

General procedure for the preparation of 4-alkyldihydropyridines

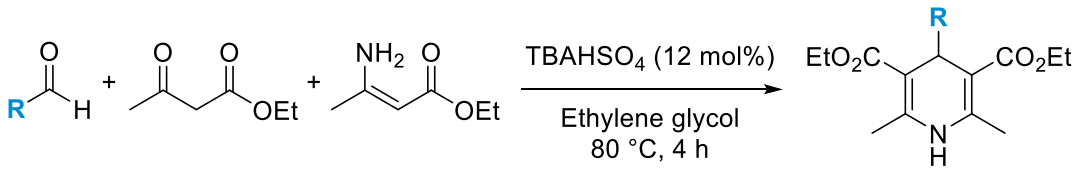

Following a reported procedure,[41,257] ethyl 3-aminocrotonate (1 equiv.) and ethylene glycol (2.5 M) were added to a flask under N_2. Ethyl acetoacetate (1 equiv.) was added, followed by aldehyde (1 equiv.) and tetrabutylammonium hydrogen sulfate (12 mol%). The reaction mixture was stirred at 80 °C for 4 h, then cooled and diluted with EtOAc. A brine solution was added, phases separated, and the aqueous solution extracted with EtOAc (x3). Organics were pooled, dried ($MgSO_4$), the solution was evaporated to dryness, and the residue purified by flash column chromatography to obtain the desired compound.

Diethyl 2,6-dimethyl-4-pentyl-1,4-dihydropyridine-3,5-dicarboxylate (67f)

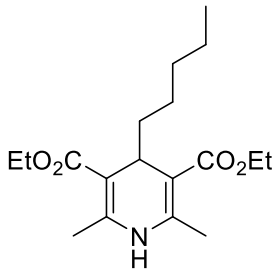

Prepared according to the general procedure using hexanal (1.2 mL, 10 mmol). The crude material was purified by flash column chromatography (eluent hexane:EtOAc 8:2) to give the corresponding product as a colorless oil (2.02 g, 62% yield). **^{1}H NMR** (500 MHz, $CDCl_3$): δ 5.59 (br s, 1H), 4.26-4.09 (m, 4H), 3.93 (t, J = 5.8 Hz, 1H), 2.28 (s, 6H), 1.34-1.16 (m, 14H), 0.85 (t, J = 7.0 Hz, 3H). The spectral data are in good agreement with those previously reported.[258]

Diethyl 2,6-dimethyl-4-(pent-4-en-2-yl)-1,4-dihydropyridine-3,5-dicarboxylate (67o)

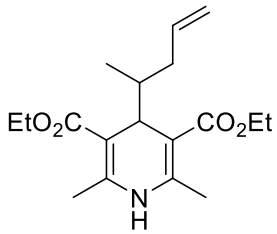

Prepared according to the general procedure using 2-methylpent-4-enal (473 mg, 4.8 mmol). The crude material was purified by flash column chromatography (eluent hexane:EtOAc 8:2) to give the corresponding product as a light yellow oil that solidifies upon standing (713 mg, 46% yield). **^{1}H NMR** (500 MHz, $CDCl_3$): δ 5.77-5.68 (m, 1H), 5.60 (s, 1H), 4.97-4.91 (m, 2H), 4.26-4.13 (m, 4H), 4.04 (d, J = 4.8 Hz, 1H), 2.31 (s, 6H), 2.18-2.11 (m, 1H), 1.72-1.64 (m, 1H), 1.54-1.46 (m, 1H), 1.30 (t, J = 7.1 Hz, 6H), 0.73 (d, J = 6.9 Hz, 3H). **^{13}C NMR** (125.6 MHz, $CDCl_3$): δ 168.6, 168.4, 144.6,

138.6, 115.0, 102.0, 101.5, 59.6, 40.9, 38.1, 37.1, 19.5, 19.4, 14.9, 14.4. **HRMS (ESI)**: Exact mass calculated for $C_{18}H_{27}NNaO_4$ [M+Na]$^+$: 344.1832, found: 344.1834.

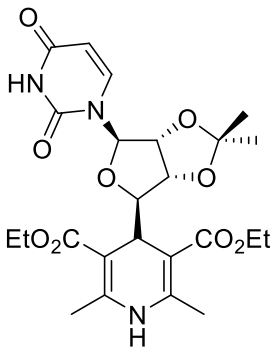

Diethyl 4-((3a*R*,4*R*,6*R*,6a*R*)-6-(2,4-dioxo-3,4-dihydropyrimidin-1(2*H*)-yl)-2,2-dimethyltetrahydrofuro[3,4-*d*][1,3]dioxol-4-yl)-2,6-dimethyl-1,4-dihydropyridine-3,5-dicarboxylate (67t)

Prepared according to the general procedure using 5′-deoxy-2′,3′-*O*-(1-methylethylidene)uridine (600 mg, 2.12 mmol). The crude material was purified by flash column chromatography (eluent CH_2Cl_2:MeOH 10:1) to give the corresponding product as a light yellow solid (759 mg, 71% yield). **^{1}H NMR** (500 MHz, $CDCl_3$): δ 8.74 (s, 1H), 7.32 (d, *J* = 8.1 Hz, 1H), 6.01 (s, 1H), 5.84 (d, *J* = 3.3 Hz, 1H), 5.73 (dd, *J* = 8.1, 2.2 Hz, 1H), 4.74 (dd, *J* = 6.6, 4.7 Hz, 1H), 4.56 (dd, *J* = 6.6, 3.3 Hz, 1H), 4.42 (d, *J* = 6.6 Hz, 1H), 4.28-4.09 (m, 4H), 3.89 (dd, *J* = 6.6, 4.7 Hz, 1H), 2.33 (s, 3H), 2.32 (s, 3H), 1.51 (s, 3H), 1.32-1.26 (m, 9H). **^{13}C NMR** (125.6 MHz, $CDCl_3$): δ 167.8, 167.7, 162.9, 149.9, 146.6, 146.0, 140.7, 114.6, 102.5, 99.1, 98.6, 89.0, 87.2, 83.7, 80.4, 60.1, 60.0, 34.0, 27.3, 25.5, 19.6, 19.5, 14.4, 14.4. **HRMS (ESI)**: Exact mass calculated for $C_{24}H_{31}N_3NaO_9$ [M+Na]$^+$: 528.1953, found: 528.1959.

6.9 Photomediated β-alkylations of enals

General procedure

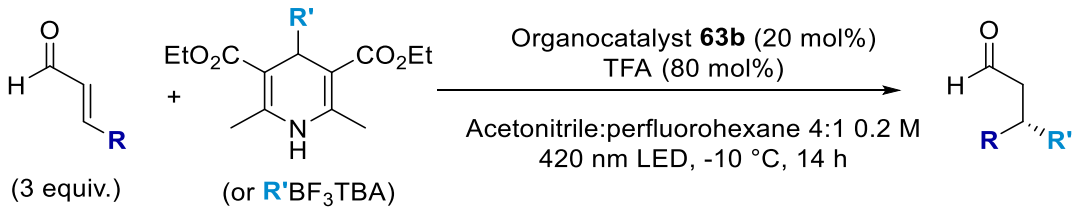

A 5 mL Ar-purged vial was charged with organocatalyst **63b** (22.1 mg, 0.02 mmol, 20 mol%), the 4-alkyl-1,4-dihydropyridine (0.1 mmol) and enal (0.3 mmol, 3 equiv., if solid or oil). The vial was put under N_2 and 0.4 mL 0.2 M TFA solution in acetonitrile was added, followed by enal (0.3 mmol, 3 equiv., if liquid) and perfluorohexane (0.1 mL). The vial was sealed with parafilm and placed in our reactor (see description in Section 6.2). The reaction was stirred for 15-40 h at -10 °C under blue light irradiation (420 nm). At completion the solvent was evaporated and the residue purified by flash column chromatography to obtain the desired compound.

NOTES: Variations in stoichiometry or components are specified in each case. Yields and enantiomeric ratios are reported as average of two runs. Enantiomeric ratio is determined on the corresponding alcohol upon reduction with $NaBH_4$.

(*R*)-3-cyclopentyl-3-phenylpropanal (68d)

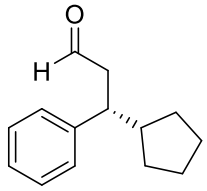

Prepared according to the general procedure using cinnamaldehyde (39.6 mg, 0.3 mmol, 3 equiv.) and diethyl 4-cyclopentyl-2,6-dimethyl-1,4-dihydropyridine-3,5-dicarboxylate (32.0 mg, 0.1 mmol). The crude material was purified by flash column chromatography (eluent pentane:Et_2O 99.7:0.3) to give the corresponding product as a colourless oil (15.1 mg, 75% yield). The enantiomeric ratio of the corresponding alcohol was determined by HPLC analysis on a Daicel Chiralpack IC-3 column (hexane:*i*-PrOH 9:1; flow rate 0.6 mL/min; λ = 215 nm); τ_{major} = 14.5 min, τ_{minor} = 11.5 min; e.r. 97:3. $[\alpha]_D^{26}$ = +15.1° (*c* 0.40, $CHCl_3$). **^{1}H NMR** (500 MHz, $CDCl_3$): δ 9.61 (t, *J* =2.2 Hz, 1H), 7.32-7.26 (m, 2H), 7.23-7.18 (m, 1H), 7.16-7.12 (m, 2H), 3.02-2.94 (m, 1H), 2.87-2.68 (m, 2H), 1.85- 1.71 (m, 2H), 1.69-1.59 (m, 2H), 1.54-1.44 (m, 2H), 1.25-1.02 (m, 3H), 1.00-0.77 (m, 2H). **^{13}C NMR** (125.6 MHz, $CDCl_3$): δ 202.6, 142.7, 128.3, 128.2, 126.4, 47.1, 46.1, 43.1, 31.0, 30.7, 26.4, 26.3. **HRMS (ESI)**: Exact mass calculated for $C_{15}H_{22}NaO_2$ $[M+MeOH+Na]^+$: 257.1512, found: 257.1513.

(*R*)-3-cyclobutyl-3-phenyl-propanal (68e)

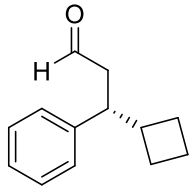

Prepared according to the general procedure using cinnamaldehyde (39.6 mg, 0.3 mmol, 3 equiv.) and tetrabutylammonium cyclobutyltrifluoroborate[XXII] (36.5 mg, 0.1 mmol), along with TFA (3 μL, 0.04 mmol, 40 mol%) in acetonitrile (0.2 mL). The crude material was purified by flash column chromatography (eluent pentane:Et_2O 99:1) to give the corresponding product as a colourless oil (5.5 mg, 29% yield). The enantiomeric ratio of the corresponding alcohol was determined by HPLC analysis on a Daicel Chiralpack IC-3 column (hexane:*i*-PrOH 9:1; flow rate 0.6 mL/min; λ = 215 nm); τ_{major} = 13.1 min, τ_{minor} = 11.5 min; e.r. 86:14. $[\alpha]_D^{26}$ = -12.1° (*c* 0.3, $CHCl_3$). **^{1}H NMR** (500 MHz, $CDCl_3$):

[XXII] This entry was performed using tetrabutylammonium cyclobutyltrifluoroborate as the radical precursor because of the photochemical inactivity of the corresponding dihydropyridine, which failed to deliver the corresponding radical upon excitation.

δ 9.65 (t, *J* = 2.3 Hz, 1H), 7.32-7.27 (m, 2H), 7.23-7.16 (m, 3H), 3.13-3.06 (m, 1H), 2.68-2.63 (m, 2H), 2.59-2.48 (m, 1H), 2.16-2.06 (m, 1H), 1.84-1.70 (m, 3H), 1.66-1.58 (m, 1H), 1.35-1.26 (m, 1H). **^{13}C NMR** (125.6 MHz, $CDCl_3$): δ 202.2, 142.1, 128.5, 127.6, 126.6, 47.8, 47.0, 41.4, 27.5, 26.8, 17.3. **HRMS (ESI)**: Exact mass calculated for $C_{14}H_{20}NaO_2$ $[M+Na+MeOH]^+$: 243.1356, found: 243.1357.

(*S*)-3,4-diphenylbutanal (68h)

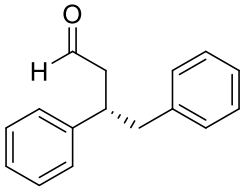

Prepared according to the general procedure using cinnamaldehyde (39.6 mg, 0.3 mmol, 3 equiv.) and diethyl 4-benzyl-2,6-dimethyl-1,4-dihydropyridine-3,5-dicarboxylate (34.3 mg, 0.1 mmol). The crude material was purified by flash column chromatography (eluent hexane:Et_2O 95:5, three consecutive purifications) to give the corresponding product as a colorless oil (10.0 mg, 44% yield). The enantiomeric ratio of the corresponding alcohol was determined by HPLC analysis on a Daicel Chiralpack IC-3 column (hexane:*i*-PrOH 9:1; flow rate 0.6 mL/min; λ = 215 nm); τ_{major} = 13.54 min, τ_{minor} = 12.59 min; e.r. 86:14. **^{1}H NMR** (400 MHz, $CDCl_3$): δ 9.62 (t, *J* = 2.0 Hz, 1H), 7.35-7.17 (m, 8H), 7.11-7.06 (m, 2H), 3.52 (quintuplet, *J* = 7.3 Hz, 1H), 2.99 (dd, *J* = 13.5, 7.1 Hz, 1H), 2.91 (dd, *J* = 13.5, 7.9 Hz, 1H), 2.84-2.72 (m, 2H). The spectral data are in good agreement with those previously reported.[174]

***tert*-Butyl (*R*)-4-(3-oxo-1-phenylpropyl)piperidine-1-carboxylate (68j)**

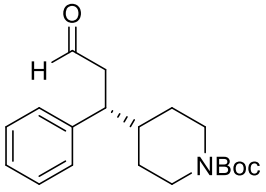

Prepared according to the general procedure using cinnamaldehyde (39.6 mg, 0.3 mmol, 3 equiv.) and diethyl 4-(1-(*tert*-butoxycarbonyl)piperidin-4-yl)-2,6-dimethyl-1,4-dihydropyridine-3,5-dicarboxylate (44.0 mg, 0.1 mmol), along with organocatalyst **63a** (14.0 mg, 0.02 mmol, 20 mol%), TFA (0.1 mmol, 1 equiv.) in CH_2Cl_2 (0.4 mL). The crude material was purified by flash column chromatography (eluent hexane:Et_2O 8:2) to give the corresponding product as a colorless oil (11.2 mg, 35% yield). The enantiomeric ratio of the corresponding alcohol was determined by HPLC analysis on a Daicel Chiralpack IC-3 column (hexane:*i*-PrOH 8:2; flow rate 0.6 mL/min; λ = 215 nm); τ_{major} = 32.3 min, τ_{minor} = 24.2 min; e.r. 86:14. $[\alpha]_D^{26}$ = -3.7° (*c* 0.55, $CHCl_3$). **^{1}H NMR** (500 MHz, $CDCl_3$): δ 9.61 (t, *J* = 2.0 Hz, 1H), 7.33-7.29 (m, 2H), 7.23 (tt,

J = 7.3, 1.3 Hz, 1H), 7.16-7.13 (m, 2H), 4.15 (br s, 1H), 4.03 (br s, 1H), 3.03- 2.97 (m, 1H), 2.88-2.73 (m, 2H), 2.66 (br s, 1H), 2.55 (br s, 1H), 1.75 (d, *J* = 12.2 Hz, 1H), 1.68-1.59 (m, 1H), 1.43 (s, 9H), 1.40-1.32 (m, 1H), 1.21-1.13 (m, 1H), 1.08-0.98 (m, 1H). **^{13}C NMR** (125.6 MHz, $CDCl_3$): δ 201.8, 154.7, 141.9, 128.6, 128.2, 126.8, 79.4, 47.0, 45.5, 41.6, 28.4. Due to rotamers, the NCH_2 carbon signal is not visible in the ^{13}C NMR spectrum, but an HSQC signal at 44 ppm is coupled to the corresponding protons. **HRMS (ESI)**: Exact mass calculated for $C_{19}H_{27}NNaO_3$ $[M+Na]^+$: 340.1883, found: 340.1894.

(3*R*, 4*RS*)-5-(4-isopropylphenyl)-4-methyl-3-phenylpentanal (68l)

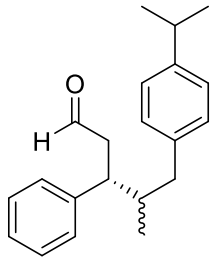

Prepared according to the general procedure using cinnamaldehyde (39.6 mg, 0.3 mmol, 3 equiv.) and diethyl 4-(1-(4-isopropylphenyl)propan-2-yl)-2,6-dimethyl-1,4-dihydropyridine-3,5-dicarboxylate (41.4 mg, 0.1 mmol). The crude material was purified by flash column chromatography (eluent hexane:Et_2O 96:4) to give the corresponding product as a colorless oil (16.2 mg, 55% yield, 1:1 mixture of diastereoisomers). The enantiomeric ratio of the corresponding alcohol was determined by SFC analysis on a IE-3 column (CO_2:acetonitrile 100:0 for 1 min, then gradient ramp to 6:4 over 5 min, curve 6; flow rate 3.0 mL/min; λ = 220 nm); first diastereoisomer: τ_{major} = 4.92 min, τ_{minor} = 5.37 min; e.r. 94:6; second diastereoisomer: τ_{major} = 5.22 min, τ_{minor} = 5.09 min; e.r. 93:7. $[\alpha]_D^{26}$ = -5.9° (*c* 0.8, $CHCl_3$). **^{1}H NMR** for diasteroisomeric mixture (400 MHz, $CDCl_3$): δ 9.63 (dt, *J* = 6.4, 2.1 Hz, 2H), 7.37- 7.30 (m, 4H), 7.26-7.18 (m, 6H), 7.16-7.11 (m, 4H), 7.07-7.03 (m, 2H), 6.99 (d, *J* = 8.1 Hz, 2H), 3.29-3.22 (m, 1H), 3.18-3.11 (m, 1H), 2.92- 2.82 (m, 6H), 2.78 (dd, *J* = 13.6, 4.9 Hz, 1H), 2.66 (dd, *J* = 13.4, 4.2 Hz, 1H), 2.23-2.11 (m, 2H), 2.10-1.98 (m, 1H), 1.25 (dd, *J* = 6.9, 6.0 Hz, 12H), 0.88 (d, *J* = 6.6 Hz, 3H), 0.74 (d, *J* = 6.7 Hz, 3H). **^{13}C NMR** for diastereoisomeric mixture (125.6 MHz, $CDCl_3$): δ 202.3, 202.2, 146.5, 146.4, 142.7, 141.4, 138.1, 137.9, 129.0, 128.9, 128.7, 128.6, 128.34, 128.25, 126.7, 126.3, 126.2, 47.3, 46.2, 45.3, 44.7, 40.8, 40.6, 40.3, 40.1, 33.68, 33.66, 24.1, 16.6, 16.2. **HRMS (ESI)**: Exact mass calculated for $C_{21}H_{26}NaO$ $[M+Na]^+$: 317.1876, found: 317.1877.

(3*R*, 4*RS*)-5-(benzo[*d*][1,3]dioxol-5-yl)-4-methyl-3-phenylpentanal (68m)

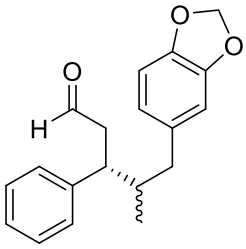

Prepared according to the general procedure using cinnamaldehyde (39.6 mg, 0.3 mmol, 3 equiv.) and diethyl 4-(1-(benzo[d][1,3]dioxol-5-yl)propan-2-yl)-2,6-dimethyl-1,4-dihydropyridine-3,5-dicarboxylate (41.5 mg, 0.1 mmol). The crude material was purified by flash column chromatography (eluent hexane:Et_2O 9:1, two consecutive purifications) to give the corresponding product as a colorless oil (15.1 mg, 51% yield, 1:1 mixture of diastereoisomers). The enantiomeric ratio of the corresponding alcohol was determined by SFC analysis on a ID-3 column (CO_2:acetonitrile 100:0 for 1 min, then gradient ramp to 6:4 over 5 min, curve 6; flow rate 3.0 mL/min; λ = 287 nm); first diastereoisomer: τ_{major} = 4.03 min, τ_{minor} = 4.73 min; e.r. 96:4; second diastereoisomer: τ_{major} = 4.47 min, τ_{minor} = 5.13 min; e.r. 95:5. $[\alpha]_D^{26}$ = -7.7° (*c* 0.38, $CHCl_3$). **^{1}H NMR** for diasteroisomeric mixture (400 MHz, $CDCl_3$): δ 9.65 (t, *J* = 2.1 Hz, 1H), 9.63 (t, *J* = 2.1 Hz, 1H), 7.37-7.31 (m, 4H), 7.25-7.18 (m, 6H), 6.74 (d, *J* = 7.9 Hz, 1H), 6.72 (d, *J* = 7.9 Hz, 1H), 6.63-6.50 (m, 4H), 5.92 (s, 2H), 5.91 (s, 2H), 3.26 (td, *J* = 8.2, 6.8 Hz, 1H), 3.13 (td, *J* = 8.2, 6.8 Hz, 1H), 2.91-2.87 (m, 2H), 2.86-2.82 (m, 2H), 2.74 (dd, *J* = 13.4, 4.8 Hz, 1H), 2.61 (dd, *J* = 13.3, 4.2 Hz, 1H), 2.16-2.03 (m, 2H), 2.06-1.92 (m, 2H), 0.88 (d, *J* = 6.6 Hz, 3H), 0.75 (d, *J* = 6.6 Hz, 3H). **^{13}C NMR** for diastereoisomeric mixture (125.6 MHz, $CDCl_3$): δ 202.2, 202.0, 147.6, 147.5, 145.7, 145.6, 142.7, 141.3, 134.7, 134.5, 128.7, 128.6, 128.4, 128.2, 126.7, 121.9, 121.8, 109.3, 109.2, 108.1, 108.0, 100.8, 100.7, 47.2, 46.3, 45.2, 44.6, 41.0, 40.7, 40.5, 40.2, 16.5, 16.0. **HRMS (ESI)**: Exact mass calculated for $C_{19}H_{20}NaO_3$ $[M+Na]^+$: 319.1305, found: 319.1313.

(3*R*, 4*RS*)-4,8-dimethyl-3-phenylnon-8-enal (68n)

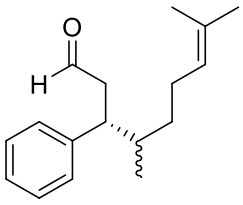

Prepared according to the general procedure using cinnamaldehyde (39.6 mg, 0.3 mmol, 3 equiv.) and diethyl 2,6-dimethyl-4-(6-methylhept-5-en-2-yl)-1,4-dihydropyridine-3,5-dicarboxylate (36.0 mg, 0.1 mmol). The crude material was purified by flash column chromatography (eluent hexane:Et_2O 99.7:0.3) to give the corresponding product as a colorless oil (11.5 mg, 47% yield, 1:1 mixture of diastereoisomers). The enantiomeric ratio of the corresponding alcohol was determined by SFC analysis on a CEL2 column (CO_2:*i*-PrOH 94:6, curve 6; flow rate 1.8 mL/min; λ = 215 nm); first

diastereoisomer: τ_{major} = 4.60 min, τ_{minor} = 3.42 min; e.r. 95:5; second diastereoisomer: τ_{major} = 3.90 min, τ_{minor} = 3.65 min; e.r. 95:5. $[\alpha]_D^{26}$ = -10.6° (*c* 0.40, $CHCl_3$). **^{1}H NMR** for diasteroisomeric mixture (400 MHz, $CDCl_3$): δ 9.61 (q, *J* = 2.2 Hz, 2H), 7.33-7.26 (m, 4H), 7.24-7.13 (m, 6H), 5.09-5.03 (m, 1H), 5.01-4.95 (m, 1H), 3.12 (dq, *J* = 14.6, 7.3 Hz, 2H), 2.82-2.73 (m, 4H), 1.97 (m, 4H), 1.77-1.68 (m, 2H), 1.68 (d, *J* = 1.4 Hz, 3H), 1.65 (d, *J* = 1.4 Hz, 3H). 1.60 (d, *J* = 1.3 Hz, 3H), 1.55 (t, *J* = 1.3 Hz, 3H), 1.50-1.39 (m, 1H), 1.37-1.19 (m, 1H), 1.12-0.97 (m, 2H), 0.91 (d, *J* = 7.2 Hz, 3H), 0.78 (d, *J* = 6.8 Hz, 3H). **^{13}C NMR** for diastereoisomer 1 (125.6 MHz, $CDCl_3$): δ 202.5, 142.8, 131.6, 128.4, 128.2, 126.5, 124.3, 46.2, 45.4, 38.0, 34.1, 25.7, 25.5, 17.6, 16.7. **^{13}C NMR** for diastereoisomer 2 (125.6 MHz, $CDCl_3$): δ 202.4, 141.9, 131.5, 128.5, 128.3, 126.5, 124.3, 47.2, 45.0, 37.7, 34.4, 25.7, 25.6, 17.7, 16.4. **HRMS (ESI)**: Exact mass calculated for $C_{17}H_{24}NaO$ $[M+Na]^+$: 267.1719, found: 267.1711.

(3*R*, 4*RS*)-4-methyl-3-phenylhept-6-enal (68o)

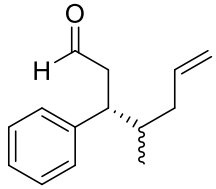

Prepared according to the general procedure using cinnamaldehyde (39.6 mg, 0.3 mmol, 3 equiv.) and dihydropyridine **67o** (32.1 mg, 0.1 mmol). The crude material was purified by flash column chromatography (eluent pentane:Et_2O 99:1) to give the corresponding product as a colorless oil (9.5 mg, 47% yield, 1.4:1 mixture of diastereoisomers). The enantiomeric ratio of the corresponding alcohol was determined by SFC analysis on a CEL2 column (CO_2:*i*-PrOH 93:7, curve 6; flow rate 1.0 mL/min; λ = 215 nm); major diastereoisomer: τ_{major} = 5.50 min, τ_{minor} = 4.39 min; e.r. 95:5; minor diastereoisomer: τ_{major} = 5.16 min, τ_{minor} = 4.75 min; e.r. 95:5. $[\alpha]_D^{26}$ = -24.0° (*c* 0.23, $CHCl_3$). **^{1}H NMR** for diasteroisomeric mixture (400 MHz, $CDCl_3$): δ 9.61 (m, 2H), 7.33-7.38 (m, 4H), 7.24-7.15 (m, 6H), 5.85-5.66 (m, 2H), 5.08-4.92 (m, 4H), 3.21-3.07 (m, 2H), 2.84-2.76 (m, 4H), 2.25-2.16 (m, 1H), 2.10-2.03 (m, 1H), 1.90-1.79 (m, 3H), 1.78-1.69 (m, 1H), 0.94 (d, *J* = 6.6 Hz, 3H), 0.78 (d, *J* = 6.6 Hz, 3H). **^{13}C NMR** for diastereoisomeric mixture (125.6 MHz, $CDCl_3$): δ 202.3, 202.1, 142.7, 141.6, 136.8, 128.6, 128.5, 128.3, 128.2, 126.6, 116.5, 116.4, 47.2, 46.4, 45.0, 44.3, 38.8, 38.7, 38.3, 37.9, 16.7, 16.4. **HRMS (ESI)**: Exact mass calculated for $C_{15}H_{22}NaO_2$ $[M+Na+MeOH]^+$: 257.1512, found: 257.1505.

(*S*)-3-((3aR,4?,6R,6aR)-6-(2,4-dioxo-3,4-dihydropyrimidin-1(2H)-yl)-2,2-dimethyltetrahydrofuro[3,4-d][1,3]dioxol-4-yl)-3-phenylpropanal (68t)

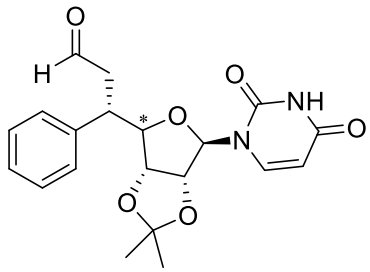

Prepared according to the general procedure using cinnamaldehyde (39.6 mg, 0.3 mmol, 3 equiv.) and dihydropyridine **67t** (50.6 mg, 0.1 mmol), along with organocatalyst **63a** (14.0 mg, 0.02 mmol, 20 mol%) in CH_2Cl_2 (0.4 mL). The crude material was purified by flash column chromatography (pure Et_2O as eluent) to give the corresponding product as a colorless oil (22.7 mg, 59% yield, 1:1.5:7 mixture of three diastereoisomers). Unfortunately we were unable to determine the exact configuration of the main diastereoisomer. **Characterisation of the major diastereoisomer: ^{1}H NMR** (500 MHz, $CDCl_3$): δ 9.64 (br s, 1H), 9.45 (br s, 1H), 7.37-7.22 (m, 5H), 7.00 (d, *J* = 8.0 Hz, 1H), 5.71 (dd, *J* = 8.0, 1.7 Hz, 1H), 5.62 (d, *J* = 2.1 Hz, 1H), 4.94 (dd, *J* = 6.6, 2.1 Hz, 1H), 4.67 (dd, *J* = 6.6, 4.3 Hz, 1H), 4.28 (dd, *J* = 8.7, 4.3 Hz, 1H), 3.72 (dt, *J* = 8.5, 7.1 Hz, 1H), 2.99 (ddd, *J* = 17.1, 6.6, 1.7 Hz, 1H), 2.76 (ddd, *J* = 17.1, 7.5, 1.6 Hz, 1H), 1.49 (s, 3H), 1.23 (s, 3H). **^{13}C NMR** (125.6 MHz, $CDCl_3$): δ 200.7, 163.3, 150.0, 142.6, 139.2, 128.9, 128.5, 127.5, 114.4, 102.8, 94.5, 90.0, 83.9, 81.8, 47.0, 42.5, 27.1, 25.2. **HRMS (ESI)**: Exact mass calculated for $C_{20}H_{22}N_2NaO_6$ $[M+Na]^+$: 409.1370, found: 409.1383.

(*R*)-4-ethyl-3-(*o*-tolyl)hexanal (68u)

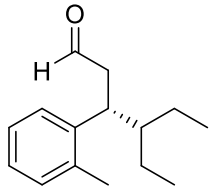

Prepared according to the general procedure using 3-(*o*-tolyl)acrylaldehyde (44.0 mg, 0.3 mmol, 3 equiv.) and diethyl 2,6-dimethyl-4-(pentan-3-yl)-1,4-dihydropyridine-3,5-dicarboxylate (32.3 mg, 0.1 mmol) in acetonitrile (0.2 mL). The crude material was purified by flash column chromatography (eluent hexane:Et_2O 99:1) to give the corresponding product as a colourless oil (10.7 mg, 49% yield). The enantiomeric ratio of the corresponding alcohol was determined by SFC analysis on a CEL2 column (CO_2:*i*-PrOH 100:0 for 1 min, then gradient ramp to 6:4 over 5 min, curve 6; flow rate 2.0 mL/min; λ = 215 nm); τ_{major} = 3.35 min, τ_{minor} = 3.59 min; e.r. 89:11. $[\alpha]_D^{26}$ = +6.5° (*c* 0.5, $CHCl_3$). **^{1}H NMR** (500 MHz, $CDCl_3$): δ 9.54 (t, *J* = 2.3 Hz, 1H), 7.19-7.08 (m, 4H), 3.49 (q, *J* = 7.6 Hz, 1H), 2.76-2.74 (m, 2H), 2.38 (s, 3H), 1.61-1.49 (m, 2H), 1.37-1.23 (m, 2H), 1.21-1.12 (m, 1H), 0.86 (t, *J* = 7.4 Hz, 3H), 0.84 (t, *J* = 7.4 Hz, 3H). **^{13}C NMR** (125.6 MHz,

$CDCl_3$): δ 202.6, 141.7, 136.2, 130.6, 126.8, 126.1, 126.0, 46.6, 45.2, 36.9, 22.3, 21.4, 20.0, 11.3, 10.3. **HRMS (ESI)**: Exact mass calculated for $C_{16}H_{26}NaO_2$ $[M+Na+MeOH]^+$: 273.1825, found: 273.1822.

(*R*)-4-ethyl-3-(*p*-tolyl)hexanal (68v)

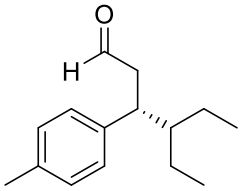

Prepared according to the general procedure using 3-(*p*-tolyl)acrylaldehyde (44.0 mg, 0.3 mmol, 3 equiv.) and diethyl 2,6-dimethyl-4-(pentan-3-yl)-1,4-dihydropyridine-3,5-dicarboxylate (32.3 mg, 0.1 mmol) in acetonitrile (0.2 mL). The crude material was purified by flash column chromatography (eluent hexane:Et_2O 99:1) to give the corresponding product as a colourless oil (14.6 mg, 67% yield). The enantiomeric ratio of the corresponding alcohol was determined by SFC analysis on a CEL2 column (CO_2:MeOH 100:0 for 1 min, then gradient ramp to 6:4 over 5 min, curve 6; flow rate 2.0 mL/min; λ = 220 nm); τ_{major} = 2.61 min, τ_{minor} = 2.71 min; e.r. 89:11. $[\alpha]_D^{26}$ = -6.3° (*c* 0.7, $CHCl_3$). **^{1}H NMR** (500 MHz, $CDCl_3$): δ 9.59 (t, *J* = 2.3 Hz, 1H), 7.12-7.04 (m, 4H), 3.21 (q, *J* = 7.4 Hz, 1H), 2.75-2.71 (m, 2H), 2.32 (s, 3H), 1.49-1.22 (m, 4H), 1.17-1.05 (m, 1H), 0.90 (t, *J* = 7.4 Hz, 3H), 0.83 (t, *J* = 7.4 Hz, 3H). **^{13}C NMR** (125.6 MHz, $CDCl_3$): δ 202.8, 139.6, 135.9, 129.1, 128.1, 46.8, 46.0, 41.5, 22.3, 21.9, 21.0, 11.1, 10.8. **HRMS (ESI)**: Exact mass calculated for $C_{15}H_{22}NaO$ $[M+Na]^+$: 241.1563, found: 241.1573.

(*R*)-3-(2-chlorophenyl)-4-ethylhexanal (68w)

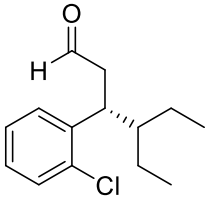

Prepared according to the general procedure using 3-(2-chlorophenyl)acrylaldehyde (50.0 mg, 0.3 mmol, 3 equiv.) and diethyl 2,6-dimethyl-4-(pentan-3-yl)-1,4-dihydropyridine-3,5-dicarboxylate (32.3 mg, 0.1 mmol) in acetonitrile (0.2 mL). The crude material was purified by flash column chromatography (eluent hexane:Et_2O 99:1) to give the corresponding product as a colourless oil (13.1 mg, 55% yield). The enantiomeric ratio of the corresponding alcohol was determined by SFC analysis on a CEL2 column (CO_2:EtOH 100:0 for 1 min, then gradient ramp to 6:4 over 5 min, curve 6; flow rate 2.0 mL/min; λ = 215 nm); τ_{major} = 3.04 min, τ_{minor} = 3.23 min; e.r. 91:9. $[\alpha]_D^{26}$ = -12.6° (*c* 0.33, $CHCl_3$). **^{1}H NMR** (500 MHz, $CDCl_3$): δ 9.57 (dd, *J* = 3.1, 1.7 Hz, 1H), 7.37 (dd, *J* = 7.9, 1.2 Hz, 1H), 7.25-7.12 (m, 3H), 3.88-3.81 (m, 1H), 2.82-2.66 (m, 2H), 1.67-1.61 (m, 1H),

1.57-1.46 (m, 1H), 1.37-1.27 (m, 2H), 1.25-1.14 (m, 1H), 0.87 (t, J = 7.4 Hz, 6H). **^{13}C NMR** (125.6 MHz, $CDCl_3$): δ 201.9, 141.4, 132.1, 129.6, 128.5, 46.7, 45.9, 41.2, 22.3, 21.9, 11.0, 10.8. **HRMS (ESI)**: Exact mass calculated for $C_{15}H_{23}ClNaO_2$ $[M+Na+MeOH]^+$: 293.1279, found: 293.1268.

(*R*)-3-(4-chlorophenyl)-4-ethylhexanal (68x)

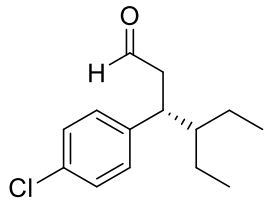

Prepared according to the general procedure using 3-(4-chlorophenyl)acrylaldehyde (50.0 mg, 0.3 mmol, 3 equiv.) and diethyl 2,6-dimethyl-4-(pentan-3-yl)-1,4-dihydropyridine-3,5-dicarboxylate (32.3 mg, 0.1 mmol) in acetonitrile (0.2 mL). The crude material was purified by flash column chromatography (eluent hexane:Et_2O 98.5:1.5) to give the corresponding product as a colourless oil (10.5 mg, 44% yield). The enantiomeric ratio of the corresponding alcohol was determined by SFC analysis on a CEL2 column (CO_2:*i*-PrOH 100:0 for 1 min, then gradient ramp to 6:4 over 5 min, curve 6; flow rate 2.0 mL/min; λ = 221 nm); τ_{major} = 3.42 min, τ_{minor} = 3.53 min; e.r. 88:12. $[\alpha]_D^{26}$ = +3.2° (*c* 0.55, $CHCl_3$). **^{1}H NMR** (500 MHz, $CDCl_3$): δ 9.62 (t, J = 2.3 Hz, 1H), 7.30-7.26 (m, 2H), 7.15-7.10 (m, 2H), 3.28-3.22 (m, 1H), 2.82-2.71 (m, 2H), 1.49-1.22 (m, 4H), 1.16-1.05 (m, 1H), 0.91 (t, J = 7.4 Hz, 3H), 0.84 (t, J = 7.4 Hz, 3H). **^{13}C NMR** (125.6 MHz, $CDCl_3$): δ 201.9, 141.4, 132.1, 129.6, 128.5, 46.7, 45.9, 41.2, 22.3, 21.9, 11.0, 10.8. **HRMS (ESI)**: Exact mass calculated for $C_{15}H_{23}ClNaO_2$ $[M+Na+MeOH]^+$: 293.1279, found: 293.1280.

(*R*)-4-ethyl-3-(4-methoxyphenyl)hexanal (68aa)

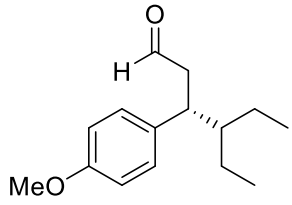

Prepared according to the general procedure using 3-(4-methoxyphenyl)acrylaldehyde (48.7 mg, 0.3 mmol, 3 equiv.) and diethyl 2,6-dimethyl-4-(pentan-3-yl)-1,4-dihydropyridine-3,5-dicarboxylate (32.3 mg, 0.1 mmol) along with TFA (0.1 mmol, 1 equiv.) in acetonitrile (0.2 mL). The crude material was purified by flash column chromatography (eluent hexane:Et_2O 9:1) to give the corresponding product as a colourless oil (16.2 mg, 69% yield). The enantiomeric ratio of the corresponding alcohol was determined by HPLC analysis on an Agilent IC-3 column (hexane:*i*-PrOH 9:1; flow rate 0.6 mL/min; λ = 215 nm); τ_{major} = 15.9 min, τ_{minor} = 13.7 min;

e.r. 80:20. $[\alpha]_D^{26}$ = -4.65° (*c* 0.82, $CHCl_3$). **^{1}H NMR** (500 MHz, $CDCl_3$): δ 9.58 (t, *J* = 2.3 Hz, , 1H), 7.10-7.05 (m, 2H), 6.85-6.81 (m, 2H), 3.79 (s, 3H), 3.20 (q, *J* = 7.2 Hz, 1H), 2.74-2.70 (m, 2H), 1.48-1.22 (m, 4H), 1.15-1.04 (m, 1H), 0.90 (t, *J* = 7.3 Hz, 3H), 0.82 (t, *J* = 7.4 Hz, 3H). **^{13}C NMR** (125.6 MHz, $CDCl_3$): δ 202.8, 158.0, 134.6, 129.1, 113.7, 55.1, 46.8, 46.1, 41.0, 22.2, 21.9, 11.1, 10.8. **HRMS (ESI)**: Exact mass calculated for $C_{15}H_{22}NaO_2$ $[M+Na]^+$: 257.1512, found: 257.1515.

6.10 Cyclic voltammetry experiments

The CV traces of compounds analysed in this document are reported. In all cases experiments were performed in acetonitrile, ferrocene was added as internal standard, and its reduction potential set to + 0.42 V *vs* SCE.[8]

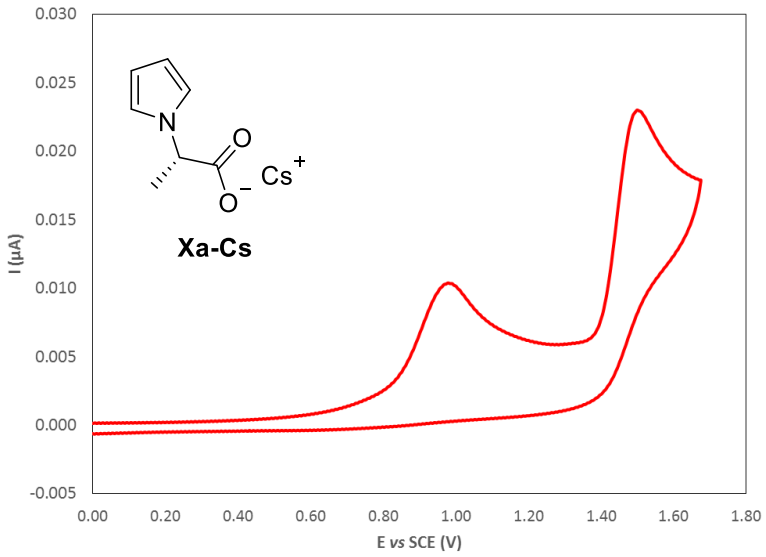

E_P (1)	+ 0.99 V
$E_{P/2}$ (1)	+ 0.90 V
E_P (2)	+ 1.50 V
$E_{P/2}$ (2)	+ 1.45 V

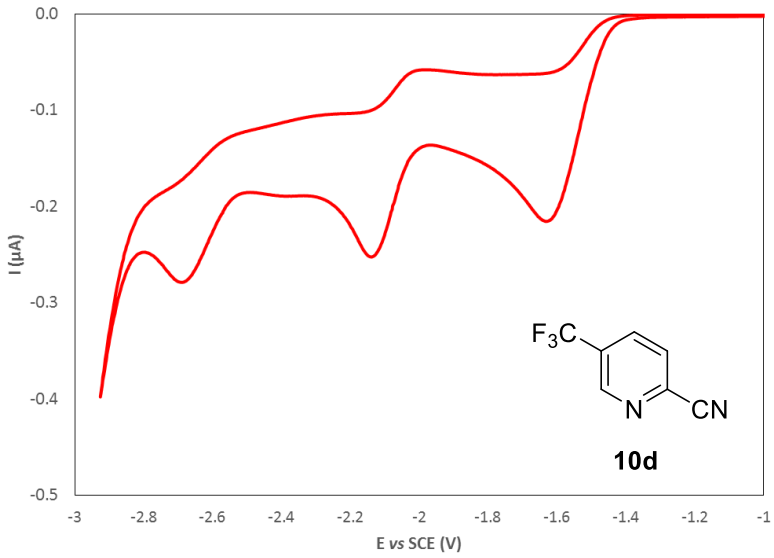

E_P (1)	- 1.62 V
$E_{P/2}$ (1)	- 1.53 V
E_P (2)	- 2.13 V
$E_{P/2}$ (2)	- 2.07 V
E_P (3)	- 2.69 V
$E_{P/2}$ (3)	- 2.61 V

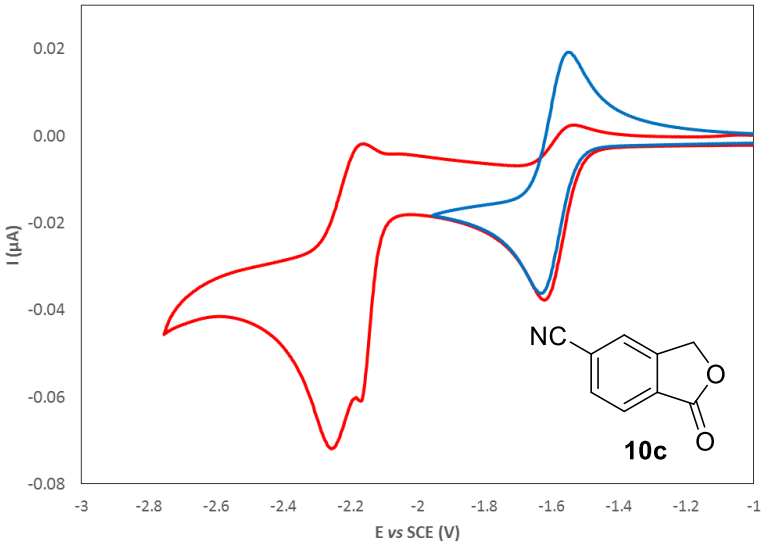

$E^{1/2}$ (1)	- 1.59 V
E^{p} (2)	- 2.25 V
$E^{p/2}$ (2)	- 2.14 V

6.11 Fluorescence quenching experiments

Results concerning quenching experiments with 4CzIPN and PXX as photocatalysts and various quenchers are summarised here. Graphs represent I_0/I in function of the concentration of quencher $[Q]$, and trend lines are in the form (Stern-Volmer relationship):[259]

$$\frac{I_0}{I} = K_{SV}[Q] + 1$$

where I_0 is the intensity of fluorescence at the specified wavelenght in the absence of quencher, I the intensity of fluorescence in the presence of a concentration $[Q]$ of quencher, and K_{SV} is the Stern-Volmer constant. This also equals to:

$$K_{SV} = k_Q \cdot \tau_0$$

where τ_0 is the lifetime of the excited state of the photocatalyst in the absence of quencher and k_Q the rate of the quenching process. K_{SV} and k_Q are useful parameters to compare quenching efficiency of different quenchers.

Quenching experiments on 4CzIPN (Chapter 2)

Emission of a 10^{-4} M solution of 4CzIPN in acetone recorded at 530 nm in the presence of selected quenchers.

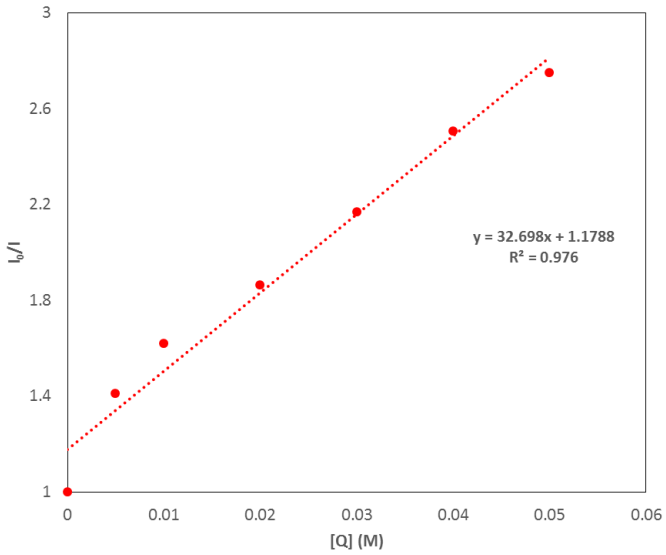
y = 32.698x + 1.1788
R² = 0.976
I₀/I
[Q] (M)

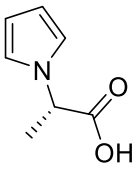

11a

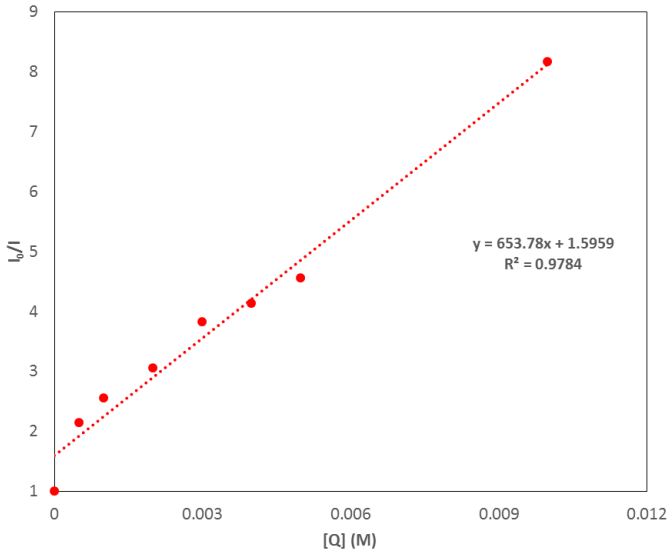
y = 653.78x + 1.5959
R² = 0.9784
I₀/I
[Q] (M)

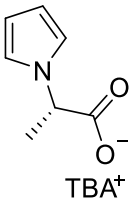

11a-TBA

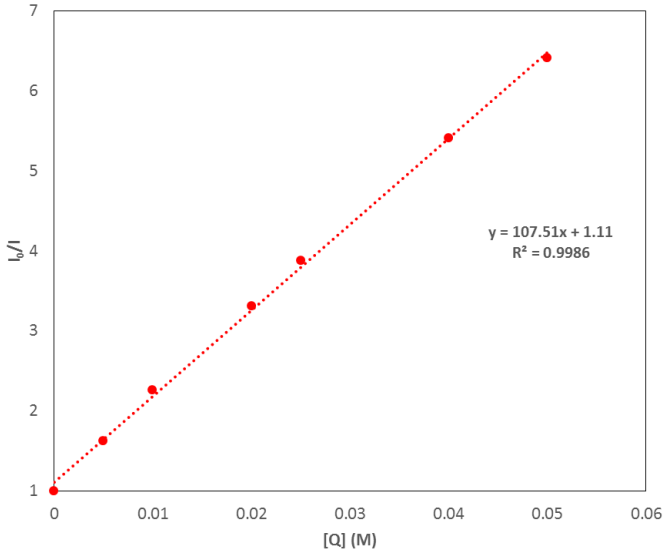
y = 107.51x + 1.11
R² = 0.9986
I₀/I
[Q] (M)

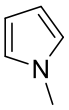

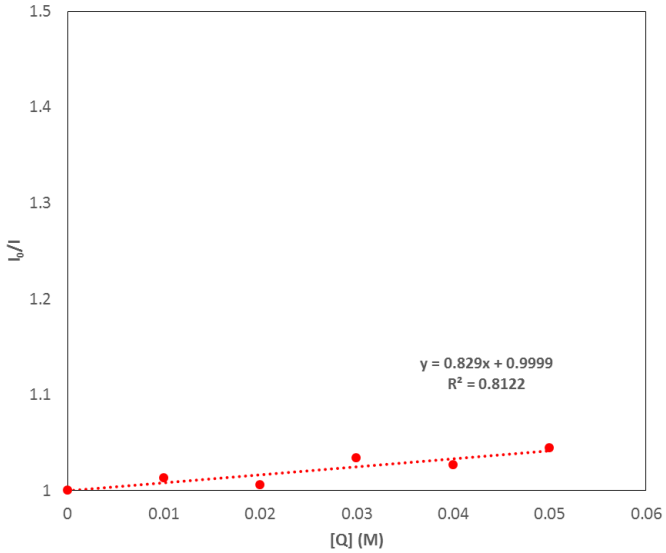

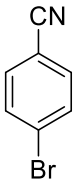

Quenching experiments on PXX (Chapter 3)

Emission of a $4 \cdot 10^{-5}$ M solution of PXX in acetonitrile recorded at 477 nm in the presence of selected quenchers.

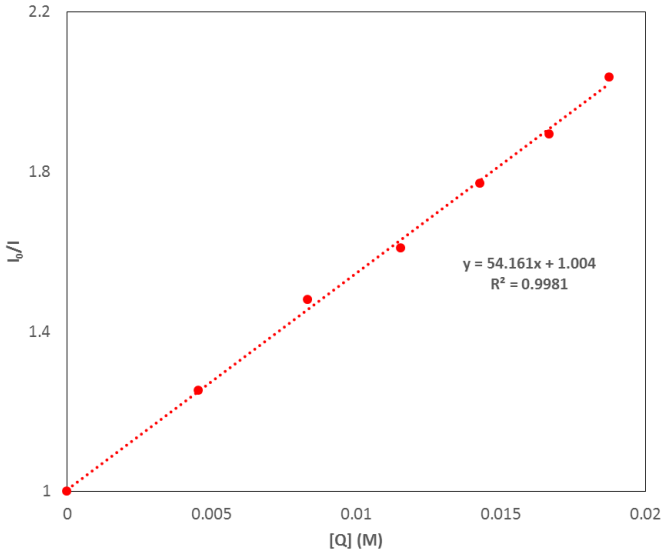

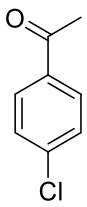

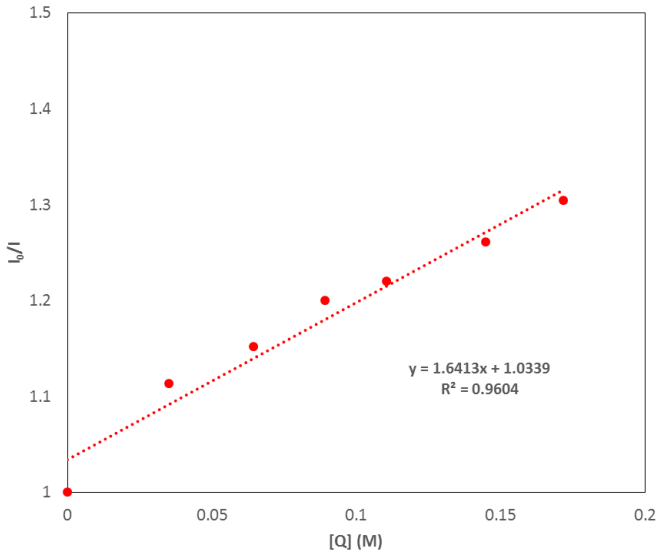
1.5
1.4
1.3
1.2
1.1
1
I_0/I
0
0.05
0.1
0.15
0.2
[Q] (M)
y = 1.6413x + 1.0339
R² = 0.9604

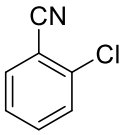
CN
Cl

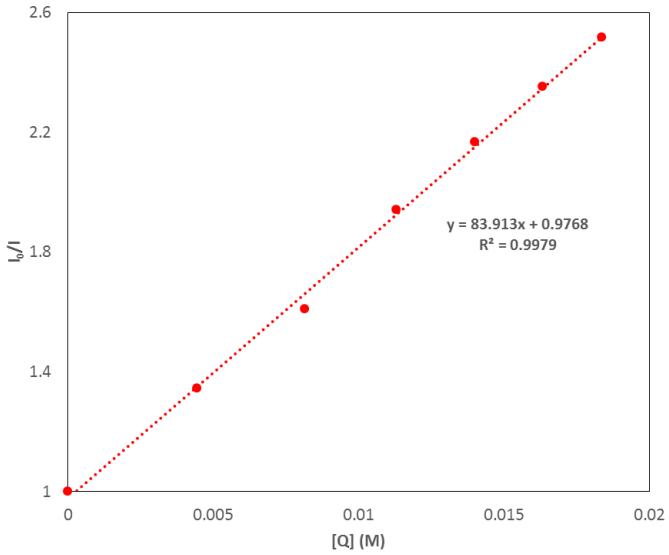
2.6
2.2
1.8
1.4
1
I_0/I
0
0.005
0.01
0.015
0.02
[Q] (M)
y = 83.913x + 0.9768
R² = 0.9979

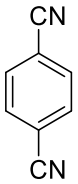
CN
CN

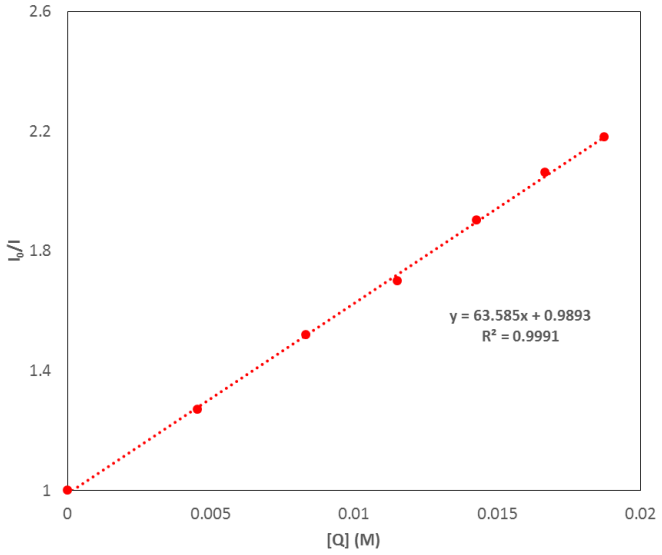
2.6
2.2
1.8
1.4
1
I_0/I
0
0.005
0.01
0.015
0.02
[Q] (M)
y = 63.585x + 0.9893
R² = 0.9991

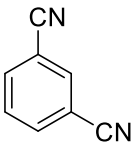
CN
CN

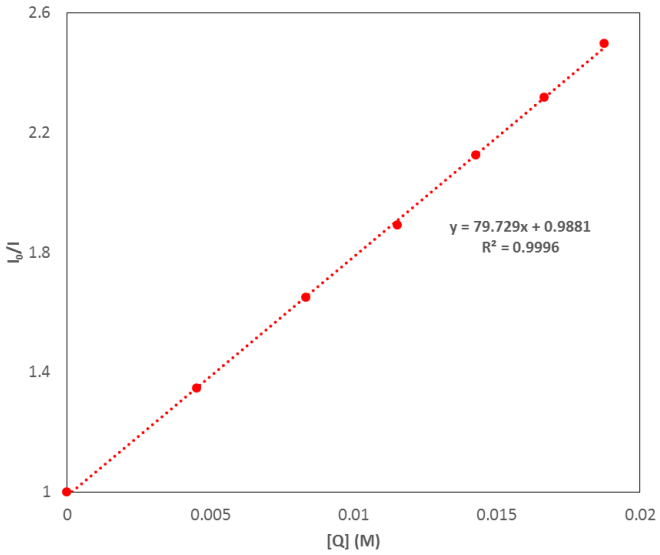
2.6
2.2
1.8
1.4
1
I_0/I
y = 79.729x + 0.9881
R² = 0.9996
0
0.005
0.01
0.015
0.02
[Q] (M)

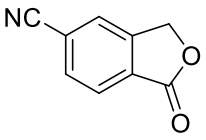
NC
O
O

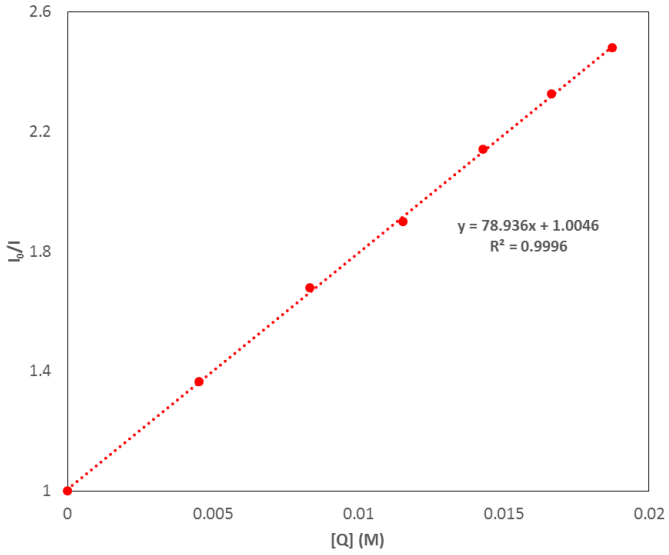
2.6
2.2
1.8
1.4
1
I_0/I
y = 78.936x + 1.0046
R² = 0.9996
0
0.005
0.01
0.015
0.02
[Q] (M)

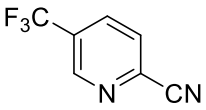
F_3C
N
CN

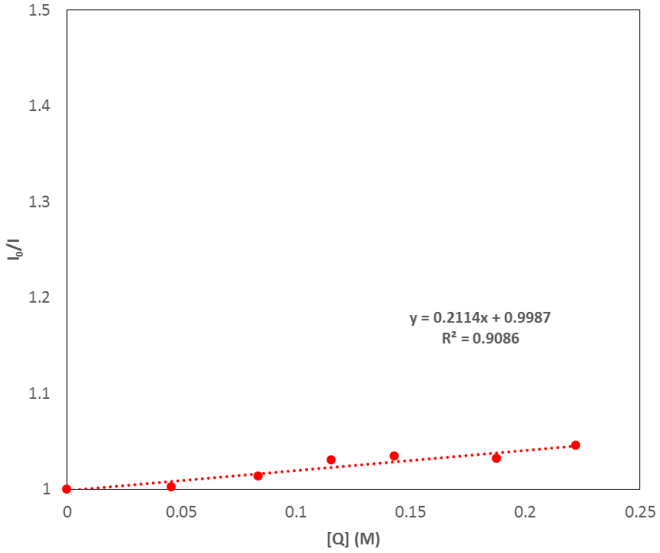
1.5
1.4
1.3
1.2
1.1
1
I_0/I
y = 0.2114x + 0.9987
R² = 0.9086
0
0.05
0.1
0.15
0.2
0.25
[Q] (M)

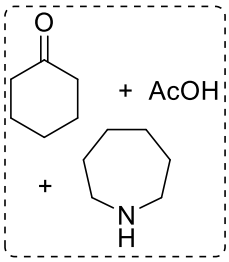
O
+ AcOH
+
N
H

1 : 1 : 1

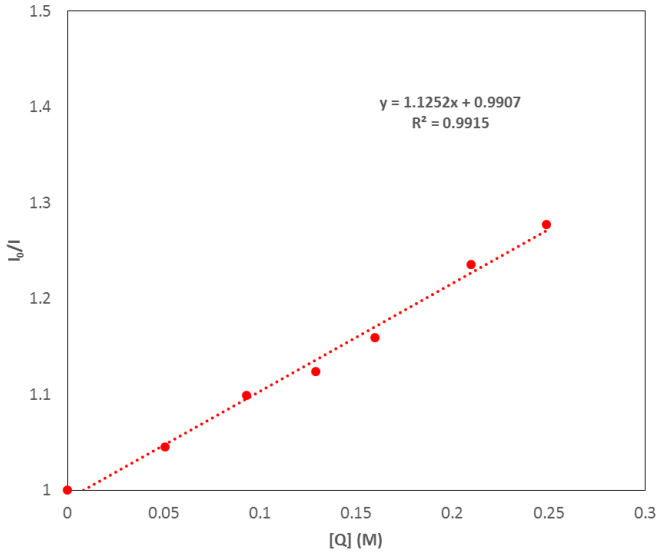
y = 1.1252x + 0.9907
R² = 0.9915
I0/I
[Q] (M)
1.5
1.4
1.3
1.2
1.1
1
0
0.05
0.1
0.15
0.2
0.25
0.3

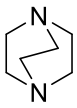
N
N

References

[1] M. Yan, J. C. Lo, J. T. Edwards, P. S. Baran, *J. Am. Chem. Soc.* **2016**, *138*, 12692–12714.

[2] M. H. Shaw, J. Twilton, D. W. C. MacMillan, *J. Org. Chem.* **2016**, *81*, 6898–6926.

[3] R. C. McAtee, E. J. Mcclain, C. R. J. Stephenson, *Trends Chem.* **2019**, *1*, 111–125.

[4] D. A. Nicewicz, D. W. C. MacMillan, *Science* **2008**, *322*, 77–80.

[5] M. A. Ischay, M. E. Anzovino, J. Du, T. P. Yoon, *J. Am. Chem. Soc.* **2008**, *130*, 12886–12887.

[6] J. M. R. Narayanam, J. W. Tucker, C. R. J. Stephenson, *J. Am. Chem. Soc.* **2009**, *131*, 8756–8757.

[7] C. K. Prier, D. A. Rankic, D. W. C. MacMillan, *Chem. Rev.* **2013**, *113*, 5322–5363.

[8] H. G. Roth, N. A. Romero, D. A. Nicewicz, *Synlett* **2016**, *27*, 714–723.

[9] M. A. Cismesia, T. P. Yoon, *Chem. Sci.* **2015**, *6*, 5426–5434.

[10] F. Strieth-Kalthoff, M. J. James, M. Teders, L. Pitzer, F. Glorius, *Chem. Soc. Rev.* **2018**, *47*, 7190–7202.

[11] K. L. Skubi, T. R. Blum, T. P. Yoon, *Chem. Rev.* **2016**, *116*, 10035–10074.

[12] J. Twilton, C. C. Le, P. Zhang, M. H. Shaw, R. W. Evans, D. W. C. Macmillan, *Nat. Rev.* **2017**, *1*, Article number: 0052.

[13] L. N. Cavalcanti, G. A. Molander, *Top. Curr. Chem.* **2016**, *374*, 39.

[14] M. Silvi, P. Melchiorre, *Nature* **2018**, *554*, 41–49.

[15] N. A. Romero, D. A. Nicewicz, *Chem. Rev.* **2016**, *116*, 10075–10166.

[16] D. Ravelli, M. Fagnoni, A. Albini, *Chem. Soc. Rev.* **2013**, *42*, 97–113.

[17] D. P. Hari, B. König, *Chem. Commun.* **2014**, *50*, 6688–6699.

[18] S. Fukuzumi, H. Kotani, K. Ohkubo, S. Ogo, N. V Tkachenko, H. Lemmetyinen, *J. Am. Chem. Soc.* **2004**, *126*, 1600–1601.

[19] A. Joshi-pangu, F. Levesque, H. G. Roth, S. F. Oliver, L. Campeau, D. Nicewicz, D. A. DiRocco, *J. Org. Chem.* **2016**, *81*, 7244–7249.

[20] J. Luo, J. Zhang, *ACS Catal.* **2016**, *6*, 873–877.

[21] C. Pezzetta, D. Bonifazi, R. W. M. Davidson, *Org. Lett.* **2019**, *21*, 8957–8961.

[22] C. Verrier, N. Alandini, C. Pezzetta, M. Moliterno, L. Buzzetti, H. B. Hepburn, A. Vega-Penaloza, M. Silvi, P. Melchiorre, *ACS Catal.* **2018**, *8*, 1062–1066.

[23] A. Sciutto, A. Fermi, A. Folli, T. Battisti, J. M. Beames, D. M. Murphy, D. Bonifazi, *Chem. Eur. J.* **2018**, *24*, 4382–4389.

[24] C. C. C. Johansson Seechurn, M. O. Kitching, T. J. Colacot, V. Snieckus, *Angew. Chem. Int. Ed.* **2012**, *51*, 5062–5085.

[25] F. González-Bobes, G. C. Fu, *J. Am. Chem. Soc.* **2006**, *128*, 5360–5361.

[26] O. Gutierrez, J. C. Tellis, D. N. Primer, G. A. Molander, M. C. Kozlowski, *J. Am. Chem. Soc.* **2015**, *137*, 4896–4899.

[27] J. C. Tellis, D. N. Primer, G. A. Molander, *Science* **2014**, *345*, 433–436.

[28] D. N. Primer, I. Karakaya, J. C. Tellis, G. A. Molander, *J. Am. Chem. Soc.* **2015**, *137*, 2195–2198.

[29] I. Karakaya, D. N. Primer, G. A. Molander, *Org. Lett.* **2015**, *17*, 3294–3297.

[30] J. C. Tellis, J. Amani, G. A. Molander, *Org. Lett.* **2016**, *18*, 2994–2997.

[31] J. Amani, E. Sodagar, G. A. Molander, *Org. Lett.* **2016**, *18*, 732–735.

[32] D. N. Primer, G. A. Molander, *J. Am. Chem. Soc.* **2017**, *139*, 9847–9850.

[33] R. Alam, G. A. Molander, *J. Org. Chem.* **2017**, *82*, 13728–13734.

[34] Z. Zuo, D. T. Ahneman, L. Chu, J. A. Terrett, A. G. Doyle, D. W. C. MacMillan, *Science* **2014**, *345*, 437–440.

[35] A. Noble, S. J. McCarver, D. W. C. Macmillan, *J. Am. Chem. Soc.* **2015**, *137*, 624–627.

[36] C. P. Johnston, R. T. Smith, S. Allmendinger, D. W. C. MacMillan, *Nature* **2016**, *536*, 322–325.

[37] N. A. Till, R. T. Smith, D. W. C. Macmillan, *J. Am. Chem. Soc.* **2018**, *140*, 5701–5705.

[38] V. Corce, L. Chamoreau, E. Derat, J. Goddard, C. Ollivier, L. Fensterbank, *Angew. Chem. Int. Ed.* **2015**, *54*, 11414–11418.

[39] M. Jouffroy, D. N. Primer, G. A. Molander, *J. Am. Chem. Soc.* **2016**, *138*, 475–478.

[40] K. Nakajima, S. Nojima, Y. Nishibayashi, *Angew. Chem. Int. Ed.* **2016**, *55*, 14106–14110.

[41] A. Gutierrez-Bonet, J. C. Tellis, J. K. Matsui, B. A. Vara, G. A. Molander, *ACS Catal.* **2016**, *6*, 8004–8008.

[42] S. O. Badir, A. Dumoulin, J. K. Matsui, G. A. Molander, *Angew. Chem. Int. Ed.* **2018**, *57*, 6610–6613.

[43] A. Dumoulin, J. K. Matsui, A. Gutierrez-Bonet, G. A. Molander, *Angew. Chem. Int. Ed.* **2018**, *57*, 6614–6618.

[44] L. Buzzetti, A. Prieto, S. Raha Roy, P. Melchiorre, *Angew. Chem. Int. Ed.* **2017**, *56*, 15039–15043.

[45] C. Remeur, C. B. Kelly, N. R. Patel, G. A. Molander, *ACS Catal.* **2017**, *7*, 6065–6069.

[46] T. Knauber, R. Chandrasekaran, J. W. Tucker, J. M. Chen, M. Reese, D. A. Rankic, N. Sach, C. Helal, *Org. Lett.* **2017**, *19*, 6566–6569.

[47] E. Dauncey, S. U. Dighe, J. J. Douglas, D. Leonori, *Chem. Sci.* **2019**, *10*, 7728–7753.

[48] D. T. Ahneman, A. G. Doyle, *Chem. Sci.* **2016**, *7*, 7002–7006.

[49] M. H. Shaw, V. W. Shurtleff, J. A. Terrett, J. D. Cuthbertson, D. W. C. MacMillan, *Science* **2016**, *352*, 1304–1308.

[50] C. Le, Y. Liang, R. W. Evans, X. Li, D. W. C. MacMillan, *Nature* **2017**, *547*, 79–83.

[51] I. B. Perry, T. F. Brewer, P. J. Sarver, D. M. Schultz, D. A. DiRocco, D. W. C. MacMillan, *Nature* **2018**, *560*, 70–75.

[52] Y. Shen, Y. Gu, R. Martin, *J. Am. Chem. Soc.* **2018**, *140*, 12200–12209.

[53] B. J. Shields, A. G. Doyle, *J. Am. Chem. Soc.* **2016**, *138*, 12719–12722.

[54] D. R. Heitz, J. C. Tellis, G. A. Molander, *J. Am. Chem. Soc.* **2016**, *2016*, 12715–12718.

[55] K. Wang, W. Kong, *Chin. J. Chem.* **2018**, *36*, 247–256.

[56] S. J. Mohan, E. C. Mohan, M. R. Yamsani, *Int. J. Pharm. Sci. Nanotechnol.* **2009**, *1*, 309–316.

[57] Z. Zuo, H. Cong, W. Li, J. Choi, G. C. Fu, D. W. C. MacMillan, *J. Am. Chem. Soc.* **2016**, *138*, 1832–1835.

[58] M. B. Smith, J. March, *March's Advanced Organic Chemistry - Reactions, Mechanisms and Structure (6th Edition)*, **2007**.

[59] E. E. Stache, T. Rovis, A. G. Doyle, *Angew. Chem. Int. Ed.* **2017**, *56*, 3679–3683.

[60] Q. Q. Zhou, F. D. Lu, D. Liu, L. Q. Lu, W. J. Xiao, *Org. Chem. Front.* **2018**, *5*, 3098–3102.

[61] X. Cheng, H. Lu, Z. Lu, *Nat. Commun.* **2019**, *10*, Article number: 3549.

[62] E. Gandolfo, X. Tang, S. Raha Roy, P. Melchiorre, *Angew. Chem. Int. Ed.* **2019**, *58*, 16854–16858.

[63] M. Baumann, I. R. Baxendale, S. V. Ley, N. Nikbin, *Beilstein J. Org. Chem.* **2011**, *7*, 442–495.

[64] E. F. Godefroi, C. A. M. van der Eijcken, *Imidazole Carboxylates. US Patent 3354173*, **1967**.

[65] D. Belelli, A. L. Muntoni, S. D. Merrywest, L. J. Gentet, A. Casula, H. Callachan, P. Madau, D. K. Gemmell, N. M. Hamilton, J. J. Lambert, K. T. Sillar, J. A. Peters, *Neuropharmacology* **2003**, *45*, 57–71.

[66] R. Desai, K. W. Miller, D. E. Raines, *Anesth. Analg* **2013**, *116*, 573–579.

[67] Y. Xiong, J. Guo, M. R. Candelore, R. Liang, C. Miller, Q. Dallas-yang, G. Jiang, P. E. Mccann, S. A. Qureshi, X. Tong, S. S. Xu, J. Shang, S. H. Vincent, L. M. Tota, M. J. Wright, X. Yang, B. B. Zhang, J. R. Tata, E. R. Parmee, *J. Med. Chem.* **2012**, *55*, 6137–6148.

[68] E. L. Meredith, G. Ksander, L. G. Monovich, J. P. N. Papillon, Q. Liu, K. Miranda, P. Morris, C. Rao, R. Burgis, M. Capparelli, Q. Hu, A. Singh, D. F. Rigel, A. Y. Jeng, M. Beil, F. Fu, C. Hu, D. LaSala, *ACS Med. Chem. Lett.* **2013**, *4*, 1203–1207.

[69] C. W. Jefford, F. De Villedon De Naide, K. Sienkiewicz, *Tetrahedron Asymmetry* **1996**, *7*, 1069–1076.

[70] C. G. M. Janssen, J. B. A. Thijssen, W. L. M. Verluyten, J. J. P. Heykants, *J. Label. C. Radiopharm.* **1987**, *24*, 909–918.

[71] M. Baumann, I. R. Baxendale, *Eur. J. Org. Chem.* **2017**, *2017*, 6518–6524.

[72] M. Manjathuru, A. N. Mayekar, Y. Derambala, P. K. Vasudeva, T. A. Arulmoli, *A Process*

for the Preparation of Etomidate. Indian Patent IN 2011CH04309, **2011**.

[73] J. K. Laha, G. D. Cuny, *J. Org. Chem.* **2011**, *76*, 8477–8482.

[74] J. K. Laha, R. A. Bhimpuria, M. K. Hunjan, *Chem. Eur. J.* **2017**, *23*, 2044–2050.

[75] I. Nilsson, R. Isaksson, *Acta Chem. Scand. B* **1985**, *39*, 531–547.

[76] D. C. Blakemore, L. Castro, I. Churcher, D. C. Rees, A. W. Thomas, D. M. Wilson, A. Wood, *Nat. Chem.* **2018**, *10*, 383–394.

[77] L. Fan, J. Jia, H. Hou, Q. Lefebvre, M. Rueping, *Chem. Eur. J.* **2016**, *22*, 16437–16440.

[78] G. A. Molander, D. Ryu, M. Hosseini-Sarvari, R. Devulapally, D. G. Seapy, *J. Org. Chem.* **2013**, *78*, 6648–6656.

[79] D. Liu, C. Liu, H. Li, A. Lei, *Angew. Chem. Int. Ed.* **2013**, *52*, 4453–4456.

[80] A. R. Katritzky, H. Lang, X. Lan, *Tetrahedron* **1993**, *49*, 2829–2838.

[81] D. Cambie, C. Bottecchia, N. J. W. Straathof, V. Hessel, T. Noël, *Chem. Rev.* **2016**, *116*, 10276–10341.

[82] S. Z. Tasker, E. A. Standley, T. F. Jamison, *Nature* **2014**, *509*, 299–309.

[83] A. H. Hoveyda, D. A. Evans, G. C. Fu, *Chem. Rev.* **1993**, *93*, 1307–1370.

[84] G. Rousseau, B. Breit, *Angew. Chem. Int. Ed.* **2011**, *50*, 2450–2494.

[85] T. T. Tsou, J. K. Kochi, *J. Am. Chem. Soc.* **1979**, *101*, 6319–6332.

[86] S. Bajo, G. Laidlaw, A. R. Kennedy, S. Sproules, D. J. Nelson, *Organometallics* **2017**, *36*, 1662–1672.

[87] D. W. Manley, J. C. Walton, *Org. Lett.* **2014**, *16*, 5394–5397.

[88] K. Donabauer, M. Maity, A. L. Berger, G. S. Huff, S. Crespi, B. König, *Chem. Sci.* **2019**, *10*, 5162–5166.

[89] J. D. Nguyen, E. M. D. Amato, J. M. R. Narayanam, C. R. J. Stephenson, *Nat. Chem.* **2012**, *4*, 854–859.

[90] H. W. Shih, M. N. Vander Wal, R. L. Grange, D. W. C. MacMillan, *J. Am. Chem. Soc.* **2010**, *132*, 13600–13603.

[91] A. Mcnally, C. K. Prier, D. W. C. Macmillan, *Science* **2011**, *334*, 1114–1117.

[92] M. T. Pirnot, D. A. Rankic, D. B. C. Martin, D. W. C. MacMillan, *Science* **2013**, *339*, 1593–1596.

[93] F. R. Petronijevic, M. Nappi, D. W. C. MacMillan, *J. Am. Chem. Soc.* **2013**, *135*, 18323.

[94] Y. Cheng, X. Gu, P. Li, *Org. Lett.* **2013**, *15*, 2664–2667.

[95] I. Ghosh, L. Marzo, A. Das, R. Shaikh, B. König, *Acc. Chem. Res.* **2016**, *49*, 1566–1577.

[96] M. Majek, A. J. Von Wangelin, *Acc. Chem. Res.* **2016**, *49*, 2316–2327.

[97] E. H. Discekici, N. J. Treat, S. O. Poelma, K. M. Mattson, Z. M. Hudson, Y. Luo, C. J. Hawker, J. R. De Alaniz, *Chem. Commun.* **2015**, *51*, 11705–11708.

[98] S. O. Poelma, G. L. Burnett, E. H. Discekici, K. M. Mattson, N. J. Treat, Y. Luo, Z. M. Hudson, S. L. Shankel, P. G. Clark, J. W. Kramer, C. J. Hawker, J. Read De Alaniz, *J. Org. Chem.* **2016**, *81*, 7155–7160.

[99] M. H. Aukland, M. Šiaučiulis, A. West, G. J. P. Perry, D. J. Procter, *Nat. Catal.* **2020**, https://doi.org/10.1038/s41929-019-0415-3.

[100] Y. Du, R. M. Pearson, C.-H. Lim, S. M. Sartor, M. D. Ryan, H. Yang, N. H. Damrauer, G. M. Miyake, *Chem. Eur. J.* **2017**, *23*, 10962–10968.

[101] M. Kudisch, C.-H. Lim, P. Thordarson, G. M. Miyake, *J. Am. Chem. Soc.* **2019**, *141*, 19479–19486.

[102] C. S. Kim, N. Iqbal, G. S. Park, K. Son, E. J. Cho, *Org. Lett.* **2019**, *21*, 9950–9953.

[103] L. Wang, J. Byun, R. Li, W. Huang, K. A. I. Zhang, *Adv. Synth. Catal.* **2018**, *360*, 4312–4318.

[104] R. Matsubara, T. Yabuta, U. Md Idros, M. Hayashi, F. Ema, Y. Kobori, K. Sakata, *J. Org. Chem.* **2018**, *83*, 9381–9390.

[105] I. Ghosh, T. Ghosh, J. I. Bardagi, B. Konig, *Science* **2014**, *346*, 725–728.

[106] L. Zeng, T. Liu, C. He, D. Shi, F. Zhang, C. Duan, *J. Am. Chem. Soc.* **2016**, *138*, 3958–3961.

[107] I. Ghosh, B. Konig, *Angew. Chem. Int. Ed.* **2016**, *55*, 7676–7679.

[108] R. S. Shaikh, S. J. S. Düsel, B. König, *ACS Catal.* **2016**, *6*, 8410–8414.

[109] A. Graml, I. Ghosh, B. König, *J. Org. Chem.* **2017**, *82*, 3552–3560.

[110] X. Li, D. Liang, W. Huang, H. Sun, L. Wang, M. Ren, B. Wang, Y. Ma, *Tetrahedron* **2017**, *73*, 7094–7099.

[111] J. I. Bardagi, I. Ghosh, M. Schmalzbauer, T. Ghosh, B. König, *Eur. J. Org. Chem.* **2018**, 34–40.

[112] M. Neumeier, D. Sampedro, M. Májek, V. A. de la Peña O'Shea, A. Jacobi von Wangelin, R. Pérez-Ruiz, *Chem. Eur. J.* **2018**, *24*, 105–108.

[113] M. Schmalzbauer, I. Ghosh, B. König, *Faraday Discuss.* **2019**, *215*, 364–378.

[114] N. G. W. Cowper, C. P. Chernowsky, O. P. Williams, Z. K. Wickens, *J. Am. Chem. Soc.* **2020**, *142*, 2093–2099.

[115] I. Ghosh, R. S. Shaikh, B. König, *Angew. Chem. Int. Ed.* **2017**, *56*, 8544–8549.

[116] M. Marchini, G. Bergamini, P. G. Cozzi, P. Ceroni, V. Balzani, *Angew. Chem. Int. Ed.* **2017**, *56*, 12820–12821.

[117] I. Ghosh, J. I. Bardagi, B. König, *Angew. Chem. Int. Ed.* **2017**, *56*, 12822–12824.

[118] M. Majek, U. Faltermeier, B. Dick, R. Pérez-Ruiz, A. J. von Wangelin, *Chem. Eur. J.* **2015**, *21*, 15496–15501.

[119] T. Miletić, A. Fermi, I. Orfanos, A. Avramopoulos, F. De Leo, N. Demitri, G. Bergamini, P. Ceroni, M. G. Papadopoulos, S. Couris, D. Bonifazi, *Chem. Eur. J.* **2017**, *23*, 2363–2378.

[120] N. Kobayashi, M. Sasaki, K. Nomoto, *Chem. Mater.* **2009**, *21*, 552–556.

[121] N. Kobayashi, M. Sasaki, T. Ohe, *Semiconductor Device, Method of Manufacturing the Same, and Method of Forming Multilayer Semiconductor Thin Film. US Patent 2012/0025173 A1*, **2012**.

[122] H. Li, F. Zhang, S. Qiu, N. Lv, Z. Zhao, Q. Li, Z. Cui, *Chem. Commun.* **2013**, *49*, 10492–10494.

[123] N. Lv, M. Xie, W. Gu, H. Ruan, S. Qiu, C. Zhou, Z. Cui, *Org. Lett.* **2013**, *15*, 2382–2385.

[124] C. Song, T. M. Swager, *Macromolecules* **2009**, *42*, 1472–1475.

[125] D. Stassen, N. Demitri, D. Bonifazi, *Angew. Chem. Int. Ed.* **2016**, *55*, 5947–5951.

[126] M. S. Oderinde, M. Frenette, D. W. Robbins, B. Aquila, J. W. Johannes, *J. Am. Chem. Soc.* **2016**, *138*, 1760–1763.

[127] A. U. Meyer, T. Slanina, C.-J. Yao, B. Konig, *ACS Catal.* **2016**, *6*, 369–375.

[128] M. Jiang, H. Yang, H. Fu, *Org. Lett.* **2016**, *18*, 5248–5251.

[129] A. Nitelet, D. Thevenet, B. Schiavi, C. Hardouin, J. Fournier, R. Tamion, X. Pannecoucke, P. Jubault, T. Poisson, *Chem. Eur. J.* **2019**, *25*, 3262–3266.

[130] D. E. Bartak, K. J. Houser, B. C. Rudy, M. D. Hawley, *J. Am. Chem. Soc.* **1972**, *94*, 7526–7530.

[131] E. C. Swift, T. M. Williams, C. R. J. Stephenson, *Synlett* **2016**, *27*, 754–758.

[132] S. Purser, P. R. Moore, S. Swallow, V. Gouverneur, *Chem. Soc. Rev.* **2008**, *37*, 320–330.

[133] W. K. Hagmann, *J. Med. Chem.* **2008**, *51*, 4359–4369.

[134] D. A. Nagib, D. W. C. MacMillan, *Nature* **2011**, *480*, 224–228.

[135] J. A. Terrett, M. D. Clift, D. W. C. MaCmillan, *J. Am. Chem. Soc.* **2014**, *136*, 6858–6861.

[136] J. L. Jeffrey, F. R. Petronijevic, D. W. C. MacMillan, *J. Am. Chem. Soc.* **2015**, *137*, 8404–8407.

[137] D. Leifert, A. Studer, *Angew. Chem. Int. Ed.* **2020**, *59*, 74–108.

[138] G. R. Buettner, *Free Radic. Biol. Med.* **1987**, *3*, 259–303.

[139] S. Narra, Y. Nishimura, H. A. Witek, S. Shigeto, *ChemPhysChem* **2014**, *15*, 2945–2950.

[140] C. Xia, J. Peon, B. Kohler, *J. Chem. Phys.* **2002**, *117*, 8855–8866.

[141] J. F. Hartwig, *Nature* **2008**, *455*, 314–322.

[142] R. Dorel, C. P. Grugel, A. M. Haydl, *Angew. Chem. Int. Ed.* **2019**, *58*, 17118–17129.

[143] C. Cavedon, P. H. Seeberger, B. Pieber, *Eur. J. Org. Chem.* **2020**, 1379–1392.

[144] E. B. Corcoran, M. T. Pirnot, S. Lin, S. D. Dreher, D. A. Dirocco, I. W. Davies, S. L. Buchwald, D. W. C. Macmillan, *Science* **2016**, *353*, 279–283.

[145] M. S. Oderinde, N. H. Jones, A. Juneau, M. Frenette, B. Aquila, S. Tentarelli, D. W. Robbins, J. W. Johannes, *Angew. Chem. Int. Ed.* **2016**, *55*, 13219–13223.

[146] T. Kim, S. Mccarver, C. Lee, D. W. C. MacMillan, *Angew. Chem. Int. Ed.* **2018**, *57*, 3488–3492.

[147] M. S. Oderinde, M. Frenette, D. W. Robbins, B. Aquila, J. W. Johannes, *J. Am. Chem. Soc.* **2016**, *138*, 1760–1763.

[148] M. Jouffroy, C. B. Kelly, G. A. Molander, *Org. Lett.* **2016**, *18*, 876–879.

[149] J. A. Terrett, J. D. Cuthbertson, V. W. Shurtleff, D. W. C. Macmillan, *Nature* **2015**, *524*, 330–334.

[150] E. R. Welin, C. Le, D. M. Arias-Rotondo, J. K. Mccusker, D. W. C. Macmillan, *Science* **2017**, *355*, 380–385.

[151] J. Xuan, T. T. Zeng, J. R. Chen, L. Q. Lu, W. J. Xiao, *Chem. Eur. J.* **2015**, *21*, 4962–4965.

[152] Z.-H. Qi, J. Ma, *ACS Catal.* **2018**, *8*, 1456–1463.

[153] C. H. Lim, M. Kudisch, B. Liu, G. M. Miyake, *J. Am. Chem. Soc.* **2018**, *140*, 7667–7673.

[154] S. Wagaw, B. H. Yang, S. L. Buchwald, *J. Am. Chem. Soc.* **1998**, *120*, 6621–6622.

[155] W. Wu, X.-H. Fan, L.-P. Zhang, L.-M. Yang, *RSC Adv.* **2014**, *4*, 3364–3367.

[156] D. Xue, S. Yu, *Method for Synthesizing N-Aryl Hydrazone through Reaction of Aryl Halide and Hydrazones Compound Catalyzed with Visible Light - CN Patent 2017-10453387*, **2017**.

[157] H. Fretz, A. Valdenaire, J. Pothier, K. Hilpert, C. Gnerre, O. Peter, X. Leroy, M. A. Riederer, *J. Med. Chem.* **2013**, *56*, 4899–4911.

[158] X. Zhang, S. R. Yeh, S. Hong, M. Freccero, A. Albini, D. E. Falvey, P. S. Mariano, *J. Am. Chem. Soc.* **1994**, *116*, 4211–4220.

[159] A. Cordova, *Catalytic Asymmetric Conjugate Reactions*, **2010**.

[160] S. Bräse, S. Höfener, *Angew. Chem. Int. Ed.* **2005**, *44*, 7879–7881.

[161] S. Ay, M. Nieger, S. Bräse, *Chem. Eur. J.* **2008**, *14*, 11539–11556.

[162] L. Palais, L. Babel, A. Quintard, S. Belot, A. Alexakis, *Org. Lett.* **2010**, *12*, 1988–1991.

[163] S. Goncalves-Contal, L. Gremaud, L. Palais, L. Babel, A. Alexakis, *Synthesis* **2016**, *48*, 3301–3308.

[164] A. Erkkila, I. Majander, P. M. Pihko, *Chem. Rev.* **2007**, *107*, 5416–5470.

[165] S. Afewerki, P. Breistein, K. Pirttilä, L. Deiana, P. Dziedzic, I. Ibrahem, A. Cordova, *Chem. Eur. J.* **2011**, *17*, 8784–8788.

[166] D. W. C. MacMillan, *Nature* **2008**, *455*, 304–308.

[167] P. Melchiorre, M. Marigo, A. Carlone, G. Bartoli, *Angew. Chem. Int. Ed.* **2008**, *47*, 6138–6171.

[168] G. Stork, A. Brizzolara, H. Landesman, J. Szmuszkovicz, R. Terrell, *J. Am. Chem. Soc.* **1963**, *85*, 207–222.

[169] B. List, I. Čorić, O. O. Grygorenko, P. S. J. Kaib, I. Komarov, A. Lee, M. Leutzsch, S. Chandra Pan, A. V. Tymtsunik, M. Van Gemmeren, *Angew. Chem. Int. Ed.* **2014**, *53*, 282–285.

[170] E. Arceo, I. D. Jurberg, A. Álvarez-Fernández, P. Melchiorre, *Nat. Chem.* **2013**, *5*, 750–756.

[171] A. Bahamonde, P. Melchiorre, *J. Am. Chem. Soc.* **2016**, *138*, 8019–8030.

[172] M. Silvi, E. Arceo, I. D. Jurberg, C. Cassani, P. Melchiorre, *J. Am. Chem. Soc.* **2015**, *137*, 6120–6123.

[173] Ł. Woźniak, J. J. Murphy, P. Melchiorre, *J. Am. Chem. Soc.* **2015**, *137*, 5678–5681.

[174] M. Silvi, C. Verrier, Y. P. Rey, L. Buzzetti, P. Melchiorre, *Nat. Chem.* **2017**, *9*, 868–873.

[175] L. Wozniak, G. Magagnano, P. Melchiorre, *Angew. Chem. Int. Ed.* **2018**, *57*, 1068–1072.

[176] D. Mazzarella, G. E. M. Crisenza, P. Melchiorre, *J. Am. Chem. Soc.* **2018**, *140*, 8439–8443.

[177] P. Bonilla, Y. P. Rey, C. M. Holden, P. Melchiorre, *Angew. Chem. Int. Ed.* **2018**, *57*, 12819–12823.

[178] L. A. Perego, P. Bonilla, P. Melchiorre, *Adv. Synth. Catal.* **2020**, *362*, 302–307.

[179] M. G. Campbell, T. Ritter, *Chem. Rev.* **2015**, *115*, 612–633.

[180] T. Liang, C. N. Neumann, T. Ritter, *Angew. Chem. Int. Ed.* **2013**, *52*, 8214–8264.

[181] W. Zhao, D. Ran, S. Xiang, F. Jiang, *Method for Preparing 3-Fluoropropionic Acid - CN Patent 2011-10416173*, **2013**.

[182] S. Ventre, F. R. Petronijevic, D. W. C. MacMillan, *J. Am. Chem. Soc.* **2015**, *137*, 5654–5657.

[183] S. Bloom, C. R. Pitts, R. Woltornist, A. Griswold, M. G. Holl, T. Lectka, *Org. Lett.* **2013**, *15*, 1722–1724.

[184] J. Miró, C. Pozo, F. D. Toste, S. Fustero, *Angew. Chem. Int. Ed.* **2016**, *55*, 9045–9049.

[185] C. Chatalove-Sazepin, R. Hemelaere, J.-F. Paquin, G. M. Sammis, *Synthesis* **2015**, *47*, 2554–2569.

[186] R. P. Singh, J. M. Shreeve, *Chem. Commun.* **2001**, 1196–1197.

[187] K. K. Laali, A. Jamalian, C. Zhao, *Tetrahedron Lett.* **2014**, *55*, 6643–6646.

[188] J. M. Antelo, J. Crugeiras, J. R. Leis, A. Ríos, *J. Chem. Soc. Perkin Trans. 2* **2000**, 2071–2076.

[189] M. Meanwell, M. B. Nodwell, R. E. Martin, R. Britton, *Angew. Chem. Int. Ed.* **2016**, *55*, 13244–13248.

[190] O. D. Cupta, R. L. Kirchemier, J. M. Shreeve, *J. Am. Chem. Soc.* **1990**, *112*, 2383–2386.

[191] X. Fan, J. Rong, H. Wu, Q. Zhou, H. Deng, J. Da Tan, W. Xue, L. Wu, H. Tao, J. Wu, *Angew. Chem. Int. Ed.* **2018**, *57*, 8514–8518.

[192] J. Dong, Q. Xia, X. Lv, C. Yan, H. Song, Y. Liu, Q. Wang, *Org. Lett.* **2018**, *20*, 5661–5665.

[193] S. Pan, J. Liu, H. Li, Z. Wang, X. Guo, Z. Li, *Org. Lett.* **2010**, *12*, 1932–1935.

[194] Q. Xia, W. Chen, H. Qiu, *J. Org. Chem.* **2011**, *76*, 7577–7582.

[195] M. K. Singh, H. K. Akula, S. Satishkumar, L. Stahl, M. K. Lakshman, *ACS Catal.* **2016**, *6*, 1921–1928.

[196] H. Aruri, U. Singh, S. Sharma, S. Gudup, M. Bhogal, S. Kumar, D. Singh, V. K. Gupta, R. Kant, R. A. Vishwakarma, P. P. Singh, *J. Org. Chem.* **2015**, *80*, 1929–1936.

[197] I. Buslov, X. Hu, *Adv. Synth. Catal.* **2014**, *356*, 3325–3330.

[198] B. Sun, Z. Yan, C. Jin, W. Su, *Synlett* **2018**, *29*, 2432–2436.

[199] Z. Pan, Z. Fan, B. Lu, J. Cheng, *Adv. Synth. Catal.* **2018**, *360*, 1761–1767.

[200] L. Zhang, H. Yi, J. Wang, A. Lei, *J. Org. Chem.* **2017**, *82*, 10704–10709.

[201] S. Stoll, A. Schweiger, *J. Magn. Reson.* **2006**, *178*, 42–55.

[202] C. G. Hatchard, C. A. Parker, *P. Roy. Soc. A - Math. Phy.* **1956**, *A235*, 518–536.

[203] J. N. Demas, W. D. Bowman, E. F. Zalewski, R. A. Velapoldi, *J. Phys. Chem.* **1981**, *85*, 2766–2771.

[204] A. Fermi, I. Orfanos, A. Avramopoulos, T. Miletic, F. De Leo, N. Demitri, G. Bergamini, P. Ceroni, M. G. Papadopoulos, S. Couris, D. Bonifazi, *Chem. Eur. J.* **2017**, *23*, 2363–2378.

[205] P. Stoessel, H. Spreizter, H. Becker, *Method for the Production of Highly Pure, Tris-Ortho-Metalated Organo-Iridium Compounds - Patent Application WO 2002060910 A1*, **2002**.

[206] S. Cañellas, C. Ayats, A. H. Henseler, M. A. Pericàs, *ACS Catal.* **2017**, *7*, 1383–1391.

[207] C. A. M. Cariou, B. M. Kariuki, J. S. Snaith, *Org. Biomol. Chem.* **2008**, *6*, 3337–3348.

[208] H. Wang, N. Li, Z. Yan, J. Zhang, X. Wan, *RSC Adv.* **2015**, *5*, 2882–2890.

[209] K. H. Jenses, J. D. Webb, M. S. Sigman, *J. Am. Chem. Soc.* **2010**, *132*, 17471–17482.

[210] H. Shimizu, J. C. Holder, B. M. Stoltz, *Beilstein J. Org. Chem.* **2013**, *9*, 1637–1642.

[211] M. S. McCammant, M. S. Sigman, *Chem. Sci.* **2015**, *6*, 1355–1361.

[212] A. G. De Crisci, K. Chung, A. G. Oliver, D. Solis-ibarra, R. M. Waymouth, *Organometallics* **2013**, *32*, 2257–2266.

[213] E. W. Werner, T. Mei, A. J. Burckle, M. S. Sigman, *Science* **2012**, *338*, 1455–1458.

[214] F. Chen, Y. Zhang, L. Yu, S. Zhu, *Angew. Chem. Int. Ed.* **2017**, *56*, 2022–2025.

[215] J. T. Binder, C. J. Cordier, G. C. Fu, *J. Am. Chem. Soc.* **2012**, *134*, 17003–17006.

[216] R. Hassani, A. Requet, S. Marque, A. Gaucher, D. Prim, Y. Kacem, B. Ben Ben, *Tetrahedron Asymmetry* **2014**, *25*, 1275–1279.

[217] M. J. Oila, J. E. Tois, A. M. P. Koskinen, *Lett. Org. Chem.* **2008**, *5*, 11–16.

[218] D.-F. Lu, G.-S. Liu, C.-L. Zhu, B. Yuan, H. Xu, *Org. Lett.* **2014**, *16*, 2912–2915.

[219] K. Manna, W. C. Everett, G. Schoendorff, A. Ellern, T. L. Windus, A. D. Sadow, *J. Am. Chem. Soc.* **2013**, *135*, 7235–7250.

[220] M. K. Tse, S. Bhor, M. Klawonn, G. Anilkumar, H. Jiao, C. Dobler, A. Spannenberg, W. Magerlein, H. Hugl, M. Beller, *Chem. Eur. J.* **2006**, *12*, 1855–1874.

[221] K. A. Nolin, R. W. Ahn, Y. Kobayashi, J. J. Kennedy-smith, F. D. Toste, *Chem. Eur. J.* **2010**, *16*, 9555–9562.

[222] B. Bhattarai, P. Nagorny, *Org. Lett.* **2018**, *20*, 154–157.

[223] J. Hall, J.-M. Lehn, A. DeCian, J. Fischer, *Helv. Chim. Acta* **1991**, *74*, 1–6.

[224] K. Tsutsumi, K. Itagaki, K. Nomura, *ACS Omega* **2017**, *2*, 3886–3900.

[225] S. Kumar, S. Krishankanth, J. Mathew, Z. Pomerantz, J.-P. Lellouche, S. Ghosh, *J. Phys. Chem. C* **2014**, *118*, 2570–2579.

[226] C. W. Jefford, Q. Tang, J. Boukouvalas, *Tetrahedron Lett.* **1990**, *31*, 995–998.

[227] J. Mao, F. Liu, M. Wang, L. Wu, B. Zheng, S. Liu, J. Zhong, Q. Bian, P. J. Walsh, *J. Am. Chem. Soc.* **2014**, *136*, 17662–17668.

[228] C. Ducloiset, P. Jouin, E. Paredes, R. Guillot, M. Sircoglou, M. Orio, W. Leibl, A. Aukauloo, *Eur. J. Inorg. Chem.* **2015**, 5405–5410.

[229] M. F. Semmelhack, A. Chlenov, D. M. Ho, *J. Am. Chem. Soc.* **2005**, *127*, 7759–7773.

[230] A. Spaggiari, D. Vaccari, P. Davoli, F. Prati, *Synthesis* **2006**, 995–998.

[231] N. J. Liverton, C. Bolea, S. Celanire, L. Yunfu, *ACS Chem. Biol.* **2017**, *12*, 244–253.

[232] N. J. Liverton, C. Bolea, S. Celanire, L. Yungu, *Tricyclic Fused Thiazolopyrazole Compounds as Allosteric Modulators of Metabotropic Glutamate Receptors. Patent Application WO 2012008999 A2*, **2012**.

[233] E. J. Reinhard, S. A. Kolodziej, D. R. Anderson, N. W. Stehle, W. F. Vernier, L. F. Lee, S. G. Hedge, *Preparation of Aminocyanopyridines, in Particular Tricyclic Derivatives, as Inhibitors of Mitogen Activated Protein Kinase-Activated Protein Kinase-2 for Treating TNFa Mediated Diseases. Patent Application US 20040127519 A1*, **2004**.

[234] E. Tokumaru, A. Tengeiji, T. Nakahara, I. Shiina, *Chem. Lett.* **2015**, *44*, 1768–1770.

[235] R. R. Ruddarraju, A. C. Murugulla, R. Kotla, M. C. B. Tirumalasetty, R. Wudayagiri, S. Donthabakthuni, R. Maroju, *Med. Chem. Commun.* **2017**, *8*, 176–183.

[236] A. Homsi, A. Kasideh, *Int. J. ChemTech Res.* **2015**, *8*, 1817–1825.

[237] S. I. Zav'yalov, O. V. Dorofeeva, E. E. Rumyantseva, L. B. Kulikova, G. I. Ezhova, N. E. Kravchenko, A. G. Zavozin, *Pharm. Chem. J.* **2002**, *36*, 440–442.

[238] D. M. Shendage, R. Frohlich, G. Haufe, *Org. Lett.* **2004**, *6*, 3675–3678.

[239] N. N. Bhuvan Kumar, O. A. Mukhina, A. G. Kutateladze, *J. Am. Chem. Soc.* **2013**, *135*, 9608–9611.

[240] L. A. Polindara-Garcia, L. D. Miranda, *Synthesis* **2012**, 1051–1056.

[241] N. K. Pahadi, M. Paley, R. Jana, S. R. Waetzig, J. A. Tunge, *J. Am. Chem. Soc.* **2009**, *131*, 16626–16627.

[242] R. T. Buck, D. M. Coe, M. J. Drysdale, L. Ferris, D. Haigh, C. J. Moody, N. D. Pearson, J. B. Sanghera, *Tetrahedron Asymmetry* **2003**, *14*, 791–816.

[243] F. Aydogan, M. Basarir, C. Yolacan, A. S. Demir, *Tetrahedron* **2007**, *63*, 9746–9750.

[244] H. E. Smith, R. K. Orr, F. M. Chen, *J. Am. Chem. Soc.* **1975**, *97*, 3126–3130.

[245] M. Nishida, H. Kimoto, S. Fujii, Y. Hayakawa, L. A. Cohen, *Bull. Chem. Soc. Jpn.* **1991**, *64*, 2255–2259.

[246] G. Varchi, A. Ricci, G. Cahiez, P. Knochel, *Tetrahedron* **2000**, *56*, 2727–2731.

[247] G. Manolikakes, A. Gavryushin, P. Knochel, *J. Org. Chem.* **2008**, *73*, 1429–1434.

[248] T. Kobatake, A. Kondoh, S. Yoshida, H. Yorimitsu, K. Oshima, *Chem. Asian J.* **2008**, *3*, 1613–1619.

[249] F. Zhu, Z. X. Wang, *Adv. Synth. Catal.* **2013**, *355*, 3694–3702.

[250] H. Zhang, Q. Cai, D. Ma, *J. Org. Chem.* **2005**, *70*, 5164–5173.

[251] D. Dehe, I. Munstein, A. Reis, W. R. Thiel, *J. Org. Chem.* **2011**, *76*, 1151–1154.

[252] X. Li, L. He, H. Chen, W. Wu, H. Jiang, *J. Org. Chem.* **2013**, *78*, 3636–3646.

[253] T. Okauchi, K. Kuramoto, M. Kitamura, *Synlett* **2010**, 2891–2894.

[254] Z. B. Dong, M. Balkenhohl, E. Tan, P. Knochel, *Org. Lett.* **2018**, *20*, 7581–7584.

[255] T. D. Machajewski, C. Wong, *Synthesis* **1999**, 1469–1472.

[256] F. Michailidou, C.-W. Chung, M. J. B. Brown, A. F. Bent, J. H. Naismith, W. J. Leavens, S. M. Lynn, S. V. Sharma, R. J. M. Goss, *Angew. Chem. Int. Ed.* **2017**, *56*, 12492–12497.

[257] S. D. Dreher, P. G. Dormer, D. L. Sandrock, G. A. Molander, *J. Am. Chem. Soc.* **2008**, *130*, 9257–9259.

[258] G. V. M. Sharma, K. L. Reddy, P. S. Lakshmi, P. R. Krishna, *Synthesis* **2006**, 55–58.

[259] V. Balzani, P. Ceroni, A. Juris, *Photochemistry and Photophysics - Concepts, Research, Applications*, **2015**.

[260] A. L. Trifonov, L. I. Panferova, V. V. Levin, V. A. Kokorekin, A. D. Dilman, *Org. Lett.* **2020**, *22*, 2409–2413.